Polish Academy of Sciences
Institute of Fundamental Technological Research

P. 262 b

INSTYTUT PODSTAWOWYCH PROBLEMÓW TECHNIKI PAN
BIBLIOTEKA

Archives of Mechanics

Archiwum Mechaniki Stosowanej

volume 49 issue 2

Polish Scientific Publishers PWN
Warszawa 1997

http://rcin.org.pl

ARCHIVES OF MECHANICS IS DEVOTED TO
Theory of elasticity and plasticity • Theory of nonclassical continua • Physics of continuous media • Mechanics of discrete media • Nonlinear mechanics • Rheology • Fluid gas-mechanics • Rarefied gas • Thermodynamics

---

FOUNDERS

M.T. HUBER • W. NOWACKI • W. OLSZAK
W. WIERZBICKI

INTERNATIONAL COMMITTEE

J.L. AURIAULT • D.C. DRUCKER • R. DVOŘÁK
W. FISZDON • D. GROSS • V. KUKUDZHANOV
G. MAIER • G.A. MAUGIN • Z. MRÓZ
C.J.S. PETRIE • J. RYCHLEWSKI • W. SZCZEPIŃSKI
G. SZEFER • V. TAMUŽS • K. TANAKA
CZ. WOŹNIAK • H. ZORSKI

EDITORIAL COMMITTEE

M. SOKOŁOWSKI — editor • L. DIETRICH
J. HOLNICKI-SZULC • W. KOSIŃSKI
W.K. NOWACKI • M. NOWAK
H. PETRYK — associate editor
J. SOKÓŁ-SUPEL • A. STYCZEK • Z.A. WALENTA
B. WIERZBICKA — secretary • S. ZAHORSKI

Copyright 1997 by Polska Akademia Nauk, Warszawa, Poland
Printed in Poland, Editorial Office: Świętokrzyska 21,
00-049 Warszawa (Poland)

e-mail: publikac@ippt.gov.pl

Arkuszy wydawniczych 14,5. Arkuszy drukarskich 13.
Papier offset. kl. III 70 g. B1. Oddano do składania w marcu 1997 r.
Druk ukończono w kwietniu 1997 r.
Skład i łamanie: "MAT-TEX"
Druk i oprawa: Drukarnia Braci Grodzickich, Żabieniec ul. Przelotowa 7

---

http://rcin.org.pl

Arch. Mech., 49, 2, pp. 243–244, Warszawa 1997

Preface

The Journal *Archives of Mechanics*, published bimonthly, has appeared for more than 40 years and is edited by the Institute of Fundamental Technological Research of the Polish Academy of Sciences. The scope of the Journal covers *mechanics and physics of continuous media, theoretical and experimental mechanics of solids and fluids, engineering structures, thermodynamics, analytical and computational methods in mechanics.*

The Editorial Committee invited the Scientific Committee of the XXXI Polish Solid Mechanics Conference – SolMec'96 organized in Mierki, September 9-14, 1996, by the Institute of Fundamental Technological Research and Committee of Mechanics of the Polish Academy of Sciences, to encourage all authors of oral and poster presentations at the SolMec'96 Conference to publish their contributions in special issues of the *Archives of Mechanics* and *Engineering Transactions*.

The present issue of *Archives of Mechanics* is the first special issue of the Journal (the second one will appear in two months) and contains the submitted and reviewed contributions of a more basic orientation.

The first special issue of the other journal, namely *Engineering Transactions* has been printed simultaneously and it contains the contributions with a more engineering character.

The number of papers presented at the XXXI Polish Solid Mechanics Conference exceeded 200, including almost 90 papers from abroad. The conference took place at the Holiday Resort Centre KORMORAN in Mierki, approximately 25 km south of Olsztyn and 200 km north of Warsaw, located in a beautiful forest on a bank of the scenic Pluszne Lake.

The program of the conference included the invited opening, 15 general and closing lectures, as well as almost 200 contributed papers presented as lectures or at the poster sessions. They were arranged according to the subject considered.

The main topics of the Conference were arranged as follows:

- mechanics and thermodynamics of solids with microstructure,
- dynamics of solids and structures,
- plasticity, damage and fracture mechanics,
- mathematical and computer methods in mechanics and engineering sciences,
- experimental methods in mechanics,
- contact and interface problems in mechanics,
- environmental mechanics,
- porous media.

http://rcin.org.pl

Special attention of the organizers and participants coming to the Conference from several academic and research centers all over the world was paid to problems of environmental mechanics. The Organizing Committee of the Conference, together with Professors Schrefler from Padova and Professor Kleiber and Dr. Gajl from Warsaw, organized a TEMPUS – sponsored Intensive Course on Environmental Mechanics during the SolMec'96 Conference.

During the Conference an INTERNET Session was organized with the help of COMP Ltd. Warszawa, Poland and after the Conference on the WWW – page of the Book of Abstracts will be still reachable under the address:

http://www.ippt.gov.pl/~solmec96.

As announced during the Conference the contributions of participants who submit their papers in an electronic form are and will be included in the SolMec'96 electronic proceedings book under the same address on the INTERNET.

The Conference hosted 238 scientists from 20 countries, including: Austria, Belgium, Czech, Finland, France, German, Great Britain, Greece, Hungary, Italy, Japan, Russia, Spain, Swiss, Turkey, Republic of South Africa, Romania, Ukraine, U.S.A.

Some of the scientists coming from Russia obtained financial support towards their travel expenses from the *International Science Foundation* and from the Organizing Committee towards a reduction of the registration fees and their living expenses.

All German participants and some Polish ones obtained financial support to reduce the registration fees from the *Stiftung für deutsch – polnische Zusammenarbeit*. Moreover, the *Stiftung* will support the publishing of a special Proceedings volume dedicated to "Problems of Environmental and Damage Mechanics".

Warszawa, February 1997

Witold Kosiński
Conference Chairman

http://rcin.org.pl

Arch. Mech., 49, 2, pp. 245–252, Warszawa 1997

Crack in an anisotropic medium

A. V. BALUEVA and S. V. KUZNETSOV (MOSCOW)

A NUMERICAL method for the 3D problem of cracks in anisotropic media is developed, based on the variational approach to the crack opening problem. Properties of the pseudo-differential operator of the crack equilibrium problem are considered. Numerical examples are presented.

1. Introduction

SOLUTION of the 3D problem of a plane crack in anisotropic medium is not simple in view of the absence of effective algorithms for determination of fundamental solutions of the equilibrium equations.

Presumably the first integro-differential equation for the plane crack in anisotropic medium was constructed in [1, 2] by means of the Fourier and Radon transforms. The main difficulty in that approach lies in the necessity of constructing several auxiliary solutions to the problem of determination of the root of elliptic polynomials in three variables. In fact, in the case of arbitrary anisotropy, the latter problem can be solved only numerically. That does not allow us to obtain qualitative and quantitative results for cracks, which are known for isotropic case [3, 4].

The method developed for solution of the 3D problem for a plane crack of arbitrary shape in anisotropic medium is based on the construction of the elliptic pseudo-differential operator (p.d.o.) and application of the Goldstein – Klein – Eskin variational method [5] for a numerical solution.

2. Basic operators

Anisotropic elastic medium is considered, for which Lamé's equations of equilibrium can be written in the form

$$\mathbf{A}(\partial_x)\mathbf{u}(\mathbf{x}) \equiv -\mathrm{div}_x \mathbf{C} \cdots \nabla_x \mathbf{u}(\mathbf{x}) = 0, \tag{2.1}$$

where $\mathbf{A}$ is the matrix differential operator of the equilibrium equations, $\mathbf{C}$ is a fourth-order elasticity tensor, assumed to be strongly elliptic, while the medium itself is assumed to be hyperelastic, and $\mathbf{u}$ is the displacement vector field.

Application of the integral Fourier transform

$$g^{\wedge}(\xi) = \int_{R^3} g(\mathbf{x}) \exp(-2\pi i \mathbf{x} \cdot \xi)\, dx$$

http://rcin.org.pl

to (2.1) yields the matrix operator $\mathbf{A}$

$$\mathbf{A}^{\wedge}(\xi) = (2\pi)^2 \xi \cdot \mathbf{C} \cdot \xi \,. \tag{2.2}$$

As it follows from (2.2), operator $\mathbf{A}^{\wedge}$ is strongly elliptic, positive definite of degree 2 and analytic in R^3.

Now, formal identity following from the definition of the fundamental solution

$$\mathbf{A}^{\wedge}(\xi) \cdot \mathbf{E}^{\wedge}(\xi) = \mathbf{I}, \tag{2.3}$$

where $\mathbf{E}^{\wedge}$ is the fundamental solution, and $\mathbf{I}$ is a unit (diagonal) matrix, enables us to write $\mathbf{E}^{\wedge}$ in the form

$$\mathbf{E}^{\wedge}(\xi) = \mathbf{A}_0^{\wedge}(\xi) / \det \mathbf{A}^{\wedge}(\xi), \tag{2.4}$$

where $\mathbf{A}_0^{\wedge}$ is the cofactor of $\mathbf{A}^{\wedge}$. This formula shows that operator $\mathbf{E}^{\wedge}$ is also strongly elliptic, positive definite of degree -2 and $\mathbf{E}^{\wedge} \in C^{\infty}(R^3 \setminus 0, R^3 \otimes R^3)$.

The inverse Fourier transform applied to the formula (2.4) leads to

PROPOSITION 1. Fundamental solution of the equilibrium equations (2.1) is positive definite of degree -1 and $\mathbf{E} \in C^{\infty}(R^3 \setminus 0, R^3 \otimes R^3)$.

REMARK 1. It should be noted that, while for some specific groups of elastic symmetry the Fourier inversion of the formula (2.4) can be performed analytically, in the general case of elastic anisotropy it can be done only numerically [6].

3. Representation of solution

The displacement field produced by a crack is represented by the double-layer potential

$$\mathbf{u}(\mathbf{x}) = \int_{\Omega} \mathbf{b}(\mathbf{y}') \cdot \mathbf{T}(\partial_y, \nu_y) \mathbf{E}(\mathbf{x} - \mathbf{y}') dy', \tag{3.1}$$

where $\mathbf{b}$ is the crack opening, $\mathbf{T}$ is the operator of surface tractions, dy' is the Lebesgue measure on the Π_ν-plane, and $\Omega \subset \Pi_\nu$ is the bounded plane region occupied by the crack at the Π_ν-plane.

Surface tractions acting at the Π_ν-plane are determined by the limits (evaluated in non-tangential direction)

$$\mathbf{t}(\mathbf{x}') = \lim_{\mathbf{x} \to \mathbf{x}'} \mathbf{T}(\partial_x, -\nu_{x'}) \int_{\Omega} \mathbf{b}(\mathbf{y}') \cdot \mathbf{T}(\partial_y, \nu_y) \mathbf{E}(\mathbf{x} - \mathbf{y}') dy', \qquad \mathbf{x}' \in \Pi_\nu \,. \tag{3.2}$$

These limits are correctly determined according to the Lyapunov–Tauber theorem for elastic potentials [7].

http://rcin.org.pl

Application of the Fourier transform to (3.2) gives the amplitude [9] of the corresponding pseudo-differential operator

$$\mathbf{G}^{\wedge}(\xi) = (2\pi)^2 \nu_y \cdot \mathbf{C} \cdots \xi \otimes \mathbf{E}^{\wedge}(\xi) \otimes \xi \cdots \mathbf{C} \cdot \nu_x . \tag{3.3}$$

Properties of the amplitude (3.3) and the associated principal symbol were investigated in [7, 8] where it was proved that condition of strong ellipticity for the elasticity tensor $\mathbf{C}$ ensures strong ellipticity for the amplitude (3.3) and principal symbol.

Reduction of the amplitude (3.3) to the Π_ν-plane gives the principal symbol we are looking for, which depends on $\xi' \in \Pi_\nu$ variables alone:

$$\mathbf{G}^{\sim}(\xi') = (2\pi)^2 \,\text{F.P.} \int_{-\infty}^{\infty} \mathbf{G}^{\wedge}(\xi)\, d\xi'', \tag{3.4}$$

where $\xi \in R^3$, $\xi' = \text{Pr}_{\Pi_\nu}\xi$, $\xi'' = \text{Pr}_{\nu}(\xi)$ so $\xi = \xi' + \xi''\nu$. In (3.4) F.P. stands for the Finite Part of the diconvergent improper integral.

4. Regularization technique

To evaluate integral in (3.4) we observe that the integrand in (3.4) has an obvious asymptotic property due to (2.4)

$$\|\mathbf{G}^{\wedge}(\xi)\| = O(|\xi|^0), \qquad |\xi| \to \infty. \tag{4.1}$$

Moreover, the limit of the integrand when $|\xi''| \to \infty$ can be easily obtained from (3.4) using Eqs. (2.3) and (2.4), that is

$$\underset{\xi' \neq 0}{\forall}\, \xi' \lim_{|\xi''| \to \infty} \mathbf{G}^{\wedge}(\xi) = \nu \cdot \mathbf{C} \cdot \nu. \tag{4.2}$$

Now, from Eqs. (4.1) and (4.2) it follows that

$$\|\mathbf{G}^{\wedge}(\xi) - \nu \cdot \mathbf{C} \cdot \nu\| = O(|\xi''|^{-1}), \qquad |\xi''| \to \infty. \tag{4.3}$$

Analysis of the expressions (4.2) and (4.3) shows that the asymptotic terms of the highest order $O(|\xi''|^{-1})$, $|\xi''| \to \infty$ are odd functions of ξ''. So, the improper integral in (3.3) exists in the Principal Value sense at any $\xi' \neq 0$:

$$\mathbf{G}^{\sim}(\xi') = \text{P.V.} \int_{-\infty}^{\infty} (\mathbf{G}^{\wedge}(\xi) - \nu \cdot \mathbf{C} \cdot \nu)\, d\xi''. \tag{4.4}$$

Taking into account oddness (with respect to ξ''-variable) of the highest asymptotic expression in (4.3), the integral in (4.4) can be finally rewritten in the following form, which can be more convenient in computations

$$\mathbf{G}^{\sim}(\xi') = \int_{-\infty}^{\infty} [\mathbf{G}^{\wedge}(\xi) - \mathbf{G}^{\wedge}(-\xi) - 2\nu \cdot \mathbf{C} \cdot \nu]\, d\xi'', \qquad \xi' \neq 0. \tag{4.5}$$

http://rcin.org.pl

5. Properties and structure of the operator $\mathbf{G}^{\sim}$

Proof of the following proposition can be found in [7, 8]:

PROPOSITION 2. a) Operator $\mathbf{G}^{\sim}$ is symmetric; b) $\mathbf{G}^{\sim}$ is positive definite of degree 1 with respect to $|\xi'|$; c) symbol $\mathbf{G}^{\sim}$ is strongly elliptic; d) work produced by the surface loadings $\mathbf{t}_0 \in H_{-1/2}(\Omega, R^3)$ acting on the crack faces

$$\int_{\Omega} \mathbf{t}_0 \cdot \mathbf{b}\, dx' > 0 \tag{5.1}$$

is positive, where $H_{-1/2}$ is the Hörmander functional space; e) quadratic functional

$$F(\mathbf{b}) \equiv \int_{\Pi_\nu} \mathbf{b}^{\sim}(\xi') \cdot \mathbf{G}^{\sim}(\xi') \cdot \overline{\mathbf{b}^{\sim}(\xi')}\, d\xi' \tag{5.2}$$

representing the elastic energy is coercive in Hörmander's space $H_{1/2}$.

COROLLARY 1. Normal loading on the crack surface $\mathbf{t}_0 = p\nu$, $p > 0$ produces crack opening and increases the crack volume, independently of the elastic anisotropy.

COROLLARY 2. Variational problem

$$\inf_{V \subset H_{1/2}} \left[\frac{1}{2} F(b) - l(b)\right], \qquad l(b) \equiv \int_{\Omega} t_0 \cdot b\, dx' = \int_{\Pi_\nu} t_0^{\sim} \cdot \overline{b}^{\sim} d\xi' \tag{5.3}$$

has a unique solution provided V is a closed subspace in $H_{1/2}(\Omega, R^3)$.

REMARK 1. It should be noted that for an anisotropic medium, normal loading of the crack surface can also produce components of displacement lying in the crack plane (together with necessarily present normal components, due to Corollary 1).

PROPOSITION 3. If anisotropic material possesses a plane of elastic symmetry and the crack lies in it, then $\mathbf{G}^{\sim}$ may be represented in the form

$$\mathbf{G}^{\sim}(\xi') = \mathbf{g}_1(\xi') + g_2(\xi')\nu \otimes \nu, \tag{5.4}$$

where $\mathbf{g}_1$ is a tensor with components lying in the Π_ν-plane: $\nu \cdot \mathbf{g}_1 = 0$, $\mathbf{g}_1 \cdot \nu = 0$, and $g_2(\xi')$ is a scalar-valued function.

P r o o f. At first we remark that if ν is the unit normal to the plane of elastic symmetry, then the fourth-order elasticity tensor $\mathbf{C}$ can have only an even number of indices corresponding to the ν-direction. Otherwise it would not satisfy the symmetry condition. Now it becomes obvious that term $\nu \cdot \mathbf{C} \cdot \nu$ in (4.3), (4.4) does not contain mixed indices, that is referring to ν and in the Π_ν-plane.

http://rcin.org.pl

Similar considerations based on the decomposition (5.4), show that both operators $\mathbf{A}^{\wedge}$ and $\mathbf{E}^{\wedge}$ consist of odd or even components with respect to ξ''-variable, provided these components have, respectively, odd or even number of indices corresponding to the ν-direction. Analysis of the formula (3.3) with the preceding remark yields the conclusion that the mixed components of $\mathbf{G}^{\wedge}$ are odd functions of the ξ''-variable. This, together with (4.3), completes the proof.

REMARK 2. When the crack lies in the plane of elastic symmetry, then in contrast to the general case noted in the Remark 1, normal loading produces only normal components of the crack opening. The preceding proposition shows that the inverse statement is also true.

6. Construction of the p.d.o.

Fourier inversion in the Π_ν-plane of the operator $\mathbf{G}^{\sim}$ which gives the p.d.o. of the crack theory, can be done by the method similar to the multipolar expansion method [6].

Let the operator $\mathbf{G}^{\sim}$ be expanded into harmonic series on the unit circle $S \subset \Pi_\nu$,

$$\mathbf{G}^{\sim}(\xi') = |\xi'|^2 \frac{\sum_n \mathbf{G}_n \exp(in\varphi)}{|\xi'|}, \qquad \xi' = (\xi_1, \xi_2), \quad \xi_1 = |\xi'|\cos\varphi, \quad \xi_2 = |\xi'|\sin\varphi. \tag{6.1}$$

Matrix coefficients $\mathbf{G}_n$ in Eq. (6.1) are determined by integration along the circle S (at $|\xi'| = 1$):

$$\mathbf{G}_n = \pi^{-1} \int_0^{2\pi} \mathbf{G}^{\sim}(\varphi) \exp(in\varphi)\, d\varphi\,. \tag{6.2}$$

REMARK 3. In the expansion (6.1) are presented harmonic functions of even order only. That is due to positive definiteness of the operator $\mathbf{G}^{\sim}$.

Now the inverse Fourier transform of (6.1) can be obtained by Bochner's inversion formula which leads to an operator with weak singularity. This gives the p.d.o. we are looking for

$$\mathbf{G}(\mathbf{x}') = (2\pi)^{-2} \frac{\sum_n i^n \mathbf{G}_n \exp(in\varphi)}{|\mathbf{x}'|} \cdot \mathbf{I}\Delta_{x'}, \qquad \mathbf{x}' = (x_1, x_2), \quad x_1 = |\mathbf{x}'|\cos\varphi, \quad x_2 = |\mathbf{x}'|\sin\varphi. \tag{6.3}$$

Remark 3 shows that formula (6.3) defines a weakly singular operator with the zero imaginary part.

http://rcin.org.pl

7. Numerical method

The variational equation relating the crack closure to the surface tractions may be written in the form

$$W(\mathbf{b}) - l(\mathbf{b}) = 0, \tag{7.1}$$
$$W(\mathbf{b}) \equiv \int_{\Omega} \mathbf{b} \cdot \mathbf{G} \cdot \mathbf{b}\, dx', \qquad l(\mathbf{b}) \equiv \int_{\Omega} \mathbf{t}_0 \cdot \mathbf{b}\, dx',$$

where W is the quadratic functional defining the energy necessary for the crack opening. The condition of vanishing of the gradient of expression (7.1) leads to the Euler equation

$$\nabla_{\mathbf{b}}[W(\mathbf{b}) - l(\mathbf{b})] = 0,$$

which coincides with (3.2). Equation (7.1) may be represented by means of the integral Fourier transform and Parseval's identity in the form

$$\int_{\Pi} \overline{\tilde{b}(\xi')} \cdot \tilde{G}(\xi') \cdot \tilde{b}(\xi')\, d\xi' = \int_{\Pi} \tilde{b}\overline{(\xi')} \cdot \tilde{t}_0(\xi')\, d\xi', \tag{7.2}$$

where Π is the plane of the crack Ω. We will find the Fourier-transform of the crack opening in the series form [10]

$$\tilde{b}(\xi') = \sum_m b_m \tilde{\varphi}_m(\xi'), \tag{7.3}$$

where $\varphi_m \in H_{1/2}$ are the coordinates, and the unknown vectorial coefficients b_m are defined from the condition of minimization of the quadratic functional (7.1). It gives the linear system enabling the determination of b_m [10]:

$$\sum_m b_m \int_{\Pi} \tilde{\varphi}_m(\xi')\overline{\tilde{\varphi}_k(\xi')\tilde{G}(\xi')}\, d\xi' = \int_{\Pi} \tilde{\varphi}_k(\xi')\overline{\tilde{t}_0(\xi')}\, d\xi', \tag{7.4}$$

or in a coordinate form

$$\sum_m b^{\beta}{}_m \int_{\Pi} \tilde{\varphi}_m(\xi')\overline{\tilde{\varphi}_k(\xi')\tilde{G}^{\alpha\beta}(\xi')}\, d\xi' = \int_{\Pi} \tilde{\varphi}_k(\xi')\overline{\tilde{t}^{\alpha}{}_0(\xi')}\, d\xi', \tag{7.5}$$

where indices α, β run from 1 to 3.

8. Example of numerical calculation

A crystal of $MgAl_2O_4$ (spinel) was taken for model calculations with the following anisotropy coefficients:

$$C_{1111} = 1, \quad C_{1122} = 0.548, \quad C_{1133} = 0.548,$$
$$C_{2222} = 1, \quad C_{2233} = 0.548, \quad C_{3333} = 1,$$
$$C_{1212} = C_{3232} = C_{1313} = 0.548,$$

http://rcin.org.pl

which correspond to the cubic crystal. The crack is placed in one of the main symmetry planes, and the crack is subjected to the normal loading.

FIG. 1. Opening of a crack of elliptical form. The semi-axes ratio 1 : 1.

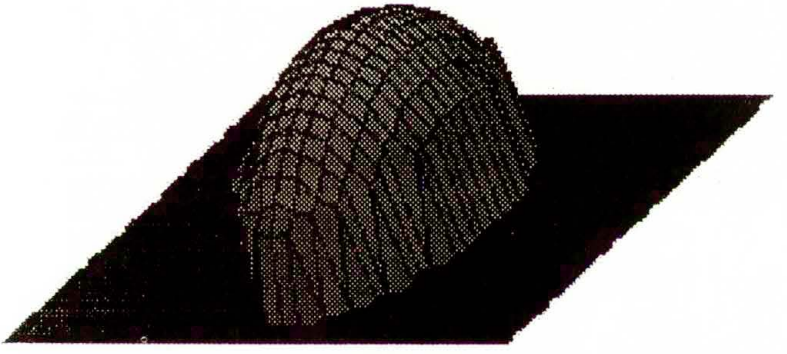

FIG. 2. Opening of a crack of elliptical form. The semi-axes ratio 2 : 1.

Two examples of a circular crack and an elliptical crack with semiaxes ratio 1 : 2 were calculated. The computer results showed that in case of this loading and crack position in the cubic crystal, only normal crack opening occurs (the tangential displacement jumps are equal to zero), what is also in a good agreement with the theoretical results. The cracks openings are represented graphically in Fig. 1 and 2.

References

1. J.R. WILLIS, *Boussinesq problems for an anisotropic halfspace*, J. Mech. Phys. Solids, **15**, 331–339, 1967.
2. J.R. WILLIS, *The stress field around an elliptic crack in an anisotropic elastic medium*, Int. J. Engng. Sci., **6**, 253–263, 1968.
3. A.E. ANDREIKIV, *Spatial problems of the crack theory* [in Russian], Naukova Dumka, Kiev 1982.

http://rcin.org.pl

4. R.V. GOLDSTEIN and V.M. ENTOV, *Variational estimates for the SIF at the front of the plane crack* [in Russian], Izv. AN SSSR, Mech. Tverdogo Tela, 3, 59–64, 1975.
5. R.V. GOLDSTEIN, V.M. ENTOV and A.F. ZAZOVSKI, *Solution of the mixed boundary value problems by the direct variational method* [in Russian], Chisl. Meth. Mech. Splosh. Sredy, 7, 5–13, 1976.
6. S.V. KUZNETSOV, *Fundamental solutions for Lamé's equations in anisotropic elasticity* [in Russian], Izv. AN SSSR, Mech. Tverdogo Tela, 4, 50–54, 1989.
7. S.V. KUZNETSOV, *Spatial problems for cracks in anisotropic media* [in Russian], Izv. AN SSSR, Mech. Tverdogo Tela, 4, 50–54, 1989.
8. S.K. KANAUN, *On the 3D problem of crack in anisotropic elastic media*, Appl. Math. Mech., **45**, 2, 1981.
9. F. TREV, *Introduction to pseudodifferential and Fourier integral operators*. Vol. 1. *Pseudodifferential operators*, Plenum Press, N. Y. and London 1982.
10. A.V. BALUEVA, *Three-dimensional problem on crack kinetics growth under gas diffusion*, Mech. of Solids, 6, 123–131, 1993.

INSTITUTE FOR PROBLEMS IN MECHANICS
RUSSIAN ACADEMY OF SCIENCES
pr. Vernadskogo, 101, 117526 Moscow, Russia.

Received October 21, 1996.

http://rcin.org.pl

Arch. Mech., 49, 2, pp. 253–283, Warszawa 1997

Symmetric boundary integral formulations of transient heat conduction: saddle-point theorems for BE analysis and BE-FE coupling

Dedicated to the memory of Professor Gaetano Fichera

A. CARINI (BRESCIA), M. DILIGENTI (PARMA) and G. MAIER (MILANO)

THE LINEAR PROBLEM of transient heat conduction over a bounded time interval in a homogeneous domain with boundary conditions for temperature and flux is formulated in terms of boundary integral equations with an integral operator which is shown to be symmetric with respect to a bilinear form (convolutive in time). This form generates a functional characterizing the solution by its stationarity. Making recourse to a suitable integral transform and to another special bilinear form, it is shown that the boundary solution over the unbounded time interval $0 \leq t < \infty$, is characterized by a saddle-point property with separation of variables. Separation means that the solution corresponds to a maximum with respect to the time history of temperatures on the Neumann boundary, and by a minimum with respect to the time history of fluxes on the Dirichlet boundary. Subsequently a domain decomposition is assumed in view of coupled BE-FE discretization and a variational basis to such heterogeneous multifield modelling is provided.

1. Introduction

IN THE LAST FEW YEARS a growing portion of the literature concerning boundary integral equation (BIE) approaches and boundary element methods (BEMs) is devoted to symmetric formulations and relevant solution procedures.

The traditional formulation rests on Somigliana's identity (generated by "static" sources) and on its space-discrete version achieved by field modelling and node-wise collocation. As for diffusion problems, representative contributions are those due to RIZZO and SHIPPY [1], SHAW [2], TANAKA and TANAKA [3], ROURES and ALARCON [4], PINA and FERNANDEZ [5], while a comprehensive survey can be found in SHARP and CROUCH [6]. In this now popular context, key operators turn out to be nonsymmetric (or non-selfadjoint). Symmetry can be conferred to these operators by suitably adopting as boundary sources both static (or *intensive* or *single layer*) and kinematic (or *extensive* or *double layer*) discontinuities and, after modelling, by enforcing two suitably chosen BIEs in a Galerkin weighted-residual sense, which implies double integrations. Thus, among various consequences, variational characterizations can be given to the solution of boundary-value problems and of their BE-discretized versions in elasticity and in potential problems such

http://rcin.org.pl

as steady-state heat conduction, Darcy filtration, Saint-Venant torsion analyses and their analogues (see e.g.: [7, 8, 9]).

Parallel results have been established in incremental plasticity for both the rate problem and the finite-step problem, by recourse to domain distributions of concentrated strain sources (and relevant additional terms in the two BIEs) and to a third integral equation for stresses over potentially yielding portions of the domain (see e.g. [10, 11, 12, 13, 14]).

No attempt is made here to survey the numerous contributions to the theoretical foundations and to related computational aspect (*in primis* double integrations of hypersingular integrands and computer implementations) of the Galerkin-symmetric BEM in linear and nonlinear boundary-value problems. Two recent books [15] and [16] provide fairly abundant information and references (updated to 1991 and 1995, respectively).

As for initial-value boundary-value problems, much less attention has been attracted so far by their symmetric Galerkin BIE formulations and consequent solution properties and BE techniques. These formulations and properties have been established making use of time-dependent discontinuity sources of two kinds, in a way basically similar to the one adopted for boundary-value problems. Thus the BIE analysis of transient heat conduction (diffusion) [17], elastodynamics [18], viscoelasticity [19] and elastic-plastic dynamics [20] have been conferred symmetry in space and time (with respect to a time-convolutive bilinear form) over the finite time-interval of interest. As a consequence, variational saddle-point characterizations of the time response of the system to a given history of external actions, have been established in all the mechanical contexts listed above.

The present paper is intended to provide a further contribution to the theoretical foundations of the symmetric, variational BIE-BE methods for time-dependent problems with reference to linear transient heat conduction.

First the diffusion problem with mixed boundary conditions is formulated in the context of the "direct" approaches by means of BIEs using boundary sources of two kinds, like in an earlier paper by the authors in the context of "indirect" approaches [17]. The integral operator arising from the set of the above BIEs is shown to be symmetric (self-adjoint) with respect to a suitably devised bilinear form. This is defined as usual in the space variables; as for the time variable, the bilinear form is generated by means of the Laplace transforms of the two functions involved and by integrating, with respect to the transform parameter s over the unbounded interval $0 \leq s \leq \infty$, the product of the two functions and a suitable weight function.

As a consequence of the symmetry achieved in the above sense, the time history of the unknown boundary temperatures and fluxes over the unbounded time interval turns out to be characterized by a saddle-point property with separation of the two kinds of variables; namely, by a minimum with respect to the temperature field (extensive, kinematic variables) and by a maximum with respect to the heat flux field (intensive, static variables).

http://rcin.org.pl

In contrast to the present saddle-point theorem, the min-max property presented earlier by the authors did not exhibit the above separation of variables. However, it had been proved over any bounded time interval, instead of over $0 \leq t \leq \infty$ only. The path of reasoning leading to the present min-max theorem is inspired by the ones followed by GURTIN [21], TONTI [22], RAFALSKI [23, 24] and REISS and HAUG [25], in order to arrive at variational principles for initial/boundary value problems formulated by partial differential equations.

Domain decomposition for coupling of BEM and FEM (Finite Element Method) has been a topic of active research since years (see e.g. [26]). The purpose is to employ each method in the subdomain where its peculiarities can be exploited at best for the numerical solution of the problem. Galerkin symmetric BEM turns out to be especially suitable to BE-FE coupled solutions, as shown by HOLZER [27], POLIZZOTTO and ZITO [28]. For the present time-dependent (transient) heat transfer problem, a contribution to heterogeneous modelling in the above sense is provided by the variational approach developed herein in Sec. 5.

2. Governing equation, Green functions and their properties

2.1. The linear diffusion problem

The thermally isotropic material considered herein is characterized by the following constant parameters: thermal conductivity k (measured e.g. in the units: $\mathrm{J\,sec^{-1}m^{-1}K^{-1}}$); specific heat γ ($\mathrm{J\,K^{-1}kg^{-1}}$); density ϱ ($\mathrm{kg\,m^{-3}}$). The heat conduction in a homogeneous body obtained by filling with the above material the open bounded domain Ω of a space with d dimensions ($\mathcal{R}^d$, with $d = 1, 2$ or 3) is governed by Fourier's and energy conservation laws. These laws combined lead to the classical equation (see e.g. [29]):

$$\frac{\partial \theta(\mathbf{x}, t)}{\partial t} - \alpha \nabla^2 \theta(\mathbf{x}, t) = \frac{1}{\gamma \varrho} Q(\mathbf{x}, t) \qquad \text{in } \Omega \times T. \tag{2.1}$$

Here $\alpha = k\gamma^{-1}\varrho^{-1}$ is the diffusivity coefficient of the material (in $\mathrm{m^2\,sec^{-1}}$); ∇^2 means Laplace operator; θ denotes temperature (in Kelvin degrees K); $\mathbf{x}$ is the d-vector of space coordinates x_i in a Cartesian reference system; t denotes time and $T \equiv [0, \bar{t}]$ the time interval over which the phenomenon is to be studied; Q represents the (given) density of heat supply rate [i.e. the production of heat per unit volume and time ($\mathrm{J\,m^{-3}\,sec^{-1}}$)].

The initial and boundary conditions are:

$$\theta(\mathbf{x}, 0) = \bar{\theta}_0(\mathbf{x}) \qquad \text{in } \Omega, \tag{2.2}$$

$$\theta(\mathbf{x}, t) = \bar{\theta}(\mathbf{x}, t) \qquad \text{on } \Gamma_\theta \times T, \tag{2.3}$$

$$q(\mathbf{x}, t) = -k \frac{\partial \theta}{\partial n}(\mathbf{x}, t) = \bar{q}(\mathbf{x}, t) \qquad \text{on } \Gamma_q \times T, \tag{2.4}$$

$$q(\mathbf{x}, t) = [\theta(\mathbf{x}, t) - \theta_\infty]\, c \qquad \text{on } \Gamma_c \times T. \tag{2.5}$$

http://rcin.org.pl

Equation $(2.4)_1$ defines the heat flux q ($\mathrm{J\,m^{-2}sec^{-1}}$) in direction $\mathbf{n}$; $\mathbf{n}$ is the outward unit normal to the boundary $\Gamma = \Gamma_\theta \cup \Gamma_q \cup \Gamma_c$ (Γ_θ, Γ_q and Γ_c being disjoint parts of Γ) and is supposed to be uniquely defined everywhere; $\bar{\theta}_0$, $\bar{\theta}$ and $\bar{q}$ are given functions; the convection coefficient c ($\mathrm{J\,sec^{-1}\,m^{-2}\,K^{-1}}$) and the far-field temperature θ_∞ (in K) are known parameters.

For the sake of formal simplicity, the present study will assume $\Gamma_c = 0$, but its results can easily be extended to Cauchy (convective) condition (2.5). The less easy extension to non-homogeneous, multidomain problems can be carried out according to the line of thought pointed out in [18]. Thermally anisotropic media are implicitly covered with recourse to the relevant fundamental solutions.

2.2. Green functions

Consider (and denote by Ω_∞) the space $\mathcal{R}^d$ embedding Ω and filled with the same material as Ω. The response of Ω_∞ to a *source* represented by a (pulse) unit heat supply, concentrated in $\boldsymbol{\xi}$ (*load* or *source* point) at the instant τ, is described by the classical formula (see e.g. [29]):

$$G_{\theta\theta}(\mathbf{x}, \boldsymbol{\xi}; t-\tau) = \frac{1}{\gamma\varrho} \frac{e^{-\frac{r^2}{4\alpha(t-\tau)}}}{[4\pi\alpha(t-\tau)]^{d/2}} \qquad \text{for } t \geq \tau, \tag{2.6}$$

where $r \equiv \|\mathbf{x} - \boldsymbol{\xi}\| = [(x_i - \xi_i)(x_i - \xi_i)]^{1/2}$ with $i = 1, \ldots, d$, denoting by $\|\cdot\|$ the Euclidean norm. The Green function or kernel (2.6) is the *fundamental solution* to Eq. (2.1), in the sense that it solves Eq. (2.1), when one sets in it $Q(\mathbf{x}, t) = Q\,\delta(\mathbf{x} - \boldsymbol{\xi})\,\delta(t - \tau)$ (δ being Dirac distribution and $Q = 1$) and assumes $\theta \to 0$ for $\|\mathbf{x}\| \to \infty$ as boundary condition (i.e. $\theta = 0$ on Γ_∞) in three-dimensional situations.

It is worth noting that the heat-impulse source which gives rise to the temperature field (2.6), can be interpreted as a unit flux discontinuity across Γ, concentrated in $\boldsymbol{\xi}$ and τ. In order to make this circumstance explicit, denote by $\boldsymbol{\xi}^+$ a point not belonging to $\Omega \cup \Gamma$ (i.e. internal to $\Omega_\infty - \Omega \cup \Gamma$) and infinitely close to $\boldsymbol{\xi} \in \Gamma$ and by Γ^+ the set of all $\boldsymbol{\xi}^+$. Similarly, denote by $\boldsymbol{\xi}^-$ and Γ^- the obvious counterparts defined for points belonging to Ω. The unit normal, indicated by $\boldsymbol{\nu}$ in $\boldsymbol{\xi}$ and $\mathbf{n}$ in $\mathbf{x}$, is assumed as outward with respect to Ω and common to Γ and Γ^-, but in $\boldsymbol{\xi}^+$ the normal is $\boldsymbol{\nu}^+ = -\boldsymbol{\nu}$ (outward with respect to $\Omega_\infty - \Omega$). By means of this notation, the above source can be described in the alternate form:

$$\Delta q\,\delta(\mathbf{z} - \boldsymbol{\xi})\,\delta(t - \tau), \tag{2.7}$$

where

$$\Delta q \equiv -q\left(\boldsymbol{\xi}^-, t\right) - q\left(\boldsymbol{\xi}^+, t\right) = 1, \qquad \mathbf{z}, \boldsymbol{\xi} \in \Gamma, \qquad t, \tau \in T. \tag{2.7'}$$

Here Δq denotes the jump of the heat flux across Γ in $\boldsymbol{\xi}$ and $\delta(\mathbf{z} - \boldsymbol{\xi})$ is the Dirac distribution defined over Γ (no longer over Ω).

http://rcin.org.pl

Other kernels, all defined for $t \geq \tau$, are derived below for later use by taking derivatives of the two-point function $G_{\theta\theta}$, Eq. (2.6), in the direction $\mathbf{n}$ of the outward normal to Γ defined in the *field* or *receiver* point $\mathbf{x}$ or/and in the direction $\boldsymbol{\nu}$ of the outward normal in the load point $\boldsymbol{\xi}$. Whenever useful to remind of these normals in the expression of a kernel G, their symbols will show up in the argument or will be replaced by / to mark their absence.

$$(2.8) \qquad G_{q\theta}(\mathbf{x}, \boldsymbol{\xi}; \mathbf{n}, /; t-\tau) \equiv -k \frac{\partial G_{\theta\theta}}{\partial x_i} n_i = \frac{k}{2\alpha(t-\tau)} (x_i - \xi_i) n_i G_{\theta\theta}(\mathbf{x}, \boldsymbol{\xi}; t-\tau),$$

$$(2.9) \qquad G_{\theta q}(\mathbf{x}, \boldsymbol{\xi}; /, \boldsymbol{\nu}; t-\tau) \equiv -k \frac{\partial G_{\theta\theta}}{\partial \xi_i} \nu_i = \frac{-k}{2\alpha(t-\tau)} (x_i - \xi_i) \nu_i G_{\theta\theta}(\mathbf{x}, \boldsymbol{\xi}; t-\tau),$$

$$(2.10) \qquad G_{qq}(\mathbf{x}, \boldsymbol{\xi}; \mathbf{n}, \boldsymbol{\nu}; t-\tau) \equiv -k \frac{\partial G_{q\theta}}{\partial \xi_i} \nu_i = -k \frac{\partial G_{\theta q}}{\partial x_i} n_i$$
$$= -\frac{k^2}{2\alpha(t-\tau)} \left[\frac{1}{2\alpha(t-\tau)} (x_i - \xi_i) n_i (x_r - \xi_r) \nu_r - n_j \nu_j \right] G_{\theta\theta}(\mathbf{x}, \boldsymbol{\xi}; t-\tau).$$

Physically interpreted, Eq. (2.8) represents the flux response in the field point $\mathbf{x}$ and direction $\mathbf{n}$ at instant t to the heat impulse acting on Ω_∞ in load point $\boldsymbol{\xi}$ at instant τ. Kernels (2.9) and (2.10) represent the temperature at $\mathbf{x}$ and t and, respectively, the flux at $\mathbf{x}$ in direction $\mathbf{n}$ at time t, which are generated in Ω_∞ by a "double layer" *source* consisting of a unit discontinuity of temperature across a surface through $\boldsymbol{\xi}$ of normal $\boldsymbol{\nu}$, concentrated in space and time. This (concentrated) temperature discontinuity source can be formally described by a counterpart to Eq. (2.7), making recourse to the same Dirac distributions δ, $\Delta\theta$ denoting a jump of temperature across Γ:

$$(2.11) \qquad \Delta\theta\, \delta(\mathbf{z} - \boldsymbol{\xi})\, \delta(t - \tau),$$

where

$$(2.11') \qquad \Delta\theta \equiv -\theta\left(\boldsymbol{\xi}^+, t\right) + \theta\left(\boldsymbol{\xi}^-, t\right) = 1, \qquad \mathbf{z}, \boldsymbol{\xi} \in \Gamma, \qquad t, \tau \in T.$$

2.3. Properties of kernels

The Green functions (2.6), (2.8), (2.9) and (2.10), all defined over Ω_∞ and for $t \geq \tau$ (causality condition), for $\mathbf{x} \to \boldsymbol{\xi}$ and $t \to \tau$ exhibit singularities which depend on the ratio $r/(t-\tau)$ when both r and $(t-\tau)$ tend to zero. However, it can be shown (see Appendix A) that the usual singularities of the (time-independent)

http://rcin.org.pl

Green functions for the stationary conduction are exhibited by the Laplace transforms of these functions; namely, in three-dimensional situations ($d = 3$):

$$\begin{aligned} &\mathcal{L}(G_{\theta\theta}) = O(r^{-1}), \qquad \mathcal{L}(G_{\theta q}) = O(r^{-2}), \\ &\mathcal{L}(G_{q\theta}) = O(r^{-2}), \qquad \mathcal{L}(G_{qq}) = O(r^{-3}). \end{aligned} \tag{2.12}$$

In Eq. (2.12) $\mathcal{L}$ means Laplace transform

$$\mathcal{L}(\phi(t), s) \equiv \int_0^\infty e^{-st}\phi(t)\,dt, \tag{2.13}$$

s being the transformation parameter and ϕ any $\mathcal{L}$-transformable function.

The following *reciprocity* relationships among the above kernels hold at any time in space for $\mathbf{x} \neq \boldsymbol{\xi}$ and can be readily justified by inspection of the relevant formulae, Eqs. (2.6), (2.8), (2.9) and (2.10):

$$G_{\theta\theta}(\mathbf{x}, \boldsymbol{\xi}; t-\tau) = G_{\theta\theta}(\boldsymbol{\xi}, \mathbf{x}; t-\tau), \tag{2.14}$$

$$G_{q\theta}(\mathbf{x}, \boldsymbol{\xi}; \mathbf{n}, /; t-\tau) = G_{\theta q}(\boldsymbol{\xi}, \mathbf{x}; /, \mathbf{n}; t-\tau), \tag{2.15}$$

$$G_{qq}(\mathbf{x}, \boldsymbol{\xi}; \mathbf{n}, \boldsymbol{\nu}; t-\tau) = G_{qq}(\boldsymbol{\xi}, \mathbf{x}; \boldsymbol{\nu}, \mathbf{n}; t-\tau). \tag{2.16}$$

The positive definiteness of $\mathcal{L}(G_{\theta\theta})$ and the negative (semi)definiteness of $\mathcal{L}(G_{qq})$ formally mean that:

$$\int_\Gamma \int_\Gamma \mathcal{L}(\Delta q(\mathbf{x}; t), s)\, \mathcal{L}(G_{\theta\theta}(\mathbf{x}, \boldsymbol{\xi}; t), s)\, \mathcal{L}(\Delta q(\boldsymbol{\xi}; t), s)\, d\Gamma\, d\Gamma > 0 \tag{2.17}$$

$$\forall \Delta q \neq 0,$$

$$\int_\Gamma \int_\Gamma \mathcal{L}(\Delta\theta(\mathbf{x}; t), s)\, \mathcal{L}(G_{qq}(\mathbf{x}, \boldsymbol{\xi}; \mathbf{n}, \boldsymbol{\nu}; t), s)\, \mathcal{L}(\Delta\theta(\boldsymbol{\xi}; t), s)\, d\Gamma\, d\Gamma \leq 0 \tag{2.18}$$

$$\forall \Delta\theta.$$

These properties are proved in Appendix B.

In view of the $O(r^{-3})$ singularity ("hypersingularity") of the Laplace transform of kernel G_{qq}, Eq. (2.10), the double integral (2.18) acquires a meaning only if special interpretations and computational provisions are adopted. These are extensively dealt with in the recent literature see e.g. [30, 31, 32 and 33]; therefore they will not be discussed here. An investigation and implementation of hypersingular integrals occurring in elastostatics are presented in [8].

It seems appropriate to mention here also the following features of the basic Green's function, Eq. (2.6), in three-dimensional situations, see e.g. [29]:

$$\lim_{t\to\infty} G_{\theta\theta} = 0, \qquad \lim_{r\to\infty} G_{\theta\theta} = 0, \qquad \lim_{t\to\tau} G_{\theta\theta} = \delta(\mathbf{x} - \boldsymbol{\xi}). \tag{2.19}$$

http://rcin.org.pl

3. Symmetric boundary integral equations and first variational formulation

In order to simplify notation and formal developments, the following provisions will be adopted henceforth. (i) Only Dirichlet Eq. (2.3) and Neumann Eq. (2.4) boundary conditions will be considered (i.e. $\Gamma_c = 0$). (ii) The differentials $d\boldsymbol{\xi}$ (and $d\mathbf{x}$) henceforth will mean $d\Gamma$ or $d\Omega$ when the integration variables are the coordinates of the source point $\boldsymbol{\xi}$ (and of the receiver point $\mathbf{x}$, respectively), as the integration domain indicated near the integral symbol will remove any ambiguity. (iii) The convolutive integration with respect to time τ will be denoted by an asterisk, namely $\int_0^t \psi(t-\tau)\psi'(\tau)\,d\tau = \psi(t) * \psi'(t)$, where ψ and ψ' are any time functions.

3.1. Two governing boundary integral equations

Consider the time history of the temperature field $\theta(\mathbf{x}, t)$ in Ω (as a part of Ω_∞) due to the following *causes* acting on Ω_∞: discontinuities of flux $\Delta q(\boldsymbol{\xi}, \tau)$ and of temperature $\Delta\theta(\boldsymbol{\xi}, \tau)$, distributed along the boundary Γ; heat supply $Q(\boldsymbol{\xi}, t)$ in the domain Ω; temperature initial condition $\bar{\theta}_0(\boldsymbol{\xi}, 0)$ in the domain Ω and $\bar{\theta}_0(\boldsymbol{\xi}, 0) = 0$ outside Ω, i.e. in $\Omega_\infty - (\Omega \cup \Gamma)$. Obviously, the last two data define the initial temperature discontinuity $\Delta\theta(\boldsymbol{\xi})$ across Γ at $\tau = 0$.

Using the kernels $G_{\theta\theta}$ and $G_{\theta q}$ as influence functions of Ω_∞ and superposing effects, we can give $\theta(\mathbf{x}, t)$ the following representation:

$$\theta(\mathbf{x};t) = \int_\Gamma G_{\theta\theta}(\mathbf{x},\boldsymbol{\xi};t) * \Delta q(\boldsymbol{\xi};t)\,d\boldsymbol{\xi} + \int_\Gamma G_{\theta q}(\mathbf{x},\boldsymbol{\xi};/,\boldsymbol{\nu};t) * \Delta\theta(\boldsymbol{\xi};t)\,d\boldsymbol{\xi} + \int_\Omega G_{\theta\theta}(\mathbf{x},\boldsymbol{\xi};t) * Q(\boldsymbol{\xi},t)\,d\boldsymbol{\xi} + \gamma\varrho \int_\Omega G_{\theta\theta}(\mathbf{x},\boldsymbol{\xi};t)\bar{\theta}_0(\boldsymbol{\xi})\,d\boldsymbol{\xi}\,. \tag{3.1}$$

The last integral containing the initial temperature $\bar{\theta}_0$ can be justified by the path of reasoning expounded in [6].

A similar integral representation is given below to the flux $q(\mathbf{x}; t)$ in Ω (as a part of Ω_∞), taking the derivatives of Eq. (3.1) with respect to $\mathbf{x}$ in direction $\mathbf{n}$ and multiplying this derivative by $-k$:

$$q(\mathbf{x};t) = \int_\Gamma G_{q\theta}(\mathbf{x},\boldsymbol{\xi};\mathbf{n},/;t) * \Delta q(\boldsymbol{\xi};t)\,d\boldsymbol{\xi} + \int_\Gamma G_{qq}(\mathbf{x},\boldsymbol{\xi};\mathbf{n},\boldsymbol{\nu};t) * \Delta\theta(\boldsymbol{\xi};t)\,d\boldsymbol{\xi} + \int_\Omega G_{q\theta}(\mathbf{x},\boldsymbol{\xi};\mathbf{n},/;t) * Q(\boldsymbol{\xi},t)\,d\boldsymbol{\xi} + \gamma\varrho \int_\Omega G_{q\theta}(\mathbf{x},\boldsymbol{\xi};\mathbf{n},/;t)\bar{\theta}_0(\boldsymbol{\xi})\,d\boldsymbol{\xi}\,. \tag{3.2}$$

Choosing a "direct" rather than an "indirect" approach, we identify now the discontinuity sources as jumps across Γ between actual quantities in the domain

http://rcin.org.pl

Ω and their counterparts in an unheated constant-temperature exterior $\Omega_\infty - (\Omega \cup \Gamma)$. Namely, we set for any $t \in T$:

$$
\begin{aligned}
&q(\boldsymbol{\xi}^+, t) = 0 \quad \text{on } \Gamma, \qquad q(\boldsymbol{\xi}^-, t) = \bar{q}(\boldsymbol{\xi}, t) \quad \text{on } \Gamma_q, \\
&q(\boldsymbol{\xi}^-, t) = q(\boldsymbol{\xi}, t) \quad \text{on } \Gamma_\theta, \qquad \theta(\boldsymbol{\xi}^+, t) = 0 \quad \text{on } \Gamma, \\
&\theta(\boldsymbol{\xi}^-, t) = \bar{\theta}(\boldsymbol{\xi}, t) \quad \text{on } \Gamma_\theta, \qquad \theta(\boldsymbol{\xi}^-, t) = \theta(\boldsymbol{\xi}, t) \quad \text{on } \Gamma_q.
\end{aligned} \tag{3.3}
$$

Now, keeping in mind Eqs. $(2.7)_2$, $(2.11)_2$ and (3.3), let us enforce Eq. (3.1) in points $\mathbf{x}^- \in \Omega$ infinitely close to the Dirichlet boundary Γ_θ, and identify the temperature in these points with the boundary data $\bar{\theta}(\mathbf{x}; t)$ assigned there. Similarly, we write Eq. (3.2) in points $\mathbf{x}^- \in \Omega$ close to Neumann boundary Γ_q, identify the heat flux in these points with the assigned boundary data $\bar{q}(\mathbf{x}; t)$. Thus Eqs. (3.1) and (3.2) yield:

for $\mathbf{x} \in \Gamma_\theta^-$

$$
\int_{\Gamma_\theta} G_{\theta\theta}(\mathbf{x}, \boldsymbol{\xi}; t) * q(\boldsymbol{\xi}; t)\, d\boldsymbol{\xi} - \int_{\Gamma_q} G_{\theta q}(\mathbf{x}, \boldsymbol{\xi}; \boldsymbol{\nu}; t) * \theta(\boldsymbol{\xi}; t)\, d\boldsymbol{\xi} = \bar{f}_\theta(\mathbf{x}; t), \tag{3.4}
$$

for $\mathbf{x} \in \Gamma_q^-$

$$
\int_{\Gamma_\theta} G_{q\theta}(\mathbf{x}, \boldsymbol{\xi}; \mathbf{n}; t) * q(\boldsymbol{\xi}; t)\, d\boldsymbol{\xi} - \int_{\Gamma_q} G_{qq}(\mathbf{x}, \boldsymbol{\xi}; \mathbf{n}, \boldsymbol{\nu}; t) * \theta(\boldsymbol{\xi}; t)\, d\boldsymbol{\xi} = -\bar{f}_q(\mathbf{x}; t), \tag{3.5}
$$

having set:

$$
\begin{aligned}
\bar{f}_\theta(\mathbf{x}; t) \equiv -\bar{\theta}(\mathbf{x}; t) &+ \int_\Omega G_{\theta\theta}(\mathbf{x}, \boldsymbol{\xi}; t) * Q(\boldsymbol{\xi}, t)\, d\boldsymbol{\xi} \\
&+ \gamma \varrho \int_\Omega G_{\theta\theta}(\mathbf{x}, \boldsymbol{\xi}; t)\, \bar{\theta}_0(\boldsymbol{\xi})\, d\boldsymbol{\xi} - \int_{\Gamma_q} G_{\theta\theta}(\mathbf{x}, \boldsymbol{\xi}; t) * \bar{q}(\boldsymbol{\xi}, t)\, d\boldsymbol{\xi} \\
&+ \int_{\Gamma_\theta} G_{\theta q}(\mathbf{x}, \boldsymbol{\xi}; \boldsymbol{\nu}; t) \bar{\theta}(\boldsymbol{\xi}; t)\, d\boldsymbol{\xi},
\end{aligned} \tag{3.6}
$$

$$
\begin{aligned}
\bar{f}_q(\mathbf{x}; t) \equiv \bar{q}(\mathbf{x}; t) &- \int_\Omega G_{q\theta}(\mathbf{x}, \boldsymbol{\xi}; \mathbf{n}; t) * Q(\boldsymbol{\xi}, t)\, d\boldsymbol{\xi} \\
&- \gamma \varrho \int_\Omega G_{q\theta}(\mathbf{x}, \boldsymbol{\xi}; \mathbf{n}; t)\, \bar{\theta}_0(\boldsymbol{\xi})\, d\boldsymbol{\xi} + \int_{\Gamma_q} G_{q\theta}(\mathbf{x}, \boldsymbol{\xi}; \mathbf{n}; t) * \bar{q}(\boldsymbol{\xi}, t)\, d\boldsymbol{\xi} \\
&- \int_{\Gamma_\theta} G_{qq}(\mathbf{x}, \boldsymbol{\xi}; \mathbf{n}, \boldsymbol{\nu}; t)\, \bar{\theta}(\boldsymbol{\xi}; t)\, d\boldsymbol{\xi}.
\end{aligned} \tag{3.7}
$$

http://rcin.org.pl

It is worth stressing that the singular integrals which intervene in Eqs. (3.4) and (3.5) must be interpreted in a suitable sense (in Cauchy and Hadamard sense for kernels $G_{\theta q}$ and $G_{q\theta}$ and for the "hypersingular" one G_{qq}, respectively). Also the existence and computability of integrals involving G_{qq} set special continuity requirements on functions θ and on interpolations to employ in its modelling. The analytical and numerical integrations in the presence of singularity and hypersingularity will not be discussed here. They are the object of the recent literature cited in Sec. 2 (and mostly concerning basically similar elastostatic and elastodynamic problems).

The boundary integral equations (3.4) and (3.5) govern the time histories, over the time interval T, of the unknown boundary fields $q(\boldsymbol{\xi};\tau)$ on Γ_θ, $\theta(\boldsymbol{\xi},\tau)$ on Γ_q. Thermal quantities which will actually occur elsewhere in the body considered will be recovered by quadratures from the boundary solution through the representation formulae (3.1) and (3.2) collocated at any point $\mathbf{x}$ and instant t of interest, account being taken of Eqs. $(2.7)_2$, $(2.11)_2$ and (3.3).

Therefore, the integral boundary equations (3.4) and (3.5) can be regarded as an alternative formulation of the original initial/boundary value problem, Eqs. (2.1)–(2.4). What follows is intended to point out some peculiar and hopefully computationally useful consequences of the above nonconventional "direct" BIE formulation (3.4)–(3.7) of linear transient heat conduction.

3.2. Symmetry and boundary variational theorem

It is convenient for subsequent developments to re-write the boundary integral equations (3.4) and (3.5) using a compact (operatorial) notation:

$$\mathbf{L}\,\mathbf{y} = \mathbf{f}. \tag{3.8}$$

In Eq. (3.8) $\mathbf{y}$ and $\mathbf{f}$ are vectors which gather boundary unknown functions and data, respectively:

$$\mathbf{y} \equiv \begin{Bmatrix} q(\boldsymbol{\xi};t) \\ \theta(\boldsymbol{\xi};t) \end{Bmatrix} \begin{matrix} \text{on} \quad \Gamma_\theta^- \times T, \\ \text{on} \quad \Gamma_q^- \times T, \end{matrix} \qquad \mathbf{f} \equiv \begin{Bmatrix} \bar{f}_\theta(\mathbf{x};t) \\ \bar{f}_q(\mathbf{x};t) \end{Bmatrix} \begin{matrix} \text{on} \quad \Gamma_\theta^- \times T, \\ \text{on} \quad \Gamma_q^- \times T, \end{matrix} \tag{3.9}$$

and $\mathbf{L}$ represents the linear integral operator:

$$\mathbf{L} \equiv \begin{bmatrix} \int\limits_{\Gamma_\theta} G_{\theta\theta} * [\cdot]\, d\boldsymbol{\xi} & -\int\limits_{\Gamma_q} G_{\theta q} * [\cdot]\, d\boldsymbol{\xi} \\ -\int\limits_{\Gamma_\theta} G_{q\theta} * [\cdot]\, d\boldsymbol{\xi} & \int\limits_{\Gamma_q} G_{qq} * [\cdot]\, d\boldsymbol{\xi} \end{bmatrix} \begin{matrix} \text{on} \quad \Gamma_\theta^- \times T, \\ \text{on} \quad \Gamma_q^- \times T. \end{matrix} \tag{3.10}$$

http://rcin.org.pl

A bilinear form over $\Gamma \times T$, *convolutive in time*, is defined as follows, $\mathbf{y}$ and $\mathbf{y}^*$ being two functions over $\Gamma \times T$ (superscript T denoting transpose):

$$(3.11) \qquad < \mathbf{y}, \mathbf{y}^* > \equiv \int_{\Gamma} \int_{0}^{\bar{t}} \mathbf{y}^T(\mathbf{x}; \bar{t} - t)\, \mathbf{y}^*(\mathbf{x}; t)\, d\mathbf{x}\, dt.$$

With reference to this notion, the two theorems stated below have been established in [16].

PROPOSITION 1. The integral operator $\mathbf{L}$, Eq. (3.10), of the governing boundary equations (3.8) is symmetric with respect to the bilinear form (3.11) convolutive in time; namely, the following equality holds for any vector of functions defined on $\Gamma \times T$ according to Eq. $(3.9)_1$:

$$(3.12) \qquad < \mathbf{Ly}, \mathbf{y}^* > = < \mathbf{Ly}^*, \mathbf{y} > \qquad \forall \quad \mathbf{y}, \mathbf{y}^*.$$

PROPOSITION 2. The time histories of boundary fields [flux $q(\mathbf{x}; t)$ on $\Gamma_\theta \times T$ and temperature $\theta(\mathbf{x}; t)$ on $\Gamma_q \times T$] which solve the diffusion problem in the direct boundary formulation (3.4)–(3.5), are characterized (as a sufficient and necessary condition) by the stationarity of the quadratic functional:

$$\begin{aligned}
(3.13) \qquad F(q(\mathbf{x}; t), \theta(\mathbf{x}; t)) \equiv{}& \frac{1}{2} < \mathbf{Ly}, \mathbf{y} > - < \mathbf{f}, \mathbf{y} > \\
={}& \frac{1}{2} \int_0^{\bar{t}} \int_{\Gamma_\theta} q(\mathbf{x}; \bar{t} - t) \int_0^{t} \int_{\Gamma_\theta} G_{\theta\theta}(\mathbf{x}, \boldsymbol{\xi}; t - \tau)\, q(\boldsymbol{\xi}; \tau)\, d\boldsymbol{\xi}\, d\tau\, d\mathbf{x}\, dt \\
&- \frac{1}{2} \int_0^{\bar{t}} \int_{\Gamma_\theta} q(\mathbf{x}; \bar{t} - t) \int_0^{t} \int_{\Gamma_q} G_{\theta q}(\mathbf{x}, \boldsymbol{\xi}; t - \tau)\, \theta(\boldsymbol{\xi}; \tau)\, d\boldsymbol{\xi}\, d\tau\, d\mathbf{x}\, dt \\
&- \frac{1}{2} \int_0^{\bar{t}} \int_{\Gamma_q} \theta(\mathbf{x}; \bar{t} - t) \int_0^{t} \int_{\Gamma_\theta} G_{q\theta}(\mathbf{x}, \boldsymbol{\xi}; t - \tau)\, q(\boldsymbol{\xi}; \tau)\, d\boldsymbol{\xi}\, d\tau\, d\mathbf{x}\, dt \\
&+ \frac{1}{2} \int_0^{\bar{t}} \int_{\Gamma_q} \theta(\mathbf{x}; \bar{t} - t) \int_0^{t} \int_{\Gamma_q} G_{qq}(\mathbf{x}, \boldsymbol{\xi}; t - \tau)\, \theta(\boldsymbol{\xi}; \tau)\, d\boldsymbol{\xi}\, d\tau\, d\mathbf{x}\, dt \\
&- \int_0^{\bar{t}} \int_{\Gamma_\theta} q(\mathbf{x}; \bar{t} - t) \bar{f}_\theta(\mathbf{x}; t)\, d\mathbf{x}\, dt - \int_0^{\bar{t}} \int_{\Gamma_q} \theta(\mathbf{x}; \bar{t} - t)\, \bar{f}_q(\mathbf{x}; t)\, d\mathbf{x}\, dt.
\end{aligned}$$

REMARKS

A. The above boundary statements have been established in [17], starting from earlier work by GURTIN [21] and TONTI [22] on variational principles for linear

http://rcin.org.pl

non-self-adjoint operators. The proof of Proposition 1 is based on the reciprocity properties (2.14)–(2.16) and the time-convolutive nature of the bilinear form (3.11). This proof is relegated to Appendix C. Proposition 2 follows from Proposition 1 through a customery path of reasoning which is outlined below. Through differentiation, and using the above symmetry (3.12), we may write:

$$\delta F = < \mathbf{Ly}, \delta\mathbf{y} > - < \mathbf{f}, \delta\mathbf{y} > + \frac{1}{2} < \mathbf{L}\delta\mathbf{y}, \delta\mathbf{y} > . \tag{3.14}$$

The first variation in (3.14) can be rewritten as $\delta^{(1)}F = < \mathbf{Ly} - \mathbf{f}, \delta\mathbf{y} >$ and this shows that indeed, the circumstance $\delta^{(1)}F = 0$ for any $\delta\mathbf{y}$ is a sufficient and necessary condition for $\mathbf{Ly} = \mathbf{f}$, i.e. for solving problem (3.4) and (3.5) in the boundary unknowns θ, q over the time T.

B. The second variation in Eq. (3.14), i.e. $\delta^{(2)}F = \frac{1}{2} < \mathbf{L}\delta\mathbf{y}, \delta\mathbf{y} >$, is not in general a sign-definite quadratic form. Therefore, the variational property stated by Proposition 2 corresponds to a saddle-point, not to an extremum of functional F. However, the saddle-point for F cannot be proved to represent an extremum point of F with respect to q and θ, separately. This remark motivates our search for stronger statements which led to the results expounded in the next Section.

C. The discretization in space and time, resting on the variational basis provided in what precedes, has been preliminarily discussed in [17] and implemented in [34] (with numerical integrations in space and analytical in time). Possible correlation between time interval and typical element length might be required in order to ensure the desired computational futures (primarily algorithmic stability). Issues of this kind, however, are beyond our present purposes.

4. Symmetry with respect to a bilinear form and a saddle-point theorem with variable separation

4.1. A further bilinear form and relevant variational theorem

Let $W(s)$ indicate an assigned function of the Laplace transform parameter s (interpreted as time). This "weight function" will be suitably chosen later within a broad class of alternatives, under the condition expressed below in (4.4), that it should be nonnegative everywhere, and not identically zero.

Taking over a concept put forward and used by RAFALSKI [23, 24] and REISS and HAUG [25] in linear initial-value problems, we introduce the following new bilinear form, denoted by the symbol $\ll \cdot, \cdot \gg$ involving the Laplace transforms of boundary field histories ($\mathbf{y}$ and $\mathbf{y}^*$) and defined over $\Gamma \times T_\infty$, denoting by T_∞ an unbounded from above time interval, namely $0 \leq t < \infty$:

$$\ll \mathbf{y}, \mathbf{y}^* \gg \equiv \int_\Gamma \int_0^\infty W(s)\,[\mathcal{L}(\mathbf{y}(\mathbf{x}; t), s)\mathcal{L}(\mathbf{y}^*(\mathbf{x}; \tau), s)]\, ds\, d\mathbf{x} \tag{4.1}$$

http://rcin.org.pl

or, more concisely:

$$\ll \mathbf{y}, \mathbf{y}^* \gg \equiv \int_\Gamma \int_0^\infty \int_0^\infty g(t+\tau)\mathbf{y}(\mathbf{x};t)\mathbf{y}^*(\mathbf{x};\tau)\, dt\, d\tau\, d\mathbf{x} \tag{4.2}$$

having set:

$$g(t+\tau) \equiv \int_0^\infty W(s) e^{-(t+\tau)s}\, ds \tag{4.3}$$

under the conditions:

$$W(s) \geq 0, \qquad W(s) \not\equiv 0. \tag{4.4}$$

On the basis of the new bilinear form (4.1) or (4.2), two further properties are stated below, as Propositions 3 and 4, which parallel Propositions 1 and 2, respectively.

PROPOSITION 3. The linear boundary operator **L**, Eq. (3.10), is symmetric with respect to the bilinear form (4.2); namely, the following equality holds for any pair of functions **y** and **y*** defined by Eq. $(3.9)_1$ over the time-unbounded set $\Gamma \times T_\infty$:

$$\ll \mathbf{L}\mathbf{y}, \mathbf{y}^* \gg = \ll \mathbf{L}\mathbf{y}^*, \mathbf{y} \gg, \qquad \forall \mathbf{y}, \mathbf{y}^*. \tag{4.5}$$

PROPOSITION 4. A time-history of flux $q(\mathbf{x};t)$ on Γ_θ and temperature $\theta(\mathbf{x};t)$ on Γ_q, both defined over the unbounded time interval T_∞, represent the actual boundary response of the body to the external input, if and only if they make the following quadratic functional stationary:

$$\begin{aligned} F^*(q(\mathbf{x};t), \theta(\mathbf{x};t)) \equiv \frac{1}{2} \ll \mathbf{L}\mathbf{y}, \mathbf{y} \gg - \ll \mathbf{f}, \mathbf{y} \gg \\ = \frac{1}{2} \int_{\Gamma_\theta} \int_0^\infty \int_0^\infty g(t+\eta) q(\mathbf{x};\eta) \int_{\Gamma_\theta} G_{\theta\theta}(\mathbf{x}, \boldsymbol{\xi}; t) * q(\boldsymbol{\xi}; t)\, dt\, d\eta\, d\boldsymbol{\xi}\, d\mathbf{x} \\ - \frac{1}{2} \int_{\Gamma_\theta} \int_0^\infty \int_0^\infty g(t+\eta) q(\mathbf{x};\eta) \int_{\Gamma_q} G_{\theta q}(\mathbf{x}, \boldsymbol{\xi}; t) * \theta(\boldsymbol{\xi}; t)\, dt\, d\eta\, d\boldsymbol{\xi}\, d\mathbf{x} \\ - \frac{1}{2} \int_{\Gamma_q} \int_0^\infty \int_0^\infty g(t+\eta) \theta(\mathbf{x};\eta) \int_{\Gamma_\theta} G_{q\theta}(\mathbf{x}, \boldsymbol{\xi}; t) * q(\boldsymbol{\xi}; t)\, dt\, d\eta\, d\boldsymbol{\xi}\, d\mathbf{x} \\ + \frac{1}{2} \int_{\Gamma_q} \int_0^\infty \int_0^\infty g(t+\eta) \theta(\mathbf{x};\eta) \int_{\Gamma_q} G_{qq}(\mathbf{x}, \boldsymbol{\xi}; t) * \theta(\boldsymbol{\xi}; t)\, dt\, d\eta\, d\boldsymbol{\xi}\, d\mathbf{x} \end{aligned} \tag{4.6}$$

http://rcin.org.pl

(4.6) [cont.]

$$- \int_{\Gamma_\theta} \int_0^\infty \int_0^\infty g(t+\eta) \bar{f}_\theta(\mathbf{x}; t) q(\mathbf{x}; \eta)\, dt\, d\eta\, d\mathbf{x}$$

$$- \int_{\Gamma_q} \int_0^\infty \int_0^\infty g(t+\eta) \bar{f}_q(\mathbf{x}; t) \theta(\mathbf{x}; \eta)\, dt\, d\eta\, d\mathbf{x}.$$

Our formal proof of Proposition 3, still resting on the reciprocity relationships (2.14)–(2.16), implies rather lengthy manipulations and, hence, is confined to Appendix D. Proposition 4 is a straightforward consequence of Proposition 3, through the same familiar argument which led from Propositions 1 to 2 and, hence, its proof will not be duplicated here. The present task, pursued below, is to strengthen Proposition 4 into a stronger statement, a purpose which was not possible to achieve for Proposition 2.

4.2. A saddle-point theorem, extremum for flux and temperature, separately

The two quadratic forms, one in flux q and the other in temperature θ, contained in functional F, Eq. (3.13), turn out to be not defined in sign in general. On the contrary, the two quadratic forms in functional F^*, Eq. (4.6), which represent the counterparts to those in Eq. (3.13), do exhibit sign-definiteness as shown below.

PROPOSITION 5. The following sign-definiteness properties hold for the quadratic forms associated with Green functions $G_{\theta\theta}$ and G_{qq}, respectively, in functional F^*:

$$\int_{\Gamma_\theta} \int_0^\infty \int_0^\infty g(t+\eta) q(\mathbf{x}; \eta) \int_{\Gamma_\theta} \int_0^t G_{\theta\theta}(\mathbf{x}, \boldsymbol{\xi}; t-\tau)\, q(\boldsymbol{\xi}; \tau)\, d\tau\, d\boldsymbol{\xi}\, d\eta\, dt\, d\mathbf{x} > 0, \quad \forall q \not\equiv 0, \tag{4.7}$$

$$\int_{\Gamma_q} \int_0^\infty \int_0^\infty g(t+\eta) \theta(\mathbf{x}; \eta) \int_{\Gamma_q} \int_0^t G_{qq}(\mathbf{x}, \boldsymbol{\xi}; t-\tau)\, \theta(\boldsymbol{\xi}; \tau)\, d\tau\, d\boldsymbol{\xi}\, d\eta\, dt\, d\mathbf{x} \leq 0, \quad \forall \theta. \tag{4.8}$$

The latter inequality can be strengthened into a strict inequality ($< 0, \forall\, \theta \not\equiv 0$, i.e. negative definiteness instead of semi-definiteness), if Γ_q splits Ω_∞ into disjoint parts.

P r o o f. Using Eq. (4.3) and the Laplace transform

$$\mathcal{L}(\mathbf{y}(t), s) \equiv \int_0^\infty e^{-st} \mathbf{y}(t)\, dt, \tag{4.9}$$

http://rcin.org.pl

the quadratic form (4.7) can be given the following alternative expression:

$$\int_{\Gamma_\theta}\int_{\Gamma_\theta}\int_{0}^{\infty} W(s)\mathcal{L}(q(\mathbf{x};t),s)\mathcal{L}(G_{\theta\theta}(\mathbf{x},\boldsymbol{\xi};t),s)\mathcal{L}(q(\boldsymbol{\xi};t),s)\,ds\,d\mathbf{x}\,d\boldsymbol{\xi}. \tag{4.10}$$

Let us combine the expression in (4.10), with the positive definiteness property (2.17) of kernel $G_{\theta\theta}$, and with the assumed nonnegativeness of $W(s)$. This straightforwardly leads to the desired conclusion (4.7).

A proof of property (4.8) follows the same path of reasoning starting from kernel property (2.18) and, hence, is omitted here for brevity.

PROPOSITION 6. (Saddle-point theorem) Let $\hat{q}(\mathbf{x};t)$ over $\Gamma_\theta \times T_\infty$ and $\hat{\theta}(\mathbf{x};t)$ over $\Gamma_q \times T_\infty$ represent the boundary solution of the diffusion problem in its integral formulation (3.4)–(3.5), and let the uncapped symbols denote any pair of fields (flux q and temperature θ) defined there. Then the following inequalities hold:

$$F^*(\hat{q},\theta) \le F^*\left(\hat{q},\hat{\theta}\right) \le F^*\left(q,\hat{\theta}\right), \tag{4.11}$$

where the equality signs hold if and only if $q = \hat{q}$ and $\theta = \hat{\theta}$.

P r o o f. Compute the varied functional F^*, Eq. (4.6), after a perturbation $\delta\hat{\theta}$, $\delta\hat{q}$ around the solution and gather the first-order and second-order terms in $\delta^{(1)}F^*$ and $\delta^{(2)}F^*$, respectively. The addend $\delta^{(1)}F^*$ which contains the first-order terms vanishes because of the variational property Proposition 4. As for $\delta^{(2)}F^*$ which collects the second-order terms we notice that setting $\delta\hat{q} = 0$, this addend is negative for any $\delta\hat{\theta} \neq 0$ by virtue of Eq. (4.8). This justifies the former of inequalities (4.11) for infinitesimal perturbations around the solution (i.e. *in the small*). However, in view of the quadratic nature of the functional, the inequality must be fulfilled also *in the large*. The latter inequality (4.11) is achieved by similar argumentation setting $\delta\hat{\theta} = 0$ and making use of Eq. (4.7).

5. Coupling

Let the domain Ω be subdivided into two disjoint complementary open subdomains Ω^F and Ω^B, separated by interface Γ^C (so that $\Gamma^C = \bar{\Omega}^F \cap \bar{\Omega}^B$, denoting by bars that boundaries are included). The present purpose is to establish a unified variational basis for approximate solutions of the initial-boundary-value problem in point by means of two discretization procedures simultaneously, namely by a finite element method in Ω^F and a symmetric Galerkin boundary element method in Ω^B. To this coupling (or "multifield modelling") purpose, we rewrite below, suitably adjusted, two "strong" formulations of the transient heat conduction problem over Ω^F and Ω^B.

http://rcin.org.pl

For the former subdomain Ω^F let the problem be formulated in terms of partial derivative equations and boundary conditions. Denoting by Γ_q^F and Γ_θ^F the Neumann and Dirichlet boundary, respectively, and being understood that all equations hold over the unbounded time interval T_∞, the initial-boundary value problem, after the domain decomposition in point, can be formulated as follows.

$$-\frac{\partial q_i^F}{\partial x_i} + Q^F = \gamma\varrho\frac{\partial \theta^F}{\partial t} \qquad \text{in } \Omega^F, \tag{5.1}$$

$$q_i^F = kp_i^F \qquad \text{in } \Omega^F, \tag{5.2}$$

$$p_i^F = -\frac{\partial \theta^F}{\partial x_i} \qquad \text{in } \Omega^F, \tag{5.3}$$

$$n_i q_i^F = \tilde{q}^F \qquad \text{on } \Gamma_q^F, \tag{5.4}$$

$$\theta^F = \tilde{\theta}^F \qquad \text{on } \Gamma_\theta^F, \tag{5.5}$$

$$\theta^F(\mathbf{x}, 0) = \tilde{\theta}_0^F \qquad \text{in } \bar{\Omega}^F. \tag{5.6}$$

For the latter subdomain Ω^B let the same problem be governed by the boundary integral equations of the symmetric kind developed in Secs. 2 and 3. These are rewritten below by referring to points $\mathbf{x} \in \Gamma$ (no longer Γ^-) and, therefore, by making explicit certain consequences of the singularities in the integrands. In fact, integrals concerning the strongly singular kernels $G_{\theta q}$ and $G_{q\theta}$, give rise to Cauchy principal parts (marked by $\neg$ in what follows) and "free terms". Similarly, integrals involving the hypersingular kernel G_{qq} lead to Hadamard finite parts (marked by $=$) and "free terms". In the above free terms the coefficient, say β, depends on the geometry of surface Γ in a neighbourhood of field point $\mathbf{x}$ with $\beta = 1/2$ in smooth points as assumed herein.

For $\mathbf{x} \in \Gamma_\theta^B$

$$\int_{\Gamma_\theta^B} G_{\theta\theta}(\mathbf{x}, \boldsymbol{\xi}; t) * q^B(\boldsymbol{\xi}; t)\, d\boldsymbol{\xi} + \int_{\Gamma^C} G_{\theta\theta}(\mathbf{x}, \boldsymbol{\xi}; t) * q^C(\boldsymbol{\xi}; t)\, d\boldsymbol{\xi} - \neg\int_{\Gamma_q^B} G_{\theta q}(\mathbf{x}, \boldsymbol{\xi}; \boldsymbol{\nu}; t) * \theta^B(\boldsymbol{\xi}; t)\, d\boldsymbol{\xi} - \neg\int_{\Gamma^C} G_{\theta q}(\mathbf{x}, \boldsymbol{\xi}; \boldsymbol{\nu}; t) * \theta^C(\boldsymbol{\xi}; t)\, d\boldsymbol{\xi} = \tilde{f}_\theta^B, \tag{5.7}$$

for $\mathbf{x} \in \Gamma_q^B$

$$-\neg\int_{\Gamma_\theta^B} G_{q\theta}(\mathbf{x}, \boldsymbol{\xi}; \mathbf{n}; t) * q^B(\boldsymbol{\xi}; t)\, d\boldsymbol{\xi} - \neg\int_{\Gamma^C} G_{q\theta}(\mathbf{x}, \boldsymbol{\xi}; \mathbf{n}; t) * q^C(\boldsymbol{\xi}; t)\, d\boldsymbol{\xi} + =\int_{\Gamma_q^B} G_{qq}(\mathbf{x}, \boldsymbol{\xi}; \mathbf{n}, \boldsymbol{\nu}; t) * \theta^B(\boldsymbol{\xi}; t)\, d\boldsymbol{\xi} + =\int_{\Gamma^C} G_{qq}(\mathbf{x}, \boldsymbol{\xi}; \mathbf{n}, \boldsymbol{\nu}; t) * \theta^C(\boldsymbol{\xi}; t)\, d\boldsymbol{\xi} = \tilde{f}_q^B, \tag{5.8}$$

http://rcin.org.pl

for $\mathbf{x} \in \Gamma^C$

$$(5.9)\qquad \int_{\Gamma_\theta^B} G_{\theta\theta}(\mathbf{x},\boldsymbol{\xi};t) * q^B(\boldsymbol{\xi};t)\, d\boldsymbol{\xi} + \int_{\Gamma^C} G_{\theta\theta}(\mathbf{x},\boldsymbol{\xi};t) * q^C(\boldsymbol{\xi};t)\, d\boldsymbol{\xi}$$
$$- \int_{\Gamma_q^B} G_{\theta q}(\mathbf{x},\boldsymbol{\xi};\boldsymbol{\nu};t) * \theta^B(\boldsymbol{\xi};t)\, d\boldsymbol{\xi} - \int_{\Gamma^C} G_{\theta q}(\mathbf{x},\boldsymbol{\xi};\boldsymbol{\nu};t) * \theta^C(\boldsymbol{\xi};t)\, d\boldsymbol{\xi} + \frac{1}{2}\theta^C = \bar{f}_\theta^C,$$

for $\mathbf{x} \in \Gamma^C$

$$(5.10)\qquad -\int_{\Gamma_\theta^B} G_{q\theta}(\mathbf{x},\boldsymbol{\xi};\mathbf{n};t) * q^B(\boldsymbol{\xi};t)\, d\boldsymbol{\xi} - \int_{\Gamma^C} G_{q\theta}(\mathbf{x},\boldsymbol{\xi};\mathbf{n};t) * q^C(\boldsymbol{\xi};t)\, d\boldsymbol{\xi}$$
$$+ \int_{\Gamma_q^B} G_{qq}(\mathbf{x},\boldsymbol{\xi};\mathbf{n},\boldsymbol{\nu};t) * \theta^B(\boldsymbol{\xi};t)\, d\boldsymbol{\xi} + \int_{\Gamma^C} G_{qq}(\mathbf{x},\boldsymbol{\xi};\mathbf{n},\boldsymbol{\nu};t) * \theta^C(\boldsymbol{\xi};t)\, d\boldsymbol{\xi} - \frac{1}{2}q^C = \bar{f}_q^C.$$

On the interface between the two subdomains, the continuity conditions concern flux and temperature, namely:

$$(5.11)\qquad n_i q_i^F + q^C = 0 \qquad \text{on } \Gamma^C,$$

$$(5.12)\qquad \theta^F - \theta^C = 0 \qquad \text{on } \Gamma^C.$$

In the BIEs, Eqs. (5.7), (5.8), (5.9) and (5.10), the terms containing data only are, respectively:

$$(5.13)\qquad \bar{f}_\theta^B = -\frac{1}{2}\bar{\theta}^B(\mathbf{x};t) - \int_{\Gamma_q^B} G_{\theta\theta}(\mathbf{x},\boldsymbol{\xi};t) * \bar{q}^B(\boldsymbol{\xi};t)\, d\boldsymbol{\xi}$$
$$+ \int_{\Gamma_\theta^B} G_{\theta q}(\mathbf{x},\boldsymbol{\xi};\boldsymbol{\nu};t) * \bar{\theta}^B(\boldsymbol{\xi};t)\, d\boldsymbol{\xi} + \int_{\Omega^B} G_{\theta\theta}(\mathbf{x},\boldsymbol{\xi};t) * Q^B(\boldsymbol{\xi};t)\, d\boldsymbol{\xi}$$
$$+ \gamma\varrho \int_{\Omega^B} G_{\theta\theta}(\mathbf{x},\boldsymbol{\xi};t)\, \bar{\theta}_0^B(\boldsymbol{\xi})\, d\boldsymbol{\xi},$$

$$(5.14)\qquad \bar{f}_q^B = \frac{1}{2}\bar{q}^B(\mathbf{x};t) + \int_{\Gamma_q^B} G_{q\theta}(\mathbf{x},\boldsymbol{\xi};\mathbf{n};t) * \bar{q}^B(\boldsymbol{\xi};t)\, d\boldsymbol{\xi}$$
$$- \int_{\Gamma_\theta^B} G_{qq}(\mathbf{x},\boldsymbol{\xi};\mathbf{n},\boldsymbol{\nu};t) * \bar{\theta}^B(\boldsymbol{\xi};t)\, d\boldsymbol{\xi} - \int_{\Omega^B} G_{q\theta}(\mathbf{x},\boldsymbol{\xi};\mathbf{n};t) * Q^B(\boldsymbol{\xi};t)\, d\boldsymbol{\xi}$$
$$- \gamma\varrho \int_{\Omega^B} G_{q\theta}(\mathbf{x},\boldsymbol{\xi};\mathbf{n};t)\, \bar{\theta}_0^B(\boldsymbol{\xi})\, d\boldsymbol{\xi},$$

http://rcin.org.pl

$$\bar{f}_\theta^C = -\int_{\Gamma_q^B} G_{\theta\theta}(\mathbf{x},\boldsymbol{\xi};t) * \bar{q}^B(\boldsymbol{\xi};t)\, d\boldsymbol{\xi} + \oint_{\Gamma_\theta^B} G_{\theta q}(\mathbf{x},\boldsymbol{\xi};\boldsymbol{\nu};t) * \bar{\theta}^B(\boldsymbol{\xi};t)\, d\boldsymbol{\xi} + \int_{\Omega^B} G_{\theta\theta}(\mathbf{x},\boldsymbol{\xi};t) * Q^B(\boldsymbol{\xi};t)\, d\boldsymbol{\xi} + \gamma\varrho \int_{\Omega^B} G_{\theta\theta}(\mathbf{x},\boldsymbol{\xi};t)\,\bar{\theta}_0^B(\boldsymbol{\xi})\, d\boldsymbol{\xi}, \tag{5.15}$$

$$\bar{f}_q^C = \oint_{\Gamma_q^B} G_{q\theta}(\mathbf{x},\boldsymbol{\xi};\mathbf{n};t) * \bar{q}^B(\boldsymbol{\xi};t)\, d\boldsymbol{\xi} - \oint\!\!\!\!\!\!= _{\Gamma_\theta^B} G_{qq}(\mathbf{x},\boldsymbol{\xi};\mathbf{n},\boldsymbol{\nu};t) * \bar{\theta}^B(\boldsymbol{\xi};t)\, d\boldsymbol{\xi} - \oint_{\Omega^B} G_{q\theta}(\mathbf{x},\boldsymbol{\xi};\mathbf{n};t) * Q^B(\boldsymbol{\xi};t)\, d\boldsymbol{\xi} - \gamma\varrho \oint_{\Omega^B} G_{q\theta}(\mathbf{x},\boldsymbol{\xi};\mathbf{n};t)\,\bar{\theta}_0^B(\boldsymbol{\xi})\, d\boldsymbol{\xi}. \tag{5.16}$$

The equations (5.1)–(5.3) concerning Ω^F, Eqs. (5.4), (5.5) concerning its boundary not in common with Ω^B and the initial conditions (5.6) can be given, respectively, the following compact operatorial formulations (in matrix notation):

$$\begin{bmatrix} -k & 1 & 0 \\ 1 & 0 & \partial(\cdot)/\partial x_i \\ 0 & -\partial(\cdot)/\partial x_i & -\gamma\varrho(\partial(\cdot)/\partial t) \end{bmatrix} \begin{bmatrix} p_i^F \\ q_i^F \\ \theta^F \end{bmatrix} = \begin{bmatrix} 0 \\ 0 \\ -Q^F \end{bmatrix} \to \mathbf{N}_1\mathbf{y}_1 = \mathbf{h}_1, \tag{5.17}$$

$$\begin{bmatrix} 0 & -n_i \\ n_i & 0 \end{bmatrix} \begin{bmatrix} q_i^F \\ \theta^F \end{bmatrix} = \begin{bmatrix} -n_i\bar{\theta} \\ \bar{q} \end{bmatrix} \begin{matrix} \text{on } \Gamma_\theta^F \\ \text{on } \Gamma_q^F \end{matrix} \to \mathbf{N}_2\mathbf{y}_2 = \mathbf{h}_2, \tag{5.18}$$

$$-\gamma\varrho\,\theta^F(\mathbf{x},0) = -\gamma\varrho\,\bar{\theta}_0^F \quad \text{on } \bar{\Omega}^F \text{ for } t = 0 \to N_3 y_3 = h_3. \tag{5.19}$$

Similarly the BIE's (5.7)–(5.10) which concern Ω^B and its boundary will be expressed in the more compact forms:

$$\begin{bmatrix} \int_{\Gamma^C} G_{\theta\theta} * [\cdot]\, d\boldsymbol{\xi} & -\oint_{\Gamma^C} G_{\theta q} * [\cdot]\, d\boldsymbol{\xi} + 1/2 & \int_{\Gamma_\theta^B} G_{\theta\theta} * [\cdot]\, d\boldsymbol{\xi} & -\oint_{\Gamma_q^B} G_{\theta q} * [\cdot]\, d\boldsymbol{\xi} \\ -\oint_{\Gamma^C} G_{q\theta} * [\cdot]\, d\boldsymbol{\xi} - 1/2 & \oint\!\!\!\!\!\!= _{\Gamma^C} G_{qq} * [\cdot]\, d\boldsymbol{\xi} & -\oint_{\Gamma_\theta^B} G_{q\theta} * [\cdot]\, d\boldsymbol{\xi} & + \oint\!\!\!\!\!\!= _{\Gamma_q^B} G_{qq} * [\cdot]\, d\boldsymbol{\xi} \\ \int_{\Gamma^C} G_{\theta\theta} * [\cdot]\, d\boldsymbol{\xi} & -\oint_{\Gamma^C} G_{\theta q} * [\cdot]\, d\boldsymbol{\xi} & \int_{\Gamma_\theta^B} G_{\theta\theta} * [\cdot]\, d\boldsymbol{\xi} & -\oint_{\Gamma_q^B} G_{\theta q} * [\cdot]\, d\boldsymbol{\xi} \\ -\oint_{\Gamma^C} G_{q\theta} * [\cdot]\, d\boldsymbol{\xi} & \oint\!\!\!\!\!\!= _{\Gamma^C} G_{qq} * [\cdot]\, d\boldsymbol{\xi} & -\oint_{\Gamma_\theta^B} G_{q\theta} * [\cdot]\, d\boldsymbol{\xi} & + \oint\!\!\!\!\!\!= _{\Gamma_q^B} G_{qq} * [\cdot]\, d\boldsymbol{\xi} \end{bmatrix} \begin{bmatrix} q^C \\ \theta^C \\ q^B \\ \theta^B \end{bmatrix} = \begin{bmatrix} \bar{f}_\theta^C \\ \bar{f}_q^C \\ \bar{f}_\theta^B \\ \bar{f}_q^B \end{bmatrix} \begin{matrix} \text{on } \Gamma^C \\ \text{on } \Gamma^C \\ \text{on } \Gamma_\theta^B \\ \text{on } \Gamma_q^B \end{matrix} \to \mathbf{N}_4\mathbf{y}_4 = \mathbf{h}_4. \tag{5.20}$$

http://rcin.org.pl

Finally, the interface conditions on Γ^C Eq. (5.11) and (5.12) are rewritten (two times) for convenience as follows.

$$\frac{1}{2}\begin{bmatrix} 0 & -n_i & 0 & n_i \\ n_i & 0 & 1 & 0 \\ 0 & 1 & 0 & -1 \\ n_i & 0 & 1 & 0 \end{bmatrix}\begin{bmatrix} q_i^F \\ \theta^F \\ q^C \\ \theta^C \end{bmatrix} = \begin{bmatrix} 0 \\ 0 \\ 0 \\ 0 \end{bmatrix} \rightarrow \mathbf{N}_5\mathbf{y}_5 = \mathbf{h}_5 . \tag{5.21}$$

Consistently with the above adopted compact notation, let us gather the (scalar) variables in the vector $\mathbf{y}^T = \left[p_i^F, q_i^F, \theta^F, q^C, \theta^C, q^B, \theta^B\right]$ (superscript T denoting transpose), the data in vector

$$\mathbf{h}^T = \left[\mathbf{h}_1^T, \mathbf{h}_2^T, h_3, \mathbf{h}_4^T, \mathbf{h}_5^T\right] = \left[0, 0, -Q^F, -n_i\bar{\theta}, \bar{q}, -\gamma\varrho\bar{\theta}_0^F, \bar{f}_\theta^C, \bar{f}_q^C, \bar{f}_\theta^B, \bar{f}_q^B, 0, 0, 0, 0\right]$$

and the operators into the matrix

$$\mathbf{N} \equiv \begin{bmatrix} \overline{\mathbf{N}}_1 \\ \overline{\mathbf{N}}_2 \\ \overline{\mathbf{N}}_3 \\ \overline{\mathbf{N}}_4 \\ \overline{\mathbf{N}}_5 \end{bmatrix}, \tag{5.22}$$

where the barred symbols have the following meaning: $\overline{\mathbf{N}}_1 = [\mathbf{N}_1, \mathbf{0}, \mathbf{0}, \mathbf{0}, \mathbf{0}]$, $\overline{\mathbf{N}}_2 = [\mathbf{0}, \mathbf{N}_2, \mathbf{0}, \mathbf{0}, \mathbf{0}, \mathbf{0}]$, $\overline{\mathbf{N}}_3 = [0, 0, N_3, 0, 0, 0, 0]$, $\overline{\mathbf{N}}_4 = [\mathbf{0}, \mathbf{0}, \mathbf{0}, \mathbf{N}_4]$, $\overline{\mathbf{N}}_5 = [\mathbf{0}, \mathbf{N}_5, \mathbf{0}, \mathbf{0}]$. Now, denoting by $\mathbf{y}$ and $\mathbf{y}'$ two vectors of fields which belong to the domain of the above defined operator $\mathbf{N}$ ($\mathbf{y}, \mathbf{y}' \in \mathcal{D}(\mathbf{N})$), a bilinear form associated to this operator $\mathbf{N}$ can be generated as follows, according to the pattern adopted in Sec. 4, Eqs. (4.1) – (4.4), on the basis of operator $\mathbf{L}$:

$$\begin{aligned} \ll \mathbf{N}\mathbf{y}, \mathbf{y}' \gg &= \int_0^\infty \int_0^\infty g(t+\tau) \left\{ \int_{\Omega^F} [\mathbf{N}_1\mathbf{y}_1(t)]^T \mathbf{y}_1'(\tau)\, d\Omega + \int_{\Gamma^F} [\mathbf{N}_2\mathbf{y}_2(t)]^T \mathbf{y}_2'(\tau)\, d\tau \right. \\ &\quad \left. + \int_{\Gamma^B+\Gamma^C} [\mathbf{N}_4\mathbf{y}_4(t)]^T \mathbf{y}_4'(\tau)\, d\Gamma + \int_{\Gamma^C} [\mathbf{N}_5\mathbf{y}_5(t)]^T \mathbf{y}_5'(\tau)\, d\Gamma \right\} dt\, d\tau \\ &\quad + \int_0^\infty \int_{\Omega^F} g(\tau)\, [N_3 y_3(t)]\, y_3'(\tau)\, d\Omega\, d\tau. \end{aligned} \tag{5.23}$$

http://rcin.org.pl

In full analogy with Eq. (4.6), we construct the quadratic functional:

$$
\begin{aligned}
(5.24)\qquad \mathcal{F}\left(p_i^F, q_i^F, \theta^F, q^C, \theta^C, q^B, \theta^B\right) &= \frac{1}{2} \ll \mathbf{N}\mathbf{y}, \mathbf{y} \gg - \ll \mathbf{h}, \mathbf{y} \gg \\
&= \int_0^\infty \int_0^\infty g(t+\tau) \left[\frac{1}{2} \int_{\Omega^F} -\gamma \varrho \frac{\partial \theta^F(t)}{\partial t} \theta^F(\tau)\, d\Omega - \frac{1}{2} \int_{\Omega^F} \frac{\partial q_i^F}{\partial x_i}(t)\, \theta^F(\tau)\, d\Omega \right. \\
&\quad - \frac{1}{2} \int_{\Omega^F} k\, p_i^F(t)\, p_i^F(\tau)\, d\Omega + \int_{\Omega^F} q_i^F(t)\, p_i^F(\tau)\, d\Omega + \frac{1}{2} \int_{\Omega^F} \frac{\partial \theta^F}{\partial x_i}(t)\, q_i^F(\tau)\, d\Omega \\
&\quad - \frac{1}{2} \int_{\Gamma_\theta^F} n_i \theta^F(t)\, q_i^F(\tau)\, d\Gamma + \frac{1}{2} \int_{\Gamma_q^F} n_i q_i^F(t)\, \theta^F(\tau)\, d\Gamma + \int_{\Omega^F} Q^F(t)\, \theta^F(\tau)\, d\Omega \\
&\quad \left. + \int_{\Gamma_\theta^F} n_i \tilde{\theta}^F(t)\, q_i^F(\tau)\, d\Gamma - \int_{\Gamma_q^F} \tilde{q}(t)\, \theta^F(\tau)\, d\Gamma \right] dt\, d\tau \\
&\quad - \frac{1}{2} \int_0^\infty g(t) \int_{\Omega^F} \gamma \varrho\, \theta^F(t) \left(\theta^F(0) - 2\tilde{\theta}_0^F \right) d\Omega\, dt \\
&\quad + \int_0^\infty \int_0^\infty g(t+\tau) \left[\frac{1}{2} \int_{\Gamma^C} \int_{\Gamma^C} G_{\theta\theta} * q^C(t)\, q^C(\tau)\, d\boldsymbol{\xi}\, d\mathbf{x} \right. \\
&\quad - \frac{1}{2} \int_{\Gamma^C} \oint_{\Gamma^C} G_{\theta q} * \theta^C(t)\, q^C(\tau)\, d\boldsymbol{\xi}\, d\mathbf{x} + \frac{1}{2} \int_{\Gamma^C} \int_{\Gamma_\theta^B} G_{\theta\theta} * q^B(t)\, q^C(\tau)\, d\boldsymbol{\xi}\, d\mathbf{x} \\
&\quad - \frac{1}{2} \int_{\Gamma^C} \oint_{\Gamma_q^B} G_{\theta q} * \theta^B(t)\, q^C(\tau)\, d\boldsymbol{\xi}\, d\mathbf{x} - \frac{1}{2} \int_{\Gamma^C} \oint_{\Gamma^C} G_{q\theta} * q^C(t)\, \theta^C(\tau)\, d\boldsymbol{\xi}\, d\mathbf{x} \\
&\quad + \frac{1}{2} \oint_{\Gamma^C} \oint_{\Gamma^C} G_{qq} * \theta^C(t)\, \theta^C(\tau)\, d\boldsymbol{\xi}\, d\mathbf{x} - \frac{1}{2} \int_{\Gamma^C} \oint_{\Gamma_\theta^B} G_{q\theta} * q^B(t)\, \theta^C(\tau)\, d\boldsymbol{\xi}\, d\mathbf{x} \\
&\quad + \frac{1}{2} \oint_{\Gamma^C} \oint_{\Gamma_q^B} G_{qq} * \theta^B(t)\, \theta^C(\tau)\, d\boldsymbol{\xi}\, d\mathbf{x} + \frac{1}{2} \int_{\Gamma_\theta^B} \int_{\Gamma^C} G_{\theta\theta} * q^C(t)\, q^B(\tau)\, d\boldsymbol{\xi}\, d\mathbf{x} \\
&\quad - \frac{1}{2} \int_{\Gamma_\theta^B} \oint_{\Gamma^C} G_{\theta q} * \theta^C(t)\, q^B(\tau)\, d\boldsymbol{\xi}\, d\mathbf{x} + \frac{1}{2} \int_{\Gamma_\theta^B} \int_{\Gamma_\theta^B} G_{\theta\theta} * q^B(t)\, q^B(\tau)\, d\boldsymbol{\xi}\, d\mathbf{x} \\
&\quad - \frac{1}{2} \int_{\Gamma_\theta^B} \oint_{\Gamma_q^B} G_{\theta q} * \theta^B(t)\, q^B(\tau)\, d\boldsymbol{\xi}\, d\mathbf{x} - \frac{1}{2} \int_{\Gamma_q^B} \oint_{\Gamma^C} G_{q\theta} * q^C(t)\, \theta^B(\tau)\, d\boldsymbol{\xi}\, d\mathbf{x}
\end{aligned}
$$

http://rcin.org.pl

(5.24) [cont.]
$$+\frac{1}{2}\int_{\Gamma_q^B}\oint_{\Gamma^C} G_{qq} * \theta^C(t)\,\theta^B(\tau)\,d\boldsymbol{\xi}\,d\mathbf{x} - \frac{1}{2}\int_{\Gamma_q^B}\oint_{\Gamma_\theta^B} G_{q\theta} * q^B(t)\,\theta^B(\tau)\,d\boldsymbol{\xi}\,d\mathbf{x}$$
$$+\frac{1}{2}\int_{\Gamma_q^B}\oint_{\Gamma_q^B} G_{qq} * \theta^B(t)\,\theta^B(\tau)\,d\boldsymbol{\xi}\,d\mathbf{x} - \int_{\Gamma^C} \bar{f}_\theta^C(t)\,q^C(\tau)\,d\mathbf{x}$$
$$-\int_{\Gamma^C} \bar{f}_q^C(t)\,\theta^C(\tau)\,d\mathbf{x} - \int_{\Gamma_\theta^B} \bar{f}_\theta^B(t)\,q^B(\tau)\,d\mathbf{x} - \int_{\Gamma_q^B} \bar{f}_q^B(t)\,\theta^B(\tau)\,d\mathbf{x}\Bigg]\,dt\,d\tau$$
$$+\int_0^\infty\int_0^\infty g(t+\tau)\left[\frac{1}{2}\int_{\Gamma^C} n_i q_i^F(t)\,\theta^C(\tau)\,d\mathbf{x} + \frac{1}{2}\int_{\Gamma^C}\theta^F(t)\,q^C(\tau)\,d\mathbf{x}\right]dt\,d\tau.$$

At this stage, the following two statements can be formulated.

PROPOSITION 7. The operator **N**, Eq. (5.22), (which is both differential and boundary-integral), is symmetric with respect to the bilinear form (5.23).

PROPOSITION 8. In the body $\bar{\Omega}$ subdivided into subdomains $\bar{\Omega}^B$ and $\bar{\Omega}^F$, and over the unbounded time $0 \le t < \infty$, flux $q^B(\mathbf{x}, t)$ on Γ_θ^B and Γ^C, temperature $\theta^B(\mathbf{x}, t)$ on Γ_q^B and Γ^C, temperature $\theta^B(\mathbf{x}, t)$ in $\bar{\Omega}^F$, flux $q_i^F(\mathbf{x}, t)$ in $\bar{\Omega}^F$ and temperature gradient $p_i^F(\mathbf{x}, t)$ also in $\bar{\Omega}^F$ represent the actual response of the body to a given time history of external actions, if and only if they make stationary the above functional $\mathcal{F}$, Eq. (5.24).

The proof of statement 7 for the present coupled formulation can be given following a rather lengthy path of reasoning similar to that adopted in Sec. 4 and Appendix D and, hence, will not be expounded here for brevity. It is worth noting that the operator symmetry disrupted by the coefficient $1/2$ and $-1/2$ of the free terms in Eq. (5.20) is recovered in the operator of the coupled problem (if there is no interface Γ^C decomposing the domain Ω, those coefficients show up only in terms of data as seen in the preceding Sections).

REMARKS

A. In the expression (5.24) of the functional $\mathcal{F}$ the first addend, denoted henceforth by symbol A_1, contains the product of the temperature field θ^F and its time derivative, over the finite element subdomain $\bar{\Omega}^F$. It is easy and computationally useful to transform A_1 into the sum of two quadratic terms in θ^F alone. In fact we may write a sequence of alternative formulations for A_1:

(5.25)
$$A_1 = \frac{1}{2}\int_{\Omega^F}\int_0^\infty\int_0^\infty\int_0^\infty \gamma\varrho\, W(s)\, e^{-(t+\tau)s}\,\frac{\partial\theta^F(t)}{\partial t}\,\theta^F(\tau)\,ds\,dt\,d\tau\,d\Omega$$

http://rcin.org.pl

(5.25) [cont.]

$$= \frac{1}{2}\int_{\Omega^F} \gamma\varrho \int_0^\infty W(s) \int_0^\infty e^{-st}\,\frac{\partial\theta^F(t)}{\partial t}\,dt \int_0^\infty e^{-s\tau}\,\theta^F(\tau)\,d\tau\,ds\,d\Omega$$

$$= \frac{1}{2}\int_{\Omega^F} \gamma\varrho \int_0^\infty W(s)\left[-\theta^F(0) + s\int_0^\infty e^{-st}\,\theta^F(t)\,dt \int_0^\infty e^{-s\tau}\,\theta^F(\tau)\,d\tau\right] ds\,d\Omega$$

$$= \frac{1}{2}\int_0^\infty\int_0^\infty g^*(t+\tau)\int_{\Omega^F} \gamma\varrho\,\theta^F(t)\,\theta^F(\tau)\,d\Omega\,d\tau\,dt$$

$$+ \frac{1}{2}\int_0^\infty g(t)\int_{\Omega^F} \gamma\varrho\,\theta^F(t)\,\theta^F(0)\,d\Omega\,dt\,.$$

The first of the above expressions of A_1 has been achieved through Eq. (4.3), the second by rearranging the integrations, the third through an integration by parts over $0 \leq t \leq \infty$, the fourth by setting:

$$g^*(t+\tau) = \int_0^\infty s\,W(s)\,e^{-(t+\tau)s}\,ds. \tag{5.26}$$

B. The functional $\mathcal{F}$ defined by Eq. (5.24) is a multifield functional in the sense that over the subdomain $\bar{\Omega}^F$ it depends on temperature θ^F, its gradient $\partial\theta^F/\partial x_i$ and heat flux q_i^F, which represent independent unknowns on the subdomain Ω^F and, as such, can independently be modelled over Ω^F as a finite element discretization. Alternatively, Eqs. (5.2) and (5.3) can be *a priori* enforced, so that $\mathcal{F}$ reduces to a functional of temperature only over $\Omega^F \times T_\infty$, besides of temperature and flux on $\Gamma_q^B \times T_\infty$ and $\Gamma_\theta^B \times T_\infty$, respectively. The former case, (multifield functional $\mathcal{F}$) might be desirable in order to construct parametric variational principles with possible computational benefits, as pointed out by FELIPPA [35] in the context of the finite element methods.

C. Operator $\mathbf{N}$ for the coupled problem turns out to be symmetric also with respect to the bilinear form (3.11) convolutive in time i.e. $< \mathbf{N}\mathbf{y}, \mathbf{y}' > = < \mathbf{N}\mathbf{y}', \mathbf{y} >$, besides with respect to the new bilinear form (4.2)–(4.4), i.e. $\ll \mathbf{N}\mathbf{y}, \mathbf{y}' \gg = \ll \mathbf{N}\mathbf{y}', \mathbf{y} \gg$, as stated by Proposition 7.

6. Closing remarks

With reference to the transient heat conduction in a homogeneous body as a typical linear initial-boundary-value problem, what precedes presented the results outlined and commented below as conclusions.

(a) A formulation in terms of boundary integral equations, constructed by means of single and double layer sources, in such way that the boundary integral operator is symmetric with respect to a bilinear form convolutive in time

http://rcin.org.pl

over the boundary and a finite time interval. The reciprocity properties of the time-dependent Green functions for the thermally homogeneous space were crucial to establish this circumstance.

(**b**) A variational characterization, corresponding to a saddle point, for the solution of the boundary problem formulated over a bounded time T_∞ as outlined at (a).

(**c**) A further, different saddle point characterization of the boundary solution over the unbounded time interval T_∞, which is shown to represent a minimum with respect to the temperature and a maximum with respect to the flux, separately. This variational property and the variable separation in it have been achieved by generating another special bilinear form in the Laplace transforms of the boundary variable fields, and by using the sign-definiteness (proved in Appendix B) of the Laplace transforms of the two Green functions for temperature and heat flux due to discontinuities (concentrated in space and time) of flux and temperature, respectively.

(**d**) An extension of the variational theorem (c), preserving the variable separation, in order to cover cases where transient heat conduction is governed in a subdomain by the symmetric system of boundary (and now interface too) integral equations, and in the complementary subdomain by the original partial differential equations (Fourier and conservation laws) and the relevant mixed (Dirichlet and Neumann) boundary conditions. The computational potentialities and applications of the results expounded in this paper and summarized above, are regarded to be beyond the present purposes and will be discussed elsewhere. However, the following remarks may envisage possible developments towards the use of these results in numerical solution methods.

(**e**) The variational approach mentioned at (b) and developed in Sec. 3, by modelling in space and time (either simultaneously or separately) the boundary fields over a time interval T, leads to a boundary element algebraic linear equation system endowed with symmetric coefficient matrix (the same is attainable from result (a) by means of a Galerkin weighted-residual approximate enforcement of the integral equations). Both the computational benefits of such symmetry and the difficulties of the hypersingular integrals are fairly well understood in the recent BEM literature, though with reference to physically different problems, see e.g. [8, 9, 14, 15, 16, 30, 31, 32, 33].

(**f**) The boundary element discretization based on the saddle-point theorem derived in Sec. 4 and above mentioned at (c) preserves symmetry in the resulting algebraic equations and appears to be computationally promising for short-duration transient analysis, in view of the use of field modelling by means of shape functions with exponential, asymptotical decay in time, as pointed out in a forthcoming paper.

(**g**) The uselfulness, in terms of computing cost-effectiveness of large-size analyses, of multifields (or heterogeneous) models when approximating initial-boundary-value problems over complex domain, has been demonstrated by a

http://rcin.org.pl

growing literature in various contexts, see e.g. [36]. This fact motivates the variational approach (d) developed in Sec. 5 in view of a domain decomposition for BE-FE coupling motivated like in other contexts [26, 27, 28]. However, further work is required to assess the expected computational merits of result (d) from this standpoint (account taken of the present more stringent continuity requirements on the temperature field, compared to those in traditional BEMs). Another issue worth being pursued elsewhere concerns parametric variational principles in the sense of FELIPPA [35], which might be generated in the symmetric BE context, with possible computational advantages.

Appendix A

With reference to Sec. 2.3 on the properties of the time-dependent Green's functions for heat conduction in isotropic space Ω_∞, the statement given there on their singularities is corroborated here below by formal developments concerning kernel $G_{\theta\theta}$ alone for brevity. In two-dimensional situations ($d = 2$), Eq. (2.6) specializes to:

$$G_{\theta\theta} = \frac{1}{4\pi\alpha t} e^{-\frac{r^2}{4\alpha t}}. \tag{A.1}$$

The Laplace transform of kernel (A.1) reads:

$$\mathcal{L}(G_{\theta\theta}) = \frac{1}{2\pi\alpha} K_0\left(\frac{r\sqrt{s}}{\sqrt{\alpha}}\right). \tag{A.2}$$

Here s is the transformation paremeter, γ denotes Euler constant ($\gamma = 0.577...$) and K_0 represents the modified zero-order Bessel function, namely, z being its argument (see [37])

$$K_0(z) = -\left[\log\left(\frac{z}{2}\right) + \gamma\right] I_0(z) + \frac{\frac{1}{4}z^2}{(1!)^2} + \left(1 + \frac{1}{2}\right)\frac{\left(\frac{1}{4}z^2\right)^2}{(2!)^2} + \left(1 + \frac{1}{2} + \frac{1}{3}\right)\frac{\left(\frac{1}{4}z^2\right)^3}{(3!)^2} + \dots, \tag{A.3}$$

where

$$I_0(z) = 1 + \frac{\frac{1}{4}z^2}{(1!)^2} + \frac{\left(\frac{1}{4}z^2\right)^2}{(2!)^2} + \frac{\left(\frac{1}{4}z^2\right)^3}{(3!)^2} + \dots. \tag{A.4}$$

http://rcin.org.pl

From Eqs. (A.2) – (A.4) it turns out that the only singular term in $\mathcal{L}(G_{\theta\theta})$ is $\log r$:

$$\log\left(\frac{z}{2}\right) = \log\left(\sqrt{\frac{s}{4\alpha}}\right) + \log r. \tag{A.5}$$

In three-dimensional problems ($d = 3$), Eq. (2.6) becomes:

$$G_{\theta\theta} = \frac{1}{[4\pi\alpha t]^{3/2}} e^{-\frac{r^2}{4\alpha t}}. \tag{A.6}$$

The Laplace transform of kernel (A.6) reads:

$$\frac{2\sqrt{\alpha}}{(4\alpha)^{3/2}\pi}\left(\frac{1}{r}\right) e^{-\frac{r\sqrt{s}}{\sqrt{\alpha}}}, \tag{A.7}$$

where it can be noticed that the only singular factor is r^{-1}.

Appendix B. A proof of sign semi-definiteness for the Laplace transforms of kernels $G_{\theta\theta}$ and G_{qq}

If Laplace integral transform (4.9) is applied to both its sides, the diffusion equation (2.1) becomes (s denoting the transform parameter):

$$\alpha\nabla^2\mathcal{L}(\theta) = s\mathcal{L}(\theta) - \theta(\mathbf{x}, 0) - \frac{1}{\gamma\varrho}\mathcal{L}(Q). \tag{B.1}$$

On the boundary Γ, interpreted as a surface in the space Ω_∞, consider a distribution of temperature discontinuities $\Delta\theta = -\theta^+ + \theta^-$ and another one of heat flux jumps $\Delta q = -q^+ - q^-$, according to Eqs. $(2.11)_2$ and $(2.7)_2$, respectively. By virtue of the Gauss lemma and of equation (B.1) in the transform space, keeping in mind that the above sources are now the only external actions on Ω_∞, we write:

$$\begin{aligned}\int_{\Gamma^-} \mathcal{L}(\theta^-)\frac{\partial\mathcal{L}(\theta^-)}{\partial n}\,d\Gamma &= \int_{\Gamma^-} \mathcal{L}(\theta^-)\frac{\partial\mathcal{L}(\theta^-)}{\partial x_i}n_i^-\,d\Gamma \\ = \int_\Omega \frac{\partial\left(\mathcal{L}(\theta)\dfrac{\partial\mathcal{L}(\theta)}{\partial x_i}\right)}{\partial x_i}\,d\Omega &= \int_\Omega \frac{\partial\mathcal{L}(\theta)}{\partial x_i}\frac{\partial\mathcal{L}(\theta)}{\partial x_i}\,d\Omega + \int_\Omega \mathcal{L}(\theta)\frac{\partial^2\mathcal{L}(\theta)}{\partial x_i\partial x_i}\,d\Omega \\ &= \int_\Omega \frac{\partial\mathcal{L}(\theta)}{\partial x_i}\frac{\partial\mathcal{L}(\theta)}{\partial x_i}\,d\Omega + \frac{s}{\alpha}\int_\Omega \mathcal{L}(\theta)\mathcal{L}(\theta)\,d\Omega \geq 0.\end{aligned} \tag{B.2}$$

http://rcin.org.pl

Similarly, denoting by Ω^* the exterior domain, $\Omega^* = \Omega_\infty - (\Omega \cup \Gamma)$, we obtain an inequality over Γ^+:

$$\text{(B.3)} \qquad \int_{\Gamma^+} \mathcal{L}(\theta^+) \frac{\partial \mathcal{L}(\theta^+)}{\partial n} \, d\Gamma = - \int_{\Gamma^+} \mathcal{L}(\theta^+) \frac{\partial \mathcal{L}(\theta^+)}{\partial x_i} n_i^+ \, d\Gamma$$

$$= - \int_{\Omega^*} \frac{\partial \left(\mathcal{L}(\theta) \dfrac{\partial \mathcal{L}(\theta)}{\partial x_i} \right)}{\partial x_i} \, d\Omega$$

$$= - \int_{\Omega^*} \frac{\partial \mathcal{L}(\theta)}{\partial x_i} \frac{\partial \mathcal{L}(\theta)}{\partial x_i} \, d\Omega - \frac{s}{\alpha} \int_{\Omega^*} \mathcal{L}(\theta) \mathcal{L}(\theta) \, d\Omega \leq 0.$$

Fourier's law, $q_i = -k \dfrac{\partial \theta}{\partial x_i}$, formulated at $\mathbf{x}^+$ and $\mathbf{x}^-$ in the Laplace transform space with $k = 1$ and $\mathbf{n}^+ = -\mathbf{n} = -\mathbf{n}^-$, yields:

$$\text{(B.4)} \qquad \frac{\partial \mathcal{L}(\theta^-)}{\partial n} = -\mathcal{L}(q^-), \qquad \frac{\partial \mathcal{L}(\theta^+)}{\partial n} = \mathcal{L}(q^+).$$

By adding inequality (B.2) to inequality (B.3) reversed in sign and, subsequently, by using Eqs. (B.4), we obtain:

$$\text{(B.5)} \qquad - \int_{\Gamma^-} \mathcal{L}(\theta^-) \frac{\partial \mathcal{L}(\theta^-)}{\partial n} \, d\Gamma + \int_{\Gamma^+} \mathcal{L}(\theta^+) \frac{\partial \mathcal{L}(\theta^+)}{\partial n} \, d\Gamma$$

$$= \int_{\Gamma^-} \mathcal{L}(\theta^-) \mathcal{L}(q^-) \, d\Gamma + \int_{\Gamma^+} \mathcal{L}(\theta^+) \mathcal{L}(q^+) \, d\Gamma \leq 0.$$

Now, like in Sec. 3 for the symmetric BIE formulation, let the sources Δq be confined to the portion Γ_θ of Γ, the sources $\Delta\theta$ to Γ_q. In terms of their Laplace transforms this means that:

$$\text{(B.6)} \qquad \left. \begin{aligned} \mathcal{L}(\Delta q) &= -\mathcal{L}(q^+) - \mathcal{L}(q^-) \\ \mathcal{L}(\theta^+) &= \mathcal{L}(\theta^-) = \mathcal{L}(\theta) \end{aligned} \right\} \quad \text{on } \Gamma_\theta,$$

$$\text{(B.7)} \qquad \left. \begin{aligned} \mathcal{L}(\Delta\theta) &= -\mathcal{L}(\theta^+) + \mathcal{L}(\theta^-) \\ -\mathcal{L}(q^+) &= \mathcal{L}(q^-) = \mathcal{L}(q) \end{aligned} \right\} \quad \text{on } \Gamma_q.$$

As a consequence of Eqs. (B.6) and (B.7), the inequality (B.5) becomes:

$$\text{(B.8)} \qquad \int_{\Gamma_\theta^-} \mathcal{L}(\theta) \mathcal{L}(q^-) \, d\Gamma + \int_{\Gamma_\theta^+} \mathcal{L}(\theta) \mathcal{L}(q^+) \, d\Gamma + \int_{\Gamma_q^-} \mathcal{L}(\theta^-) \mathcal{L}(q) \, d\Gamma$$

$$- \int_{\Gamma_q^+} \mathcal{L}(\theta^+) \mathcal{L}(q) \, d\Gamma = - \int_{\Gamma_\theta} \mathcal{L}(\theta) \mathcal{L}(\Delta q) \, d\Gamma + \int_{\Gamma_q} \mathcal{L}(\Delta\theta) \mathcal{L}(q) \, d\Gamma \leq 0.$$

http://rcin.org.pl

In view of the definitions and mechanical interpretations of the Green functions $G_{\theta\theta}$ and G_{qq} in Sec. 2, Eq. (B.8) can be re-written in the form:

$$(B.9) \qquad -\int_{\Gamma_\theta}\int_{\Gamma_\theta} \mathcal{L}(\Delta q)\mathcal{L}\,(G_{\theta\theta})\,\mathcal{L}(\Delta q)\,d\Gamma\,d\Gamma + \int_{\Gamma_q}\int_{\Gamma_q} \mathcal{L}(\Delta\theta)\mathcal{L}\,(G_{qq})\,\mathcal{L}(\Delta\theta)\,d\Gamma\,d\Gamma \leq 0.$$

Since the source fields are arbitrary (so that $\mathcal{L}(\Delta q) \equiv 0$ and $\mathcal{L}(\Delta\theta) \equiv 0$ are feasible choices), Eq. (B.9) yields the two inequalities which embody the sign-semidefiniteness of the two kernels in Laplace transform space:

$$(B.10) \qquad \begin{aligned} &\int_{\Gamma_\theta}\int_{\Gamma_\theta} \mathcal{L}(\Delta q)\mathcal{L}\,(G_{\theta\theta})\,\mathcal{L}(\Delta q)\,d\Gamma\,d\Gamma \geq 0 \qquad \forall\,\Delta q, \\ &\int_{\Gamma_q}\int_{\Gamma_q} \mathcal{L}(\Delta\theta)\mathcal{L}\,(G_{qq})\,\mathcal{L}(\Delta\theta)\,d\Gamma\,d\Gamma \leq 0 \qquad \forall\,\Delta\theta \qquad \text{q. e. d.} \end{aligned}$$

Appendix C. A proof of the symmetry of the boundary integral operator with respect to a time-convolutive bilinear form over $\Gamma \times T$ (Proposition 1)

In order to prove Eq. (3.12), let us write the bilinear form (3.11), in terms of $\mathbf{y}$ according to Eq. $(3.9)_1$ and of $\mathbf{y}^*$ interpreted as the integral transform of another field $\mathbf{y}'$ through operator (3.10):

$$(C.1) \qquad \begin{aligned} &< \mathbf{L}\mathbf{y}, \mathbf{y}' > \\ &= \int_0^{\bar t}\int_{\Gamma_\theta} \left[\int_0^t\int_{\Gamma_\theta} G_{\theta\theta}\,(\mathbf{x},\boldsymbol{\xi};t-\tau)\,q\,(\boldsymbol{\xi};\tau)\,d\boldsymbol{\xi}\,d\tau\right] q'\,(\mathbf{x};\bar t-t)\,d\mathbf{x}\,dt \\ &- \int_0^{\bar t}\int_{\Gamma_\theta} \left[\int_0^t\int_{\Gamma_q} G_{\theta q}\,(\mathbf{x},\boldsymbol{\xi};t-\tau)\,\theta\,(\boldsymbol{\xi};\tau)\,d\boldsymbol{\xi}\,d\tau\right] q'\,(\mathbf{x};\bar t-t)\,d\mathbf{x}\,dt \\ &- \int_0^{\bar t}\int_{\Gamma_q} \left[\int_0^t\int_{\Gamma_\theta} G_{q\theta}\,(\mathbf{x},\boldsymbol{\xi};t-\tau)\,q\,(\boldsymbol{\xi};\tau)\,d\boldsymbol{\xi}\,d\tau\right] \theta'\,(\mathbf{x};\bar t-t)\,d\mathbf{x}\,dt \\ &+ \int_0^{\bar t}\int_{\Gamma_q} \left[\int_0^t\int_{\Gamma_q} G_{qq}\,(\mathbf{x},\boldsymbol{\xi};t-\tau)\,\theta\,(\boldsymbol{\xi};\tau)\,d\boldsymbol{\xi}\,d\tau\right] \theta'\,(\mathbf{x};\bar t-t)\,d\mathbf{x}\,dt. \end{aligned}$$

http://rcin.org.pl

Let us change the integration order and use the Heaviside function $H(t-\tau)$ (= 0 for $\tau > t$; = 1 for $\tau < t$):

$$\text{(C.2)} \quad \int_0^{\bar{t}} \int_0^{\bar{t}} \left[\int_{\Gamma_\theta} \int_{\Gamma_\theta} q(\boldsymbol{\xi};\tau)\, G_{\theta\theta}(\mathbf{x},\boldsymbol{\xi};t-\tau)\, q'(\mathbf{x};\bar{t}-t)\; d\boldsymbol{\xi}\, d\mathbf{x} - \int_{\Gamma_\theta} \int_{\Gamma_q} \theta(\boldsymbol{\xi};\tau)\, G_{\theta q}(\mathbf{x},\boldsymbol{\xi};t-\tau)\, q'(\mathbf{x};\bar{t}-t)\; d\boldsymbol{\xi}\, d\mathbf{x} - \int_{\Gamma_q} \int_{\Gamma_\theta} q(\boldsymbol{\xi};\tau)\, G_{q\theta}(\mathbf{x},\boldsymbol{\xi};t-\tau)\, \theta'(\mathbf{x};\bar{t}-t)\; d\boldsymbol{\xi}\, d\mathbf{x} + \int_{\Gamma_q} \int_{\Gamma_q} \theta(\boldsymbol{\xi};\tau)\, G_{qq}(\mathbf{x},\boldsymbol{\xi};t-\tau)\, \theta'(\mathbf{x};\bar{t}-t)\; d\boldsymbol{\xi}\, d\mathbf{x} \right] H(t-\tau)\; d\tau\, dt.$$

Now take into account the kernel reciprocity properties, Eqs. (2.14)–(2.16), and adopt for convenience new time variables $\sigma \equiv \bar{t} - \tau$, $s \equiv \bar{t} - t$:

$$\text{(C.3)} \quad \int_0^{\bar{t}} \int_0^{\bar{t}} \left[\int_{\Gamma_\theta} \int_{\Gamma_\theta} q(\boldsymbol{\xi};\bar{t}-\sigma)\, G_{\theta\theta}(\mathbf{x},\boldsymbol{\xi};\sigma-s)\, q'(\mathbf{x};s)\; d\boldsymbol{\xi}\, d\mathbf{x} - \int_{\Gamma_\theta} \int_{\Gamma_q} \theta(\boldsymbol{\xi};\bar{t}-\sigma)\, G_{\theta q}(\mathbf{x},\boldsymbol{\xi};\sigma-s)\, q'(\mathbf{x};s)\; d\boldsymbol{\xi}\, d\mathbf{x} - \int_{\Gamma_q} \int_{\Gamma_\theta} q(\boldsymbol{\xi};\bar{t}-\sigma)\, G_{q\theta}(\mathbf{x},\boldsymbol{\xi};\sigma-s)\, \theta'(\mathbf{x};s)\; d\boldsymbol{\xi}\, d\mathbf{x} + \int_{\Gamma_q} \int_{\Gamma_q} \theta(\boldsymbol{\xi};\bar{t}-\sigma)\, G_{qq}(\mathbf{x},\boldsymbol{\xi};\sigma-s)\, \theta'(\mathbf{x};s)\; d\boldsymbol{\xi}\, d\mathbf{x} \right] H(\sigma-s)\; d\sigma\, ds.$$

By re-arranging Eq. (C.3), using again symbol t instead of σ and τ instead of s, and, finally, by interpreting the role of the Heaviside function in terms of integration intervals, an expression is achieved from which the symmetry property to prove clearly emerges:

$$\text{(C.4)} \quad \int_0^{\bar{t}} \int_{\Gamma_\theta} \left[\int_0^{t} \int_{\Gamma_\theta} G_{\theta\theta}(\mathbf{x},\boldsymbol{\xi};t-\tau)\, q'(\mathbf{x};\tau)\; d\boldsymbol{\xi}\, d\tau \right] q(\boldsymbol{\xi};\bar{t}-t)\; d\boldsymbol{\xi}\, dt - \int_0^{\bar{t}} \int_{\Gamma_\theta} \left[\int_0^{t} \int_{\Gamma_q} G_{\theta q}(\mathbf{x},\boldsymbol{\xi};t-\tau)\, q'(\mathbf{x};\tau)\; d\mathbf{x}\, d\tau \right] \theta(\boldsymbol{\xi};\bar{t}-t)\; d\boldsymbol{\xi}\, dt$$

http://rcin.org.pl

(C.4) [cont.]

$$- \int_0^{\bar{t}} \int_{\Gamma_q} \left[\int_0^t \int_{\Gamma_\theta} G_{q\theta}(\mathbf{x}, \boldsymbol{\xi}; t-\tau)\, \theta'(\mathbf{x}; \tau)\, d\mathbf{x}\, d\tau \right] q(\boldsymbol{\xi}; \bar{t}-t)\, d\boldsymbol{\xi}\, dt$$

$$+ \int_0^{\bar{t}} \int_{\Gamma_q} \left[\int_0^t \int_{\Gamma_q} G_{qq}(\mathbf{x}, \boldsymbol{\xi}; t-\tau)\, \theta'(\mathbf{x}; \tau)\, d\mathbf{x}\, d\tau \right] \theta(\boldsymbol{\xi}; \bar{t}-t)\, d\boldsymbol{\xi}\, dt$$

$$= < \mathbf{Ly}', \mathbf{y} > \qquad \text{q. e. d.}$$

Appendix D. A proof of the symmetry of the boundary integral operator with respect to a new bilinear form over $\Gamma \times T_\infty$ (Proposition 3)

A path of reasoning similar to that in Appendix C can be followed here again with reference to the bilinear form defined by Eq. (4.2) in order to prove the symmetry property expressed by Eq. (4.5), with the same interpretation of $\mathbf{y}$, $\mathbf{y}'$ and $\mathbf{L}$ as in Appendix C.

(D.1)

$$\ll \mathbf{Ly}, \mathbf{y}' \gg$$

$$= \int_{\Gamma_\theta} \int_0^\infty \int_0^\infty g(t+\eta)\, q'(\mathbf{x}; \eta) \int_{\Gamma_\theta} \int_0^t G_{\theta\theta}(\mathbf{x}, \boldsymbol{\xi}; t-\tau)\, q(\boldsymbol{\xi}; \tau)\, d\tau\, d\boldsymbol{\xi}\, d\eta\, dt\, d\mathbf{x}$$

$$- \int_{\Gamma_\theta} \int_0^\infty \int_0^\infty g(t+\eta)\, q'(\mathbf{x}; \eta) \int_{\Gamma_q} \int_0^t G_{\theta q}(\mathbf{x}, \boldsymbol{\xi}; t-\tau)\, \theta(\boldsymbol{\xi}; \tau)\, d\tau\, d\boldsymbol{\xi}\, d\eta\, dt\, d\mathbf{x}$$

$$- \int_{\Gamma_q} \int_0^\infty \int_0^\infty g(t+\eta)\, \theta'(\mathbf{x}; \eta) \int_{\Gamma_\theta} \int_0^t G_{q\theta}(\mathbf{x}, \boldsymbol{\xi}; t-\tau)\, q(\boldsymbol{\xi}; \tau)\, d\tau\, d\boldsymbol{\xi}\, d\eta\, dt\, d\mathbf{x}$$

$$+ \int_{\Gamma_q} \int_0^\infty \int_0^\infty g(t+\eta)\, \theta'(\mathbf{x}; \eta) \int_{\Gamma_q} \int_0^t G_{qq}(\mathbf{x}, \boldsymbol{\xi}; t-\tau)\, \theta(\boldsymbol{\xi}; \tau)\, d\tau\, d\boldsymbol{\xi}\, d\eta\, dt\, d\mathbf{x}.$$

Let us now take into account again the definition (4.2) and invert the integration sequence, to obtain:

(D.2)

$$\int_{\Gamma_\theta} \int_{\Gamma_\theta} \int_0^\infty W(s) \int_0^\infty e^{-s\eta} q'(\mathbf{x}; \eta)\, d\eta \int_0^\infty e^{-st} G_{\theta\theta}(\mathbf{x}, \boldsymbol{\xi}; t)\, dt$$

$$\times \int_0^\infty e^{-s\tau} q(\boldsymbol{\xi}; \tau)\, d\tau\, ds\, d\boldsymbol{\xi}\, d\mathbf{x}$$

http://rcin.org.pl

(D.2) [cont.]

$$
\begin{aligned}
&- \int_{\Gamma_\theta}\int_{\Gamma_q}\int_0^\infty W(s)\int_0^\infty e^{-s\eta} q'(\mathbf{x};\eta)\,d\eta \int_0^\infty e^{-st} G_{\theta q}(\mathbf{x},\boldsymbol{\xi};t)\,dt \\
&\qquad \times \int_0^\infty e^{-s\tau}\theta(\boldsymbol{\xi};\tau)\,d\tau\,ds\,d\boldsymbol{\xi}\,d\mathbf{x} \\
&- \int_{\Gamma_q}\int_{\Gamma_\theta}\int_0^\infty W(s)\int_0^\infty e^{-s\eta}\theta'(\mathbf{x};\eta)\,d\eta \int_0^\infty e^{-st} G_{q\theta}(\mathbf{x},\boldsymbol{\xi};t)\,dt \\
&\qquad \times \int_0^\infty e^{-s\tau} q(\boldsymbol{\xi};\tau)\,d\tau\,ds\,d\boldsymbol{\xi}\,d\mathbf{x} \\
&+ \int_{\Gamma_q}\int_{\Gamma_q}\int_0^\infty W(s)\int_0^\infty e^{-s\eta}\theta'(\mathbf{x};\eta)\,d\eta \int_0^\infty e^{-st} G_{qq}(\mathbf{x},\boldsymbol{\xi};t)\,dt \\
&\qquad \times \int_0^\infty e^{-s\tau}\theta(\boldsymbol{\xi};\tau)\,d\tau\,ds\,d\boldsymbol{\xi}\,d\mathbf{x}.
\end{aligned}
$$

The reciprocity properties (2.14)-(2.16) of the Green functions in point lead to a final expression which evidences the new symmetry of operator **L**, as stated by Proposition 3:

(D.3)

$$
\begin{aligned}
&\int_{\Gamma_\theta}\int_0^\infty\int_0^\infty g(t+\eta)\,q(\mathbf{x};\eta)\int_{\Gamma_\theta}\int_0^t G_{\theta\theta}(\mathbf{x},\boldsymbol{\xi};t-\tau)\,q'(\boldsymbol{\xi};\tau)\,d\tau\,d\boldsymbol{\xi}\,d\eta\,dt\,d\mathbf{x} \\
&- \int_{\Gamma_\theta}\int_0^\infty\int_0^\infty g(t+\eta)\,\theta(\mathbf{x};\eta)\int_{\Gamma_q}\int_0^t G_{\theta q}(\mathbf{x},\boldsymbol{\xi};t-\tau)\,q'(\boldsymbol{\xi};\tau)\,d\tau\,d\boldsymbol{\xi}\,d\eta\,dt\,d\mathbf{x} \\
&- \int_{\Gamma_q}\int_0^\infty\int_0^\infty g(t+\eta)\,q(\mathbf{x};\eta)\int_{\Gamma_\theta}\int_0^t G_{q\theta}(\mathbf{x},\boldsymbol{\xi};t-\tau)\,\theta'(\boldsymbol{\xi};\tau)\,d\tau\,d\boldsymbol{\xi}\,d\eta\,dt\,d\mathbf{x} \\
&+ \int_{\Gamma_q}\int_0^\infty\int_0^\infty g(t+\eta)\,\theta(\mathbf{x};\eta)\int_{\Gamma_q}\int_0^t G_{qq}(\mathbf{x},\boldsymbol{\xi};t-\tau)\,\theta'(\boldsymbol{\xi};\tau)\,d\tau\,d\boldsymbol{\xi}\,d\eta\,dt\,d\mathbf{x} \\
&\qquad = \ll \mathbf{L}\mathbf{y}', \mathbf{y} \gg \qquad \text{q. e. d.}
\end{aligned}
$$

Acknowledgments

Authors acknowledge with thanks a research grant from MURST (so-called 40% programme).

http://rcin.org.pl

References

1. F.J. RIZZO and D.H. SHIPPY, *A method of solution for certain problems of transient heat conduction*, AIAA J., **8**, 2004–2009, 1970.
2. R.P. SHAW, *An integral approach to diffusion*, Int. J. Heat Mass Transfer, **16**, 693–699, 1974.
3. K. TANAKA and M. TANAKA, *Time space boundary elements for transient heat conduction problems*, Appl. Math. Modelling, **4**, 331–334, 1980.
4. V. ROURES and E. ALARCON, *Transient heat conduction problems using BIEM*, Computers and Structures, **16**, 717–730, 1983.
5. M.L.G. PINA and J.L.M. FERNANDEZ, *Applications in heat conduction by BEM*, [in:] Topics in Boundary Elements Research, C.A. BREBBIA [Ed.], Springer-Verlag, Berlin, 41–58, 1984.
6. S. SHARP and L. CROUCH, *Heat conduction, thermoelasticity and consolidation*, [in:] Boundary Element Methods in Mechanics, D.E. BESKOS [Ed.], Elsevier, Amsterdam, 439–498, 1987.
7. C. POLIZZOTTO, *An energy approach to the boundary element method*, Part I. *Elastic solids*, Comp. Meth. Appl. Mech. Engng., **69**, 167–184, 1988.
8. S. SIRTORI, G. MAIER, G. NOVATI and S. MICCOLI, *A Galerkin symmetric boundary element method in elasticity: formulation and implementation*, Int. J. Num. Meth. Engng., **35**, 255–282, 1992.
9. J.H. KANE and C. BALAKRISHNA, *Symmetric Galerkin boundary formulations employing curved elements*, Int. J. Num. Meth. Engng., **36**, 2157–2187, 1993.
10. G. MAIER and C. POLIZZOTTO, *A Galerkin approach to boundary elements elastoplastic analysis*, Comp. Meth. Appl. Mec. Engng., **60**, 175–194, 1987.
11. C. POLIZZOTTO, *An energy approach to the boundary element method*, Part II. *Elastic-plastic solids*, Comp. Meth. Appl. Mech. Engng., **69**, 263–276, 1988.
12. C. COMI and G. MAIER, *Extremum, convergence and stability properties of the finite-increment problem in elastic-plastic boundary element analysis*, Int. J. Solid Struct., **29**, 249–270, 1992.
13. G. MAIER, S. MICCOLI, G. NOVATI and S. SIRTORI, *A Galerkin symmetric boundary element method in plasticity: formulation and implementation*, [in:] Advance in Boundary Element Techniques, H. KANE, G. MAIER, N. TOSAKA and S.N. ATLURI [Eds.], Springer-Verlag, Berlin, 288–328, 1993.
14. G. MAIER, S. MICCOLI, G. NOVATI and U. PEREGO, *Symmetric Galerkin boundary element method in plasticity and gradient plasticity*, Computational Mech., **17**, 115–129, 1995.
15. J.H. KANE, *Boundary element analysis in engineering continuum mechanics*, Prentice Hall, Englewood Cliffs, N.Y. 1994.
16. M. BONNET, *Equations intégrales et éléments de frontière*, Coll. Sciences de l'Ingénieur, Eyrolles/CNRS, 1995.
17. A. CARINI, M. DILIGENTI and G. MAIER, *Variational formulation of the boundary element method in transient heat conduction*, Math. Comp. Modelling, **15**, 71–80, 1991.
18. G. MAIER, M. DILIGENTI and A. CARINI, *A variational approach to boundary element elastodynamic analysis and extension to multidomain problems*, Comp. Meth. Appl. Mech. Engng., **92**, 193–213, 1991.
19. A. CARINI, M. DILIGENTI and G. MAIER, *Boundary equation analysis in linear viscoelasticity: variational and saddle point formulation*, Comp. Mech., **8**, 87–98, 1991.
20. T. PANZECA, C. POLIZZOTTO and M. ZITO, *Dynamic plasticity analysis by boundary-interior elements*, Analysis with Boundary Elem., **14**, 113–120, 1994.
21. M.E. GURTIN, *Variational principles in the linear theory of viscoelasticity*, Arch. Ration. Mech. Anal., **13**, 179–191, 1963.
22. E. TONTI, *On the variational formulation for linear initial value problems*, Annali di Matematica Pura ed Applicata, **45**, 4, 331–359, 1073.
23. P. RAFALSKI, *Orthogonal projection method. I. Heat conduction boundary problem*, Bull. Acad. Polon. Sci., Sér. Sci. Techn., **17**, 63–67, 1969.
24. P. RAFALSKI, *Orthogonal projection method. II. Thermoelastic problem*, Bull. Acad. Polon. Sci., Sér. Sci. Techn., **17**, 69–74, 1969.
25. R. REISS and E.J. HAUG, *Extremum principles for linear initial-value problems of mathematical physics*, Int. J. Engng. Sci., **16**, 231–251, 1978.
26. W.L. WENDLAND, *On the coupling of finite elements and boundary elements*, [in:] Discretization methods in structural mechanics, G. KUHN and H. MANG [Eds.], Springer-Verlag, Vienna, 405–414, 1990.

http://rcin.org.pl

27. S. HOLZER, *On the engineering analysis of 2D problems by the symmetric Galerkin boundary element method and coupled BEM-FEM*, [in:] Advances in Boundary Element Techniques, J.H. KANE, G. MAIER, N. TOSAKA and S. ATLURI [Eds.], Springer-Verlag, Berlin, 187–208, 1992.
28. C. POLIZZOTTO and M. ZITO, *Variational formulations for coupled BE/FE methods in elastostatics*, Z. Angew. Math. Mech., **74**, 533–543, 1994.
29. H.S. CARSLAW and J.C. JAEGER, *Conduction of heat in solids*, University Press, Oxford 1959.
30. M. GUIGGIANI, G. KRISHNASAMY, T.J. RUDOLPHI and F.J. RIZZO, *A general algorithm for the numerical solution of hypersingular boundary integral equations*, ASME J. Appl. Mech., **59**, 604–614, 1992.
31. M. BONNET and H.D. BUI, *Regularization of the displacements and traction BIE for 3D elastodynamics using indirect methods*, [in:] Advances in Boundary Element Techniques, J. KANE, G. MAIER, N. TOSAKA and S.N. ATLURI [Eds.], Springer-Verlag, Berlin, 1–29, 1993.
32. S. HOLZER, *How to deal with hypersingular integrals in the symmetric BEM*, Comm. Num. Meth. Engng., **9**, 219–232, 1993.
33. M. DILIGENTI and G. MONEGATO, *Finite-part integrals: their occurence and computation*, Rendiconti del Circolo Matematico di Palermo, **33**, 39–61, 1993.
34. A. CARINI, M. DILIGENTI and A. SALVADORI, *Analytical time integrations for a symmetric boundary element method in transient heat conduction*, Joint Conference of Italian Group of Computational Mechanics and Ibero-Latin American Association of Computational Methods in Engineering, Padova, Sept. 25-27, 1996 [to appear].
35. C.A. FELIPPA, *A survey of parametrized variational principles and applicational mechanics*, Comp. Meth. Appl. Mech. Engng., **113**, 109–139, 1994.
36. A. QUARTERONI and A. VALLI, *Numerical approximation of partial differential equations*, Springer- Verlag, Berlin 1994.
37. M. ABRAMOWITZ and I. STEGUN, *Handbook of mathematical functions*, Dover, New York 1965.

DEPARTMENT OF CIVIL ENGINEERING, UNIVERSITY OF BRESCIA,
via Branze 38, 25123 Brescia, Italy,
DEPARTMENT OF MATHEMATICS, UNIVERSITY OF PARMA,
via M. D'Azeglio 85, 43100 Parma, Italy
and
DEPARTMENT OF STRUCTURAL ENGINEERING, TECHNICAL UNIVERSITY (POLITECNICO),
P. Leonardo Da Vinci 32, 20133 Milano, Italy.

Received August 26, 1996.

http://rcin.org.pl

Arch. Mech., 49, 2, pp. 285–291, Warszawa 1997

On hyperbolic heat conduction

K. FRISCHMUTH (ROSTOCK) and V.A. CIMMELLI (POTENZA)

IN A PREVIOUS PAPER [5], numerical solutions of initial-boundary value problems for the *semi-empirical* model of heat conduction were compared with available experimental results. In [6] the model was modified by introducing more realistic approximations of the constitutive functions, basing on measured specific heat, heat conductivities and second sound speeds for NaF at low temperatures (10 ... 20° K). In the present paper we suggest a method to choose the free parameters entering the constitutive functions by minimizing an *error functional*, measuring the differences between the theoretical and experimental heat pulses.

1. Introduction

IN A SERIES OF PAPERS [1, 2, 3], KOSIŃSKI and co-workers introduced a model based on thermodynamics with internal state variables, describing heat conduction at low temperatures. Such a hyperbolic model avoids the paradox of infinite thermal wave speed. According to Kosiński's point of view the absolute temperature, as a concept of thermodynamical equilibrium, is not appropriate to describe the thermal evolution of systems far from equilibrium, such as dielectric crystals at low temperatures (bismuth and sodium fluoride) in which thermal waves, called second sound, can be detected. The introduction of a non-equilibrium temperature as an internal state variable is the main idea of his approach. A kinetic equation describes the evolution of that non-equilibrium temperature with time. CIMMELLI and KOSIŃSKI call such a variable *semi-empirical temperature scale*, [1].

The new model contains three physical material functions: heat conductivity, specific heat and thermal relaxation time, which can be determined by experiments. The mentioned parameter functions enter the constitutive equations for the heat flux, internal energy and the right-hand side of the kinetic equation.

On the background of the existing experimental data it is reasonable to restrict our considerations to the 1D case. For certain choices of physical parameters, length of the specimen, initial temperatures and initial thermal increments at one side of the specimen, the model equations have been solved numerically, cf. FRISCHMUTH and CIMMELLI, [5], and the results are in good accordance with the experimental data. However, some of the parameters used in the model were choosen by hand. Hence it seems to be of some interest to try to find an objective procedure for the choice of all unknown parameters which minimizes the difference between theoretical and experimental results. To this end we define a functional, called *error functional*, measuring the degree of deviation between theoretical and experimental heat pulses.

http://rcin.org.pl

Finally, we minimize the above error functional by an appropriate choice of the free constitutive parameters. Note that the evaluation of the error functional for a given set of parameters requires the solution of an initial boundary value problem for a hyperbolic system of balance laws. Previously, [6], the comparison between theoretical results and measured heat pulses was based only on the wave speed which was taken as the characteristic speed for the theoretical solutions.

2. The direct problem

In order to keep the paper possibly self–contained, let us shortly outline the assumptions of the semi-empirical theory of heat conduction. First we have the basic equation of energy balance for a rigid heat conductor([1])

$$\dot{\varepsilon} + \operatorname{div} q = r\,. \tag{1}$$

By r we denoted heat sources and by q the heat flux vector. We assume the energy to depend only on temperature: $\varepsilon = \varepsilon(\theta)$ and thus $c_v = c_v(\theta) := \varepsilon'(\theta)$([2]). Especially for NaF, we have

$$\varepsilon = \varepsilon_0\theta^4/4 + \varepsilon_1\theta^5/5\,, \tag{2}$$

which is a generalization of the classical Debye's law, and which has been proposed on the basis of data obtained by HARDY and JASWAL [7].

We postulate the existence of a scalar field β, the semi-empirical temperature, whose evolution is governed by the kinetic equation

$$\dot{\beta} = f(\theta, \beta), \tag{3}$$

and define the heat flux via a Fourier-like law of the type

$$q(x,t) = -\alpha\nabla_x\beta(x,t), \tag{4}$$

where α means the heat conductivity.

We assume further that ε, respectively the specific heat c_v, can be measured directly [7], and that these functions should be independent of the considered theory of heat conduction.

The functions $\alpha : \mathbb{R}^+ \to \mathbb{R}^+$ and $f : \mathbb{R}^+ \times \mathbb{R}^+ \to \mathbb{R}$ can be approximately determined by measuring the heat flux and the equilibrium wave speed [6], i.e. the speed of a wave travelling into a medium where $q = 0$. As far as that last

([1]) A more realistic model should include the effects due to the anisotropy together with those related to the elastic behaviour of the materials. Actually, bismuth and sodium fluoride possess both properties. However, as a first approximation we will limit ourselves to consider a one-dimensional rigid heat conductor.

([2]) For convenience, we refer all quantities to volume measures and not to mass, following the experimental papers [8, 7]. Specifically, in the 1-D case, all quantities are referred to the unit of length.

http://rcin.org.pl

function is concerned, satisfactory numerical fits of experimental data were given by COLEMANN and NEUMANN [4] and by CIMMELLI and FRISCHMUTH [6]([3]).

For practical purposes it is necessary to replace $\mathbb{R}^+$ by a small temperature range $\mathcal{R} = [\theta_{\min}, \theta_{\max}]$ which is covered by experiments and where the hyperbolic effects are relevant. We choose $\theta_{\min} = 10$ and $\theta_{\max} = 20$([4]), bearing in mind the available data for NaF.

3. Heat pulse experiments

We consider a 1-D NaF specimen, occupying the domain $W = [0, L] \subset \mathbb{R}$. Typical values of L are about 1 cm. Moreover, we suppose that on the left-hand boundary of W, a heat pulse of the form

$$\theta_L(t) = \theta_0 + \Delta\theta(H(t - t_0) - H(t - t_0 - \Delta t)), \tag{5}$$

with H some appropriate Heaviside-like function, is applied. Inside the specimen, the following equations hold

$$c_v\dot{\theta} + \operatorname{div} q = r, \tag{6}$$

$$q = -\alpha\nabla\beta, \tag{7}$$

$$\dot{\beta} = f(\theta, \beta). \tag{8}$$

On the right-hand side, Neumann or mixed type boundary conditions of the type

$$q_n = -\alpha(\theta)\beta_{,x} = -p(\theta - \theta_0) \tag{9}$$

are assumed to hold. Their meaning is rather clear: $p = 0$ represents thermal insulation, i.e. pure Neumann conditions, while $p > 0$ corresponds to a more realistic interface condition.

We assume that either the heat source r vanishes uniformly – which corresponds to an ideally insulated lateral surface of the specimen – or rather impose an analogous interface condition of the type([5])

$$r = r(\theta) = -\pi(\theta - \theta_0), \tag{10}$$

with $\pi > 0$. By solving the initial value-boundary problem given by (5)–(10), we can define a transition functional such that

$$\theta_L \mapsto \theta_r =: \theta(L, \cdot) \tag{11}$$

([3]) In our opinion the experimental calculation of α, the most crucial physical parameter, is not completely satisfactory since often the equations of the underlying theory are already used in the experiment for transforming the measured electrical quantities into the caloric ones.

([4]) Through this paper, all temperatures are in K, all lengths in cm, times in μs and masses in g.

([5]) Note that here we are neglecting the dependence on x in the constitutive functions. Furthermore, a realistic r should contain a term representing the mechanical work due to velocity and stress fields. Of course, in our simplification to a rigid heat conductor, these effects are disregarded in our considerations.

http://rcin.org.pl

i.e. giving the measured pulse on the right-hand side as a result of the transmitted impulse applied on the left-hand side. Obviously, the transition causes a delay and a change in shape and amplitude of the wave. Further, it depends on the physical setup which is determined by the parameters: θ_0 – temperature of the environment, L – length of the specimen, π – energy losses under way, p – right boundary condition, together with the constitutive functions c_v, α and f. Now we want to compare the theoretical transition functional with the experimental results. Some additional difficulties arise from the scaling of the experimental data. Indeed, in [7, 8] only the arrival time of the pulse was of interest so that the electrical signals have been measured but not calibrated. As a consequence, we cannot give the experimental transition operator absolutely but only up to an affine transformation. In what follows we consider a theoretical result θ_r to be in accordance with a measured output pulse $\bar{\theta}_r$ if there exist two coefficients λ_0 and λ_1 such that

$$\lambda_0 + \lambda_1 \bar{\theta}_r = \theta_r \,. \tag{12}$$

Otherwise we consider the term

$$\psi = \min_{\lambda_0, \lambda_1} \int [\lambda_0 + \lambda_1 \bar{\theta}_r(t) - \theta_r(t)]\, dt \tag{13}$$

as a measure of the deviation between theory and experimental data.

4. The error functional

In the previous section we have described a mathematical method to compare numerical solutions of the model equations with the experimental data, for given fixed conditions of the conductor and the experimental setup. These conditions are described by three different types of quantities:

(a) some constants, which are well known (e.g. L, ε_0, ε_1);

(b) some parameters, varying in a certain range but which are well documented in the experiments (e.g. the temperature θ_0 of the environment, coinciding with the temperature of the unperturbed initial state);

(c) some physical quantities to be determined under minimization of the error (e.g. α, f, p, π, $\Delta\theta$, Δt).

After fixing all the well known quantities let us introduce two denotations:
u, representing the collection of all unknown quantities;
v, representing the collection of the variable quantities.
Then, according to he previous section, we have the quantity

$$\psi = \psi(u, v) \tag{14}$$

http://rcin.org.pl

as a measure of the model error. Finally, we introduce the functional

$$\Psi = \Psi(u) = \int_V \psi(u, v)\, dv \tag{15}$$

as a measure of the global performance of the considered model over the range V of the variable experimental conditions. For practical purposes we can choose V to be finite and calculate the integral with respect to a discrete measure, i.e. a weighted sum. Analogously, the integral definition of the local error will be replaced by a sum of the squared errors on the time steps of the numerical solution. According to the previous considerations we can state the following identification problem:

Choose the unknown parameters u of the model in such a way that the global error functional

$$\Psi = \Psi(u) = \int_V \psi(u, v)\, dv = \int_V \min_{\lambda_0, \lambda_1} \int [\lambda_0 + \lambda_1 \theta_m r(t) - \theta_r(t)]\, dt\, dv \tag{16}$$

attains a minimum over the domain of all feasable parameters u.

5. A reduced problem and its numerical realization

The minimization problem, such as stated in the previous section, is still too general and difficult to solve, so that some further simplifications seem to be necessary.

Till now, the unknown parameters in the above "least squares" problem contain still the functional parameters α and f, i.e. scalar functions on $\mathcal{R}$, resp. $\mathcal{R} \times \mathcal{R}$. Bearing in mind that our experimental evidence is rather very limited ($|V| = 10$), a reduction of the problem is imperative.

To this end we use – as the first attempt – a very restrictive approach – hoping that a more refined version will be prepared in the near future. First, we use a thermodynamical argument in order to replace one function on $\mathcal{R} \times \mathcal{R}$ by two functions on $\mathcal{R}$. Then we postulate a certain compatibility to the classical case, assuming $\beta = \theta$ at relaxed states, and $\alpha = \kappa$. Finally, we need hence just to identify one scalar function f_1 (because $f_2 = f_1$, $f(\theta, \beta) = f_1(\theta) - f_1(\beta)$) which in turn is approximated by a linear spline f_1^s with the coefficients $s = (s_1, \ldots, s_d) \in \mathbb{R}$.

Hence, for the numerical realization, the unknown parameter u is substituted by the spline coefficients s. In order to avoid more notations, we still denote the functionals by Ψ and Φ:

$$\Psi(s) = \sum_{v \in V} \psi(s, v). \tag{17}$$

http://rcin.org.pl

In this case the variable parameter is identified with the temperature θ_0. So we have

$$\Psi(s) = \sum_{\theta_0=\theta_{\min}}^{\theta_{\max}} \psi(s, \theta_0). \tag{18}$$

The results of our optimization are shown in Fig. 1 in form of a comparison between theoretical and measured pulses at 15 K.

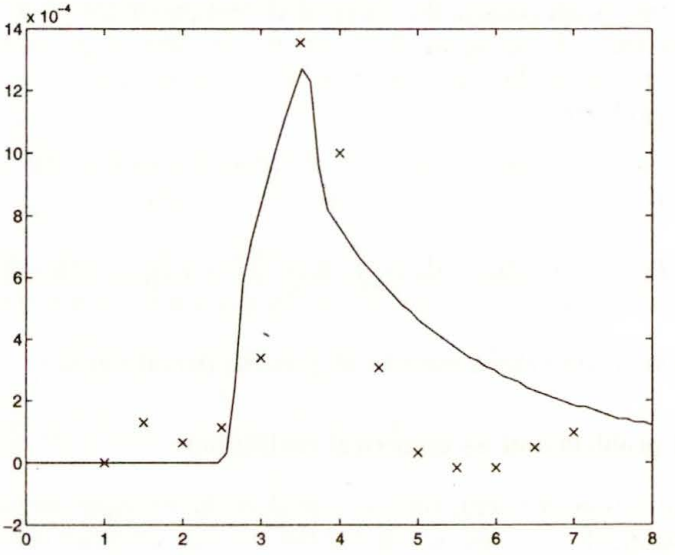

FIG. 1. Theoretical and measured pulses at 15 K.

6. Conclusions

We solved an inverse problem arising in semi-empirical heat conduction theory, in order to find the optimal values of physical parameters characterizing the model. The first results, obtained in this paper, seem to be encouraging. However, it is obvious that there is still some considerable model error. More refined numerical techniques should allow us to avoid some of the additional simplifications of Sec. 5, and thus to reduce the remaining error. This will be the subject of a forthcoming paper.

References

1. V.A. CIMMELLI and W. KOSIŃSKI, *Nonequilibrium semi-empirical temperature in materials with thermal relaxation*, Arch. Mech., **43**, 6, 753, 1991.
2. V.A. CIMMELLI and W. KOSIŃSKI, *Heat waves in dielectric crystals at low temperatures*, University of Basilicata, Quaderni del Dipartimento di Matematica, Report n.6/1992.

http://rcin.org.pl

3. V.A. CIMMELLI, W. KOSIŃSKI and K. SAXTON, *A new approach to the theory of heat conduction with finite wave speeds*, [in:] Proc. VI International Conference on Waves and Stability in Continuous Media, S. RIONERO, G. MULONE, F. SALEMI [Eds.], Acireale, Italy 1991.
4. B.D. COLEMAN and D.C. NEUMANN, *Implications of a nonlinearity in the theory of second sound in solids*, Phys. Rev. B, **32**, 1492, 1988.
5. K. FRISCHMUTH and V.A. CIMMELLI, *Numerical reconstruction of heat pulse experiments*, Int. J. Engng. Sci., **33**, 2, 215, 1995.
6. V.A. CIMMELLI and K. FRISCHMUTH, *Determination of material functions through second sound measurements in a hyperbolic heat conduction theory*, Mathematical and Computer Modelling, 1996 [in press].
7. R.J. HARDY and S.S. JASWAL, *Velocity of second sound in NaF*, Phys. Rev. B, **3**, 4385, 1971.
8. H.E. JACKSON and C.T. WALKER, *Thermal conductivity, second sound, and phonon-phonon interactions in NaF*, Phys. Rev. Letters, **3**, 4, 1428, 1971.

UNIVERSITÄT ROSTOCK, FACHBEREICH MATHEMATIK,
D-18051 ROSTOCK, GERMANY
e-mail: kurt@sun2.math.uni-rostock.de

and

UNIVERSITÁ DELLA BASILICATA,
DIPARTIMENTO DI MATEMATICA, I-85100 POTENZA, ITALY
e-mail: Cimmelli@unibas.it

Received November 8, 1996.

http://rcin.org.pl

Arch. Mech., 49, 2, pp. 293–319, Warszawa 1997

Nonlinear transport equation and macroscopic properties of microheterogeneous media

A. GAŁKA, J. J. TELEGA and S. TOKARZEWSKI (WARSZAWA)

THE AIM of this paper is a study of the quasi-linear transport equation, for instance the stationary heat equation. For periodically microheterogeneous media, asymptotic homogenization has been performed with the local problem formulated as a minimization problem. The Hashin-Shtrikman type bounds and Golden–Papanicolaou integral representation theorem have been extended. In the case of layered composites, exact analytical formula for the effective coefficients have been derived. The possibility of applying Padé approximants and the Ritz method has been shown. Specific cases and examples have also been examined.

1. Introduction

THE NONLINEAR Eq. (2.1) below is here called a nonlinear transport equation. It is obvious that from the physical point of view, the study of such an equation is very important. Typical examples are the stationary heat conduction and a nonlinear dielectric. The small parameter $\varepsilon > 0$ characterizes a microstructure of the material. We have thus to deal with composite materials. Performing homogenization or passing with ε to zero one obtains the homogenized (effective) coefficients a_{ij}^{ε} $(i, j = 1, 2, 3)$. Of our main interest will be the periodic homogenization, cf. [1, 2]. We shall also extend to the nonlinear problem studied, the results due to GOLDEN and PAPANICOLAOU [20] on the integral representation of the effective coefficients in the linear case when $a_{ij}(y, \omega)(y \in \mathbb{R}^3, \omega \in \Omega)$ are stationary matrix-valued random fields; here $(\Omega, \mathcal{F}, \mathcal{P})$ is a probability space. Such an extension is possible since in the local problem the macroscopic field $u^{(0)}$, say the macroscopic temperature $T = u^{(0)}$ in the case of the heat conduction, plays the role of a parameter only. It is thus also possible to exploit the Hashin - Shtrikman variational principles and bounds, elaborated for the linear transport equation.

Extensive literature is concerned with the linear conductivity i.e. when the coefficients a_{ij}^{ε} do not depend on the solution u^{ε}. The reader may refer to [1–21] for more details on the results achieved so far. In contrast to the linear case, there seems to exist only a few papers on the homogenization of the quasi-linear Eq. (2.1), cf. [22–25]. Those papers are purely theoretical and provide no examples of applications to composite materials. Also, the problem of the estimation of the effective coefficients has been left open, though a particular case has been studied by MITYUSHEV [26]. However, the definition of the effective conductivity used by this author is different from the formula obtained by homogenization. We observe that a_{ij}^{ε} depend on $u^{(0)}$, where $u^{(0)}$ is a weak limit of u^{ε} when $\varepsilon \to 0$.

http://rcin.org.pl

For instance, in the case of the heat conduction, a_{ij}^{ε} depend on the macroscopic temperature T. Such a dependence is in general a nonlinear one, even then when in each of phases constituting the composite a_{ij}^{ε} depend linearly on T; specific examples are provided in Secs. 5, 6 and 7 of our paper. A nonlinear dependence of the conductivities on the temperature is of vital importance not only in the study of engineering materials and structures [27, 28], but also for modelling the behaviour of biological tissues [29, 30].

The determination of the effective coefficients a_{ij}^{ε} is of interest not only for undeformable bodies; such a problem arises quite naturally as an independent problem in the study of thermo- and piezo-electric composites [31, 32] and in thermodiffusion [33].

The objective of this paper is to study the quasi-linear heat equation (2.1) and provide some applications. Brief description of the contents of the paper reveals very well our aim. In Sec. 2 the method of two-scale asymptotic expansions is used in order to derive in a rather simple manner the homogenized coefficients $a_{ij}^{\varepsilon}(u^{(0)})$; in the case of heat conduction $u^{(0)} = T$. The formulation of the local problem in the form of a minimization problem, in which the macroscopic field $u^{(0)}$ (for instance T) plays the role of a parameter is also delivered. In Sec. 3 variational principles and bounds of the Hashin - Shtrikman type are given. Section 4 deals with a straightforward extension of the GOLDEN - PAPANICOLAOU [19] representation theorem to the investigated quasi-linear problem. This theorem provides an integral representation of the effective coefficients $a_{ij}^{\varepsilon}(u^{(0)})$ for two-component composites made of isotropic materials. In Sec. 5 analytical formulae for the homogenized coefficients of layered composites are derived. Section 6 reveals a possibility of an application of the Ritz method to the determination of local functions. A specific two-dimensional problem is also given. In the last section it is shown how to apply the powerful tool of Padé approximants to finding bounds on the effective coefficients.

2. Homogenization of quasi-linear heat equation with periodic coefficients

Let $V \subset \mathbb{R}^3$ be a bounded regular domain and $\Gamma = \partial V$ its boundary. We introduce a parameter $\varepsilon = l/L$, where l, L are typical length scales associated with microinhomogeneities and the region V, respectively.

We shall study the quasi-linear transport equation

$$
\begin{aligned}
-\frac{\partial}{\partial x_i}\left(a_{ij}^{\varepsilon}(x, u^{\varepsilon})\frac{\partial u^{\varepsilon}}{\partial x_j}\right) &= f \quad \text{in } V, \\
u^{\varepsilon}|_{\Gamma} &= 0 \quad \text{on } \Gamma,
\end{aligned}
\tag{2.1}
$$

where $a_{ij}^{\varepsilon}(x, u^{\varepsilon}) = a_{ij}\left(\frac{x}{\varepsilon}, u^{\varepsilon}\right)$, $x \in V$. By Y we denote the so-called basic cell [1, 2], for instance $Y = (0, Y_1) \times (0, Y_2) \times (0, Y_3)$. For the sake of simplicity we assume

http://rcin.org.pl

that $a_{ij} = a_{ji}$, $i, j = 1, 2, 3$. As usual, we apply the summation convention. The material coefficients $a_{ij}(y, r)$ are Y-periodic in the first argument. More precisely,

$$a_{ij} : (y, r) \to a_{ij}(y, r),$$
$$\mathbb{R}^3 \times \mathbb{R} \to \mathbb{R}$$

are assumed to satisfy the following conditions:

(i) For each $r \in \mathbb{R}$, $y \to a_{ij}(y, r)$ are mesurable and Y-periodic functions.

(ii) There exists a constant $\alpha > 0$ such that for every $r \in \mathbb{R}$, i.e. $y \in Y$ and for all $i, j = 1, 2, 3$, $|a_{ij}(y, r)| \leq \alpha$.

(iii) There exists a constant $k > 0$ such that

$$|a_{ij}(y, r_1) - a_{ij}(y, r_2)| \leq k|r_1 - r_2|,$$

for all $y \in \mathbb{R}^3$ and $r_1, r_2 \in \mathbb{R}$.

(iv) There exists $\alpha_0 > 0$ such that

$$a_{ij}(y, r)\xi_i\xi_j \geq \alpha_0|\xi|^2,$$

for all $\xi \in \mathbb{R}^3$ and $r \in \mathbb{R}$.

We note that for a fixed $\varepsilon > 0$ the material functions $a_{ij}^{\varepsilon}(x, r) = a_{ij}\left(\frac{x}{\varepsilon}, r\right)$ are εY-periodic in $x \in V$. After passage to the limit as $\varepsilon \to 0$, the homogenized coefficients a_{ij}^{e} will be obtained.

2.1. Method of two-scale asymptotic expansions

According to this method we make the following assumption (*ansatz*), cf. [1, 2]

$$u^{\varepsilon}(x) = u^{(0)}(x, y) + \varepsilon\, u^{(1)}(x, y) + \varepsilon^2\, u^{(2)}(x, y) + \cdots, \tag{2.2}$$

where $y = x/\varepsilon$, and the functions $u^{(0)}(x, \cdot)$, $u^{(1)}(x, \cdot)$, $u^{(2)}(x, \cdot)$, etc. are Y-periodic. Then we may write

$$a_{ij}(y, u^{(0)} + \varepsilon u^{(1)} + \varepsilon^2 u^{(2)} + \cdots) = a_{ij}(y, u^{(0)}) + \varepsilon u^{(1)} \frac{\partial a_{ij}(y, u^{(0)})}{\partial u^{(0)}}$$
$$+ \varepsilon^2 \left(u^{(2)}(x, y) \frac{\partial a_{ij}(y, u^{(0)})}{\partial u^{(0)}} + \frac{1}{2}(u^{(1)}(x, y))^2 \frac{\partial^2 a_{ij}(y, u^{(0)})}{\partial^2 u^{(0)}} \right) + \cdots.$$

It is tacitly assumed that all derivatives appearing in the procedure of asymptotic homogenization make sense. We recall that for a function $f(x, y)$, where $y = x/\varepsilon$, the differentiation operator $\partial/\partial x_i$ should be replaced by $\dfrac{\partial}{\partial x_i} + \dfrac{1}{\varepsilon}\dfrac{\partial}{\partial y_i}$. According to the method of asymptotic expansions we compare the terms associated with

http://rcin.org.pl

the same power of ε. Proceeding similarly as in the linear case we successively obtain:

$\underline{\varepsilon^{-2}}$

$$\frac{\partial}{\partial y_j}\left(a_{ij}(y, u^{(0)}(x,y))\frac{\partial u^{(0)}(x,y)}{\partial y_i}\right) = 0.$$

This equation will be satisfied provided that $u^{(0)}$ does not depend on the local variable y, i.e. $u^{(0)} = u^{(0)}(x)$. This statement holds true under the assumption that the coefficients $a_{ij}(\cdot, u^{(0)}(x,\cdot))$ are Y-periodic.

$\underline{\varepsilon^{-1}}$

$$\frac{\partial}{\partial y_j}\left(a_{ij}(y, u^{(0)}(x))\left(\frac{\partial u^{(1)}(x,y)}{\partial y_i} + \frac{\partial u^{(0)}(x)}{\partial x_i}\right)\right) = 0.$$

$\underline{\varepsilon^{0}}$ (after integration over Y)

$$\frac{\partial}{\partial x_j}\left(\frac{1}{|Y|}\int_Y a_{ij}(y, u^{(0)}(x))\left(\frac{\partial u^{(1)}(x,y)}{\partial y_i} + \frac{\partial u^{(0)}(x)}{\partial x_i}\right) dY\right) = -f(x),$$

where

$$u^{(1)}(x,y) = \frac{\partial u^{(0)}(x)}{\partial x_k}\chi^{(k)}(y, u^{(0)}).$$

The local functions $\chi^{(k)}(y, u^{(0)})$ are solutions to the local problem

$$\frac{\partial}{\partial y_j}\left(a_{ij}(y, u^{(0)})\left(\frac{\partial \chi^{(k)}(y, u^{(0)})}{\partial y_i} + \delta_{ik}\right)\right) = 0. \tag{2.3}$$

Let us introduce the space of Y-periodic functions defined by

$$H_{\text{per}}(Y) = \left\{\phi \in H^1(Y) | \phi \text{ assumes equal values at the opposite faces of } Y\right\}. \tag{2.4}$$

The weak (variational) formulation of Eq. (2.3) reads: find $\chi^{(k)}(\cdot, u^{(0)}) \in H_{\text{per}}(Y)$ such that

$$\int_Y \left[a_{ij}(y, u^{(0)})\left(\frac{\partial \chi^{(k)}(y, u^{(0)})}{\partial y_i} + \delta_{ik}\right)\right]\frac{\partial v(y)}{\partial y_j} dy = 0, \tag{2.5}$$

for each $v \in H_{\text{per}}(Y)$. Then the homogenized equation has the following form

$$-\frac{\partial}{\partial x_j}\left(a^e_{ij}(u^{(0)})\frac{\partial u^{(0)}}{\partial x_i}\right) = f, \tag{2.6}$$

http://rcin.org.pl

where the homogenized (effective) coefficients are given by

$$a_{ij}^{\varepsilon}(u^{(0)}) = \frac{1}{|Y|}\int_Y \left[a_{ij}(y, u^{(0)}) + a_{kj}(y, u^{(0)})\frac{\partial \chi^{(i)}}{\partial y_k}\right] dy. \tag{2.7}$$

In the case of the heat conduction $u^{(0)} = T$, where T is the macroscopic temperature.

Both in (2.5) and (2.6) the transport coefficients satisfy only the earlier specified conditions (i)–(iv). We observe that in the local problem (2.5) $u^{(0)}$ plays the role of a parameter. This simple, but crucial observation means that (2.5) is equivalent to a convex minimization problem:

$$(\mathcal{P}_{\text{loc}}) \quad \left| \begin{array}{l} \text{Find} \\ W(u^{(0)}, \mathbf{E}) = \inf\left\{ \dfrac{1}{2|Y|}\displaystyle\int_Y a_{ij}(y, u^{(0)})\left(\frac{\partial v}{\partial y_i} + E_i\right)\left(\frac{\partial v}{\partial y_j} + E_j\right) dy \;\middle|\; \right. \\ \qquad\qquad \left. v \in H_{\text{per}}(Y)\right\} \end{array} \right.$$

provided that $a_{ij} = a_{ji}$; here $E_i = \partial u^{(0)}/\partial x_i$. A solution $\overline{v} \in H_{\text{per}}(Y)$ exists and is unique up to a constant $c(u^{(0)})$. Due to linearity of $\overline{v}$ with respect to $\mathbf{E} = (E_i)$ we may write

$$\overline{v}(y, u^{(0)}) = \chi^{(k)}(y, u^{(0)})E_k\,. \tag{2.8}$$

In contrast to the local problem $(\mathcal{P}_{\text{loc}})$, problem (2.1) *cannot* be formulated as a minimization problem. Note also that

$$W(u^{(0)}, \mathbf{E}) = \frac{1}{2}a_{ij}^{\varepsilon}(u^{(0)})E_iE_j$$

is the macroscopic potential. For instance, for dielectric composites the macroscopic displacement vector $\mathbf{D} = (D_i)$ has the form

$$D_i = \frac{\partial W}{\partial E_i} = a_{ij}^{\varepsilon}(u^{(0)})E_j\,, \tag{2.9}$$

where $u^{(0)}$ is the electric field, say φ and $E_i = -\partial\varphi/\partial x_i$ (the sign of E_i in $(\mathcal{P}_{\text{loc}})$ is not important in the sense that one may consider either $\chi^{(k)}$ or $(-\chi^{(k)})$).

Knowing that the local problem can be formulated as the minimization problem $(\mathcal{P}_{\text{loc}})$ we come to a *very important conclusion*: all the variational bound techniques, including Hashin–Shtrikman bounds, developed for the linear transport equation can be applied to the estimation of the effective coefficients (2.7). In the next section we shall provide more details.

http://rcin.org.pl

2.2. Justification: G-convergence

From the mathematical point of view the results presented in the previous subsection are formal. Rigorous proof concerning the convergence when in Eq. (2.1) ε tends to zero have been given by ARTOLA, DUVAUT [22] and next extended in [23, 25] to the case of not necessarily periodic coefficients. Having in mind applications to physical problems we have assumed that $a_{ij} = a_{ji}$. In fact, to perform homogenization either by the asymptotic method or by the method of H-convergence, such a symmetry is not required, cf. [22, 23]. H-convergence is the G-convergence generalized to the case of nonsymmetric coefficients, cf. [1, 23–25] for more details. The main result of ARTOLA and DUVAUT [22] is summarized in the form of

THEOREM 1. *Under the assumptions* (i)–(iv) *and*

$$f \in L^2(V), \tag{2.10}$$

there exists a subsequence $u^{\varepsilon'}$ *of* u^{ε} *and* $p > 2$ *such that*

$$u^{\varepsilon'} \rightharpoonup u^{(o)} \quad \text{in } W_0^{1,p}(V) \text{ weakly}, \tag{2.11}$$

where $u^{(o)} \in W_0^{1,p}(V)$ *is a solution of* Eq. (2.6).

REMARK 1. A weak solution of Eq. (2.1) is sought in the space $H_0^1(V)$. The existence theorem provided by ARTOLA and DUVAUT [22] requires that $f \in W^{-1,p}(V)$; $p > 2$ depends on V, α, α_0 and space dimension. We observe that in [22] the coefficients a_{ij}^{ε} are not necessarily symmetric.

3. Hashin–Shtrikman variational principles and bounds

The local problem $(\mathcal{P}_{\text{loc}})$ can be used for finding variational bounds on the effective coefficients $a_{ij}^{e}(u^{(0)})$ similarly as in the linear case. Consider the case of the heat conduction; then, according to our notations $u^{(0)} = T$. For the dielectric coefficients $a_{ij}^{e}(\varphi)$ the considerations which follow are quite similar.

In this and in the next section we are interested in composite materials made by mixing two isotropic materials with conductivities $\lambda_1(T)$ and $\lambda_2(T)$, $0 < \lambda_1(T) < \lambda_2(T)$, in specified proportions θ_1 and $\theta_2 = 1 - \theta_1$. The conductivity of the composite is then given by

$$\lambda(y, T) = \lambda_1(T)\psi_1(y) + \lambda_2(T)\psi_2(y), \tag{3.1}$$

where $\psi_1(y)$ and $\psi_2(y)$ denote the characteristic functions of the sets where λ equals λ_1 and λ_2, respectively. Then the volume fractions are

$$\theta_1 = \frac{1}{|Y|}\int_Y \psi_1(y)\,dy, \qquad \theta_2 = \frac{1}{|Y|}\int_Y \psi_2(y)\,dy. \tag{3.2}$$

http://rcin.org.pl

The local problem takes the form

$$(3.3)\qquad < \mathbf{a}^e(T)\mathbf{E}, \mathbf{E} >= \inf\left\{ \frac{1}{|Y|}\int_Y \lambda(y,T)\left(\frac{\partial v}{\partial y_i} + E_i\right)\left(\frac{\partial v}{\partial y_i} + E_i\right) dy \;\Big|\; v \in H_{\mathrm{per}}(Y)\right\},$$

where $\mathbf{E} \in \mathbb{R}^3$ and $< \mathbf{a}^e(T)\mathbf{E}, \mathbf{E} >= a^e_{ij}(T)E_iE_j$. Hence elementary bounds on $\mathbf{a}^e$ readily follow, cf. [3]

$$(3.4)\qquad \Lambda_1(T)\mathbf{I} \le \mathbf{a}^e(T) \le \Lambda_2(T)\mathbf{I},$$

where $\mathbf{I} = (\delta_{ij})$ and

$$(3.5)\qquad \Lambda_1(T) = \left[\frac{1}{|Y|}\int_Y (\lambda(y,T))^{-1}\, dy\right]^{-1} = \left[(\lambda_1(T))^{-1}\theta_1 + (\lambda_2(T))^{-1}\theta_2\right]^{-1},$$

$$(3.6)\qquad \Lambda_2(T) = \frac{1}{|Y|}\int_Y \lambda(y,T)\, dy = \lambda_1(T)\theta_1 + \lambda_2(T)\theta_2\,.$$

Recall that if $\mathbf{A}$ and $\mathbf{B}$ are matrices, then $\mathbf{A} \ge \mathbf{B}$ means that $< \mathbf{AE}, \mathbf{E} >\ge < \mathbf{BE}, \mathbf{E} >$ for each $\mathbf{E} \in \mathbb{R}^3$.

We pass now to a brief discussion of Hashin - Shtrikman variational principles. We follow the paper by KOHN and MILTON [3], which is restricted to the linear case.

3.1. Variational principle for bounding $\mathbf{a}^e(T)$ from below and lower bound

Suppose that a "comparison medium" is characterized by a conductivity $\lambda^c(T)$, independent of $y \in Y$. If $\lambda^c(T)$ is restricted to the range $0 < \lambda^c(T) < \lambda_1(T)$, then $\lambda(y,T) - \lambda^c(T) > 0$ and proceeding similarly to KOHN and MILTON [3], we arrive at the variational principle of Hashin - Shtrikman type for bounding $\mathbf{a}^e(T)$ from below

$$(3.7)\qquad \frac{1}{2} < (\mathbf{a}^e(T) - \lambda^c(T)\mathbf{I})\,\mathbf{E}, \mathbf{E} > = \sup_{\boldsymbol{\sigma}} \frac{1}{|Y|}\int_Y \Big[< \boldsymbol{\sigma}, \mathbf{E} > - \frac{1}{2}(\lambda(y,T) - \lambda^c(T))^{-1}\,|\boldsymbol{\sigma}|^2 - \frac{1}{2\lambda^c(T)} < \boldsymbol{\sigma}, \nabla_y \Delta_y^{-1}\mathrm{div}_y\boldsymbol{\sigma} > \Big]\, dy.$$

Here $\boldsymbol{\sigma} = (\sigma_i)$ is a Y-periodic vector field and $|\boldsymbol{\sigma}|^2 = \sigma_i\sigma_i$; moreover $(\nabla_y v)_i = \partial v/\partial y_i$ and Δ_y denotes the Laplacian with respect to y, while Δ_y^{-1} is its inverse.

http://rcin.org.pl

To derive from (3.7) the Hashin-Shtrikman type lower bound, the test field $\boldsymbol{\sigma}$ is chosen in the form

$$\boldsymbol{\sigma}(y) = \psi_2(y)\boldsymbol{\eta}, \tag{3.8}$$

where $\boldsymbol{\eta}$ is a constant vector.

Following KOHN and MILTON [3] we finally obtain

$$\operatorname{tr}\left[(\mathbf{a}^e(T) - \lambda_1(T)\mathbf{I})^{-1}\right] \leq \frac{n}{(\lambda_2(T) - \lambda_1(T))\theta_2} + \frac{1-\theta_2}{\lambda_1(T)\theta_2} = \frac{n-1}{\Lambda_2(T) - \lambda_1(T)} + \frac{1}{\Lambda_1(T) - \lambda_1(T)}, \tag{3.9}$$

where $\operatorname{tr}\mathbf{A} = A_{ii}$ and n denotes the space dimension ($n = 3$ in the three-dimensional case).

3.2. Variational principle for bounding $\mathbf{a}^e(T)$ from above and upper bound

If $\lambda^c(T)$ is restricted to the range $\lambda_2(T) < \lambda^c(T) < \infty$, then $\lambda(y,T) - \lambda^c(T)$ is negative and the Hashin-Shtrikman type variational principle for bounding $\mathbf{a}^e(T)$ from above has the following form

$$\frac{1}{2} < (\mathbf{a}^e(T)\mathbf{E}, \mathbf{E} > = \inf_{\boldsymbol{\sigma}} \frac{1}{|Y|} \int_Y \left[< \boldsymbol{\sigma}, \mathbf{E} > - \frac{1}{2}(\lambda(y,T) - \lambda^c(T))^{-1} |\boldsymbol{\sigma}|^2 - \frac{1}{2\lambda^c(T)} < \boldsymbol{\sigma}, \nabla_y \Delta_y^{-1} \operatorname{div}_y \boldsymbol{\sigma} > \right] dy. \tag{3.10}$$

Substituting

$$\boldsymbol{\sigma}(y) = \psi_1(y)\boldsymbol{\eta} \tag{3.11}$$

into (3.10) and proceeding similarly as in [3] we obtain that

$$\operatorname{tr}\left[(\lambda_2(T)\mathbf{I} - \mathbf{a}^e(T))^{-1}\right] \leq \frac{n}{(\lambda_2(T) - \lambda_1(T))\theta_1} - \frac{1-\theta_1}{\lambda_2(T)\theta_2} = \frac{n-1}{\lambda_2(T) - \Lambda_2(T)} + \frac{1}{\lambda_2(T) - \Lambda_1(T)}. \tag{3.12}$$

4. Two-phase isotropic composites and integral representation of the homogenized coefficients

BOCCARDO and MURAT [23] have studied the convergence of solutions of Eq. (2.1) without the assumption of periodicity of the coefficients $a_{ij}^{\varepsilon}(\cdot, u^{\varepsilon})$; the

http://rcin.org.pl

symmetry of those coefficients has also not been required. Under some conditions, it has been shown that

$$\mathbf{a}^{\varepsilon}(\cdot, r) \xrightarrow{H} \bar{\mathbf{a}}(\cdot, r) \qquad (r - \text{fixed}, \quad \varepsilon \to 0). \tag{4.1}$$

Here H denotes "H-convergence". In the case of periodic coefficients, we obviously have $\bar{\mathbf{a}}(x, r) = \mathbf{a}^{e}(r)$, where $\mathbf{a}^{e}(r)$ is given by (2.7); $r \in \mathbb{R}$. To find $\bar{\mathbf{a}}(x, r)$ one needs additional information on the microstructure (we observe, that in the general case the effective coefficients may still depend on the macroscopic variable $x \in V$). For instance, such an information is available for statistically homogeneous ergodic (S.H.E) media [34]. Stochastically periodic media are a specific case of S.H.E. media. For more information on stochastic homogenization the reader should refer to [19] and to the references cited therein. Our aim in this section is not to discuss the stochastic homogenization of Eq. (2.1), which can be done by a straightforward extension of the results due to PAPANICOLAOU and VARADHAN [18] as well as to GOLDEN and PAPANICOLAOU [19]. Instead, we are going to continue the study of periodic homogenization of two-phase isotropic composites. As it has been observed by SAB [34], periodic media are a special case of S.H.E. media. Indeed, for periodic media the probability space $(\Omega, \mathcal{F}, \mathcal{P})$ is defined by the basic cell: $\Omega = [0, Y_1) \times [0, Y_2) \times [0, Y_3)$ if $Y = (0, Y_1) \times (0, Y_2) \times (0, Y_3)$; $\mathcal{F}$ is the Lebesgue σ-algebra and $P = \dfrac{1}{|Y|} dy$. It means that the results obtained in [18, 19] are also valid for the case of periodic homogenization. Particularly, recalling that in Eq. (2.7) the macroscopic field $u^{(0)}$ plays the role of a parameter, we can extend the integral representation formula due to GOLDEN and PAPANICOLAOU [19], cf. also [20, 21]. For a two-phase composite made of isotropic materials we write

$$a_{ij}(y, u^{(0)}) = a(y, u^{(0)}) \delta_{ij}\,, \tag{4.2}$$

where, for a fixed $u^{(0)}$, $a(y, u^{(0)})$ assumes only two values $a_1(u^{(0)})$ and $a_2(u^{(0)})$ with $0 < a_1(u^{(0)}) < a_2(u^{(0)})$. Thus we have, cf. (3.1)

$$a(y, u^{(0)}) = a_1(u^{(0)}) \psi_1(y) + a_2(u^{(0)}) \psi_2(y). \tag{4.3}$$

Hence we conclude that important is only the ratio

$$h(u^{(0)}) = \frac{a_2(u^{(0)})}{a_1(u^{(0)})} \qquad \left(\text{or} \quad h(u^{(0)}) = \frac{a_1(u^{(0)})}{a_2(u^{(0)})} \right). \tag{4.4}$$

In view of Eq. (2.7) we write

$$a_{ij}^{e}(u^{(0)}) = a_1(u^{(0)}) \int_Y \left[\psi_1(y) + h(u^{(0)}) \psi_2(y) \right] \tilde{E}_j^{(i)}\, dy, \tag{4.5}$$

http://rcin.org.pl

where $\tilde{E}_j^{(i)} = \dfrac{\partial \chi^{(i)}(y, u^{(0)})}{\partial y_j} + \delta_{ij}$ provided that $Y = (0,1)^3$ (for the sake of simplicity). Thus the effective transport coefficients are functions of $h(u^{(0)})$; we write $a_{ij}^e(u^{(0)}) = \tilde{a}_{ij}(h(u^{(0)}))$.

Suppose now that $h(u^{(0)})$ is a complex variable, cf. [19]. It means that the coefficients $a_1(u^{(0)})$ and $a_2(u^{(0)})$ are treated as complex-valued coefficients. Physically, imaginary parts characterize dissipative properties of the composite.

From the mathematical point of view, it is then possible to apply the theorem on the resolvent representation [19–21].

PROPOSITION 1. The function $\tilde{a}_{ij}$ is an analytic function of the complex variable $h(u^{(0)})$ everywhere except on the negative real axis.

P r o o f. For $u^{(0)}$ fixed, it is similar to the one given in [19], provided that in the formula (4.7) of the last paper one takes $\mathcal{P}(d\omega) = dy$, $\Omega = Y$ (more precisely $\Omega = [0,1)^3$). □

Equation (4.5) may be written as follows

$$m_{ij}(h(u^{(0)})) = \frac{a_{ij}^e(u^{(0)})}{a_1(u^{(0)})} = \int_Y \left[\psi_1(y) + h(u^{(0)})\psi_2(y)\right] \tilde{E}_j^{(i)}\, dy. \tag{4.6}$$

Now we are in a position to state the main result of this section

THEOREM 2 (REPRESENTATION FORMULA). *Let*

$$s(u^{(0)}) = \frac{1}{1 - h(u^{(0)})}, \qquad F_{ij}(s(u^{(0)})) = \delta_{ij} - m_{ij}(h(u^{(0)})). \tag{4.7}$$

There exist finite Borel measures $\mu_{ij}(dz)$ defined for $0 \le z \le 1$ such that the diagonals $\mu_{ii}(dz)$ (no summation over i) are positive measures satisfying

$$F_{ij}(s(u^{(0)})) = \int_0^1 \frac{\mu_{ij}(dz)}{s(u^{(0)}) - z}, \qquad i,j = 1,2,3 \tag{4.8}$$

for all complex $s(u^{(0)})$ outside $0 \le \operatorname{Re} s(u^{(0)}) \le 1$, $\operatorname{Im} s(u^{(0)}) = 0$.

P r o o f. For a fixed $u^{(0)}$ it is quite similar to the proof of the representation formula given by GOLDEN and PAPANICOLAOU [19], where h, $\mathcal{P}(d\omega)$, s and L_i should by replaced by $h(u^{(0)})$, dy, $s(u^{(0)})$ and $\partial/\partial y_i$, respectively.

COROLLARY 1. Suppose that the medium is macroscopically isotropic. Then $m_{ij}\left(h(u^{(0)})\right) = m(h(u^{(0)}))\delta_{ij}$ and

$$1 - m(h(u^{(0)})) = F(s(u^{(0)})) = \int_0^1 \frac{\mu(dz)}{s(u^{(0)}) - z}, \quad s(u^{(0)}) \text{ outside } [0,1]. \tag{4.9}$$

http://rcin.org.pl

In the literature, one can find alternative forms of the integral in the r.h.s. of the last relation like the one we shall use in the next section, cf. also [35]

$$m(h(u^{(0)})) - 1 = \eta(u^{(0)}) f_1(\eta(u^{(0)})), \tag{4.10}$$

where

$$f_1(\eta(u^{(0)})) = \int_0^1 \frac{\mu(dz)}{1 + \eta(u^{(0)})z}, \qquad \eta(u^{(0)}) = h(u^{(0)}) - 1, \tag{4.11}$$

is a Stieltjes function defined in the cut $(-\infty \leq \eta(u^{(0)}) \leq -1)$ complex plane; here $s(u^{(0)}) = -(1/\eta(u^{(0)}))$.

Just this representation formula will be used in Sec. 7 for the determination of universal curves allowing for finding lower and upper bounds on the effective conductivity $\lambda_e(T)$ for an isotropic, heat conducting medium by applying Padé approximants.

REMARK 2. To the best of our knowledge, in the available literature a generalization of the very nice representation formula (4.8) to composites made of more than two isotropic components or of anisotropic materials is still lacking. Partial results have been presented in [20, 21] by using several complex variables.

5. Microperiodic layered composite

Layered composites are often used in engineering practice. In this section we shall derive the explicit form of the homogenized coefficients for the lamination in the direction y_1, provided that the composite is made of two materials. More general cases of layering can be treated similarly.

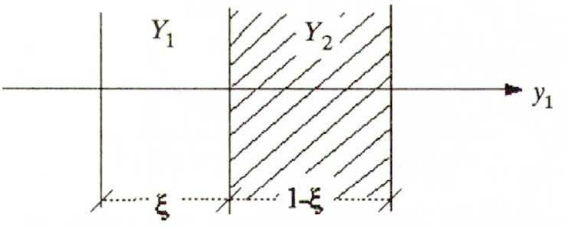

FIG. 1. Basic cell for two-phase layered composites.

Now the basic cell reduces to an interval, say (0,1). Thus the material coefficients of such a composite are specified by

$$a_{ij}(y,T) = \begin{cases} a_{ij}^{(1)}(T) & \text{if} \quad y_1 \in (0,\xi), \\ a_{ij}^{(2)}(T) & \text{if} \quad y_1 \in (\xi,1). \end{cases} \tag{5.1}$$

http://rcin.org.pl

After lengthy, though simple calculations the local functions can be found in a closed form; they are piecewise linear, cf. [32, 33]

$$\frac{\partial \chi^{(k)}(y_1, T)}{\partial y_1} = \begin{cases} -(1-\xi)\frac{1}{A(\xi,T)}[\![a_{1k}(T)]\!] & \text{if} \quad y_1 \in (0, \xi), \\ \xi \frac{1}{A(\xi,T)}[\![a_{1k}(T)]\!] & \text{if} \quad y_1 \in (\xi, 1). \end{cases} \tag{5.2}$$

From Eq. (2.7) we obtain the homogenized coefficients

$$a^{\varepsilon}_{kl}(T) = < a_{kl}(y_1, T) > -\xi(1-\xi)\frac{1}{A(\xi, T)}[\![a_{1k}(T)]\!][\![a_{1l}(T)]\!], \tag{5.3}$$

where

$$\begin{aligned} < a_{kl}(y_1, T) > &= \xi a^{(1)}_{kl}(T) + (1-\xi)a^{(2)}_{kl}(T), \\ A(\xi, T) &= \xi a^{(2)}_{11}(T) + (1-\xi)a^{(1)}_{11}(T), \\ [\![a_{ij}(T)]\!] &= a^{(2)}_{ij}(T) - a^{(1)}_{ij}(T). \end{aligned}$$

If $a^{(1)}_{ij} = 0$ for $i \neq j$ and $a^{(2)}_{ij} = 0$ for $i \neq j$ then the coefficients $a^h_{11}(T)$, $a^h_{22}(T)$, $a^h_{33}(T)$ are given by

$$\begin{aligned} a^h_{11}(T) &= \frac{1}{\xi \dfrac{1}{a^{(1)}_{11}(T)} + (1-\xi)\dfrac{1}{a^{(2)}_{11}(T)}}, \\ a^h_{22}(T) &= < a_{22}(T, y) >, \qquad a^h_{33}(T) = < a_{33}(T, y) > . \end{aligned} \tag{5.4}$$

If we set

$$h(T) = \frac{a^{(1)}_{11}(T)}{a^{(2)}_{11}(T)},$$

then Eq. $(5.4)_1$ takes the form

$$\frac{a^h_{11}(T)}{a^{(2)}_{11}(T)} = \frac{h(T)}{\xi + (1-\xi)h(T)}. \tag{5.5}$$

Consider now a particular case by assuming that layers are made of isotropic materials while the dependence on the temperature is linear:

$$a_{ij}(y_1, T) = \begin{cases} \delta_{ij}(\alpha_1 + \beta_1 T) & \text{if} \quad y_1 \in (0, \xi), \\ \delta_{ij}(\alpha_2 + \beta_2 T) & \text{if} \quad y_1 \in (\xi, 1). \end{cases} \tag{5.6}$$

Then we have

$$[\![a_{ij}]\!] = ([\![\alpha]\!] + [\![\beta]\!]T)\,\delta_{ij}, \tag{5.7}$$

http://rcin.org.pl

and

$$a_{ij}^{e}(T) = \delta_{ij}\{[\xi\alpha_1 + (1-\xi)\alpha_2)] + T[\xi\beta_1 + (1-\xi)\beta_2]\} - \delta_{i1}\delta_{1j}\xi(1-\xi)\frac{[\alpha_2 - \alpha_1 + T(\beta_2 - \beta_1)]^2}{\xi\alpha_2 + (1-\xi)\alpha_1 + T[\xi\beta_2 + (1-\xi)\beta_1]}. \tag{5.8}$$

From the last relation we conclude that the only nontrivial homogenized coefficient is given by (the remaining effective coefficients are merely averages):

$$a_{11}^{e}(T) = a(\xi) + b(\xi)T + \frac{c(\xi)}{T - d(\xi)}, \tag{5.9}$$

where

$$a(\xi) = \overline{\alpha}(\xi) - \xi(1-\xi)\left[2\frac{[\![\alpha]\!][\![\beta]\!]}{\tilde{\beta}(\xi)} - \tilde{\alpha}(\xi)\left(\frac{[\![\beta]\!]}{\tilde{\beta}(\xi)}\right)^2\right],$$

$$b(\xi) = \overline{\beta}(\xi) - \xi(1-\xi)\frac{([\![\beta]\!])^2}{\tilde{\beta}(\xi)},$$

$$c(\xi) = -\frac{\xi(1-\xi)}{\tilde{\beta}}\left([\![\alpha]\!] - [\![\beta]\!]\frac{\tilde{\alpha}}{\tilde{\beta}(\xi)}\right)^2,$$

$$d(\xi) = \frac{\tilde{\alpha}(\xi)}{\tilde{\beta}(\xi)},$$

$$\overline{\alpha} = \xi\alpha_1 + (1-\xi)\alpha_2, \qquad \overline{\beta} = \xi\beta_1 + (1-\xi)\beta_2,$$

$$\tilde{\alpha} = \xi\alpha_2 + (1-\xi)\alpha_1, \qquad \tilde{\beta} = \xi\beta_2 + (1-\xi)\beta_1.$$

We note that though in both layers the conductivity coefficients depend linearly on the temperature, yet the dependence of a_{11}^{e} on T is nonlinear.

5.1. Temperature distribution in layered and homogenized composites

Let us investigate a two-phase isotropic composite consisting of n layers made of a material with the conductivity coefficient $\lambda_1(T) = \alpha_1 + \beta_1 T$ and n layers with the conductivity coefficient $\lambda_2(T) = \alpha_2 + \beta_2 T$, cf. Fig. 2.

The layers with odd and even numbers have the thickness l_1/n and l_2/n, respectively. Obviously, $l = l_1 + l_2$ denotes the thickness of the composite. The conductivity coefficient in the composite is thus given by

$$\lambda(x,T) = \begin{cases} \lambda_1(T) & \text{if } x \in \Delta_i \text{ and } i \text{ is odd,} \\ \lambda_2(T) & \text{if } x \in \Delta_i \text{ and } i \text{ is even,} \end{cases}$$

http://rcin.org.pl

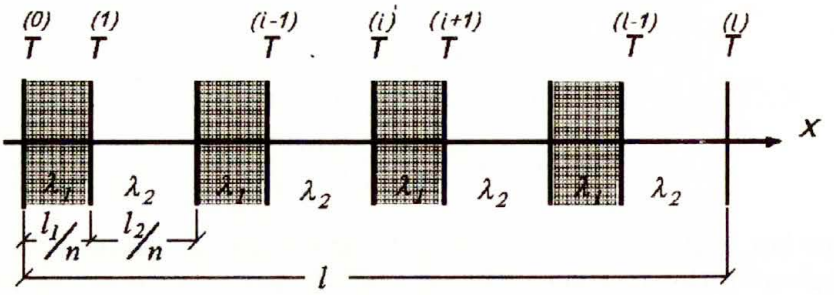

FIG. 2. Layered composite.

where $\Delta_i = (x_{i-1}, x_i)$; moreover

$$x_i = \begin{cases} \dfrac{l}{2n} i & \text{if } i \text{ is even,} \\ \dfrac{l}{2n}(i-1) + \dfrac{l_1}{n} & \text{if } i \text{ is odd.} \end{cases}$$

Denote by $\overset{(i)}{T}(x)$ the temperature distribution in the interval Δ_i; $\overset{(i-1)}{T}$ and $\overset{(i)}{T}$ are temperatures at the end point of Δ_i. The axis $0x$ is perpendicular to the layers.

The heat equation in the layers with odd numbers is given by

$$\frac{d}{dx}\left[\left(\alpha_1 + \beta_1 \overset{(i)}{T}(x)\right)\frac{d}{dx}\overset{(i)}{T}(x)\right] = 0. \tag{5.10}$$

Similarly, in the layers with even numbers we have

$$\frac{d}{dx}\left[\left(\alpha_2 + \beta_2 \overset{(i)}{T}(x)\right)\frac{d}{dx}\overset{(i)}{T}(x)\right] = 0. \tag{5.11}$$

Solving Eq. (5.10) we obtain

$$\overset{(i)}{T}(x) = \frac{1}{k_1}\left[1 - \sqrt{1 + 2k_1(\overset{(i)}{A}_1 x + \overset{(i)}{B}_1)}\right], \quad x \in \Delta_i \quad (i - \text{odd}), \tag{5.12}$$

where $k_1 = \beta_1/\alpha_1$ and

$$\overset{(i)}{A}_1 = \frac{n}{l_1}\left[\overset{(i)}{T} - \overset{(i-1)}{T} + \frac{k_1}{2}(\overset{(i)}{T}^2 - \overset{(i-1)}{T}^2)\right],$$

$$\overset{(i)}{B}_1 = \frac{n}{l_1}\left[x_i \overset{(i)}{T} - x_{i-1}\overset{(i-1)}{T} + \frac{k_1}{2}(x_i \overset{(i)}{T}^2 - x_{i-1}\overset{(i-1)}{T}^2)\right].$$

http://rcin.org.pl

Similarly Eq. (5.11) yields

$$\overset{(i)}{T}(x) = \frac{1}{k_2}\left[1 - \sqrt{1 + 2k_2(\overset{(i)}{A}_2 x + \overset{(i)}{B}_2)}\right], \quad x \in \Delta_i \quad i - \text{even}, \tag{5.13}$$

where $k_2 = \beta_2/\alpha_2$ and

$$\overset{(i)}{A}_2 = \frac{n}{l_2}\left[\overset{(i)}{T} - \overset{(i-1)}{T} + \frac{k_2}{2}(\overset{(i)}{T}^2 - \overset{(i-1)}{T}^2)\right],$$

$$\overset{(i)}{B}_2 = \frac{n}{l_2}\left[x_i \overset{(i)}{T} - x_{i-1} \overset{(i-1)}{T} + \frac{k_2}{2}(x_i \overset{(i)}{T}^2 - x_{i-1} \overset{(i-1)}{T}^2)\right].$$

Assuming continuity of the heat flux at the points x_i $(i = 1, \ldots, 2n-1)$

$$\left(\alpha_1 + \beta_1 \overset{(i)}{T}(x_i)\right) \frac{d}{dx} \overset{(i)}{T}(x_i) = \left(\alpha_2 + \beta_2 \overset{(i+1)}{T}(x_i)\right) \frac{d}{dx} \overset{(i+1)}{T}(x_i), \quad i - \text{odd},$$

$$\left(\alpha_2 + \beta_2 \overset{(i)}{T}(x_i)\right) \frac{d}{dx} \overset{(i)}{T}(x_i) = \left(\alpha_1 + \beta_1 \overset{(i+1)}{T}(x_i)\right) \frac{d}{dx} \overset{(i+1)}{T}(x_i), \quad i - \text{even},$$

we obtain

$$\overset{(i)}{A}_1 = \overset{(i+1)}{A}_2 \quad \text{if } i \text{ is odd}, \qquad \overset{(i)}{A}_2 = \overset{(i+1)}{A}_1 \quad \text{if } i \text{ is even}.$$

Hence we derive the recurrence formula for the determination of $\overset{(i)}{T}$ $(i = 1, \ldots, 2n-1)$ provided that $\overset{(0)}{T}$ and $\overset{(l)}{T}$ are prescribed:

$$\overset{(i)}{T} = \begin{cases} -C + \sqrt{C^2 + \frac{2C}{l}\left[l_2 \overset{(i+1)}{T} + l_1 \overset{(i-1)}{T} + k_1 l_2 \overset{(i+1)}{T}^2 + k_2 l_1 \overset{(i-1)}{T}^2\right]}, & \text{for } i \text{ even}, \\ -C + \sqrt{C^2 + \frac{2C}{l}\left[l_2 \overset{(i-1)}{T} + l_1 \overset{(i+1)}{T} + k_1 l_2 \overset{(i-1)}{T}^2 + k_2 l_1 \overset{(i+1)}{T}^2\right]}, & \text{for } i \text{ odd}, \end{cases} \tag{5.14}$$

where

$$2C = \frac{l}{l_1 k_2 + l_2 k_1}.$$

In the interior of the intervals Δ_i the temperature is given by (5.12) and (5.13).

Now we shall compare the temperature at the interfaces with the (*one-dimensional*) homogenized solution. The homogenized equation has the form

$$\frac{d}{dx}\left[a_{11}^e(T(x))\frac{d}{dx}T(x)\right] = 0.$$

http://rcin.org.pl

We recall that $a_{11}^{\varepsilon}(T)$ is now specified by (5.9). Then the solution of the last (homogenized) equation is given by

$$aT + \frac{b}{2}T^2 + c\ln|T + d| = Ax + B, \tag{5.15}$$

where

$$A = \frac{1}{x_l - x_0}\left(a\left(\overset{(l)}{T} - \overset{(0)}{T}\right) + \frac{b}{2}\left(\overset{(l)}{T}{}^2 - \overset{(0)}{T}{}^2\right) + c\ln\left|\frac{\overset{(l)}{T} + d}{\overset{(0)}{T} + d}\right|\right),$$

$$B = \frac{1}{x_l - x_0}\left(a\left(x_l\overset{(0)}{T} - x_0\overset{(l)}{T}\right) + \frac{b}{2}\left(x_l\overset{(0)}{T}{}^2 - x_0\overset{(l)}{T}{}^2\right) + c\ln\left|\frac{\left(\overset{(l)}{T} + d\right)^{x_0}}{\left(\overset{(0)}{T} + d\right)^{x_l}}\right|\right)$$

provided that the boundary conditions are:

$$T(x_0) = \overset{(0)}{T}, \qquad T(x_l) = \overset{(l)}{T}.$$

5.2. Example

Let us assume that

$$\lambda_1(T) = 0.5 + 2T, \qquad \lambda_2(T) = 0.8 + 1.5T,$$

$$l = 10, \qquad n = 5, \qquad \frac{l_1}{l} = 0.4, \qquad \overset{(0)}{T} = 0, \qquad \overset{(l)}{T} = 15.$$

In Fig. 3 the dots denote the interface temperatures calculated according to (5.14). The continuous curve represents the temperature distribution obtained from the solution of the homogenized problem, cf. (5.15).

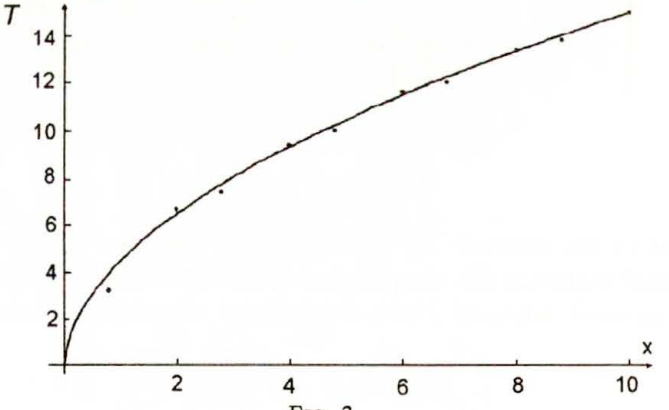

FIG. 3.

http://rcin.org.pl

6. Ritz method

The Ritz method offers a possibility of determination of local functions in an approximate manner.

6.1. General case

We shall be looking for an approximate solution of the local problem by the Ritz method. Accordingly, we take, cf. [32, 33]

$$\chi^{(m)}(y,T) = \chi_a^{(m)}(T)\phi^a(y) = \sum_a \chi_a^{(m)}(T)\phi^a(y). \tag{6.1}$$

Here $\phi^a(y)$, $a = 1, 2, \ldots, \overline{a}$ are prescribed Y-periodic functions and $\chi_a^m(T)$ are unknown constants.

The local problem (2.5) should now be satisfied for test functions of the form

$$v = v_a\phi^a(y). \tag{6.2}$$

To determine the unknown constants one has to solve the following algebraic equations:

$$\chi_a^{(m)}A^{ab} = B^{mb}, \tag{6.3}$$

where

$$A^{ab}(T) = \int_Y a_{ij}(y,T)\phi^a_{,i}\phi^b_{,j}\,dy,$$

$$B^{ja}(T) = -\int_Y a_{ji}(y,T)\phi^a_{,i}\,dy,$$

with $\phi^a_{,i} = \dfrac{\partial\phi^a}{\partial y_i}$. For a given macroscopic temperature T the solution is

$$\chi_a^{(k)}(T) = (\mathbf{A}^{-1}(T))_{ab}B^{kb}(T).$$

Here $\mathbf{A}^{-1}$ is the inverse matrix of $\mathbf{A}$.

We finally obtain

$$a^e_{ij}(T) = < (a_{ij}(y,T) > + (\mathbf{A}^{-1}(T))_{ab}B^{ib}(T)B^{ja}(T). \tag{6.4}$$

http://rcin.org.pl

6.2. Specific two-dimensional problem: two-phase composite

To illustrate the outlined general procedure we consider a two-phase composite material with the conductivity coefficients given by

$$a_{ij}(y,T) = \begin{cases} \lambda_1(T)\delta_{ij} & \text{if } y \in Y_1, \\ \lambda_2(T)\delta_{ij} & \text{if } y \in Y_2. \end{cases} \tag{6.5}$$

Now $y = (y_1, y_2)$, $\phi^a_{,3} = \dfrac{\partial \phi^a}{\partial y_3} = 0$ and $A^{a,b}(T)$ takes the form

$$A^{a,b}(T) = \lambda_2(T)F[a,b,i,i] - [\![\lambda(T)]\!]f[a,b,i,i], \tag{6.6}$$

$$B^{ja}(T) = [\![\lambda(T)]\!]f[a,j]. \tag{6.7}$$

Here

$$f[a,b,i,j] = \int_{Y_1} \frac{\partial \phi^a}{\partial y_i}\frac{\partial \phi^b}{\partial_j} dy_1\, dy_2, \qquad F[a,b,i,j] = \int_{Y} \frac{\partial \phi^a}{\partial y_i}\frac{\partial \phi^b}{\partial y_j} dy_1 dy_2, \tag{6.8}$$

$$f[a,i] = \int_{Y_1} \frac{\partial \phi^a}{\partial y_i} dy_1\, dy_2, \qquad [\![\lambda(T)]\!] = \lambda_2(T) - \lambda_1(T).$$

Consider now a particular case of a square inclusion as presented in Fig. 4.

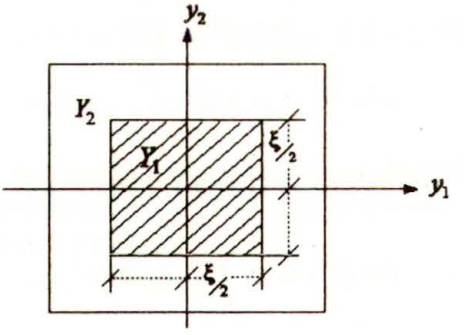

FIG. 4.

The base functions are assumed in the following form

$$\phi^1(y_1,y_2) = \begin{cases} \xi y_1 + \dfrac{\xi}{2} & \text{if } y_1 \in \left(-\dfrac{1}{2}, -\dfrac{\xi}{2}\right), \\ -(1-\xi)y_1 & \text{if } y_1 \in \left(-\dfrac{\xi}{2}, \dfrac{\xi}{2}\right), \\ \xi y_1 - \dfrac{\xi}{2} & \text{if } y_1 \in \left(\dfrac{\xi}{2}, \dfrac{1}{2}\right); \end{cases} \tag{6.9}$$

http://rcin.org.pl

$$\phi^2(y_1,y_2)=\begin{cases}\xi y_2+\dfrac{\xi}{2} & \text{if } y_2\in\left(-\dfrac{1}{2},-\dfrac{\xi}{2}\right),\\ -(1-\xi)y_2 & \text{if } y_2\in\left(-\dfrac{\xi}{2},\dfrac{\xi}{2}\right),\\ \xi y_2-\dfrac{\xi}{2} & \text{if } y_2\in\left(\dfrac{\xi}{2},\dfrac{1}{2}\right);\end{cases} \tag{6.10}$$

$$\phi^3(y_1,y_2)=\cos(\pi y_1)\sin(2\pi y_2), \tag{6.11}$$

$$\phi^4(y_1,y_2)=\cos(\pi y_2)\sin(2\pi y_1). \tag{6.12}$$

Next, we calculate

$$\phi^1_{,1}(y_1,y_2)=\begin{cases}-(1-\xi) & \text{if } y_1\in\left(-\dfrac{\xi}{2},\dfrac{\xi}{2}\right),\\ \xi & \text{if } y_1\in\left(\dfrac{-1}{2},-\dfrac{\xi}{2}\right)\cup\left(\dfrac{\xi}{2},\dfrac{1}{2}\right);\end{cases} \tag{6.13}$$

$$\phi^1_{,2}(y_1,y_2)=0,\qquad \phi^2_{,1}(y_1,y_2)=0; \tag{6.14}$$

$$\phi^2_{,2}(y_1,y_2)=\begin{cases}-(1-\xi) & \text{if } y_2\in\left(-\dfrac{\xi}{2},\dfrac{\xi}{2}\right),\\ \xi & \text{if } y_2\in\left(-\dfrac{1}{2},-\dfrac{\xi}{2}\right)\cup\left(\dfrac{\xi}{2},\dfrac{1}{2}\right);\end{cases} \tag{6.15}$$

$$\begin{aligned}\phi^3_{,1}(y_1,y_2)&=-\pi\sin(\pi y_1)\sin(2\pi y_2),\\ \phi^3_{,2}(y_1,y_2)&=2\pi\cos(\pi y_1)\cos(2\pi y_2);\end{aligned} \tag{6.16}$$

$$\begin{aligned}\phi^4_{,1}(y_1,y_2)&=2\pi\cos(2\pi y_1)\cos(\pi y_2),\\ \phi^4_{,2}(y_1,y_2)&=-\pi\sin(2\pi y_1)\sin(\pi y_2).\end{aligned} \tag{6.17}$$

Substituting (6.13)–(6.17) into (6.8), from (6.4) we can determine the dependence of the approximate value of the effective conductivity coefficient λ_e on the macroscopic temperature T. To find such a dependence it has been assumed that

$$\theta=\frac{|Y_1|}{|Y|}=\xi^2=0.75,$$

while the conductivity coefficients of the phases are given by:

a) (see Fig. 5) $\lambda_1=0.21+0.005T$, $\lambda_2=37.25+0.048T$,

b) (see Fig. 6) $\lambda_1=37.25+0.048T$, $\lambda_2=0.21+0.005T$.

http://rcin.org.pl

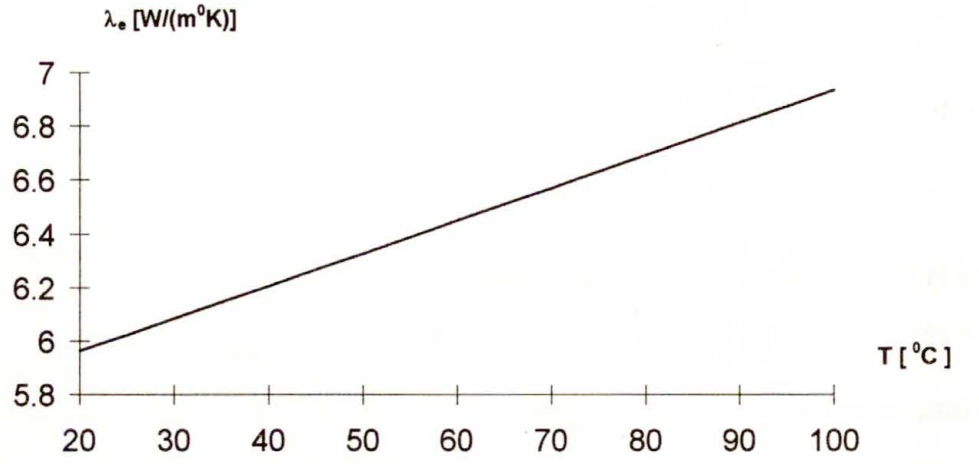

FIG. 5. The effective conductivity versus temperature; in the inclusion: $\lambda_1 = 0.21 + 0.005T$, in the matrix: $\lambda_2 = 37.25 + 0.048T$, volume ratio: $\theta = 0.75$.

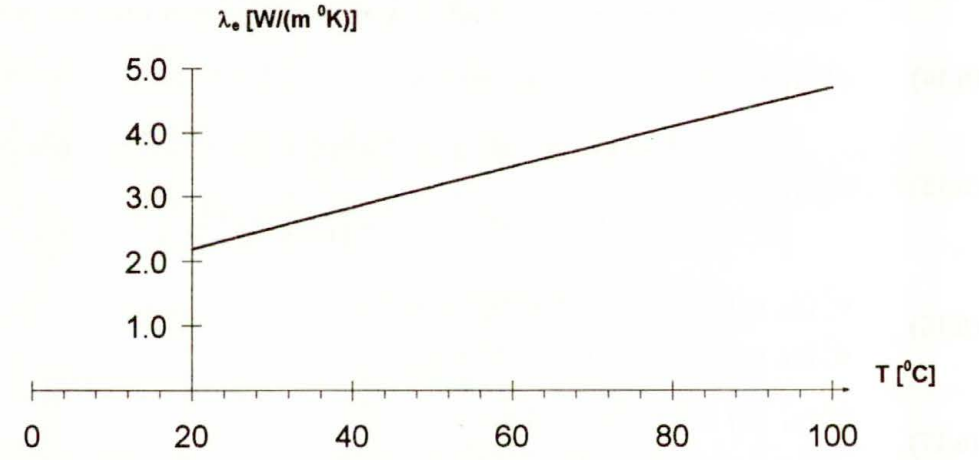

FIG. 6. The effective conductivity versus temperature; in the inclusion: $\lambda_1 = 37.25 + 0.048T$, in the matrix: $\lambda_2 = 0.21 + 0.005T$, volume ratio: $\theta = 0.75$.

7. Bounds on the effective conductivity of two-phase composites. Padé approximants method

In this section we shall use the formulae for finding bounds on the effective heat conductivity $\lambda_e(\eta(T))$ by assuming that at the macroscopic scale the composite is isotropic. Towards this end the method of Padé approximants is applied. The same procedure can also be used for the determination of bounds on the diagonal elements of the effective conductivity matrix, what follows from Theorem 2. For macroscopically isotropic materials the Stieltjes integral representation

http://rcin.org.pl

of the effective conductivity $\lambda_e(\eta(T))/\lambda_2(T)$ is given by, cf. (4.11),

$$\frac{\lambda_e(\eta(T))}{\lambda_2(T)} - 1 = \eta(T) f_1(\eta(T)) = \eta(T) \int_0^1 \frac{d\gamma_1(z)}{1+\eta(T)z}, \quad 0 \le z \le 1. \tag{7.1}$$

Moreover the following inequality is satisfied, cf. [19]

$$\lim_{\eta(T)\to -1^+} \eta(T) f_1(\eta(T)) \ge -1. \tag{7.2}$$

Consider the power expansion of $\eta(T)f_1(\eta(T))$ at $\eta(T) = 0$:

$$\eta(T) f_1(\eta(T)) = \sum_{n=1}^{\infty} c_n \eta^n(T), \tag{7.3}$$

where

$$c_n = (-1)^{n+1} \int_0^1 z^{n-1} d\gamma_1(z). \tag{7.4}$$

The one-point Padé approximants $[p/M']$ and $[p/M'']$ to the effective conductivity $\lambda_e(\eta(T))/\lambda_2(T)$ represented by $\eta(T)f_1(\eta(T))$ are given by:

$$[p/M'] = \frac{a'_1\eta(T) + a'_2\eta^2(T) + \cdots + a'_{M'}\eta^{p-M'}(T)}{1 + b'_1\eta(T) + b'_2\eta^2(T) + \cdots + b'_{M'}\eta^{M'}(T)}, \quad M' = E(p/2), \tag{7.5}$$

$$[p/M''] = \frac{a''_1\eta(T) + a''_2\eta^2(T) + \cdots + a''_{M''}\eta^{p+1-M''}(T)}{1 + b''_1\eta(T) + b''_2\eta^2(T) + \cdots + b''_{M''}\eta^{M''}(T)}, \tag{7.6}$$

$$M'' = E((p+1)/2).$$

Here $E(w)$ is the entier function, i.e. the greatest natural number not exceeding w. Observe that now $[p/M']$ and $[p/M'']$ depend on the macroscopic temperature T.

Consider the power expansions of $[p/M']$ and $[p/M'']$ at $\eta(T) = 0$:

$$[p/M'] = \sum_{n=1}^{\infty} c'_n \eta^n(T), \qquad [p/M''] = \sum_{n=1}^{\infty} c''_n \eta^n(T). \tag{7.7}$$

DEFINITION 1. *The rational functions* (7.5), (7.6) *are the one-point Padé approximants to the Stieltjes function* (7.1):

(i) *of the type* $[p/M']$, $M' = E(p/2)$, *if*

$$c'_n = c_n^{(1)} \qquad \text{for } n = 1, 2, \ldots, p; \tag{7.8}$$

http://rcin.org.pl

(ii) *of the type* $[p/M'']$, $M'' = E((p+1)/2)$, *if*

$$c_n'' = c_n^{(1)} \quad \text{for } n = 1, 2, \ldots, p, \qquad [p/M''] = -1 \quad \text{for } \eta(T) = -1. \tag{7.9}$$ □

The parameter p *appearing in this definition denotes a number of available coefficients of the power series* (7.3) *matched by Padé approximants* $[p/M']$ *and* $[p/M'']$.

Let us recall the basic results of the paper [38].

THEOREM 3. *The one-point Padé approximants* $[p/M']$ *and* $[p/M'']$ *satisfy the following inequalities:*

(i) *If* $-1 < \eta(T) < 0$ *then*

$$[p/M'] > [p+1/M'], \tag{7.10}$$

$$[p/M''] < [p+1/M''], \tag{7.11}$$

$$[p/M'] \geq \eta(T) f_1(\eta(T)) \geq [p/M'']. \tag{7.12}$$

(ii) *If* $0 < \eta(T) < \infty$ *then*

$$(-1)^p [p/M'] < (-1)^p [p+2/M'], \tag{7.13}$$

$$(-1)^p [p/M''] > (-1)^p [p+2/M''], \tag{7.14}$$

$$(-1)^p [p/M'] \leq (-1)^p \eta(T) f_1(\eta(T)) \leq (-1)^p [p/M'']. \tag{7.15}$$

Moreover

$$\eta(T) f_1(\eta(T)) = \lim_{p\to\infty} [p/M'] = \lim_{p\to\infty} [p/M''].$$

The inequalities (7.10) – (7.12) *and* (7.13) – (7.15) *have the consequence that Padé approximants* $[p/M']$ *and* $[p/M'']$ *form the best upper and lower bounds on* $\eta(T) f_1(\eta(T))$ *obtainable using only* p *coefficients of a series* (7.3), *and that the use of additional coefficients (higher* p*) improves the bounds.* □

It is convenient to represent the Padé approximants $[p/M']$ and $[p/M'']$ by S-continued fractions, cf. [36],

$$[p/M'] = \frac{g_1\eta(T)}{1} + \frac{g_2\eta(T)}{1} + \cdots + \frac{g_{p-2}\eta(T)}{1} + \frac{g_{p-1}\eta(T)}{1} + \frac{g_p\eta(T)}{1}, \tag{7.16}$$

$$[p/M''] = \frac{g_1\eta(T)}{1} + \frac{g_2\eta(T)}{1} + \cdots + \frac{g_{p-1}\eta(T)}{1} + \frac{g_p\eta(T)}{1} + \frac{V_{p+1}\eta(T)}{1}, \tag{7.17}$$

where

$$\frac{g_1\eta(T)}{1} + \frac{g_2\eta(T)}{1} + \cdots = \frac{g_1\eta(T)}{1 + \dfrac{g_2\eta(T)}{1 + \cdots}}.$$

http://rcin.org.pl

The coefficients g_m $(m = 1, 2, \ldots, p)$ are determined by the following recurrence relations

$$(7.18)\qquad \begin{cases} m = 1, 2, \ldots, p, \quad g_m = c_1^{(m)}, \\ \begin{cases} n = 1, 2, \ldots, p - m, \\ c_0^{(1+m)} = 1, \quad c_n^{(1+m)} = -\dfrac{1}{c_1^{(m)}} \left\{ \sum_{j=0}^{n-1} c_j c_{n+1-j}^{(m)} \right\}, \end{cases} \end{cases}$$

with input data c_m $(m = 1, 2, \ldots, p)$ given by (7.3), cf. [41]. Also a simple recurrence formulae determine the coefficients V_{p+1}

$$(7.19)\qquad V_1 = 1, \qquad V_{1+j} = \frac{V_j - g_j}{V_j}, \quad j = 1, 2, \ldots, p$$

and the Padé approximants $[p/M']$ $([p/M''])$

$$(7.20)\qquad \begin{gathered} Q^{(0)} = V_{p+1} = 0 \quad \text{for} \quad [p/M'], \qquad (Q^{(0)} = \eta(T) V_{p+1} \quad \text{for} \quad [p/M'']), \\ Q^{(j+1)} = \frac{\eta(T) g_{p-j}}{1 + Q^{(j)}}, \qquad j = 0, 1, \ldots, p - 1, \\ [p/M'] = Q^{(p)}, \qquad ([p/M'] = Q^{(p)}). \end{gathered}$$

Relations (7.18) – (7.20) allow us to compute Padé approximants bounds on $\lambda_e(\eta(T))/\lambda_2(T)$ in terms of $[p/M']$ and $[p/M'']$, from power expansion given by (7.3).

Let us pass now to an application of the Padé approximants method for the determination of the nonlinear effective conductivity $\lambda_e(T)$ of a composite, which consists of the regularly spaced and equally-sized cylinders of the conductivity $\lambda_2(T)$ embedded in a matrix material of the conductivity $\lambda_1(T)$. We set: $\theta = \pi\rho^2$-volume fraction, ρ-radius of cylinders, $\eta(T) = (\lambda_1(T)/\lambda_2(T)) - 1$-nondimensional conductivity. The input data for determining the Padé bounds given by power series, cf. (7.3),

$$(7.21)\qquad \eta(T) f_1(\eta(T)) = \sum_{n=1}^{\infty} (\pi d_1^{(n)} \rho^2) \eta^n(T), \qquad c_n = \pi d_1^{(n)} \rho^2,$$

have been computed by means of the recurrence formulae derived in [39]:

$$(7.22)\qquad d_m^{n+1} = -\sum_{k=1}^{\infty} d_k^n \left(\frac{1}{2} \delta_{mk} + a_{km} \frac{m \rho^{k+m}}{2k!} \right), \qquad d_m^{(1)} = \delta_{m1},$$

$$(7.23)\qquad a_{km} = (-1)^k \frac{(m + k)!}{m!} \left(A_{km} + \frac{1}{2} \pi \delta_{(m+k)2} \right), \qquad \delta_{mk} = \begin{cases} 1, & \text{if } m = k, \\ 0, & \text{if } m \neq k. \end{cases}$$

Here A_{km} are the coefficients of the Wigner potential evaluated in [42, 43]. The low order Padé bounds $[p/M']$ and $[p/M'']$ on $\lambda_e(\eta(T))/\lambda_2(T)$ of a square array of cylinders are depicted in Fig. 7. According to (4.11) the obtained bounds are

http://rcin.org.pl

universal, i.e., they are valid for arbitrary, continuous functions $\lambda_2(T)$ and $\lambda_1(T)$. From those universal bounds one can pass to bounds on λ_e as a function of T, cf. Figs. 8, 9.

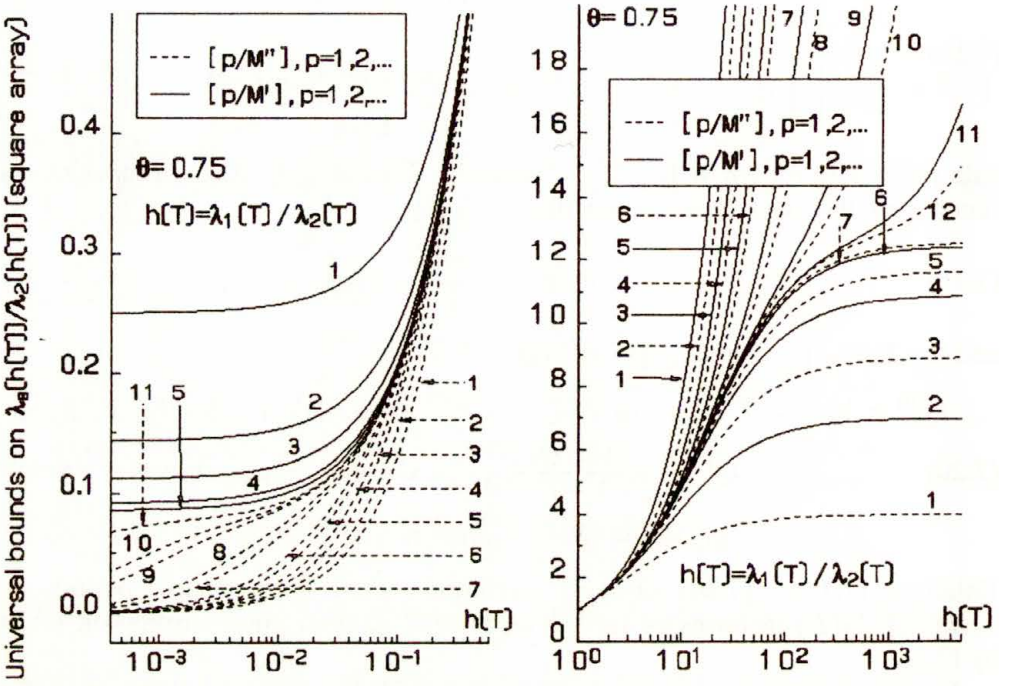

FIG. 7. Sequences of Padé approximants forming upper and lower bounds on the effective conductivity of a square array of cylinders.

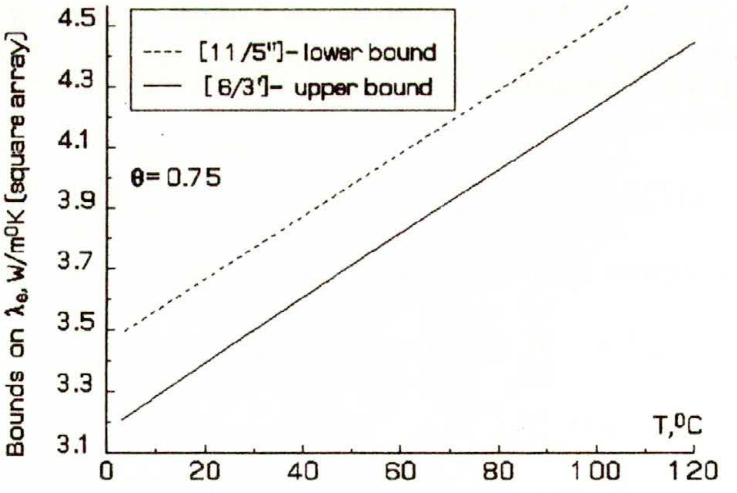

FIG. 8. Upper and lower bounds on the effective conductivity for square array of cylinders (epidian 53, $\lambda_1 = 0.21 + 0.005T$), embedded in a matrix (steel 15NiCuMoNb5, $\lambda_2 = 37.25 + 0.048T$), cf. [44].

http://rcin.org.pl

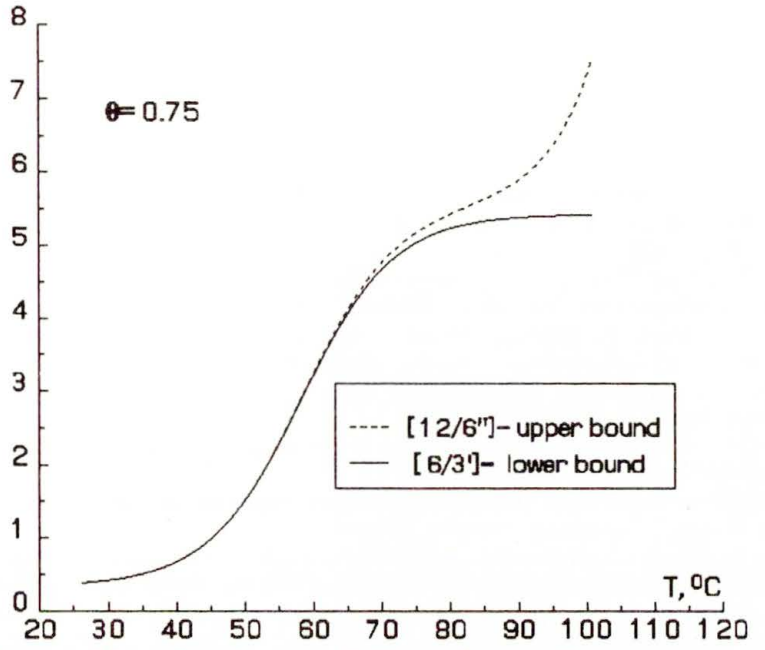

FIG. 9. Upper and lower bounds on the effective conductivity of human tissues: bones with $\lambda_1 = 0.349$ and muscles with $\lambda_2 = 0.29 + 0.29\exp((0.15(T - 36.7))$, cf. [29].

To illustrate the above procedure we have evaluated the effective conductivity λ_e versus temperature T for the composite consisting of the steel 15NiCuMoNb5 with $\lambda_1 = 37.25 + 0.048T$ and epidian 53 with $\lambda_2 = 0.21 + 0.005T$, cf. Fig. 8. The next example deals with live tissues: bone with $\lambda_2 = 0.436$ and muscles with $\lambda_1 = 0.29 + 0.29\exp 0.15(T - 36.7)$, cf. Fig. 9. All conductivities are given in [W/m°K].

Acknowledgment

This work was supported by the State Committee for Scientific Research (Poland) through the grant No. 3 P404 013 06.

References

1. A. BENSOUSSAN, J.-L. LIONS and G. PAPANICOLAOU, *Asymptotic analysis for periodic structures*, North-Holland, Amsterdam 1978.
2. E. SANCHEZ–PALENCIA, *Non-homogeneous media and vibration theory*, Springer-Verlag, Berlin 1980.
3. R.V. KOHN and G.W. MILTON, *On bounding the effective conductivity of anisotropic composites*, [in:] Homogenization and Effective Moduli of Materials and Media, pp. 97–125, J.L. ERICKSEN, D. KINDERLEHRER, R.V. KOHN, J.-L. LIONS [Eds.], Springer-Verlag, New York 1986.
4. S. MAY, S. TOKARZEWSKI, A. ZACHARA and B. CICHOCKI, *The effective conductivity of two-component composite with two-dimensional structure* [in Polish], IFTR Reports, 24/1992.

http://rcin.org.pl

5. W. MITYUSHEV, *Application of functional equations to the determination of the effective thermal conductivity of composite materials* [in Polish], Słupsk Pedagogical University, 1996.
6. O. BRUNO, *Effective moduli of strongly heterogeneous composites*, [in:] Calculus of Variations, Homogenization and Continuum Mechanics, pp. 99–115, G. BOUCHITTÉ, G. BUTTAZZO, P. SUQUET [Eds.], World Scientific, Singapore 1994.
7. D. BERGMAN, J.-L. LIONS, G. PAPANICOLAOU, F. MURAT, L. TARTAR and E. SANCHEZ-PALENCIA, *Les méthodes de l'homogénéisation: Théorie et applications en physique*, Eyrolles, Paris 1985.
8. G. DAL MASO and G.F. DELL'ANTONIO [Eds.], *Composite media and homogenization theory*, World Scientific, Singapore 1995.
9. K.A. LURIE and A.V. CHERKAEV, *Exact estimates of conductivity of mixtures composed of two isotropic media taken in prescribed proportion*, Proc. R. Soc. Edinburgh, **A 99**, 71–87, 1984.
10. A.V. CHERKAEV and L.V. GIBIANSKY, *Variational principles for complex conductivity, viscoelasticity, and similar problems in media with complex moduli*, J. Math. Phys., **35**, 1–22, 1994.
11. G.W. MILTON and R.V. KOHN, *Variational bounds on the effective moduli of anisotropic composites*, J. Mech. Phys. Solids, **36**, 597–629, 1988.
12. D. CAILLERIE, *Homogénéisation des équations de la diffusion stationaire dans les domaines cylindriques aplatis*, RAIRO, Num. Anal., **15**, 295–319, 1981.
13. H. ATTOUCH and G. BUTTAZZO, *Homogenization of reinforced periodic one-codimensional structures*, Publications AVAMAC, Université de Perpignan, No 86–06, 1986.
14. M. HNID, *Etude de transmission à travers des inclusions minces faiblement conductrices de "codimension un": homogénéisation et optimisation des structures*, Math. Modelling and Numer. Anal., **24**, 627–650, 1990.
15. A.V. CHERKAEV and R.V. KOHN [Eds.], *Topics on mathematical modelling of composite materials*, Birkhäuser, 1997 [in press].
16. G.F. DELL'ANTONIO and V. NESI, *A scalar inequality which bounds the effective conductivity of composites*, Proc. R. Soc. London, **A 431**, 519–530, 1990.
17. R.T. BONNECAZE and J.F. BRADY, *The effective conductivity of random suspensions of spherical particles*, Proc. R. Soc. London, **A 432**, 445–465, 1991.
18. G. PAPANICOLAOU and S. VARADHAN, *Boundary value problems with rapidly oscillating random coefficients*, pp. 835–873, [in:] Colloquia Mathematica Societatis János Bolyai 27, Random Fields, Esztergom (Hungary) 1979, Nord-Holland, Amsterdam 1982.
19. K. GOLDEN and G. PAPANICOLAOU, *Bounds for effective parameters of heterogeneous media by analytic continuation*, Commun. Math. Phys., **90**, 473–491, 1983.
20. K. GOLDEN and G. PAPANICOLAOU, *Bounds for effective parameters of multicomponent media by analytic continuation*, J. Statist. Physics., **40**, 655–667.
21. K. GOLDEN, *Bounds on the complex permittivity of a multicomponent material*, J. Mech. Phys. Solids, **34**, 333–358, 1986.
22. M. ARTOLA and G. DUVAUT, *Un résultat d'homogénéisation pour une classe de problèmes de diffusion nonlinéaires stationnaires*, Ann. Fac. Sc. Toulouse, **4**, 1–27, 1982.
23. L. BOCCARDO and F. MURAT, *Homogénéisation de problèmes quasi-linéaires*, [in:] Atti del Convegno "Studio di Problemi-limite della Analisi Funzionale", pp. 13–51, Bressanone, 7-9 Settembre 1981, Pitagora Editrice Bologna 1982.
24. N. FUSCO and G. MOSCARIELLO, *On the homogenization of quasilinear divergence structure operators*, Ann. Math. Pura Appl., **146**, 1–13, 1987.
25. T. DEL VECCHIO, *On the homogenization of a class of pseudomonotone operators in divergence form*, Boll. U.M.I., **5-B**, 369–388, 1991.
26. W. MITYUSHEV, *First order approximation of the effective thermal conductivity for a family of non-linear composites*, J. Tech. Phys., **36**, 429–432, 1995.
27. N. NODA, *Thermal stresses in materials with temperature-dependent properties*, Appl. Mech. Reviews, **44**, 383–397, 1991.
28. A.K. NOOR and W.S. BURTON, *Computational models for high-temperature multilayered composite plates and shells*, Appl. Mech. Reviews, **45**, 419–445, 1992.
29. F. BARDATI and G. GEROSA, *On the solution of the non-linear bio-heat equation*, J. Biomechanics, **23**, 791–798, 1990.

http://rcin.org.pl

30. S. WEINBAUM and L.M. JIJI, *A new simplified bioheat equation for the effect of blood flow on local average tissue temperature*, J. Biomech. Engng., **107**, 131–139, 1985.

31. S. BRAHIM-OTSMANE, G.A. FRANCFORT and F. MURAT, *Homogenization in thermoelasticity*, [in:] Random Media and Composites, pp. 13–45, R.V. KOHN and G.W. MILTON, SIAM, Philadelphia 1989.

32. A. GAŁKA, J.J. TELEGA and R. WOJNAR, *Some computational aspects of homogenization of thermopiezoelectric composites*, Comp. Assisted Mech. and Engng. Sci., **3**, 133–154, 1996.

33. A. GAŁKA, J.J. TELEGA and R. WOJNAR, *Thermodiffusion in heterogeneous elastic solids and homogenization*, Arch. Mech., **46**, 267–314, 1994.

34. K. SAB, *Homogenization of non-linear random media by a duality method. Application to plasticity*, Asymptotic Anal., **9**, 311–336.

35. A. BULTHEEL, P. GONZÁLEZ–VERA and R. ORIVE, *Quadrature on the half-line and two-point Padé approximants to Stieltjes function*. Part I. *Algebraic aspects*, J. Comp. Appl. Math., **65**, 57–72, 1995.

36. G.A. BAKER, *Essentials of Padé approximants*, Academic Press, London 1975.

37. S. MAY, S. TOKARZEWSKI, A. ZACHARA and B. CICHOCKI, *Continued fraction representation for the effective thermal conductivity coefficient of a periodic two-component composite*, Int. J. Heat and Mass Transf., **37**, pp. 2165–2173, 1994.

38. S. TOKARZEWSKI, *Inequalities for the effective transport coefficients of two-component composite materials*, Arch. Mech., **46**, 611–623, 1994.

39. S. TOKARZEWSKI, J. BŁAWZDZIEWICZ, I.V. ANDRIANOV, *Effective conductivity of densely packed highly conducting cylinders*, Appl. Phys., **A 59**, 601–604, 1994.

40. S. TOKARZEWSKI, J.J. TELEGA, *S-continued fractions to complex transport coefficient of two-phase composite*, Comp. Assis. Mech. and Engng. Sc., **3**, 109–119, 1996.

41. S. TOKARZEWSKI and J.J. TELEGA, *Two-point Padé approximants to Stieltjes series representation of bulk moduli of regular composites*, Comp. Assis. Mech. and Engng. Sc., **3**, 121–132, 1996.

42. W.T. PERRINS, D.R. MCKENZIE and R.C. MCPHEDRAN, *Transport properties of regular array of cylinders*, Proc. Roy. Soc. Lond., **A 369**, 207–225, 1979.

43. B. CICHOCKI and B. FELDERHOF, *Electrostatic interaction in two-dimensional Coulomb systems with periodic boundary conditions*, Physica, **A 158**, 706–722, 1989.

44. A.M. OSMAN and J.V. BECK, *Investigation of transient heat transfer coefficients in quenching experiments*, Transactions of the ASME, J. Heat Transfer, **112**, 843–848, 1990.

POLISH ACADEMY OF SCIENCES
INSTITUTE OF FUNDAMENTAL TECHNOLOGICAL RESEARCH

e-mail: agalka@ippt.gov.pl
e-mail: jtelega@ippt.gov.pl
e-mail: stokarz@ippt.gov.pl

Received November 7, 1996.

http://rcin.org.pl

Arch. Mech., 49, 2, pp. 321–343, Warszawa 1997

Outlooks in Saint–Venant theory
III. Torsion and flexure in sections of variable thickness by formal expansions

F. dell' ISOLA and G.C. RUTA (ROMA)

WE STUDY the Saint–Venant shear stress fields [1] arising in a family of sections we call Bredt-like [2, 3, 4], i.e. in a set of plane regions $\mathcal{D}_\varepsilon$ whose thickness we scale by a parameter ε. For each ε we build a coordinate mapping from a fixed plane domain $\mathcal{D}$ onto $\mathcal{D}_\varepsilon$. The shear stress field in $\mathcal{D}_\varepsilon$ can be represented by a Prandtl-like stress flow function [5, 6]. This is naturally done in torsion (*torsion*, [1]), while in flexure (*flexion inégale*, [1]) we face a gauge choice whose physical interpretation is uncertain [6]. We then consider the Helmholtz operator in a fixed system of coordinates in $\mathcal{D}$ and represent the shear stress field in a basis field which is not the covariant basis associated to any coordinate system. Formal ε-power series expansions for the shear stress field, the warping, the resultant force and torque and the shear shape factors tensor lead to hierarchies of perturbation problems for their coefficients. We obtain all the technical formulae at the lowest iteration steps and their generalization at higher steps – i.e., for thicker sections. No attempt is made to apply the methods proposed in [16] to estimate the distance between the generalized formulae we provide and the true solutions for the Saint–Venant shear stress problem.

1. Geometry of Bredt-like sections

WE CALL Bredt-like sections all the regions included in a plane $\mathcal{P}$ obtained by symmetrically thickening a curve $\mathcal{L} \in \mathcal{P}$ (*middle line*) along its Frenet normal with regularly varying thickness. The position vector field of the points of $\mathcal{L}$ with respect to any point $o \in \mathcal{P}$ is given as a function of its arc length s:

$$\mathcal{L} := \{q \in \mathcal{P} \,|\, q - o = \mathbf{r}_0(s), \qquad s \in [0, l]\}, \tag{1.1}$$

l is the length of $\mathcal{L}$. The Frenet orthonormal basis for the middle line is

$$\mathbf{l}(s) := \frac{\partial \mathbf{r}_0(s)}{\partial s} = \mathbf{r}_{0,s}(s), \qquad \mathbf{m}(s) := -* \frac{\partial \mathbf{r}_0(s)}{\partial s} = -* \mathbf{r}_{0,s}(s), \tag{1.2}$$

$*$ is Hodge operator in $\mathcal{P}$ ($\pi/2$ rotation in the positive orientation of $\mathcal{P}$); the comma denotes a derivative with respect to the indicated variable.

We define the ε-Bredt-like section as the collection of all the lines symmetrically shifted along $*\mathbf{l}(s)$ starting from $\mathcal{L}$, the total shift $\delta(s)$ being a regular function of s:

$$\mathcal{D}_\varepsilon := \{y \in \mathcal{P} \,|\, y - o = \mathbf{r}(s, z) = \mathbf{r}_0(s) + \varepsilon z \delta(s) * \mathbf{l}(s), \quad s \in [0, l], \quad z \in [-1, 1]\}; \tag{1.3}$$

http://rcin.org.pl

z is a coordinate along $\mathbf{l}(s)$ and ε is a thickness perturbation parameter. We regard s, z as rescaled coordinates over $\mathcal{D}_\varepsilon$, [7]; Eq. (1.3) implicitly defines a coordinate mapping from $\mathcal{D} := [0, l] \times [-1, 1]$ onto $\mathcal{D}_\varepsilon$.

The natural (covariant) basis associated with the coordinate system (s, z) is [8]

$$\begin{aligned} \mathbf{g}_1(s) &:= \frac{\partial \mathbf{r}}{\partial s} = [1 - \varepsilon z \kappa(s)\delta(s)]\,\mathbf{l}(s) + \varepsilon z \delta_{,s}(s) * \mathbf{l}(s), \\ \mathbf{g}_2(s) &:= \frac{\partial \mathbf{r}}{\partial z} = \varepsilon \delta(s) * \mathbf{l}(s); \end{aligned} \tag{1.4}$$

$\kappa(s)$ is the (suitably regular) curvature of the middle line. Henceforth, to lighten the notation we will drop the dependence of the indicated functions on the coordinates, when there is no risk of confusion.

The covariant components and the determinant of the metric tensor are

$$\begin{aligned} &g_{11} = (1 - \varepsilon z \kappa \delta)^2 + (\varepsilon z \delta_{,s})^2, \qquad g_{12} = g_{21} = z\varepsilon^2 \delta \delta_{,s}, \\ &g_{22} = \varepsilon \delta^2, \qquad g \doteq g_{11} g_{22} - (g_{11})^2 = (\varepsilon\delta)^2 (1 - \varepsilon z \kappa \delta)^2. \end{aligned} \tag{1.5}$$

The basis dual to the natural one is given by $\mathbf{g}^i \cdot \mathbf{g}_j = \delta^i_j$, where $\cdot$ stands for the usual scalar product in the vector space $\mathcal{V}$ of the translations of $\mathcal{P}$:

$$\mathbf{g}^1 = \frac{\mathbf{l}}{1 - \varepsilon z \kappa \delta}, \qquad \mathbf{g}^2 = -\frac{z\delta_{,s}}{\delta(1 - \varepsilon z \kappa \delta)}\mathbf{l} + \frac{1}{\varepsilon\delta} * \mathbf{l}. \tag{1.6}$$

As the section has variable thickness, the coordinate system (s, z) is not, in general, orthogonal (it is on the middle line, by construction). The Christoffel symbols (of second kind) associated with the coordinates s, z, according to $\left\{ {j \atop k\ l} \right\} := \mathbf{g}_{k,l} \cdot \mathbf{g}^j$, [3, 4, 8], are:

$$\begin{aligned} \left\{ {1 \atop 1\ 1} \right\} &= -\frac{\varepsilon z (2\kappa\delta_{,s} + \kappa_{,s}\delta)}{1 - \varepsilon z \kappa \delta}, \\ \left\{ {2 \atop 1\ 1} \right\} &= \frac{z^2 \varepsilon \delta_{,s} (2\kappa\delta_{,s} + \kappa_{,s}\delta)}{\delta(1 - \varepsilon z \kappa \delta)} + \frac{\kappa(1 - \varepsilon z \kappa \delta) + z\delta_{,ss}}{\varepsilon\delta}, \\ \left\{ {1 \atop 2\ 2} \right\} &= \left\{ {2 \atop 2\ 2} \right\} = 0, \\ \left\{ {1 \atop 2\ 1} \right\} &= \left\{ {1 \atop 1\ 2} \right\} = -\frac{\varepsilon\kappa\delta}{1 - \varepsilon z \kappa \delta}, \\ \left\{ {2 \atop 2\ 1} \right\} &= \left\{ {2 \atop 1\ 2} \right\} = \frac{\delta_{,s}}{\delta(1 - \varepsilon z \kappa \delta)}. \end{aligned} \tag{1.7}$$

The centroid of area b of the section is given, according to Eq. (1.3), by

$$b - o = \frac{\int_{\mathcal{D}_\varepsilon} (y - o)}{A_{\mathcal{D}_\varepsilon}} = \frac{\int_0^l \delta \mathbf{r}_0 - \frac{\varepsilon^2}{3} \int_0^l \delta^3 \kappa * \mathbf{l}}{\int_0^l \delta} =: \mathbf{b}_0 - \varepsilon^2 \mathbf{b}_2, \tag{1.8}$$

http://rcin.org.pl

$A_{\mathcal{D}_\varepsilon}$ is the area of the section. In all the integrals the measure of integration is understood.

2. The elliptic problem for the shear stress field

The shear stress field $\mathbf{t}$ arising in the ε-section of a Saint-Venant cylinder is subjected to the elliptic problem [1, 6, 9]

$$\text{(2.1)} \qquad \operatorname{div}\mathbf{t} = Y\mathbf{k}\cdot[*(y-b)] \qquad \text{in} \quad \mathcal{D}_\varepsilon^o,$$

$$\text{(2.2)} \qquad \operatorname{curl}\mathbf{t} = 2G[\tau + \nu\mathbf{k}\cdot(y-o)] \qquad \text{in} \quad \mathcal{D}_\varepsilon^o,$$

$$\text{(2.3)} \qquad \mathbf{t}\cdot\mathbf{n} = 0 \qquad \text{along} \quad \partial\mathcal{D}_\varepsilon,$$

$$\text{(2.4)} \qquad \oint_{\mathcal{C}} \mathbf{t}\cdot\mathbf{l}_{\mathcal{C}} = 2GA_{\mathcal{S}}[\tau + \nu\mathbf{k}\cdot(b_{\mathcal{S}} - o)] \qquad \forall\mathcal{C} \subset \mathcal{D}_\varepsilon.$$

In the former, Y, G, ν are the longitudinal (Young) elastic modulus, the tangential elastic modulus and Poisson's ratio, respectively; $\mathbf{n}$ is the outer unit normal to $\partial\mathcal{D}_\varepsilon$; $\mathcal{C}$ is a curve and $\mathbf{l}_{\mathcal{C}}$ is its unit tangent; $\mathcal{S}$ is the inner Jordan region of $\mathcal{C}$, $A_{\mathcal{S}}$ is its area and $b_{\mathcal{S}}$ its centroid; τ is the kinematic characteristic parameter of the torsion, representing the unit angle of twist (with respect to the point o); $\mathbf{k}$ is the kinematic characteristic parameter of the flexure, representing the (linear) variation of the curvature of the initially straight axis of the cylinder through o. Equation (2.1) describes local balance of contact force; Eq. (2.2) is a local compatibility condition, necessary and sufficient if the section is simply connected; Eq. (2.3) expresses the traction-free condition of the lateral surface of the cylinder; Eq. (2.4) is a global compatibility condition for sections with connection higher than 1.

It is well known that in general the problem (2.1)–(2.4) has no analytical solution in closed form, especially for sections with multiple connection. This makes it clear that for technical applications at least approximate solutions are to be found. So far as we know, in the literature there are no approximate formulae providing reliable results for the shear stress arising in thick sections. The aim of this paper is to look for such formulae, starting from a geometry of the section in which the thickening process depends on one parameter. No attempt will be done to estimate the error made in considering the formulae given here instead of the true solutions. This is a complicated mathematical issue to be faced with the methods proposed in [16].

As Eqs. (2.1)–(2.4) are linear in the two kinematical parameters, it is customary to divide the general problem of the shear stress field into two systems, each depending only on one parameter.

The system depending on τ describes the torsion:

$$\text{(2.5)} \qquad \operatorname{div}\mathbf{t} = 0 \qquad \text{in} \quad \mathcal{D}_\varepsilon^o,$$

http://rcin.org.pl

$$\operatorname{curl}\mathbf{t} = 2G\tau \qquad \text{in } \mathcal{D}_\varepsilon^o, \tag{2.6}$$

$$\mathbf{t}\cdot\mathbf{n} = 0 \qquad \text{along } \partial\mathcal{D}_\varepsilon, \tag{2.7}$$

$$\oint_{\mathcal{C}} \mathbf{t}\cdot\mathbf{l}_{\mathcal{C}} = 2GA_{\mathcal{S}}\tau \qquad \forall \mathcal{C} \subset \mathcal{D}_\varepsilon. \tag{2.8}$$

Equations (2.5) – (2.7) suggest that a flow function for $\mathbf{t}$ may be introduced, named after Prandtl [5]. Starting from such function, there are technical formulae providing approximate shear stress fields for thin sections with both simple and multiple connection [10, 11, 12]; in the latter case, the formula is due to BREDT [13].

In some previous works [2, 3, 4] the torsion problem, defined over a Bredt-like section, has been considered: the stress flow function turns out to depend on the thickness parameter. Once the *Ansatz* is made that the Prandtl function admits a formal ε-power series expansion, one obtains, starting from Eqs. (2.5) – (2.8), a hierarchy of perturbation problems. In [2, 3, 4] it has been shown that the solutions of this hierarchy provide all the known approximate formulae at the lowest steps (i.e., when the section is thin), plus their generalization at the following steps (when the section becomes thick).

The system depending on $\mathbf{k}$ describes the flexure:

$$\operatorname{div}\mathbf{t} = Y\mathbf{k}\cdot[*(y-b)] \qquad \text{in } \mathcal{D}_\varepsilon^o, \tag{2.9}$$

$$\operatorname{curl}\mathbf{t} = 2G\nu\mathbf{k}\cdot(y-o) \qquad \text{in } \mathcal{D}_\varepsilon^o, \tag{2.10}$$

$$\mathbf{t}\cdot\mathbf{n} = 0 \qquad \text{along } \partial\mathcal{D}_\varepsilon, \tag{2.11}$$

$$\oint_{\mathcal{C}} \mathbf{t}\cdot\mathbf{l}_{\mathcal{C}} = 2GA_{\mathcal{S}}\nu\mathbf{k}\cdot(b_{\mathcal{S}}-o) \qquad \forall \mathcal{C} \subset \mathcal{D}_\varepsilon. \tag{2.12}$$

In this case there is a technical formula, based on the integral counterpart of Eq. (2.9), due to Jouravski [10, 11, 12]; it provides a mean value for the shear stress component along $\mathcal{L}$, which is an accurate estimate of that component when the section is thin.

Let $\mathbf{t}_o$, $\mathbf{t}_{o'}$ be the field solutions of Eqs. (2.9) – (2.12) associated with any two arbitrarily chosen points o, $o' \in \mathcal{P}$. The field $\mathbf{t}_o - \mathbf{t}_{o'}$ satisfies the system

$$\operatorname{div}(\mathbf{t}_o - \mathbf{t}_{o'}) = 0 \qquad \text{in } \mathcal{D}_\varepsilon^o, \tag{2.13}$$

$$\operatorname{curl}(\mathbf{t}_o - \mathbf{t}_{o'}) = 2G\nu\mathbf{k}\cdot(o'-o) \qquad \text{in } \mathcal{D}_\varepsilon^o, \tag{2.14}$$

$$(\mathbf{t}_o - \mathbf{t}_{o'})\cdot\mathbf{n} = 0 \qquad \text{along } \partial\mathcal{D}_\varepsilon, \tag{2.15}$$

$$\oint_{\mathcal{C}} (\mathbf{t}_o - \mathbf{t}_{o'})\cdot\mathbf{l}_{\mathcal{C}} = 2GA_{\mathcal{S}}\nu\mathbf{k}\cdot(o'-o) \qquad \forall \mathcal{C} \subset \mathcal{D}_\varepsilon. \tag{2.16}$$

If we let $\bar{\tau} := \nu\mathbf{k}\cdot(o'-o)$ (both sides of this definition have the same physical dimensions), Eqs. (2.13) – (2.16) describe a torsion problem whose kinematic characteristic parameter is $\bar{\tau}$. That is to say, the choice of the origin o adds

http://rcin.org.pl

a torsional solution to the system of equations which describe the flexure. We are so free to choose a particular origin to simplify the search for a solution of Eqs. (2.9) – (2.12).

Let us choose $o = b$; it may be proven [6] that the field

$$\tilde{\mathbf{t}} = \frac{G}{4}\{(3 + 2\nu)[*(y - b) \otimes (y - b)] - (1 - 2\nu)[(y - b) \otimes *(y - b)]\}\mathbf{k}, \tag{2.17}$$

defined on the whole plane $\mathcal{P} \supset \mathcal{D}_\varepsilon$, is a particular solution of Eqs. (2.9) – (2.10). It turns out that

$$\int_{\mathcal{C}} *\tilde{\mathbf{t}} \cdot \mathbf{n}_{\mathcal{C}} \oint_{\mathcal{C}} \tilde{\mathbf{t}} \cdot \mathbf{l}_{\mathcal{C}} = 2GA_{\mathcal{S}}\nu\mathbf{k} \cdot (b_{\mathcal{S}} - b) \quad \forall \mathcal{C} \subset \mathcal{D}_\varepsilon \tag{2.18}$$

and the divergence and the curl of the field $\mathbf{t} - \tilde{\mathbf{t}}$ vanish. As a consequence, it is reasonable to look for a generalized stress flow function.

This can be easily done for simply connected sections and for sections whose symmetry group is that of the rectangle. In fact, (i) in simply connected sections the global compatibility condition, Eq. (2.12), is implied by the local condition Eq. (2.10), (ii) in sections with two axes of symmetry it is $b_{\mathcal{S}} = b$. In both cases, Eqs. (2.9) – (2.10), (2.12), (2.17) – (2.18) affirm the existence of a generalized stress flow function $\Psi : \mathcal{D}_\varepsilon \to \mathbb{R}$ [6]. Indeed, let $\mathcal{Q} \subset \mathcal{D}_\varepsilon$ be a region and $\mathcal{M} := \partial\mathcal{Q} \backslash \partial\mathcal{D}_\varepsilon$; we have

$$\begin{aligned} 0 = \int_{\mathcal{Q}} \operatorname{div}(\mathbf{t} - \tilde{\mathbf{t}}) = \int_{\partial\mathcal{Q}} (\mathbf{t} - \tilde{\mathbf{t}}) \cdot \mathbf{n}_{\partial\mathcal{Q}} = \oint_{\partial\mathcal{Q}} *(\mathbf{t} - \tilde{\mathbf{t}}) \cdot \mathbf{l}_{\partial\mathcal{Q}} \\ = \oint_{\mathcal{M}} *(\mathbf{t} - \tilde{\mathbf{t}}) \cdot \mathbf{l}_{\mathcal{M}} \Rightarrow \mathbf{t} = \tilde{\mathbf{t}} - *(\nabla\Psi), \end{aligned} \tag{2.19}$$

∇ being the spatial gradient operator in $\mathcal{P}$. For simply connected sections and for sections with double connection and two axes of symmetry it is then possible to build perturbation hierarchies similar to those obtained in [2, 3, 4] for torsion, and their iteration solution provides the known Jouravski formula at the lowest step and its generalization at higher steps [6].

Unfortunately, this procedure faces a serious *empasse* in the case of non-symmetrical sections with multiple connection. Indeed, Eq. (2.12) implies the existence of stress sources in the lacunae with given flow across all the closed lines $\mathcal{M}$. Now, there are infinitely many divergence-free stress fields which are gradients of Prandtl-like functions and whose flow coincides with that given by Eq. (2.18), so that we are to face a gauge choice whose physical meaning is rather uncertain [6].

It is then clear that, in order to provide a perturbation technique valid for all Bredt-like sections, we must change our point of view and abandon the method of the generalized stress flow function. The simpler idea is then to look for a perturbation method to be applied directly to the shear stress field $\mathbf{t}$.

http://rcin.org.pl

3. The Helmholtz operator in the Bredt basis field

The ε parameter in (1.3) magnifies the thickness of sections with the same "shape". We look for a hierarchy of perturbation problems for $\mathbf{t}$ in ε, whose solution at each step should provide generalized approximate formulae for the shear stress field of thick sections. On this purpose, we will write the Helmholtz operator in Eqs. (2.1)–(2.4) in the coordinate system (s, z) in $\mathcal{D}$ as a function of the thickness parameter ε.

We define the *Bredt basis field* $\mathcal{B}$ in $\mathcal{D}_\varepsilon$ as:

$$\mathcal{B} : (s, z) \mapsto \mathbf{l}(s),\ *\mathbf{l}(s); \tag{3.1}$$

the components of its Lie bracket [14] in (s, z) are

$$[\mathbf{l}, *\mathbf{l}]_1 = \frac{\kappa}{(1 - \varepsilon z \kappa \delta)^2}, \qquad [\mathbf{l}, *\mathbf{l}]_2 = -\frac{z \kappa \delta_{,s}}{\delta (1 - \varepsilon z \kappa \delta)^2}. \tag{3.2}$$

As the Lie bracket of $\mathcal{B}$ is not, in general, the zero vector field, $\mathcal{B}$ is not, in general, the covariant natural basis associated with any coordinate system [15].

We do not represent the shear stress in the natural basis of the (s, z) coordinate system, but in the Bredt basis, as it is usually done in the applications:

$$\mathbf{t} = t^1 \mathbf{g}_1 + t^2 \mathbf{g}_2 = t_1 \mathbf{g}^1 + t_2 \mathbf{g}^2 = t_s \mathbf{l} + t_z * \mathbf{l}. \tag{3.3}$$

According to (3.3), we find the relations between contravariant and Bredt components of the shear stress:

$$t^1 = \frac{t_s}{1 - \varepsilon z \kappa \delta}, \qquad t^2 = \frac{1}{\varepsilon \delta} t_z - \frac{z \delta_{,s}}{\delta (1 - z \kappa \varepsilon \delta)} t_s. \tag{3.4}$$

Because of Eqs. (3.3)–(3.4), the divergence operator is written as [8]

$$\begin{aligned} \operatorname{div} \mathbf{t} = (\nabla \mathbf{t})^i_i = t^1_{,s} + \left\{ \begin{matrix} 1 \\ j\ 1 \end{matrix} \right\} t^j + t^2_{,z} + \left\{ \begin{matrix} 2 \\ j\ 2 \end{matrix} \right\} t^j \\ = \frac{t_{s,s}}{1 - \varepsilon z \kappa \delta} - \frac{\kappa t_z}{1 - \varepsilon z \kappa \delta} + \frac{t_{z,z}}{\varepsilon \delta}. \end{aligned} \tag{3.5}$$

The same expression is obtained for Bredt-like sections with constant thickness, i.e., when the coordinates s, z are orthogonal at each point [14]. That is to say, the divergence operator expressed in terms of t_s, t_z does not change its form also when the section has variable thickness and (s, z) becomes a non-orthogonal coordinate system. This is somehow physically reasonable, as the divergence operator is more linked to the variation of the field along the middle line than to that along the thickness. This also justifies the success of the approximate formulae for the shear stress of thin sections.

http://rcin.org.pl

The covariant components of the shear stress may be found in terms of the Bredt components by $t_i = g_{ij}t^j$, once Eq. (3.3) is given:

$$t_1 = (1 - \varepsilon z\kappa\delta)t_s + \varepsilon z\delta_{,s}t_s\,, \qquad t_2 = \varepsilon\delta t_z\,. \tag{3.6}$$

We use Eq. (3.6) to calculate the curl operator and express it in terms of the Bredt components:

$$\operatorname{curl}\mathbf{t} = \frac{1}{\sqrt{g}}(\nabla_1 t_2 - \nabla_2 t_1) = \frac{t_{2,s} - \left\{ \begin{matrix} j \\ 1\ 2 \end{matrix} \right\} t_j - t_{1,z} + \left\{ \begin{matrix} j \\ 2\ 1 \end{matrix} \right\} t_j}{\varepsilon\delta(1 - \varepsilon z\kappa\delta)} \tag{3.7}$$

$$= \frac{t_{2,s} - t_{1,z}}{\varepsilon\delta(1 - \varepsilon z\kappa\delta)} = \frac{t_{z,s}}{1 - \varepsilon z\kappa\delta} - \frac{t_{s,z}}{\varepsilon\delta} + \frac{\kappa t_s}{1 - \varepsilon z\kappa\delta} - \frac{z\delta_{,s}t_{z,z}}{\delta(1 - \varepsilon z\kappa\delta)}.$$

Equation (3.7) differs only in the fourth term from the expression obtained for sections with constant thickness [14]. The additional term is proportional to the derivative of the z-component of the field with respect to z and to the variation of the thickness along $\mathcal{L}$. This is physically reasonable, as the curl operator is linked with the variation of the field along the thickness.

The gradient of a scalar function w in terms of the coordinates s, z is given by

$$\nabla w = \frac{\partial w}{\partial s}\mathbf{g}^1 + \frac{\partial w}{\partial z}\mathbf{g}^2 = \left[\frac{\delta w_{,s} - \varepsilon z\delta_{,s}w_{,z}}{\varepsilon\delta(1 - \varepsilon z\kappa\delta)}\right]\mathbf{l} + \frac{w_{,z}}{\varepsilon\delta} * \mathbf{l}; \tag{3.8}$$

Eq. (3.8) reduces to the expression of the gradient of a scalar function in an orthogonal system of coordinates [14] if we let $\delta_{,s} = 0$.

4. Formal expansions for the shear stress

As the thickness parameter describes a geometrical feature of the section, it is reasonable to let $\mathbf{t}$ be a function of ε as well as of s, z. We propose the following formal series expansion for $\mathbf{t}$ [7]:

$$\mathbf{t}(s, z; \varepsilon) = \sum_{n=0}^{N} \varepsilon^n \mathbf{t}_n(s, z) + o(\varepsilon^N), \tag{4.1}$$

where $o(\varepsilon^N)$ stands for terms of order higher than ε^N. Similar formal expansions hold for both components of the shear stress field with respect to the Bredt basis.

If we substitute Eqs. (4.1), (3.5) and (3.7) into Eqs. (2.5) – (2.8), (2.9) – (2.12), we now obtain two hierarchies of perturbation problems for the shear stress.

http://rcin.org.pl

The first hierarchy describes the case of torsion:

$$\frac{\sum_{n=0}^{N}\{\varepsilon^{n+1}\delta[t_{sn,s}-\kappa(t_{zn}+zt_{zn,z})]+\varepsilon^{n}t_{zn,z}\}}{\varepsilon\delta(1-\varepsilon z\kappa\delta)}=0, \tag{4.2}$$

$$\frac{\sum_{n=0}^{N}\{\varepsilon^{n+1}[\delta t_{zn,s}+\kappa\delta(t_{sn}+zt_{sn,z})-z\delta_{,s}t_{zn,z}]-\varepsilon^{n}t_{sn,z}\}}{\varepsilon\delta(1-\varepsilon z\kappa\delta)}=2G\tau, \tag{4.3}$$

$$\sum_{n=0}^{N}\varepsilon^{n}\mathbf{t}\cdot\mathbf{n}=0, \tag{4.4}$$

$$\sum_{n=0}^{N}\oint_{z=0}\varepsilon^{n}t_{sn}=2G\tau A_{\mathcal{R}}(b_{\mathcal{R}}-o). \tag{4.5}$$

The other hierarchy describes the case of flexure:

$$\frac{\sum_{n=0}^{N}\{\varepsilon^{n+1}\delta[t_{sn,s}-\kappa(t_{zn}+zt_{zn,z})]+\varepsilon^{n}t_{zn,z}\}}{\varepsilon\delta(1-\varepsilon z\kappa\delta)}=Y\mathbf{k}\cdot(*\bar{\mathbf{r}}_0-\varepsilon z\delta\mathbf{l}+\varepsilon^2\mathbf{b}_2), \tag{4.6}$$

$$\frac{\sum_{n=0}^{N}\{\varepsilon^{n+1}[\delta t_{zn,s}+\kappa\delta(t_{sn}+zt_{sn,z})-z\delta_{,s}t_{zn,z}]-\varepsilon^{n}t_{sn,z}\}}{\varepsilon\delta(1-\varepsilon z\kappa\delta)}=2G\nu\mathbf{k}\cdot(\mathbf{r}_0+\varepsilon z\delta*\mathbf{l}), \tag{4.7}$$

$$\sum_{n=0}^{N}\varepsilon^{n}\mathbf{t}\cdot\mathbf{n}=0, \tag{4.8}$$

$$\sum_{n=0}^{N}\oint_{z=0}\varepsilon^{n}t_{sn}=2G\nu\mathbf{k}\cdot A_{\mathcal{R}}(b_{\mathcal{R}}-o). \tag{4.9}$$

In Eqs. (4.2)–(4.9) the terms of order higher than ε^N have been dropped; in Eq. (4.6) $\bar{\mathbf{r}}_0 := \mathbf{r}_0 - \mathbf{b}_0$; the outer normal vector $\mathbf{n}$ in Eqs. (4.4), (4.8) is evaluated in the following Eqs. (4.10), (4.13), (4.14); in Eqs. (4.5), (4.9) $\mathcal{R}$ is the inner Jordan region (if any) enclosed by $\mathcal{L}$ ($z = 0$) and $b_{\mathcal{R}}$ is its centroid.

If the section has double connection, we will call it *closed*, referring to its middle line, which is homotopic to a circumference. In this case, there are two different connected elements which compose the boundary of the section. The outer vector field normal to the boundary is given by

$$\mathbf{n}|_{z=-1}=-\varepsilon\delta_{,s}\mathbf{l}-(1+\varepsilon\kappa\delta)*\mathbf{l}, \qquad \mathbf{n}|_{z=1}=-\varepsilon\delta_{,s}\mathbf{l}+(1-\varepsilon\kappa\delta)*\mathbf{l}, \tag{4.10}$$

http://rcin.org.pl

so that the boundary conditions for closed sections are, dropping the terms $o(\varepsilon^N)$,

$$\sum_{n=0}^{N} |\varepsilon^{n+1}(\delta_{,s}t_{sn} + \kappa\delta t_{zn}) + \varepsilon^n t_{zn}|_{z=-1} = 0, \tag{4.11}$$

$$\sum_{n=0}^{N} | - \varepsilon^{n+1}(\delta_{,s}t_{sn} + \kappa\delta t_{zn}) + \varepsilon^n t_{zn}|_{z=1} = 0. \tag{4.12}$$

If the section is simply connected, we will call it *open*, always referring to its middle line, now homotopic to a segment. The boundary is composed by a unique connected element, divided into four regular components. The outer vector field normal to the boundary is represented by

$$\mathbf{n}|_{s=0} = -\mathbf{l}, \qquad \mathbf{n}|_{z=-1} = -\varepsilon\delta_{,s}\mathbf{l} - (1 + \varepsilon\kappa\delta) * \mathbf{l}, \tag{4.13}$$

$$\mathbf{n}|_{s=l} = \mathbf{l}, \qquad \mathbf{n}|_{z=1} = -\varepsilon\delta_{,s}\mathbf{l} + (1 - \varepsilon\kappa\delta) * \mathbf{l}, \tag{4.14}$$

so that the boundary conditions for open sections are, always dropping the terms $o(\varepsilon^N)$,

$$\sum_{n=0}^{N} |\varepsilon^n t_{sn}|_{s=0} = 0, \tag{4.15}$$

$$\sum_{n=0}^{N} |\varepsilon^{n+1}(\delta_{,s}t_{sn} + \kappa\delta t_{zn}) + \varepsilon^n t_{zn}|_{z=-1} = 0, \tag{4.16}$$

$$\sum_{n=0}^{N} |\varepsilon^n t_{sn}|_{s=l} = 0, \tag{4.17}$$

$$\sum_{n=0}^{N} | - \varepsilon^{n+1}(\delta_{,s}t_{sn} + \kappa\delta t_{zn}) + \varepsilon^n t_{zn}|_{z=1} = 0. \tag{4.18}$$

In the next sections we will look for the solution of the hierarchies of perturbation problems (4.2)–(4.9), with the appropriate substitution of the boundary conditions (4.11)–(4.12), (4.15)–(4.18), both for closed and open sections.

As the structure of both hierarchies is the same, the only difference being brought in by the right-hand sides in Eqs. (4.2)–(4.3), (4.6)–(4.7), we obtain (see next section) the same recursive structure for the coefficients in Eq. (4.1), no matter if we study torsion or flexure.

In particular, there are common features of the two hierarchies which are worth remarking:

a. Each step can be solved within an unknown function of the coordinate s, which is determined only by solving the local balance equation, together with the boundary conditions, at the next step. This is a very well known possible feature of perturbation series [7].

http://rcin.org.pl

b. Both for closed and open sections, the structure of the perturbation problem is the same but for two different boundary conditions. Anyway, in the case of open sections, we cannot force a system of *second* order to fulfill *four* independent boundary conditions. This is another well known phenomenon of perturbation procedures, when being in presence of a boundary layer (in this case, in a neighbourhood of the "short" sides of the section [2, 3, 4, 7]). We should provide two different expansions, called *outer* and *inner* [7], and then match them; but for the aim of this paper we will content ourselves with the outer expansion, valid outside the region of the boundary layer.

4.1. Shear stress coefficients in torsion

We will first give the solutions of the first steps of our perturbation series in the case of simply connected (open) sections. We remind that the following coefficients are those of the outer formal series expansion for the shear stress. It is

$$\mathbf{t}_0 = \mathbf{0}, \tag{4.19}$$

$$\mathbf{t}_1 = -(2G\tau z\delta)\mathbf{l}, \tag{4.20}$$

$$\mathbf{t}_2 = G\tau\left\{\left[(1-z^2)\kappa\delta^2 - \frac{2}{3}\int_0^s \delta(\kappa\delta^2)_{,s}\right]\mathbf{l} + \delta\delta_{,s}(z^2-3) * \mathbf{l}\right\}. \tag{4.21}$$

Equation (4.19) is a known result, though never explicitly affirmed in the literature: when the thickness vanishes, the only solution of the torsion problem is the zero field. Equation (4.20) is the result usually provided in the literature for thin sections, sometimes attributed to Kelvin [2, 3, 4, 10, 11, 12]; Eq. (4.21) is the generalization of this formula when the section becomes thicker.

Equation (4.19) verifies all the boundary conditions; Eq. (4.20) verifies the boundary conditions at the "short" sides of the section as a mean over the thickness; Eq. (4.21) verifies only the boundary conditions at the "long" sides of the sections. This implies that, even if at the lowest step of the hierarchy the zero field is a suitable solution also near the "short" sides, at the successive iteration steps a boundary layer in that region arises, named after Kelvin. We will provide in Sec. 6.1 a measure of this effect, the same as that presented in the literature.

In the case of sections with double connection (closed) we have

$$\mathbf{t}_0 = 2G\tau\frac{A_{\mathcal{R}}}{\delta\oint_{\mathcal{L}}\frac{1}{\delta}}\mathbf{l} =: t_{s0}\mathbf{l}, \tag{4.22}$$

$$\mathbf{t}_1 = z[\delta(\kappa t_{s0} - 2G\tau)\mathbf{l} + \delta_{,s} * \mathbf{l}], \tag{4.23}$$

http://rcin.org.pl

$$\mathbf{t}_2 = \left[z^2\kappa\delta^2(\kappa t_{s0} - 2G\tau) - z^2\delta_{,s}t_{s0} + \frac{z^2}{2}\delta\delta_{,s}t_{s0} + \bar{t}_{s2}\right]\mathbf{l} + \left\{\delta\delta_{,s}\left[(z^2+1)\kappa t_{s0} + (z^2-3)G\tau\right] - \frac{z^2-1}{2}\delta^2\kappa_{,s}t_{s0}\right\} * \mathbf{l}. \tag{4.24}$$

Equation (4.22) is the well known Bredt formula [2, 3, 4, 10, 11, 12, 13]; Eqs. (4.23)–(4.24) provide its generalization when the section is thicker. In Eq. (4.24) $\bar{t}_{s2}$ is an unknown function of s alone, to be determined by solving the next step of the perturbation procedure.

We remark that for closed section we have a non-vanishing $\mathbf{t}_0$: this is physically grounded, because the stress flow runs along all the closed lines which fill the section; on the contrary, in open section the condition that the shear stress flow be zero necessarily implies that the shear stress must also be zero at the lowest step of the hierarchy.

If we let $\delta_{,s} = 0$ (δ = constant along $\mathcal{L}$) in the Eqs. (4.19)–(4.22), we recover all the results provided in [2] for sections with constant thickness.

4.2. Shear stress coefficients in flexure

As it has been done in the case of torsion, we will begin providing the solutions of the first steps of our perturbation procedure for open sections; these are also in this case the coefficients of an outer formal expansion. It is

$$\mathbf{t}_0 = Y\mathbf{k}\cdot\frac{\int_0^s \delta * \bar{\mathbf{r}}_0}{\delta}\mathbf{l} =: t_{s0}\mathbf{l}, \tag{4.25}$$

$$\mathbf{t}_1 = z[\delta(\kappa t_{s0} - 2G\nu\mathbf{k}\cdot\mathbf{r}_0)\mathbf{l} + \delta_{,s} * \mathbf{l}], \tag{4.26}$$

$$\mathbf{t}_2 = \left\{\left[z^2\delta^2\kappa(\kappa t_{s0} - 2G\nu\mathbf{k}\cdot\mathbf{r}_0) - G\nu\mathbf{k}\cdot * \mathbf{l}\right] + \frac{z^2}{2}\left[\delta(\delta_{,s}t_{s0})_{,s} - \delta_{,s}^2 t_{s0}\right]\right\}\mathbf{l} + \left\{\delta\delta_{,s}\left[(z^2+1)\kappa t_{s0} + (z^2-3)G\nu\mathbf{k}\cdot\mathbf{r}_0\right] - \frac{z^2-1}{2}\delta^2\left[\kappa_{,s}t_{s0} + \mathbf{k}\cdot(\mathbf{l} + Y\kappa * \bar{\mathbf{r}}_0)\right]\right\} * \mathbf{l}. \tag{4.27}$$

Equation (4.25) is the known Jouravski formula and it may be found in all the textbooks on strength of materials [10, 11, 12]: the integral in t_{s0} is the first moment of area of the part of the section enclosed by the values 0 and s of the arc length of the middle line. Jouravski formula in the literature is written in terms of the resultant shear stress; it is easy, though, to recognize the same expression once having remembered the linear relationship between the kinematic parameter $\mathbf{k}$ and the resultant shear stress $\mathbf{q}$ [1, 6, 9]. We will discuss this in Sec. 6.2, where we calculate the coefficients of a formal expansion for the resultant shear stress.

http://rcin.org.pl

The component along $*\mathbf{l}$ of Eq. (4.26) is another known formula. In the literature it is sometimes found by means of heuristic and graphic deduction and it is said, also on heuristic grounds, that its magnitude is small if compared with that provided by Jouravski formula. From the point of view of our technique, this result is clearly interpreted as a higher order effect in terms of the perturbation parameter.

The components along $\mathbf{l}$ of Eq. (4.26) and Eq. (4.27) are not found in the literature, so far as we know. They are the first generalization of Jouravski formula for open sections which become thick.

Exactly as we have found in the case of torsion, Eq. (4.25) verifies all the boundary conditions; Eq. (4.26) verifies the boundary conditions at the "short" sides of the section as a mean over the thickness; Eq. (4.27) verifies only the boundary conditions at the "long" sides of the sections. That is, also in flexure a boundary layer near the 'short' sides arises, a measure of which we provide in Sec. 6.2.

In the case of sections with double connection (closed) we have

$$\mathbf{t}_0 = \left\{ \frac{Y\mathbf{k}}{\delta} \cdot \left[\int_0^s (\delta * \bar{\mathbf{r}}_0) - \frac{\oint_{\mathcal{L}} \int_0^s (\delta * \bar{\mathbf{r}}_0)}{\oint_{\mathcal{L}} \frac{1}{\delta}} \right] + \frac{2GA_{\mathcal{R}} \nu \mathbf{k} \cdot (b_{\mathcal{R}} - o)}{\delta \oint_{\mathcal{L}} \frac{1}{\delta}} \right\} \mathbf{l} =: t_{s0}\mathbf{l}, \tag{4.28}$$

$$\mathbf{t}_1 = z\{\delta[\kappa t_{s0} - 2G\nu \mathbf{k} \cdot \mathbf{r}_0]\mathbf{l} + (\delta_{,s} t_{s0}) * \mathbf{l}\}, \tag{4.29}$$

$$\mathbf{t}_2 = \left\{ \frac{z^2}{2} \left[\delta(\delta_{,s} t_{s0})_{,s} - \delta_{,s}^2 t_{s0} \right] + z^2 \delta^2 \left[\kappa^2 t_{s0} - G\nu \mathbf{k} \cdot (\kappa \mathbf{r}_0 + *\mathbf{l}) \right] + \bar{t}_{s2} \right\} \mathbf{l} + \left\{ \delta \delta_{,s} \left[(z^2 + 1)\kappa t_{s0} + (z^2 - 3) G\nu \mathbf{k} \cdot \mathbf{r}_0 \right] + (1 - z^2)\delta^2 \left[\frac{\kappa_{,s} t_{s0}}{2} + \mathbf{k} \cdot (G\mathbf{l} + Y\kappa * \bar{\mathbf{r}}_0) \right] \right\} * \mathbf{l}. \tag{4.30}$$

Equation (4.28) is the Jouravski formula for thin closed section, which in the literature is found by an application of Volterra distorsions and the principle of virtual power [11, 12]. The second addend in t_{s0} is sometimes called "torsion in the section as a whole", because it has the same form of a Bredt field in the torsion of a thin closed section [2, 3, 4, 10, 11, 12, 13]; on the basis of our procedure, this similarity is more strict, as both come from the integral condition of compatibility, Eq. (2.4) [2, 3, 4]. Equations (4.29) – (4.30) provide a generalization of Jouravski formula for closed sections when the section is thicker. In Eq. (4.30) $\bar{t}_{s2}$ is an unknown function of s alone, determined in an implicit form by solving the next step of the procedure.

http://rcin.org.pl

5. Formal expansions for the warping

There is the following relationship between the shear stress field and the warping w of a section of a Saint-Venant cylinder [1, 6, 9]:

$$\mathbf{t} = G(\mathbf{v}' + \nabla w). \tag{5.1}$$

In Eq. (5.1) $\mathbf{v}'$ is a known function, given by

$$\mathbf{v}' = \tau * \mathbf{r} + \nu\{(\mathbf{r} \otimes *\mathbf{r}) + [*(y - b) \otimes \mathbf{r}\}\mathbf{k}; \tag{5.2}$$

it expresses the variation along the axis of the cylinder of the displacement of its substantial points in the plane of its sections. In Eq. (5.2) we dropped the addends which expressed a rigid contribution and used the definition $(\mathbf{a} \otimes \mathbf{b})\mathbf{c} := (\mathbf{a} \cdot \mathbf{c})\mathbf{b}$. The warping is then directly linked with the solution of the elliptic problem (2.1)–(2.4), and it is natural to try to integrate Eq. (5.1) to find its expression.

We assume that the following formal expansion holds:

$$w(s, z; \varepsilon) = \sum_{n=0}^{N} \varepsilon^n w_n(s, z) + o(\varepsilon^N). \tag{5.3}$$

Equation (5.3), substituted into Eqs. (3.8), (5.1)–(5.2), leads to a hierarchy of perturbation problems for the coefficients of the formal expansion of the warping. Due to the linearity of the problem in the two kinematical parameters, it is suggestive to split the hierarchy into two ones.

The first hierarchy describes the warping in torsion:

$$\sum_{n=0}^{N} \left[\varepsilon^{n+1}(\delta w_{n,s} - z\delta_{,s} w_{n,z})\mathbf{l} + \varepsilon^n(1 - \varepsilon z\kappa\delta) w_{n,z} * \mathbf{l}\right] = \frac{\sum_{n=0}^{N} \varepsilon^n (1 - \varepsilon z\kappa\delta)\delta \mathbf{t}_n}{G} - \tau\varepsilon\delta\left[*\mathbf{r}_0 - \varepsilon z\delta(\kappa * \mathbf{r}_0 + \mathbf{l}) + \varepsilon^2 z^2 \kappa \delta^2 \mathbf{l}\right]. \tag{5.4}$$

The second hierarchy describes the warping in flexure:

$$\sum_{n=0}^{N} \left[\varepsilon^{n+1}(\delta w_{n,s} - z\delta_{,s} w_{n,z})\mathbf{l} + \varepsilon^n(1 - \varepsilon z\kappa\delta) w_{n,z} * \mathbf{l}\right] = \frac{\sum_{n=0}^{N} \varepsilon^n (1 - \varepsilon z\kappa\delta)\delta \mathbf{t}_n}{G} - \nu\Big\{\mathrm{sym}(\mathbf{r}_0 \otimes *\mathbf{r}_0) - *\mathbf{b}_0 \otimes \mathbf{r}_0 + \varepsilon z\delta[\mathrm{sym}(*\mathbf{l} \otimes *\mathbf{r}_0 - \mathbf{r} \otimes \mathbf{l}) - (*\mathbf{b}_0 \otimes *\mathbf{l})] + \varepsilon^2[z^2\delta^2 \mathrm{sym}(*\mathbf{l} \otimes \mathbf{l}) - (*\mathbf{b}_2 \otimes \mathbf{r}_0)] + \varepsilon^3 z\delta(*\mathbf{b}_2 \otimes *\mathbf{l})\Big\}\mathbf{k}, \tag{5.5}$$

where sym stands for the symmetric part of the indicated tensor.

http://rcin.org.pl

In both Eqs. (5.4) – (5.5) we have dropped the terms of order higher than ε^N. The two hierarchies have the same structure, and the only difference is brought in by the right-hand sides, just like in the problems of determining the coefficients of the formal expansion of the shear stress. It is important to remark that the structure of the hierarchies decouples the system of partial differential equations into a system of *ordinary* equations, which significantly simplifies all the calculation. In the following we will give the results of the first coefficients of the formal expansions for the warping, dropping the constant values of integration which will only imply an (inessential) rigid contribution.

5.1. Warping coefficients in torsion

We provide at first the results for open sections, for which we have

$$w_0 = -2\tau\Omega(s), \tag{5.6}$$

$$w_1 = -\tau z\delta\mathbf{r}_0\cdot\mathbf{l}. \tag{5.7}$$

In Eq. (5.6) $\Omega(s)$ is the area of the inner Jordan region of the curve composed by the position vectors $\mathbf{r}(0)$, $\mathbf{r}(s)$ and the arc $0, s$ of $\mathcal{L}$ (sectorial area). Equation (5.6) is a formula which is found in the literature in the framework of the so-called Vlasov theory of thin-walled beams [11]. Equation (5.7) coincides with a fundamental assumption of the aforementioned theory: it states that for thicker sections the warping will be a linear function of the coordinate along the thickness. Vlasov does not consider a Saint – Venant cylinder, but regards a thin-walled beam as a shell and postulates that the section of the shell (which we have interpreted as the section of a Saint – Venant cylinder) is not affected by any deformation in its own plane. In Vlasov theory Eq. (5.6) is a consequence of the introduction of Kirchhoff-type internal constraints given by Eq. (5.7). From the point of view of our perturbation approach, this result is naturally obtained solving the lowest step of the hierarchy, which corresponds to thin sections. Moreover, our procedure shows that Kirchhoff-type constraints seem to be naturally satisfied by Saint – Venant displacement fields.

For closed sections we have

$$w_0 = 2\tau\left[\frac{A_{\mathcal{R}}}{\oint_{\mathcal{L}}\frac{1}{\delta}}\int_0^s\frac{1}{\delta} - \Omega(s)\right], \tag{5.8}$$

$$w_1 = -\tau z\delta\mathbf{r}_0\cdot\mathbf{l}. \tag{5.9}$$

Equation (5.8) gives again the warping according to the law of the sectorial area; this also is a known result for thin sections, based on Vlasov's theory. The additional term present in Eq. (5.8) with respect to Eq. (5.6) takes into account the necessity for the warping function to be periodical along the middle line.

http://rcin.org.pl

Equation (5.9) affirms that the first higher order correction to the warping of thin sections is the same as that for open sections. This is physically reasonable because the behaviour of the warping along the thickness does not have to depend on the section being open or closed.

The same results presented in Eqs. (5.6)–(5.9) were obtained also in [2, 3, 4] by means of the Prandtl stress flow function. It is worth remarking that in [2] we obtained the same equations dealing with Bredt-like sections of constant thickness: that is, at the first two steps of the iteration procedure, the coefficients of the formal expansion for the warping are not affected by the variable thickness.

5.2. Warping coefficients in flexure

In the case of flexure we have

$$w_0 = \frac{1}{G}\int_0^s t_{s0} - \nu \mathbf{k}\cdot\int_0^s [\mathrm{sym}\,(\mathbf{r}_0 \otimes *\mathbf{r}_0) - \mathbf{r}_0 \otimes *\mathbf{b}_0]\mathbf{l}\,, \tag{5.10}$$

$$w_1 = -\nu z\delta\left\{[\mathrm{sym}\,(\mathbf{r}_0 \otimes *\mathbf{r}_0) - *\mathbf{b}_0 \otimes \mathbf{r}_0]\mathbf{k}\cdot(*\mathbf{l}) + 2\mathbf{k}\cdot\int_0^s \mathbf{r}_0\right\}. \tag{5.11}$$

Equation (5.10) is the warping for thin sections, according to the interpretation of the thickness perturbation parameter; Eq. (5.11) is its generalization. As in the case of torsion, the first order coefficient of the formal expansion of the warping is a linear function of the z-coordinate.

We remark that the structure of the solution is the same both for open and closed sections, the difference being brought in only by the different expression of t_{s0}. This behaviour could be seen also in the expressions of the warping coefficients of the torsion. So far as we know, such a general formulation for the warping cannot be found in the literature.

6. Formal expansions for the resultant force and torque and for the shear shape factors

In Saint–Venant cylinders the kinematic characteristic parameters on which the general solution of the problem depends are linearly related to the resultant actions (force and torque) which act on the basis of the cylinder. This is of great relevance from the point of view of the applications, because it makes it possible to project the results obtained in the three-dimensional Saint–Venant theory onto the one-dimensional beam theory. In this way, the stiffness of a beam is a global property which results from an integral defined over the section of a Saint–Venant cylinder. So, it is rather important to check if our perturbation procedure is able to provide good approximate results also for the resultant force and torque.

http://rcin.org.pl

In the case of torsion, there is only one non-vanishing resultant action, which is the resultant torque due to the shear stress distribution:

$$T := \int_{\mathcal{D}_\varepsilon} [*(y - \bar{x})] \cdot \mathbf{t}, \tag{6.1}$$

where $\bar{x}$ is any point in $\mathcal{P}$, chosen as reduction pole for the torque. It is convenient (but unnecessary, of course) to put $\bar{x} = o$, so that the lever arm of the torque distribution is just the position vector of the places of the section, for which we have an ε-dependent expression, Eq. (1.3).

Also for the torque we obtain

$$T(\varepsilon) = \sum_{n=0}^{N} \varepsilon^n T_n = \int_{-1}^{1} \int_{0}^{l} \sqrt{g}(*\mathbf{r}_0 - \varepsilon z \delta \mathbf{l}) \cdot \sum_{n=0}^{N} \varepsilon^n \mathbf{t}_n , \tag{6.2}$$

where, as usual, we have dropped the terms $o(\varepsilon^N)$. On the basis of the results obtained in Sec. 4.1, we will calculate the coefficients of the formal expansion of the resultant torque and, as a consequence, the torsional rigidity (simply defined as the ratio of the torque and the unit angle of twist).

In the case of flexure, the peculiar resultant action is the shearing force:

$$\mathbf{q} := \int_{\mathcal{D}_\varepsilon} \mathbf{t}, \tag{6.3}$$

as a matter of fact, the resultant torque of the shear stress distribution is an effect of the choice of the origin of the plane $\mathcal{P}$, Eqs. (2.13) – (2.16), and vanishes when the so-called shear centre, or centre of flexure [9, 10, 11, 12] is chosen as origin. For $\mathbf{q}$ we obtain

$$\mathbf{q}(\varepsilon) = \sum_{n=0}^{N} \varepsilon^n \mathbf{q}_n = \int_{-1}^{1} \int_{0}^{l} \sqrt{g} \sum_{n=0}^{N} \varepsilon^n \mathbf{t}_n , \tag{6.4}$$

always dropping the terms $o(\varepsilon^N)$.

There is also another expression for $\mathbf{q}$, given by the theory of Saint-Venant [1, 6, 9]:

$$\mathbf{q} = Y * \mathbf{J}_b \mathbf{k}, \tag{6.5}$$

$$\mathbf{J}_b := \int_{\mathcal{D}_\varepsilon} [*(y - b) \otimes *(y - b)], \tag{6.6}$$

where $\mathbf{J}_b$ is a tensor of inertia of the section with respect to its centroid. Substituting the expression of the position vector of the places of the section, Eq. (1.3),

http://rcin.org.pl

into Eqs. (6.5), (6.6) it is found that $\mathbf{J}_b$ is a polynomial function of the thickness parameter:

$$\mathbf{J}_b = 2\varepsilon \int_0^l \delta(*\bar{\mathbf{r}}_0 \otimes *\bar{\mathbf{r}}_0) + \frac{4}{3}\varepsilon^3 \int_0^l \delta^3[\mathbf{l} \otimes \mathbf{l} + \operatorname{sym}(\bar{\mathbf{r}}_0 \otimes \kappa\mathbf{l})] \tag{6.7}$$

$$=: \varepsilon \mathbf{J}_{b1} + \varepsilon^3 \mathbf{J}_{b3}.$$

According to Eqs. (6.5) – (6.7), then, the resultant shearing force may be written as

$$\mathbf{q} = Y * (\varepsilon \mathbf{J}_{b1} + \varepsilon^3 \mathbf{J}_{b3})\mathbf{k} =: \varepsilon \mathbf{q}_1 + \varepsilon^3 \mathbf{q}_3 . \tag{6.8}$$

In Sec. 6.2 we will compare the results obtained by substituting the coefficients of the shear stress given in Sec. 4.2 in Eq. (6.4) with the result given by Eqs. (6.5)–(6.8).

In the technical literature the symmetric tensor $\mathbf{K}$ of the shear shape factors is introduced, according to the following equivalence in power:

$$\frac{1}{2}\mathbf{q}\cdot\mathbf{K}\frac{\mathbf{q}}{GA_{\mathcal{D}_\varepsilon}} = \frac{1}{2G}\int_{\mathcal{D}_\varepsilon}(\mathbf{t}\cdot\mathbf{t}) \;\Rightarrow\; \mathbf{q}\cdot\mathbf{K}\mathbf{q} = A_{\mathcal{D}_\varepsilon}\int_{\mathcal{D}_\varepsilon}(\mathbf{t}\cdot\mathbf{t}). \tag{6.9}$$

An ε-formal power series expansion holds also for $\mathbf{K}$, as, from Eq. (6.9), we easily obtain the following expression:

$$\left(\sum_{n=0}^{N}\varepsilon^n\mathbf{q}_n\right)\cdot\left(\sum_{n=0}^{N}\varepsilon^n\mathbf{K}_n\sum_{n=0}^{N}\varepsilon^n\mathbf{q}_n\right) \tag{6.10}$$

$$= 2\varepsilon\int_0^l \delta\int_{-1}^{1}\int_0^l \sqrt{g}\left(\sum_{n=0}^{N}\varepsilon^n\mathbf{t}_n\right)\cdot\left(\sum_{n=0}^{N}\varepsilon^n\mathbf{t}_n\right);$$

in the former, we have dropped the terms $o(\varepsilon^N)$.

6.1. Resultant torque coefficients in torsion

As previously done, we will first give the results for open sections, for which we have found only an outer expansion of the shear stress distribution:

$$T_0 = T_1 = T_2 = 0, \tag{6.11}$$

$$T_3 = \frac{4}{3}G\tau\int_0^l\left\{\left[\int_0^s \kappa\delta^2\delta_{,s}\right](*\mathbf{r}_0\cdot\mathbf{l}) - 4\delta^2\delta_{,s}(\mathbf{r}_0\cdot\mathbf{l}) + \delta^3(1 + *\mathbf{r}_0\cdot\kappa\mathbf{l})\right\}. \tag{6.12}$$

Equation (6.11) expresses a known result, which is not clearly affirmed in the literature, though: the resultant torque in the torsion of an open section of a

http://rcin.org.pl

Saint-Venant cylinder appears only with the third power of the thickness. From the point of view of our technique, this is a natural result of the perturbation method.

Equation (6.12) is the generalization of another known result, that is to say, the so-called Kelvin formula for the resultant torque of thin sections. So far as we know, in the literature there is no general formula like Eq. (6.12). All the results given in the literature for each particular open section may be found starting from Eq. (6.12): this is particularly evident in the case of sections with constant thickness, for which we immediately recover the expressions given in [2, 3] and in the technical literature [10, 11, 12].

For instance, from Eq. (6.12) one obtains the exact resultant torque in the case of a semicircular section with constant thickness. In this case, the boundary layer effect, named after Kelvin, vanishes because of geometrical effects, and the outer expansion of the shear stress provides a very good approximation of the global effects of the actual distribution.

This does not happen in the case of rectangular sections, for which we obtain from Eq. (6.12)

$$T_3 = \frac{G\tau(2\delta)^3 l}{6}, \tag{6.13}$$

which is only one half of the actual resultant torque. The outer expansion of **t** loses information on the actual stress distribution near the short edges of the rectangle. The portion of resultant torque missing in Eq. (6.13) is a measure of the boundary layer (Kelvin) effect, and was already obtained in some previous works [2, 3, 4, 6].

We remark, though, that, if we start studying the torsion from a formal expansion of the Prandtl stress flow function, as was done in [2, 3, 4, 6], we obtain the exact result for the resultant torque. This is reasonable, because Prandtl function is in some sense a primitive for the shear stress (see Sec. 2), that is to say, it is richer in information. Thus, if we calculate the resultant torque as the integral of Prandtl function over the section [1, 6, 9, 12], we are able to recover also the global contribution of the boundary layer (but not its actual local behaviour).

In the case of closed sections we obtain

$$T_0 = 0, \tag{6.14}$$

$$T_1 = 4G\tau \frac{A_{\mathcal{R}}^2}{\oint_{\mathcal{L}} \frac{1}{2\delta}}, \tag{6.15}$$

$$T_2 = 0. \tag{6.16}$$

Equation (6.14) is a known result, though never explicitly affirmed in the literature: the resultant torque must vanish when the thickness of the section fades.

http://rcin.org.pl

Equation (6.15) is another well known result, that is to say, Bredt formula [10, 11, 12, 13]; the same expression was obtained also starting from Prandtl stress flow function in [2, 3, 4]. Equation (6.16) is a new result which affirms that the first generalization of Bredt formula has to be searched at orders higher than two in the thickness parameter: this is a justification of the validity of Bredt formula in all the applications.

6.2. Resultant force and shear shape factors coefficients in flexure

For both open and closed sections we obtain

$$\mathbf{q}_0 = \mathbf{0}, \tag{6.17}$$

$$\mathbf{q}_1 = Y * \mathbf{J}_{b1}\mathbf{k}, \tag{6.18}$$

$$\mathbf{q}_2 = \mathbf{0}. \tag{6.19}$$

As usual, Eq. (6.17) affirms that the resultant action must be zero for fading thickness. The most interesting result is represented by Eqs. (6.18) – (6.19): they show that, no matter if we use Eq. (6.4) or Eqs. (6.5) – (6.8), we obtain the same results. We remark also that the resultant shearing force, as a global result, does not take into account the section being open or closed, and the different forms of Jouravski formula in the two cases, Eqs. (4.25), (4.28). Equations (6.17) – (6.19) imply that Kelvin effect in flexure is at least a third order effect in ε. Such a phenomenon has been studied in [6] in the case of open Bredt-like sections with constant thickness. In [6] the flexure is studied starting from a generalized stress flow function; there it is shown that such a function verifies all boundary conditions up to the second order in an ε-formal expansion – i.e., a boundary effect arises only starting from the third order in ε.

Equations (6.18) – (6.19) confirm that, even if Jouravski formula was originally obtained in a heuristic way, its validity is really great for all the applications. Indeed it is simple to use and provides good global approximate results. We also think that, as we have been able to find and rationally justify these results, our generalization perturbation technique is meaningful.

As for the coefficients of the formal expansion of the shear shape factors tensor (6.10), we obtain

$$\mathbf{q}_1 \cdot \mathbf{K}_0 \mathbf{q}_1 = 4 \int_0^l \delta \int_0^l \delta(x t_0 \cdot \mathbf{t}_0), \tag{6.20}$$

$$\mathbf{q}_1 \cdot \mathbf{K}_1 \mathbf{q}_1 = 0 \quad \Rightarrow \quad \mathbf{K}_1 = \mathbf{0}, \tag{6.21}$$

$$\mathbf{q}_1 \cdot \mathbf{K}_2 \mathbf{q}_1 = 4 \int_0^l \delta \int_0^l \left[(2\mathbf{t}_0 \cdot \mathbf{t}_2 + \mathbf{t}_1 \cdot \mathbf{t}_1)\delta - 2z\kappa\delta^2 \mathbf{t}_1 \cdot \mathbf{t}_0 \right]. \tag{6.22}$$

It is easy and meaningful to calculate the coefficient given by Eq. (6.20) at least for simply connected (open) sections, using Eqs. (4.25) and (6.18). If we make

http://rcin.org.pl

use of an orthonormal basis whose elements are directed along the principal axes of inertia of the section, it is

$$\mathbf{K}_0 = \frac{A_{\mathcal{D}_\varepsilon}}{2} \begin{pmatrix} \dfrac{1}{J_{b1\,22}^2} \displaystyle\int_0^l \frac{S_2^2}{\delta} & \dfrac{1}{J_{b1\,11} J_{b1\,22}} \displaystyle\int_0^l \frac{S_1 S_2}{\delta} \\ \dfrac{1}{J_{b1\,11} J_{b1\,22}} \displaystyle\int_0^l \frac{S_1 S_2}{\delta} & \dfrac{1}{J_{b1\,11}^2} \displaystyle\int_0^l \frac{S_1^2}{\delta} \end{pmatrix}, \tag{6.23}$$

S_1, S_2 are the first moments of area with respect to the 1 and 2 directions as functions of the s coordinate.

So far as we know, Eq. (6.23) is not given in the literature; usually only one of the components of the main diagonal is calculated [11, 12], and coincides with that given in Eq. (6.23).

7. Applications

We will at first consider the torsion of an isosceles trapezium whose height is l and whose bases are $2h_1$, $2h_2$. We let the s coordinate run along the height; as the s coordinate line is a portion of a straight line, its curvature vanishes. An orthonormal basis $(\mathbf{e}_1, \mathbf{e}_2)$ is given whose first element is parallel to the height of the trapezium,

$$\begin{aligned} &\mathbf{r}_0 = s\mathbf{e}_1, \quad 0 \leq s \leq l \;\Rightarrow\; \mathbf{l} = \mathbf{e}_1, \\ &\delta(s) = h_1 + (h_2 - h_1)\frac{s}{l} \;\Rightarrow\; \delta_{,s} = \frac{h_2 - h_1}{l}. \end{aligned} \tag{7.1}$$

Obviously, if $h_2 = 0$ the section reduces to an isosceles triangle and if $h_2 = h_1$, the trapezium degenerates into a rectangle.

Let us determine, as a meaningful example, the first nonvanishing term of the resultant torque coefficient given according to Eq. (6.12):

$$\frac{T_3}{G\tau} = \frac{4}{3}\int_0^l (\delta^3 - 4\delta^2\delta_{,s}\mathbf{r}_0 \cdot \mathbf{l}) = \frac{4}{3} l \left[\frac{7}{12} h_1 (h_1^2 + h_1 h_2 + h_2^2) - \frac{3}{4} h_2^3\right]. \tag{7.2}$$

If $h_1 \approx h_2$, we obtain once again the same result provided by Eq. (6.13), which was to be expected, as we have used only an outer expansion for $\mathbf{t}$. If $h_2 = 0$ (isosceles triangle), it is

$$\frac{T_3}{G\tau} = \frac{7}{72}(2h_1)^3 l. \tag{7.3}$$

http://rcin.org.pl

In [11] we found that the value for $T_3/G\tau$ is $[(2h_1)^3 l]/6$; then Eq. (7.3) overestimates the actual torsional rigidity. The difference between the value given by Eq. (7.3) and that in [11] is a measure of Kelvin effect for isosceles triangles: it is less relevant than that for the rectangle, as the vertex of the triangle is a stagnation point for the shear stress flow and its contribution to the resultant torque is negligible. The result given in [3] was obtained by using Prandtl stress flow function. We remarked in the last section that Prandtl function provides more accurate results because, at least at the lowest steps of a perturbation hierarchy, it is not affected by a boundary layer effect as it happens for the formal expansion for **t** used in this paper.

As a second application of our method, let us consider the flexure of an isosceles triangle of height l and basis $2h$; as for the trapezium studied before, the s coordinate runs along the height and the curvature κ of the middle line (which coincides with the height) vanishes. Let us assume that the kinematical parameter **k** is orthogonal (the resultant shearing force is parallel, Eqs. (6.5), (6.6)) to the height, as it is usually done in the literature. An orthonormal basis $(\mathbf{e}_1, \mathbf{e}_2)$ is given whose first element is parallel to the height of the triangle,

$$\begin{aligned} &\mathbf{r}_0 = s\mathbf{e}_1, \quad 0 \le s \le l \quad \Rightarrow \quad \mathbf{l} = \mathbf{e}_1, \\ &\delta(s) = \frac{h}{l}(l - s) \quad \Rightarrow \quad \delta_{,s} = -\frac{h}{l}. \end{aligned} \tag{7.4}$$

It is known from elementary geometry that

$$b - o = \mathbf{b}_0 = \frac{l}{3}\mathbf{e}_1 \quad \Rightarrow \quad \tilde{\mathbf{r}}_0 = \left(s - \frac{l}{3}\right)\mathbf{e}_1 . \tag{7.5}$$

Besides, the coordinates s, z run along the principal axes of inertia of the domain, so that (see Eq. (6.7))

$$\mathbf{J}_b = \begin{pmatrix} J_s & 0 \\ 0 & J_z \end{pmatrix} = \begin{pmatrix} J_{b3} & 0 \\ 0 & J_{b1} \end{pmatrix}, \qquad J_{b1} = \frac{hl^3}{18}. \tag{7.6}$$

The coefficients of the formal expansion of the shear stress fields are, with respect to $(\mathbf{l}, *\mathbf{l}) \equiv (\mathbf{e}_1, \mathbf{e}_2)$, (see Eqs. (4.25) – (4.27))

$$\mathbf{t}_0 = \frac{6s}{hl^3}(l - s)\mathbf{e}_1 =: t_{s0}\mathbf{e}_1 , \tag{7.7}$$

$$\mathbf{t}_1 = z\delta_{,s} t_{s0}\mathbf{e}_2 , \tag{7.8}$$

$$\mathbf{t}_2 = G\frac{\delta^2}{3}(2\nu - 1)\left(\frac{10}{3} - z^2\right)\mathbf{e}_1 , \tag{7.9}$$

Eqs. (7.7) – (7.8) are known in literature [10, 11, 12]; the first one represents the Jouravski mean shear stress field, and the second is orthogonal to the direction

http://rcin.org.pl

of the first. In the literature it is said, on heuristic grounds, that the field given by Eq. (7.8) is of small magnitude if compared with the Jouravski field. Our procedure gives a rational justification of this result, since Eq. (7.8) is simply a coefficient of higher order in a formal expansion of **t**. Equation (7.9), so far as we know, is a new result, providing an estimate of the shear stress field in thick isosceles triangles.

8. Conclusions

In this paper we have presented a rational procedure of formal expansion of the shear stress field for a Saint - Venant cylinder, using techniques from differential geometry. The class of domains which we are able to describe is large enough to embrace many of the sections used in typical technological applications. We are able to obtain a general formulation of the elliptic problem both for torsion and flexure. The results we find cover all the known technical formulae given in the literature at the first steps of the formal expansion, that is to say, when the section is thin. We are also able to provide new approximate formulae which seem to be meaningful.

Further investigations should be addressed to the numerical testing of the new approximate expressions and to an attempt to regularize the procedure, which we know to supply – in the present form – diverging series [17]. Finally, it may be mathematically interesting, using the methods developed in [16], to estimate the distance between the generalized Jouravski formulae we provide and the true solutions to Saint - Venant shear stress problem.

References

1. A. CLEBSCH, *Théorie de l'élasticité des corps solides* (Traduite par MM. Barré de Saint–Venant et Flamant, avec des Notes étendues de M. Barré de Saint–Venant), Dunod, Paris 1883 [Reprinted by Johnson Reprint Corporation, New York 1966].
2. F. DELL'ISOLA and G.C. RUTA, *Outlooks in Saint–Venant theory. I. Formal expansions for torsion of Bredt-like sections*, Arch. Mech., **46**, 6, 1005–1027, 1994.
3. F. DELL'ISOLA and L. ROSA, *Outlooks in Saint-Venant theory. II. Torsional rigidity, shear stress, "and all that" in the torsion of cylinders with sections of variable thickness*, Arch. Mech., **48**, 4, 753–763, 1996.
4. F. DELL'ISOLA and L. ROSA, *An extension of Kelvin and Bredt formulas*, Math. and Mech. of Solids, **1**, 2, 243–250, 1996.
5. L. PRANDTL, *Zur Torsion von Prismatischen Stäben*, Phys. Zeits., **4**, 758, 1903.
6. G.C. RUTA, *Espansioni formali per il problema di Saint–Venant*, Ph. D. Thesis, University of Roma "La Sapienza", 1996.
7. A.H. NAYFEH, *Perturbation methods*, John Wiley and Sons, New York 1973.
8. L.E. MALVERN, *Introduction to the mechanics of a continuous medium*, Prentice- Hall, Englewood Cliffs, N.J. 1969.
9. B.M. FRAEIJS DE VEUBEKE, *A course in elasticity*, Springer-Verlag, New York 1979.
10. V.I. FEODOSYEV, *Strength of materials* [in Russian], MIR, Moskva 1968 [Italian translation: *Resistenza dei materiali*, Editori Riuniti, Roma 1977].
11. A. GJELSVIK, *The theory of thin-walled bars*, John Wiley and Sons, New York 1981.

http://rcin.org.pl

12. C. GAVARINI, *Lezioni di Scienza delle Costruzioni*, 3rd ed., Masson ed. ESA, Milano 1996.
13. R. BREDT, *Kritische Bemerkungen zur Elastizität*, Zeits. Ver. Deutsch. Ing., **40**, 785–816, 1896.
14. V.I. ARNOLD, *Mathematical methods of classical mechanics* [in Russian], MIR, Moskva 1979 [Italian translation: *Metodi matematici della meccanica classica*, Editori Riuniti, Roma 1992].
15. B. SCHUTZ, *Geometrical methods of mathematical physics*, Cambridge University Press, 1990.
16. L. WHEELER and C.O. HORGAN, *Upper and lower bounds for the shear stress in the Saint–Venant theory of flexure*, J. Elasticity, **6**, 4, 383–403, Noordhoff, Leyden 1976.
17. K. FRISCHMUTH, M. HÄNLER and F. DELL'ISOLA, *Numerical methods versus asymptotic expansion for torsion of hollow elastic beams*, preprint 95/20 Fachbereich Mathematik der Universität Rostock 1995.

DIPARTIMENTO DI INGEGNERIA STRUTTURALE E GEOTECNICA,
and
DOTTORATO DI RICERCA IN MECCANICA TEORICA E APPLICATA
UNIVERSITA DI ROMA "I.A SAPIENZA", FACOLTA D'INGEGNERIA,
via Eudossiana 18, I-00184 Roma, Italia
e-mail: isola@scilla.ing.uniroma1.it
e-mail: ruta@scilla.ing.uniroma1.it

Received January 17, 1997.

http://rcin.org.pl

Arch. Mech., 49, 2, pp. 345–358, Warszawa 1997

Transport properties of finite and infinite composite materials and Rayleigh's sum

V. MITYUSHEV (SŁUPSK)

THE TRANSPORT properties of a regular array of cylinders embedded in a homogeneous matrix material have been studied by the following method. Let us bound a part of the infinite material by a closed curve γ. Knowing the transport properties of this finite amount of material, we can evaluate the transport properties of the infinite material when γ tends to infinity. This method allows us to justify the method of Lord RAYLEIGH [1] for rectangular arrays of cylinders. Moreover, it is shown that in order to improve the Clausius–Mossotti approximation for a rectangular array, it is necessary to evaluate Rayleigh's sum.

1. Introduction

A REGULAR array of cylinders is embedded in a homogeneous matrix material. The transport properties of this composite material can be studied by two approaches. The first approach is based on studying a boundary value problem in a cell representing a regular structure. A highly developed theory is used in this approach, from general investigations of homogenization to computation of the effective conductivity of the special composite materials. Results of this study are due to Lord RAYLEIGH [1], BERGMAN and DUNN [22] KOŁODZIEJ [9], MANTEUFEL and TODREAS [10], MCPHEDRAN *et al.* [4–7], MITYUSHEV [8, 11, 23], PERRINS *et al.* [2], POLADIAN *et al.* [3], SANGANI and ACRIVOS [21] and many others. The previous results concern mainly isotropic homogenized materials: the square and hexagonal arrays of cylinders. Exceptions are [1, 11, 23], where general anisotropic homogenized materials are considered by analytical methods. Using the method of collocations, KOŁODZIEJ [9] computed also the effective conductivity in a fixed direction for the special arrays including anisotropic regular structures.

The present paper presents the direct approach which is based on the following idea. Let us bound a part of the infinite material body by a closed curve γ (Fig. 1). Suppose that we can study the transport properties of this finite composite material bounded by γ. Let the curve γ tend to infinity. We set up the hypothesis that the limit transport properties coincide with the transport properties of regular infinite material bodies. Anyway, it follows from the theory of homogenization. Therefore evaluating the limits, we can get the values in question for the infinite material.

We shall investigate the limit properties in the simplest case of circular cylinders packed in a rectangular array. However, following [23] it is easy to transfer the results to arbitrary arrays of parallelograms. The sides of the rectangle will be

http://rcin.org.pl

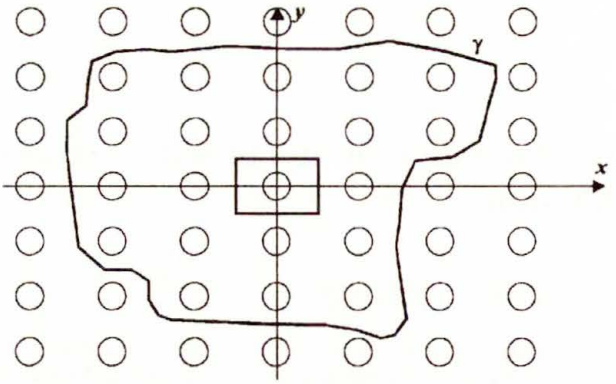

FIG. 1. Infinite rectangular array of circular cylinders and finite material bounded by γ.

denoted by α and β, and the radius of the cylinders by r. Assume that $\beta = \alpha^{-1}$, hence the area of the rectangle is equal to 1. We shall also assume that the state of the media is described by the two-dimensional Laplace equation. If the volume fraction of the cylinders is very small, then the effective conductivity can be evaluated by the Clausius - Mossotti formula (see Sec. 4, formula (4.5)). In order to improve this formula for the rectangular array of cylinders, Lord RAYLEIGH [1] introduced the absolutely divergent sum

$$S_2 := \sum{}' \frac{1}{(m_1\alpha + im_2\beta)^2},$$

where m_1 and m_2 run over all integers except $m_1 = m_2 = 0$ ($i^2 = -1$). The sum S_2 is conditionally convergent. Its value is dependent upon the shape of the exterior boundary of the pairs (m_1, m_2) which tends to infinity. The sum S_2 can be expressed by the integral

$$S_2 = \iint_{\mathbb{R}} \frac{1}{z^2} dx\, dy,$$

where $z = x + iy$. Lord RAYLEIGH [1] proposed to calculate S_2 by summation over a "needle-shaped" region, infinitely more extended along the x-axis than along the y-axis (Fig. 2). In this case

$$S_2 = S_2(\alpha^2) = \frac{2\pi^2}{\alpha^2}\left(\sum_{m=1}^{\infty} \sin^{-2}(im\pi\alpha^{-2}) + \frac{1}{6}\right). \tag{1.1}$$

Let us note that $S_2(1) = \pi$. Applying the theory of generalized functions MITYUSHEV [8] obtained the same result: $S_2(1) = \pi$. Since the sum S_2 is conditionally convergent, we can get any value for S_2 changing the shape of the exterior boundary. Using the effects of polarization, MCPHEDRAN *et al.* [7], PERRINS *et al.* [2]

http://rcin.org.pl

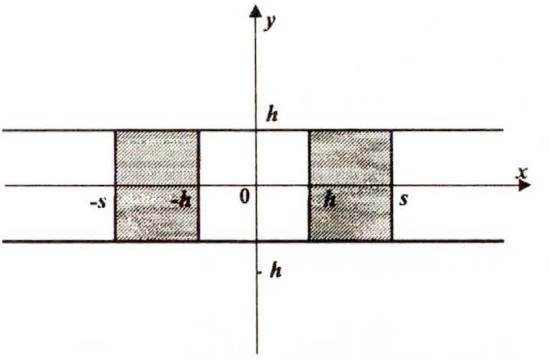

FIG. 2. Rayleigh's method of summation:

$$S_2 := \lim_{h\to\infty}\lim_{s\to\infty}\int_{-h}^{+h}\left(\int_{-s}^{-h}+\int_{h}^{s}\right)\frac{dxdy}{(x+iy)^2}. \quad \text{It is assumed that} \quad \int_{-h}^{+h}\int_{-h}^{+h}\frac{dxdy}{(x+iy)^2}=0.$$

proposed an explanation of this strange fact. In the present paper this fact has been explained completely.

At the beginning we consider two problems corresponding to infinite and finite material bodies separately. Then we shall compare the limiting effective conductivity of finite body and the effective conductivity of infinite body.

Let us assume the following independent variables. We shall write $z = x + iy$ if we consider a point inside the domain, and $t = x + iy$ if we consider a boundary point. Throughout the paper z and t are complex, x and y are real numbers.

2. Finite material body

Let G be a simply connected domain in the complex plane $\mathbb{C} := \{z = x + iy\}$ with the Lyapunov boundary γ. Let us introduce the points $a_1, a_2, ..., a_n \in G \cap E$ in the complex plane $\mathbb{C}$, where $E := \{m_1\alpha + im_2\alpha^{-1}$, m_1 and m_2 are integers$\}$. Consider mutually disjoint circles $D_k := \{z \in \mathbb{C},\ |z - a_k| < r\}$ $(k = 1, 2, ..., n)$ contained within the domain G. Suppose that $\bigcup_{k=1}^{n} D_k$ and $D := G \setminus \bigcup_{k=1}^{n} D_k$ are occupied by two isotropic materials with conductivities λ_1 and λ, respectively. In order to determine the transport properties of G, we find the potentials $u(x, y)$, $u_1(x, y)$, $u_2(x, y)$, ..., $u_n(x, y)$ which are harmonic in the respective domains D, D_1, D_2, ..., D_n, continuously differentiable in the closures of these domains with the boundary conditions

$$\begin{aligned} &u = u_k, \qquad \lambda\frac{\partial u}{\partial n} = \lambda_1\frac{\partial u_k}{\partial n} \\ &\qquad\qquad \text{on } \partial D_k := \{t \in \mathbb{C},\ |t - a_k| = r\}, \qquad k = 1, 2, ..., n, \\ &u = f \qquad \text{on } \gamma, \end{aligned} \tag{2.1}$$

http://rcin.org.pl

where $\partial/\partial n$ is a normal derivative, f is a given continuous function. We shall study the transport properties in the x-direction. Hence, we may take $f(t) = \operatorname{Re} t = x$. It is convenient to make the change

$$U_k(x,y) := \frac{\lambda_1 + \lambda}{2\lambda} u_k(x,y), \qquad k = 1,2,...,n.$$

Then the problem (2.1) takes the form

$$(2.2) \qquad u = (1-\varrho)U_k\,, \qquad \frac{\partial u}{\partial n} = (1+\varrho)\frac{\partial U_k}{\partial n} \qquad \text{on } \partial D_k\,, \quad u = f \quad \text{on } \gamma,$$

where $\varrho := (\lambda_1 - \lambda)/(\lambda_1 + \lambda)$.

General theory of the problem (2.2) is based on integral equations constructed by GAKHOV [13], MIKHAJLOV [14]. The problem (2.2) has been solved in an analytic form by MITYUSHEV [15, 16].

Let us consider certain auxiliary problems. The Dirichlet problem $V = f$ on ∂D for the function $V(x,y)$ harmonic in the domain D has the unique solution

$$V(z) = V(x,y) = \int_{\partial D} f \frac{\partial g}{\partial n} ds =: Sf(x,y) = Sf(z), \qquad z = x + iy \in D,$$

where g is Green's function of the domain D. The operator $S : f \to V$ transforms a continuously differentiable function into a function harmonic in D and continuously differentiable in $\overline{D}$ if ∂D is a smooth curve. Let us consider the domain $D_k^- := \{z \in \mathbb{C}, \ |z - a_k| > r\}$ $(k = 1,2,...,n)$. We shall use the operators S_k corresponding to D_k^- and the operator S_γ corresponding to G. If $V(z)$ is harmonic in D_k, then

$$S_k V(z) = V(z_k^*), \qquad z \in D_k^-\,, \quad k = 1,2,...,n,$$

where points $z_k^* := r^2/(\overline{z - a_k}) + a_k$ and z are symmetric with respect to the circumference $|t - a_k| = r$. Let us consider the next auxiliary boundary value problem

$$(2.3) \qquad \frac{\partial U_0}{\partial n} + \frac{\partial S_\gamma U_0}{\partial n} = h \quad \text{on } \gamma,$$

for the function $U_0(z)$ harmonic in $\overline{\mathbb{C}}\backslash\overline{G}$ and vanishing at infinity.

LEMMA (MITYUSHEV [18]). Let h be a function continuously differentiable on γ. Then the boundary value problem (2.3) has a unique solution continuously differentiable in $\overline{\mathbb{C}}\backslash\gamma$.

http://rcin.org.pl

If the function $u(x,y)$ from (2.2) is known, then using the above lemma, introduce the function $U_0(z)$ with $h = \partial u/\partial n - \partial x/\partial n$. Let us consider the function

$$\Phi(z) = \begin{cases} U_k(z) + \varrho \sum\limits_{\substack{m=1 \\ m\neq k}}^{n} U_m(z_m^*) + S_\gamma U_0(z) - x, & |z-a_k| \leq r, \quad k = 1,2,...,n, \\ U_0(z) + \varrho \sum\limits_{m=1}^{n} U_m(z_m^*), & z \in \overline{\mathbb{C}}\backslash G, \\ u(z) + \varrho \sum\limits_{m=1}^{n} U_m(z_m^*) + S_\gamma U_0(z) - x, & z \in D, \end{cases}$$

harmonic in $\mathbb{C}\backslash\partial D$. Using the boundary conditions (2.2) and (2.3), calculate the jumps of Φ on ∂D_k and γ

$$\Phi^+(t) - \Phi^-(t) = u(t) + \varrho U_k(t) - U_k(t) = 0, \qquad t \in \partial D_k, \quad k = 1,2,...,n,$$
$$\Phi^+(t) - \Phi^-(t) = u(t) + S_\gamma U_0(t) - x - U_0(t) = 0 \quad \text{on} \quad \gamma.$$

Here $\Phi^+(t) := \lim\limits_{\substack{z\to t \\ z\in D}} \Phi(z)$, $\Phi^-(t) := \lim\limits_{\substack{z\to t \\ z\in D_k}} \Phi(z)$. Along the same lines

$$\frac{\partial \Phi^+}{\partial n}(t) - \frac{\partial \Phi^-}{\partial n}(t) = \frac{\partial u}{\partial n}(t) + \varrho \frac{\partial}{\partial n}(U_k(t_k^*)) - \frac{\partial U_k}{\partial n}(t)$$
$$= \frac{\partial u}{\partial n}(t) - (1+\varrho)\frac{\partial U_k}{\partial n}(t) = 0, \qquad t \in \partial D_k, \quad k = 1,2,...,n,$$

since

$$\frac{\partial}{\partial n}(U_k(t_k^*)) = -\frac{\partial U_k}{\partial n}(t) \quad \text{on} \quad \partial D_k.$$

Taking into account (2.3), we calculate

$$\frac{\partial \Phi^+}{\partial n}(t) - \frac{\partial \Phi^-}{\partial n}(t) = \frac{\partial u}{\partial n}(t) - \frac{\partial S_\gamma U_0}{\partial n}(t) - \frac{\partial x}{\partial n} - \frac{\partial U_0}{\partial n}(t) = 0 \qquad \text{on} \quad \gamma.$$

The function $\Phi(z)$ is harmonic in $\overline{\mathbb{C}}\backslash\partial D$ and $\Phi^+ = \Phi^-$, $\partial\Phi^+/\partial n = \partial\Phi^-/\partial n$ on ∂D. According to the theorem of harmonic (analytic) continuation and Liouville's theorem we conclude that $\Phi(z) = c = \text{const}$. From the definition of $\Phi(z)$ we obtain the formulae

$$U_k(z) = -\varrho \sum_{\substack{m=1 \\ m\neq k}}^{n} U_m(z_m^*) - S_\gamma U_0(z) + x + c, \quad |z-a_k| \leq r, \quad k = 1,2,...,n,$$

$$U_0(z) = -\varrho \sum_{m=k}^{n} U_m(z_m^*) + c, \quad z \in \overline{\mathbb{C}}\backslash G.$$

http://rcin.org.pl

From the last equality we determine $S_\gamma U_0(z)$ and substitute it in the previous equalities. As a result, we have the following system of functional equations

$$U_k(z) = -\varrho \left[\sum_{\substack{m=1 \\ m\neq k}}^{n} [U_m(z_m^*) - S_\gamma U_m(t_m^*)(z) \right] + \varrho S_\gamma U_k(t_k^*)(z) + x, \tag{2.4}$$

$$|z - a_k| \leq r, \qquad k = 1, 2, \ldots, n,$$

for $U_k(z)$ $(k = 1, 2, \ldots, n)$. Each harmonic function in a simply connected domain is the real part of an analytic function, which is uniquely determined with accuracy to an additive imaginary constant. Hence there exists such a function $\phi_k(z)$ analytic in $|z - a_k| \leq r$ that $\operatorname{Re} \phi_k(z) = U_k(z)$. Let us introduce the operator T_γ^m which transforms a function $\phi_m(z)$ analytic in G in the following way. At the beginning calculate $\operatorname{Re} \phi_m(t_m^*) = U_m(t_m^*)$ on γ. Further on, by applying S_γ we obtain a harmonic function which is the real part of the analytic function $T_\gamma^m \phi_m(z)$. Actually in the last step we used the Schwarz operator of G studied by MIKHLIN [17]. We do not determine a pure imaginary constant in $T_\gamma^m \phi_m(z)$ because it does not affect the final result. So the system (2.4) is reduced to the following system of functional equations

$$\phi_k(z) = -\varrho \sum_{\substack{m=1 \\ m\neq k}}^{n} \left[\overline{\phi_m(z_m^*)} - T_\gamma^m \phi_m(z) \right] + \varrho T_\gamma^k \phi_k(z) + z,$$

$$|z - a_k| \leq r, \quad k = 1, 2, \ldots, n.$$

Let us differentiate this system and obtain

$$\phi_k'(z) = \varrho \sum_{\substack{m=1 \\ m\neq k}}^{n} \left[\left(\frac{r}{z - a_m} \right)^2 \overline{\phi_m'(z_m^*)} + V_\gamma^m \phi_m'(z) \right] + \varrho V_\gamma^k \phi_k'(z) + 1, \tag{2.5}$$

$$|z - a_k| \leq r, \quad k = 1, 2, \ldots, n,$$

where $V_\gamma^m \phi_m'(z) := (T_\gamma^m \phi_m)'(z)$. The operator V_γ^m is correctly defined because MIKHLIN [17] has proved that T_γ^m is an integral operator.

THEOREM 1 (MITYUSHEV [15, 16, 18, 23]). *The system of functional equations* (2.5) *for the functions* $\phi_k'(z)$ *analytic in* $|z - a_k| < r$ *and continuous in* $|z - a_k| \leq r$ $(k = 1, 2, \ldots, n)$ *has a unique solution. That solution can be found by the method of successive approximations converging uniformly in* $|z - a_k| \leq r$ $(k = 1, 2, \ldots, n)$.

This theorem has the following important consequence.

THEOREM 2. *The function* $\dfrac{\partial U_k}{\partial x}(a_k) = \operatorname{Re} \phi_k'(a_k)$ *is analytic in the unit disc* $|\varrho| < 1$ *with respect to the variable* ϱ:

$$\operatorname{Re} \phi_k'(a_k) = \sum_{p=1}^{\infty} A_p(k, n) \varrho^p,$$

http://rcin.org.pl

where

$$A_0(k,n) = 1, \qquad A_1(k,n) = \operatorname{Re}\left[\sum_{\substack{m=1 \\ m\neq k}}^{n}\left[\left(\frac{r}{a_k - a_m}\right)^2 + V_\gamma^m 1(a_k)\right] + V_\gamma^k 1(a_k)\right].$$

3. Infinite material

A rectangular array of circular cylinders of conductivity λ_1 is embedded in a matrix of conductivity λ. Let us study the transport properties of the composite material in the x-direction. So we have the following problem in the cell $Q_0 := \{(x,y) \in \mathbb{R}^2,\ -\alpha/2 < x < \alpha/2,\ -1/(2\alpha) < y < 1/(2\alpha)\}$: find the potentials $w_1(x,y)$ and $w(x,y)$ harmonic in $Q_1 := \{(x,y) \in \mathbb{R}^2,\ x^2 + y^2 < r^2\}$ and $Q := Q_0 \backslash \overline{Q_1}$ respectively, continuously differentiable in the closures of these domains with the boundary conditions

$$w = w_1, \qquad \lambda \frac{\partial w}{\partial n} = \lambda_1 \frac{\partial w_1}{\partial n} \quad \text{on the circumference} \quad x^2 + y^2 = r^2, \tag{3.1}$$

$$w(x+\alpha, y) = w(x,y) + \alpha, \qquad w(x, y + \alpha^{-1}) = w(x,y). \tag{3.2}$$

If $\lambda_1 = \lambda$ then $w = w_1 = x$, and the current $\mathbf{j} = -\operatorname{grad} x = (-1, 0)$.

References to papers with effective solutions of the problem (3.1), (3.2) are given in Sec. 1.

The problem (3.1), (3.2) is equivalent to the following boundary $\mathbb{R}$-value problem

$$\phi(t) = \phi_1(t) - \varrho\overline{\phi_1(t)} - t, \qquad |t| = r, \tag{3.3}$$

where the unknown functions $\phi(z)$ and $\phi_1(z)$ are analytic in D and D_1, respectively, continuously differentiable in the closures of these domains. The function $\phi(z)$ is quasi-periodic:

$$\phi(z + \alpha) + i\gamma_1 = \phi(z) = \phi(z + i\alpha^{-1}) + i\gamma_2,$$

where γ_1 and γ_2 are real constants. The harmonic and analytic functions are related by the identities $w(x,y) = \operatorname{Re}(\phi(z) + z)$, $w_1(x,y)(\lambda + \lambda_1)/2\lambda = \operatorname{Re}\phi_1(z)$. The first condition (3.1) coincides with the real part of (3.3). The second condition (3.1) complies with the imaginary part of (3.3) differentiated along the tangential vector.

We assume that ϱ is a small parameter. A method of perturbation consists in finding a solution of the problem (3.3) in the form of the following expansions:

$$\phi(z) = \phi^0(z) + \varrho\phi^1(z) + \ldots, \qquad \phi_1(z) = \phi_1^0(z) + \varrho\phi_1^1(z) + \ldots.$$

http://rcin.org.pl

By substituting these expansions in the boundary condition (3.3) and collecting terms with equal powers of ϱ^m, we obtain a cascade of the problems. The number zero problem is

$$\phi^0(t) = \phi_1^0(t) - t, \qquad |t| = r.$$

The first one is

$$\phi^1(t) = \phi_1^1(t) - \overline{\phi_1^0(t)}, \qquad |t| = r.$$

Since the solution of the zero problem has the form $\phi_1^0(z) = z$, the first problem becomes

$$\phi^1(t) = \phi_1^1(t) - \frac{r^2}{t}, \qquad |t| = r.$$

The last equality means that $\phi^1(z)$ is analytically continued into $1 < |z| < r$. Hence, the function $\phi^1(z)$ is analytic and quasi-periodic in $Q_0 \backslash \{z = 0\}$:

$$\phi^1(z + \alpha) + i\gamma_1^1 = \phi^1(z) = \phi^1(z + i\alpha^{-1}) + i\gamma_2^1. \tag{3.4}$$

It has a pole at the point $z = 0$. The residue of $\phi^1(z)$ at $z = 0$ is equal to $(-r^2)$. It follows from the theory of elliptic functions that

$$\phi^1(z) = r^2(Az - \zeta(z)), \tag{3.5}$$

where A is a constant, ζ is the Weierstrass function [19]. The relation (3.4) implies the equalities

$$\operatorname{Re}\left[\phi^1(z + \alpha) - \phi^1(z)\right] = \operatorname{Re}\left[\phi^1(z + i\alpha^{-1}) - \phi^1(z)\right] = 0.$$

Substituting (3.5) into the last relations we obtain that $\alpha \operatorname{Re} A = \eta_1$, $\operatorname{Im} A = 0$, where $\eta_1 := 2\zeta(\alpha/2)$ is a real number, hence $A = \alpha^{-1}\eta_1$. So we arrive at the following asymptotic representations

$$\phi_1(z) = z + \varrho r^2\left[\alpha^{-1}\eta_1 z - (\zeta(z) - 1/z)\right] + o(\varrho), \qquad \text{as } \varrho \to 0,$$

and

$$\phi_1'(0) = 1 + \varrho r^2 \alpha^{-1}\eta_1 + o(\varrho), \qquad \text{as } \varrho \to 0. \tag{3.6}$$

Let us consider the system (2.5). Let $R = R_0 h(\theta)$ be the equation of the curve γ in the polar coordinates (R, θ), R_0 is a positive constant. We shall say that γ tends to infinity ($\gamma \to \infty$) with a fixed shape if in the equation $R = R_0 h(\theta)$ the value R_0 tends to infinity ($R_0 \to \infty$). Let us fix $h(\theta)$. If we fix the shape of γ in such a way that the operators V_γ^m disappear in the limit $n \to \infty$, then the limiting system for infinite materials becomes

$$\psi(z) = \varrho \sum_m{}' \left(\frac{r}{z - a_m}\right)^2 \overline{\psi\left(\frac{r^2}{z - a_m}\right)} + 1, \qquad |z| \le r. \tag{3.7}$$

http://rcin.org.pl

The sum $\sum_m'$ means that the term $a_0 = 0$ is missing. The unknown function $\psi(z) = \lim_{\gamma\to\infty} \phi_k'(z)$. It is analytic in $|z| < r$, continuous in $|z| \leq r$ and periodic: $\psi(z) = \psi(z + a_k)$ for each $a_k \in E = \{m_1\alpha + im_2\alpha^{-1}\}$, m_1 and m_2 are integers. The infinite sum in (3.7) is understood in the following sense

$$\sum_m' \left(\frac{1}{z-a_m}\right)^2 \overline{\psi\left(\frac{r^2}{z-a_m}\right)} := \sum_m' \left(\frac{1}{z-a_m}\right)^2 \left(\overline{\left(\psi\frac{r^2}{z-a_m}\right)} - \overline{\psi(0)}\right) + \overline{\psi(0)}\left(\mathcal{P}(z) - \frac{1}{2} + S_2\right), \tag{3.8}$$

where S_2 is an undetermined quantity, and

$$\mathcal{P}(z) = \frac{1}{z^2} + \sum_m' \left[\left(\frac{1}{z-a_m}\right)^2 - \frac{1}{a_m^2}\right]$$

is the Weierstrass function [19]. If $\psi(z) \equiv 1$ and $z = 0$ in (3.8) then $\sum_m' \frac{1}{a_m^2} = S_2$. Using the method of successive approximations we conclude from (3.7) that

$$\psi(0) = 1 + \varrho r^2 \sum_m' \frac{1}{a_m^2} + o(\varrho) = 1 + \varrho r^2 S_2 + o(\varrho), \quad \text{as } \varrho \to 0. \tag{3.9}$$

So we have the following quantities: $\phi_1'(0)$ from the problem for infinite material and $\psi(0)$ as the limit of $\phi_k'(a_k)$ with the special shape of γ. Since we assume that $\phi_1'(0) = \psi(0)$, then we conclude from (3.6) and (3.9) that $S_2 := \alpha^{-1}\eta_1$ for this special shape of γ. It follows from the theory of elliptic functions [19] that S_2 can be written in the form (1.1). This justifies the formula of Lord Rayleigh (1.1).

Let us show that the system of functional equations (3.7) is a continuous form of the infinite algebraic system of the method of Rayleigh. Introduce now the Taylor series for the function $\psi(z)$ inside the circle $z < r$

$$\psi(z) = \sum_{k=0}^{\infty} \psi_k z^k.$$

Then

$$\sum_m' \left(\frac{r}{z-a_m}\right)^2 \overline{\psi\left(\frac{r^2}{z-a_m}\right)} = \sum_{k=0}^{\infty} \overline{\psi}_k r^{2(k+1)} \mathcal{S}_{k+2}(z,\alpha),$$

where

$$\mathcal{S}_{k+2}(z,\alpha) := \sum_m' \frac{1}{(z-a_m)^2} = \sum_m' \left(-\sum_{s=0}^{\infty} \frac{z^s}{a_m^{s+1}}\right)^{k+2}, \qquad k = 0, 1, 2, \ldots.$$

http://rcin.org.pl

The function $\mathcal{S}_2(z,\alpha)$ is understood in the following sense: $\mathcal{S}_2(z,\alpha) := \mathcal{P}(z) - \frac{1}{z^2} + S_2$. If $z = 0$ then $\mathcal{S}_2(0,\alpha) = S_2$. Substituting all series in (3.7) we arrive at an infinite system of linear algebraic equations. The real parts of this system coincide with the infinite system of Lord RAYLEIGH [1], MCPHEDRAN *et al.* [4–7], PERRINS *et al.* [2], POLADIAN *et al.* [3] for $\alpha = 1$. We will show it only for the number zero equation. Substituting $z = 0$ into (3.7) we obtain

$$\psi_0 = \varrho \sum_{k=0}^{\infty} \overline{\psi_k}\, r^{2(k+1)} \mathcal{S}_{k+2}(0,1) + 1,$$

where

$$\mathcal{S}_{k+2}(0,1) = \sum_m{}' \frac{1}{a_m^{k+2}}.$$

If we replace ψ_k by

$$\beta_{k+1} = (k+1)\varrho\, r^{2(k+1)} \operatorname{Re} \psi_k,$$

then we obtain the first equation of [2].

4. Effective conductivity and the sum S_2

Let us introduce the value

$$\lambda_e^x(n) = \frac{<j>}{<e>},$$

where

$$<e> = J + \sum_{k=1}^{n} j_k, \qquad <j> = \lambda J + \sum_{k=1}^{n} \lambda_k j_k,$$

$$j_k := \iint\limits_{D_k} \frac{\partial u_k}{\partial x} dx\, dy = (1-\varrho) \iint\limits_{D_k} \frac{\partial U_k}{\partial x} dx\, dy = (1-\varrho) J_k,$$

$$J := \iint\limits_{D} \frac{\partial u}{\partial x} dx\, dy.$$

Using the Green's formula $\iint\limits_G \frac{\partial v}{\partial x} dx\, dy = \int\limits_\gamma v\, dy$ we obtain

$$\frac{\lambda_e^x(n)}{\lambda} = 1 + 2\varrho \frac{1}{|G|} \sum_{k=1}^{n} J_k,$$

http://rcin.org.pl

where $|G|$ is the area of the domain G. Applying the mean value theorem to the integral J_k we have

$$\iint_{D_k} \frac{\partial U_k}{\partial x} dx\, dy = \pi r^2 \frac{\partial U_k}{\partial x}(a_k) = \pi r^2 \operatorname{Re} \phi_k'(a_k).$$

Therefore

$$\frac{\lambda_e^x(n)}{\lambda} = 1 + 2\varrho \frac{\pi r^2 n}{|G|} \frac{1}{n} \sum_{k=1}^{n} \operatorname{Re} \phi_k'(a_k). \tag{4.1}$$

It follows from the Theorem 2 of Sec. 2 that

$$\operatorname{Re} \phi_k'(a_k) = 1 + \operatorname{Re} \left[r^2 \sum_{\substack{m=1 \\ m \neq k}} \left(\frac{1}{a_k - a_m} \right)^2 + \sum_{m=1}^{n} V_\gamma^m 1(a_k) \right] \varrho + o(\varrho), \quad \text{as } \varrho \to 0.$$

Substituting this relation into (4.1) we have

$$\frac{\lambda_e^x(n)}{\lambda} = 1 + 2\varrho \frac{\pi r^2 n}{|G|} + 2\varrho^2 \frac{\pi r^2 n}{|G|} \kappa(n) + o(\varrho^2), \quad \text{as } \varrho \to 0,$$

where

$$\kappa(n) := r^2 \operatorname{Re} \left(S_2(n, \gamma) + \mu(n, \gamma) \right), \qquad S_2(n, \gamma) := \frac{1}{n} \sum_{k=1}^{n} \sum_{\substack{m=1 \\ m \neq k}} \left(\frac{1}{a_k - a_m} \right)^2,$$

$$\mu(n, \gamma) := \frac{1}{n} \sum_{k=1}^{n} \sum_{m=1}^{n} V_\gamma^m 1(a_k). \tag{4.2}$$

Calculating the limit $n \to \infty \Leftrightarrow \gamma$ tends to infinity, we arrive at the relation

$$\frac{\lambda_e^x}{\lambda} = 1 + 2\varrho v + 2\varrho^2 v \lim_{n \to \infty} \kappa(n) + o(\varrho^2), \quad \text{as } \varrho \to 0, \tag{4.3}$$

where v is the volume fraction of the inclusion. On the other hand, calculating λ_e^x in the cell Q_0 representing infinite material and using (3.6) we have

$$\frac{\lambda_e^x}{\lambda} = 1 + 2\varrho v \operatorname{Re} \phi_1'(0) = 1 + 2\varrho v + 2\varrho^2 v^2 \operatorname{Re} \frac{\eta_1}{\pi \alpha} + o(\varrho^2), \quad \text{as } \varrho \to 0. \tag{4.4}$$

Comparing (4.3) and (4.4) we conclude that $\lim_{n \to \infty} \kappa(n)$ must be equal to $\operatorname{Re}(v\eta_1/\pi\alpha)$. This conclusion allows us to explain strange properties of the sum S_2 (see Sec. 1). Let us fix the shape of γ and introduce the limits

$$S_2(\gamma) = \lim_{n \to \infty} S_2(n, \gamma), \qquad \mu(\gamma) = \lim_{n \to \infty} \mu(n, \gamma).$$

http://rcin.org.pl

Thus we have the two equalities:

$$\kappa(n) = r^2 \mathrm{Re}\, S_2(n,\gamma) + \mu(n,\gamma) \qquad \text{and} \qquad \frac{v\eta_1}{\pi\alpha} = r^2 S_2(\gamma) + \mu(\gamma).$$

In the last equality the value $v\eta_1/\pi\alpha$ is independent of γ. It means that one may assume an arbitrary shape of γ and define $S_2(\gamma)$ at will. But it is necessary to account for the term $\mu(\gamma)$. For instance, if we take γ in such a way that $S_2(\gamma) = (\eta_1/\alpha)$, then $\mu(\gamma)$ must be equal to zero.

If $\alpha = 1$ then $\eta_1 = \pi$ and $\lim_{n\to\infty} \kappa(n) = v$. In this case we arrive at the asymptotic formula

$$\frac{\lambda_e^x}{\lambda} = 1 + 2\varrho v + 2\varrho^2 v^2 + o(\varrho^2), \qquad \text{as} \quad \varrho \to 0,$$

derived by Bergman and Milton. Thorough investigations of such representations involve the bounds on the effective tensor. The most important papers on those bounds are cited in the recent work by CLARK and MILTON [20].

The formula (4.4) is closely related to the famous Clausius - Mossotti approximation

$$\frac{\lambda_e}{\lambda} = \frac{1+\varrho v}{1-\varrho v} + o(v), \qquad \text{as} \quad v \to 0. \tag{4.5}$$

Let us note that $\varrho \to 0$ in (4.4) and $v \to 0$ in (4.5). It follows from [23, p. 63–75] that

$$\frac{\lambda_e^x}{\lambda} = \frac{1 + \varrho v(2 - S_2/\pi) + \dfrac{6}{\pi^4} S_4^2 \varrho^3 v^5 \left[1 + \dfrac{S_2}{\pi}\varrho v - \varrho^2 v^2 \left(\dfrac{S_2}{\pi}\right)^2\right]}{1 - \varrho v S_2/\pi - \dfrac{6}{\pi^4} S_4^2 \varrho^3 v^5 \left[1 - \left(2 - \dfrac{S_2}{\pi}\right)\varrho v - \varrho^2 v^2 \left(2 - \dfrac{S_2}{\pi}\right)^2\right]} + o(v^7) \quad \text{as} \quad v \to 0, \tag{4.6}$$

where $S_4 := \sum_m' a_m^{-4}$ is the absolutely convergent Rayleigh sum of the fourth order [1]. Therefore, in order to improve (4.5) as $v \to 0$ or $\varrho \to 0$, we must use the value S_2. Calculation of the higher order Rayleigh sums S_{2n} $(n > 1)$ is only a computation problem, because they are absolutely convergent. Let us note that an exact formula for λ_e^x/λ has been derived in [8, 23], and formula (4.6) is an approximate consequence of this result. However, (4.6) is of a very simple form and can be easily used in technical calculations.

Applying the Dykhne - Keller identity [24] to (4.6) it is possible to get an analogous formula for λ_e^y/λ. Following [23] it is necessary to replace S_2 with $(2 - S_2/2)$.

http://rcin.org.pl

5. Conclusions

In addition to the physical explanation of the equality $S_2 = \pi$ of MCPHEDRAN *et al.* [7] and PERRINS *et al.* [2] and the rigorous definition of S_2 of MITYUSHEV [8, 23], in the present paper we have given the rigorous mathematical explanation when and why the formula (1.1) is true. We have also analyzed the Rayleigh sum S_2 and its application to analytic formulae, determining the properties of the tensor. Moreover, we have justified the method of Lord Rayleigh.

Appendix

We shall prove that the value $S_2(\gamma)$ is correctly defined. Let us fix $h(\theta)$ in the equation $R = R_0 h(\theta)$ of the curve γ in the polar coordinates system (R, θ). According to [8]

$$J := v.p. \iint\limits_G \frac{1}{z^2} dx\, dy = \lim_{\varepsilon \to 0} \iint\limits_{G_\varepsilon} \frac{1}{z^2} dx\, dy,$$

$$G_\varepsilon := G \backslash \left\{ z \in \mathbb{C}, \quad |z| > \varepsilon \right\}.$$

Following to [8] we arrive at the formula

$$J = \int\limits_\gamma \operatorname{Re} \frac{1}{z} dy - \lim_{\varepsilon \to 0} \int\limits_{|z|=\varepsilon} \operatorname{Re} \frac{1}{z} dy = \frac{1}{2} \int\limits_0^{2\pi} \frac{h'(\theta)}{h(\theta)} (\sin 2\theta + i \cos 2\theta)\, d\theta.$$

Since $S_2(\gamma)$ can be considered as a limit of the Riemannian sum of the integral J, we have

$$S_2(\gamma) = \lim_{n \to \infty} S_2(n, \gamma) = \lim_{R_0 \to \infty} J.$$

One can see that J is independent of R_0. Hence $S_2(\gamma)$ is correctly defined by the integral

$$S_2(\gamma) = \frac{1}{2} \int_0^{2\pi} \frac{h'(\theta)}{h(\theta)} (\sin 2\theta + i \cos 2\theta)\, d\theta.$$

Acknowledgments

The author gratefully acknowledges R.C. MCPHEDRAN and N.A. NICOROVICI for indicating the wide literature on the question considered.

This paper was supported by the State Committee for Scientific Research (Poland) through Grant N 3P404 013 06.

http://rcin.org.pl

References

1. Lord RAYLEIGH, *On the influence of obstacles arranged in rectangular order upon the properties of a medium*, Phil. Mag., **34**, 481–502, 1892.
2. W.T. PERRINS, D.R. MCKENZIE and R.C. MCPHEDRAN, *Transport properties of regular arrays of cylinders*, Proc. R. Soc. Lond., **A 369**, 207–225, 1979.
3. L. POLADIAN and R.C. MCPHEDRAN, *Effective transport properties of periodic composite materials*, Proc. R. Soc. Lond., **A 408**, 45–59, 1986.
4. R.C. MCPHEDRAN, *Transport properties of cylinder pairs and the square array of cylinders*, Proc. R. Soc. Lond., **A 408**, 31–43, 1986.
5. R.C. MCPHEDRAN and G.W. MILTON, *Transport properties of touching cylinder pairs and of the square array of touching cylinders*, Proc. R. Soc. Lond., **A 411**, 313–326, 1987.
6. R.C. MCPHEDRAN, L. POLADIAN and G.W. MILTON, *Asymptotic studies of closely spaced, highly conducting cylinders*, Proc. R. Soc. Lond., **A 415**, 185–196, 1988.
7. R.C. MCPHEDRAN and D.R. MCKENZIE, *The conductivity of lattices of spheres, 1. The simple cubic lattice*, Proc. R. Soc. Lond., **A 359**, 45–63, 1978.
8. V. MITYUSHEV, *Rayleigh's integral and effective conductivity of the square array of cylinders*, Arch. Mech., **47**, 1, 27–37, 1995.
9. J. KOŁODZIEJ, *Determination of the effective heat conductivity of composites by the collocation method* [in Polish], Mech. Teoret. Stos., **23**, 3–4, 355–373, 1985.
10. R.D. MANTEUFEL and N.E. TODREAS, *Analytic formulae for the effective conductivity of a square or hexagonal array of parallel tubes*, Int. J. Heat Mass Transfer, **37**, 4, 647–657, 1994.
11. V.V. MITYUSHEV, *Steady heat conduction of two-dimensional composites*, Prace IX Symp. Wymiany Ciepła i Masy, Augustów, vol. **2**, 93–100, 1995.
12. L.V. GIBIANSKY, *Bounds on the effective moduli of composite materials*, School of Homogenization, Lecture Notes, Trieste 1993.
13. F.D. GAKHOV, *Boundary value problems*, Pergamon Press, Oxford 1966.
14. L.G. MIKHAJLOV, *A new class of singular integral equations*, Wolters-Noordhoff Publ., Gröningen 1970.
15. V.V. MITYUSHEV, *Plane problem for the steady heat conduction of material with circular inclusions*, Arch. Mech., **45**, 2, 211–215, 1993.
16. V.V. MITYUSHEV, *Solution of the Hilbert boundary value problem for a multiply connected domain*, Słupskie Prace Mat.-Przyr., 9a, 37–69, 1994.
17. S.G. MIKHLIN, *Integral equations*, Pergamon Press, New York 1964.
18. V. MITYUSHEV, *Generalized method of Schwarz and addition theorems in mechanics of materials containing cavities*, Arch. Mech., **47**, 6, 1169–1181, 1995.
19. A. HURWITZ and R. COURANT, *Allgemeine Funktionentheorie und elliptische Funktionen*, Springer-Verlag, Berlin 1964.
20. K.E. CLARK and G.W. MILTON, *Optimal bounds correlating electric, magnetic and thermal properties of two-phase, two-dimensional composites*, Proc. R. Soc. Lond., **A 448**, 161–190, 1995.
21. A.S. SANGANI and C. YAO, *Trasport properties in random arrays of cylinders. 1. Thermal conduction*, Phys. Fluids, **31**, 2426–2434, 1988.
22. D.J. BERGMAN and K.-J. DUNN, *Bulk effective dielectric constant of a composite with a periodic microgeometry*, Phys. Rev., **45**, 13262–13271, 1992.
23. W. MITYUSHEV, *Application of functional equations to the determination of effective thermal conductivity of composite materials* [in Polish], WSP, Słupsk 1996.
24. J.B. KELLER, *A theorem on the conductivity of a composite material*, J. Math. Phys., **5**, 4, 548–549, 1964.

DEPARTMENT OF MATHEMATICS
PEDAGOGICAL COLLEGE OF SŁUPSK

Received October 14, 1996.

http://rcin.org.pl

Arch. Mech., 49, 2, pp. 359–369, Warszawa 1997

Spalling fracture experiments with ceramic bars at elevated temperatures

J. NAJAR and M. MÜLLER-BECHTEL (MUNICH)

SPALLING EXPERIMENTS with alumina bars at temperatures up to 1500°C have been conducted in a new testing apparatus. A slender uninstrumented specimen is loaded by a compressive pulse reflected from its free end. A bridging piece is placed into the transition zone between the instrumented wave-transmitter and the specimen within the furnace. High-temperature corrections are taking into account the drop in the wave velocity and the continuous drop of the impedance in the bridging piece, which results in the incremental reflections of the pulse. The results of the experiments indicate that the decay of the strength with the increase of the temperature up to 1500°C is much stronger than that anticipated in preliminary tests. The observations can be interpreted within a continuum damage model.

1. Introduction

SPALLING EXPERIMENTS with alumina bars performed at elevated temperatures up to 1500°C have been conducted in a new testing apparatus. A description of the measuring and evaluation technique for high temperatures is given in the paper.

A slender cylindrical uninstrumented specimen located in an open-end furnace is loaded by the reflection of a compressive pulse of sufficient amplitude from its free end. A bridging piece is placed in the transition zone between the instrumented wave-transmitter (measuring rod) and the specimen, the latter being located in the homogeneous part of the thermal field within the furnace.

The data acquisition consists in measuring the incoming and reflected pulses in the transmitter, the temperature distribution in the furnace, and the positions of the spalling sites in the specimen. The evaluation procedure is based on the corresponding one for the room temperature. High-temperature corrections are taking into account two kinds of effects: the drop in the wave velocity, which changes the pulse length, and the continuous drop of the impedance in the bridging piece resulting in incremental reflections of the pulse.

2. Experimental arrangement

The set-up combines the principles of pulse initiation and its measurement, typical for split Hopkinson pressure bar, with the spalling phenomenon at tensile dynamic loading, due to the reflections of a compressive stress wave from specimen's free end. The compressive pulse is introduced into the transmitter bar by projectile impact, Fig. 1. It is registered at gauge stations of the measuring bar

http://rcin.org.pl

and stored. The same happens to the reflected pulse in the bar resulting from the difference of the impedances between the transmitter and the specimen. The transmitted compressive pulse propagates in the specimen, causing basically no material damage. Upon its arrival at the specimen's free end, it gets reflected as a tensile pulse and superposed upon the still arriving compressive tail.

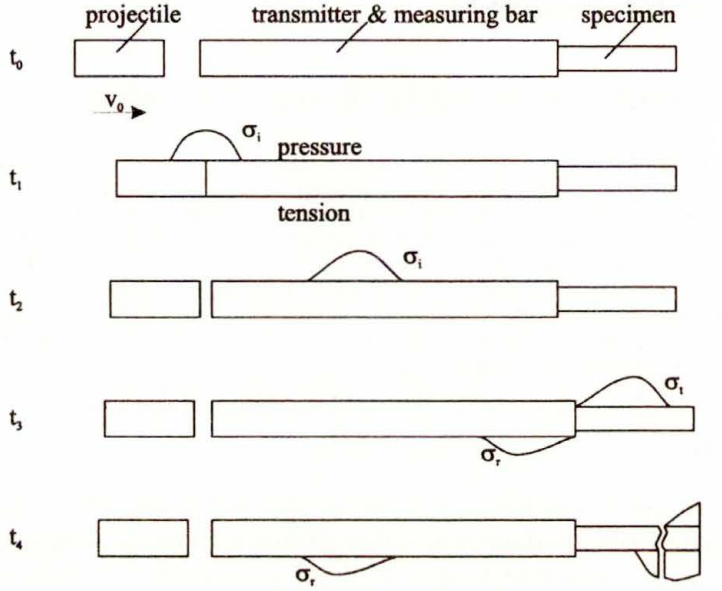

FIG. 1. Experimental arrangement.

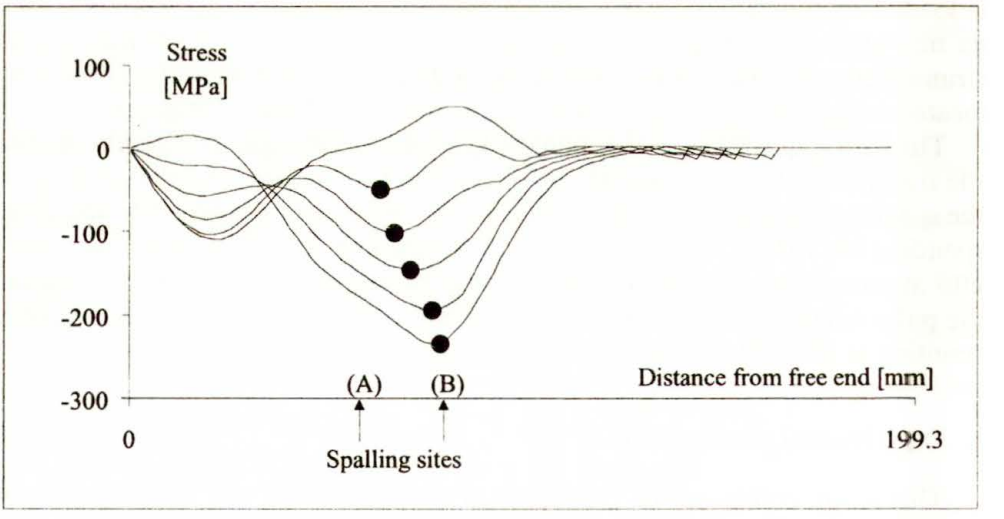

FIG. 2. Resulting transient pulses in the specimen, in a time-step sequence of 0.5μs.

The resulting stress distribution leads to tensile stresses fast growing in time at some distance from the free end. Wherever the peak value of the resulting stress

http://rcin.org.pl

distribution reaches the level of the tensile strength of the material, spalling develops immediately due to the negligible fracture activation delay in ceramics. By comparing the sites of spall with the evolution of the stress distribution maxima, the spalling strength and the primary site are determined uniquely, Fig. 2.

3. High temperature arrangement

Having in mind applications of ceramics at thermal exposures, experiments have been conducted at elevated temperatures. The specimen is placed in an open-end furnace placed along the axis of the set-up, Fig. 3. The furnace with 204 mm diameter and 356 mm length of the heating area makes possible to conduct the experiments up to 1500°C. The specimen must be shorter than the length of the furnace in order to be placed in its internal homogeneous temperature field. On the other hand, the measuring bar must not reach into the area of elevated temperature due to its limited resistance to thermal load and limited temperature range of application of the strain gauges.

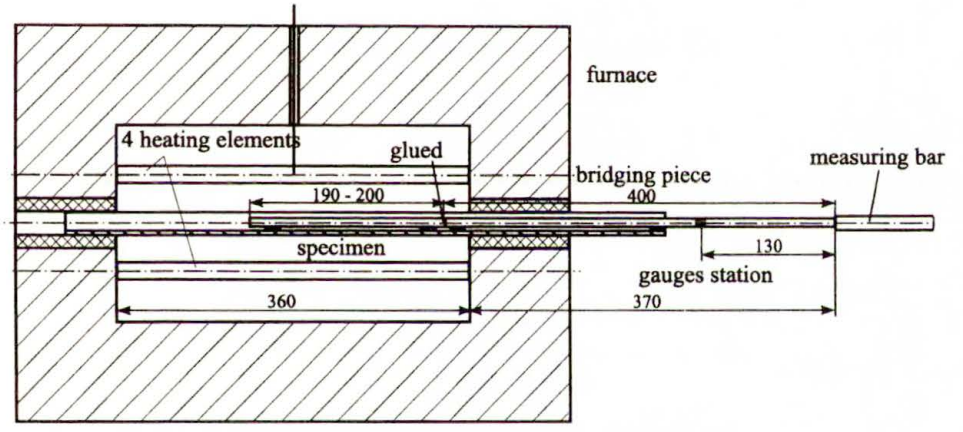

FIG. 3. Experimental set-up at elevated temperatures.

An extension piece made of the same material as the specimen is placed between it and the transmitter bar, in order to bridge over the thermally inhomogeneous field at the opening of the furnace. The bridging piece is glued to the specimen what ensures proper transmission of the pulse into the specimen, and at the same time makes easier the handling of the specimen within the furnace. The unit bridging piece – specimen can be lined up according to the axis of the set-up as a whole from without the furnace, which enables proper positioning of the unit.

The presence of the bridging piece has some influence on the transmission of the pulse into the specimen since there are some slight pulse reflections at the glued joint. Our experience shows, however, that the proper choice of the

http://rcin.org.pl

extension piece length enables direct pulse measurements on the bridging element and thus takes into account the joint reflection losses. The fracture phenomena in the specimen itself are not influenced by the presence of the bridging piece since the reflected pulse reaches the glued joint only some time after the primary fracture has occurred.

4. Temperature effects

The axial temperature distribution in the bridging piece – specimen unit has been measured with thermoelements on the surface of the specimen. The results are shown in Fig. 4. Inside the furnace the temperature is nearly constant and decreases at a high gradient within the insulation. From the experimental data for some furnace temperatures, the temperature distribution in the bridging piece and in the specimen is interpolated for the temperatures of the tests.

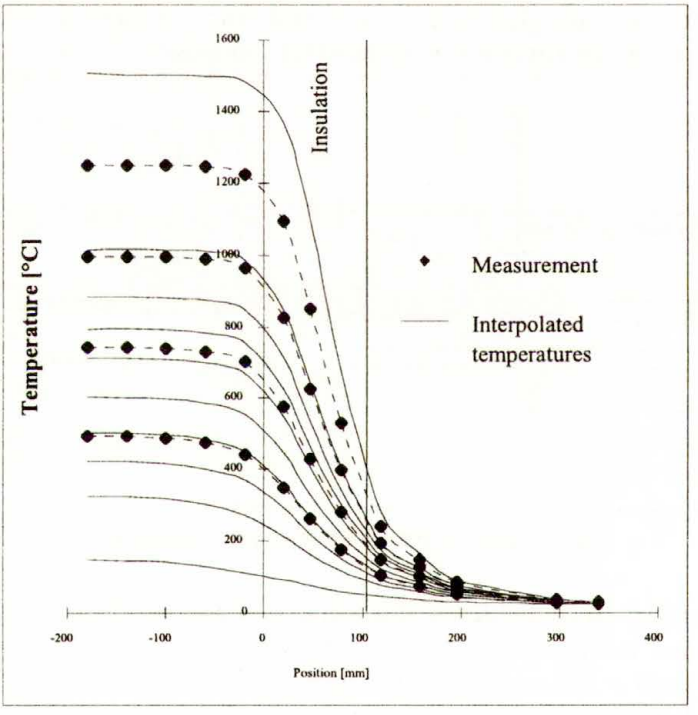

FIG. 4. Temperature distribution in the unit bridging piece – specimen.

Due to the change in the elastic modulus and the thermal expansion of the ceramics, the wave velocity decreases. For the measurement of the wave velocity at elevated temperature, an instrumented specimen is placed in two positions relative to the furnace, Fig. 5. Two gauge stations measure the travel times for each position. The difference of the travel times gives the wave velocity in the

http://rcin.org.pl

measuring length, which shows a nearly linear decrease at temperatures up to 1000°C and an enhanced decrease above that temperature, Fig. 6.

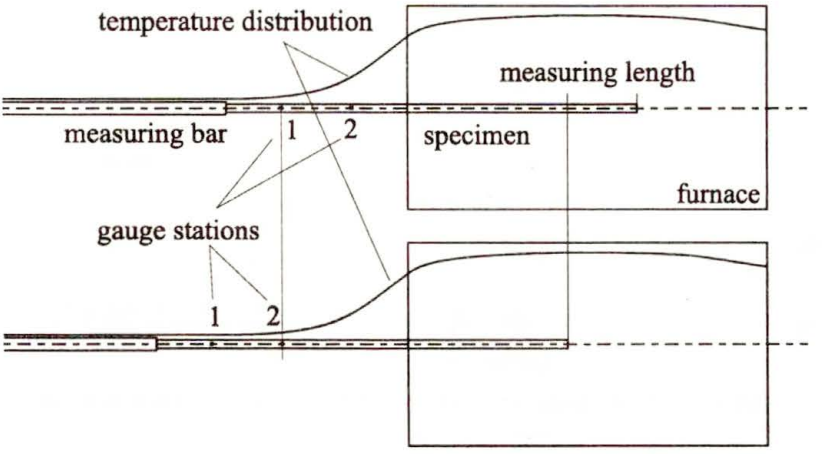

FIG. 5. Measurement of the wave velocity at elevated temperatures.

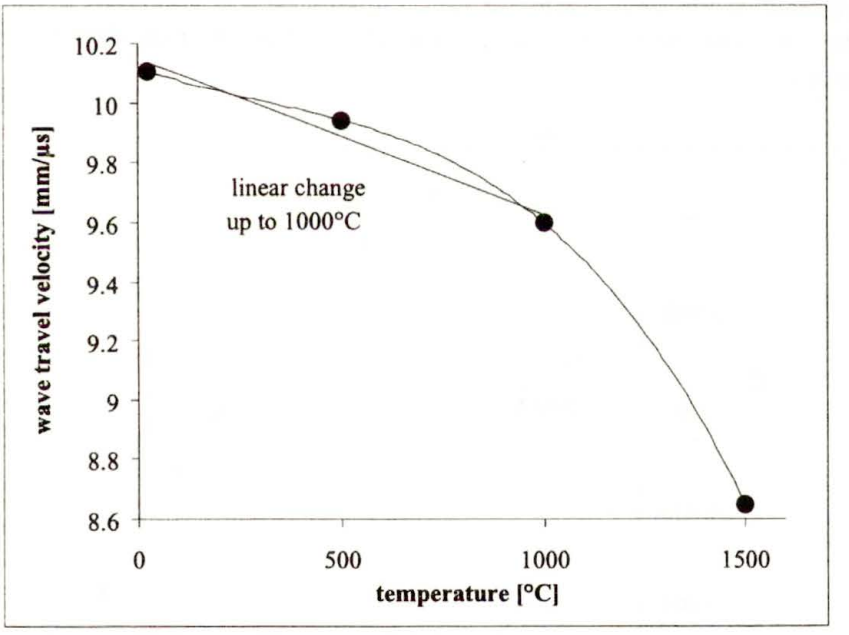

FIG. 6. Temperature dependence of the wave velocity.

The decrease of the wave velocity influences the pulse length in the specimen, the geometrical dispersion and the pulse transmission through the bridging piece.

The stress distribution in the specimen becomes shorter with the decreasing wave velocity at elevated temperature and similar stress distributions arrive with

http://rcin.org.pl

delay. This effect leads to a new identification of the primary spalling site, and thus of the spalling strength, Fig. 7.

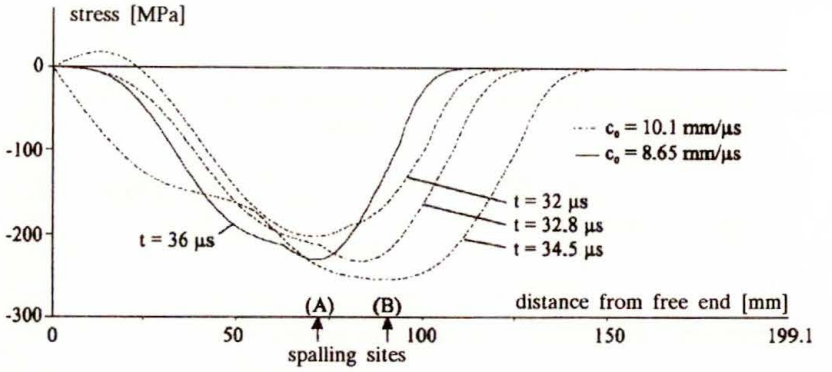

FIG. 7. Influence of decreasing wave velocity on the stress distribution in the specimen.

Like the stress distribution, the wave lengths of the Fourier components of the pulse become shorter. With the increasing ratio of the radius to wave-length the velocity of the components drops compared with the uniaxial wave velocity c_0. But the values in Fig. 8 show that this effect of geometrical dispersion can be neglected.

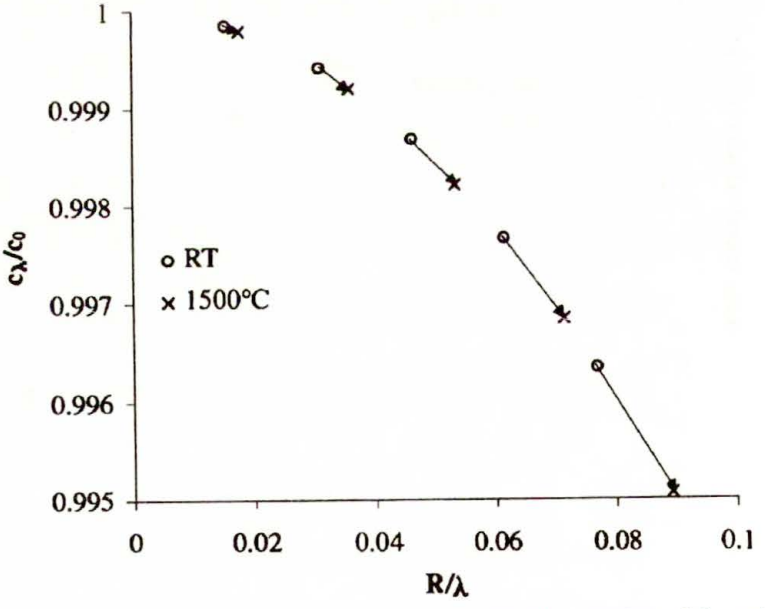

FIG. 8. Influence of the wave velocity on the geometrical dispersion of the pulse.

With the changing wave velocity, the thermal expansion of the cross-section area and the thermal change in the density, the bar impedance $I = A\varrho c$ de-

http://rcin.org.pl

creases with the temperature distribution in the bridging piece. We will check the effect in a simplified model with linear temperature distribution in the bridging piece, Fig. 9. In two calculations we assume a linear temperature-dependence of the wave velocity up to 1000°C and a third-degree polynomial dependence up to 1500°C.

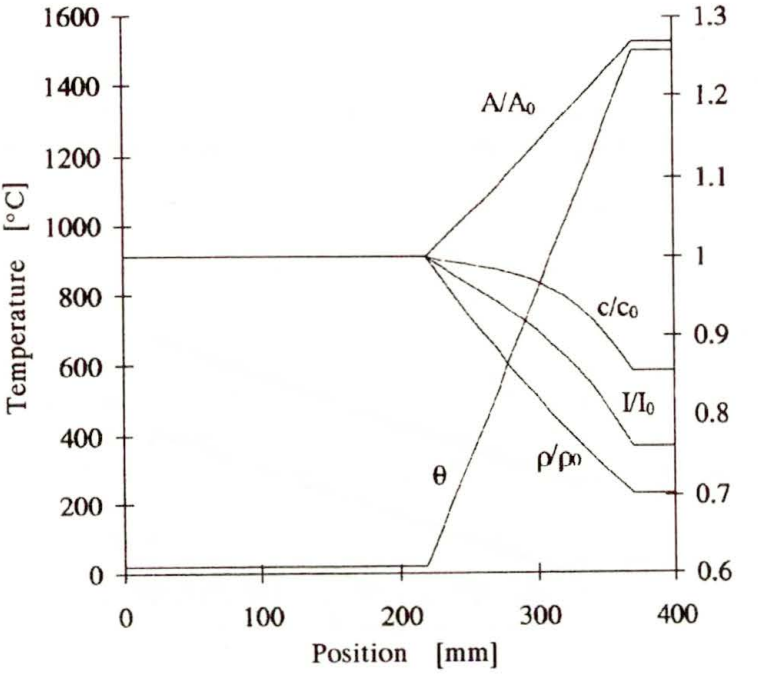

FIG. 9. Linear temperature distribution and influence on the cross-sectional area, wave velocity, density and bar impedance.

In finite bar elements we assume the applicability of the linear wave theory. At the boundary of an element, a part of the pulse in the first element is transmitted to the next element, and the other part is reflected back in the element, Fig. 10.

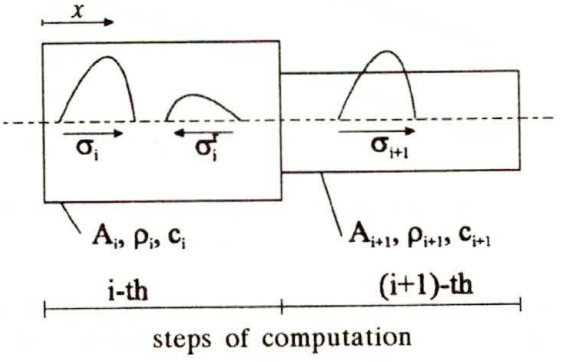

FIG. 10. Partial reflection at the element boundary.

http://rcin.org.pl

The transmitted part is obtained from formula (4.1), the reflected one from (4.2).

$$\sigma_{i+1} = \frac{A_i \varrho_{i+1} c_{i+1}}{I_i + I_{i+1}} \sigma_i , \tag{4.1}$$

$$\sigma_i^r = \frac{I_{i+1} - I_i}{I_{i+1} + I_i} \sigma_i . \tag{4.2}$$

The secondary reflected part of the pulse is obtained by the reflection of the reflected one and is transmitted to the specimen with delay. In Fig. 11 the transmitted, the reflected and the secondary reflected pulses are superposed.

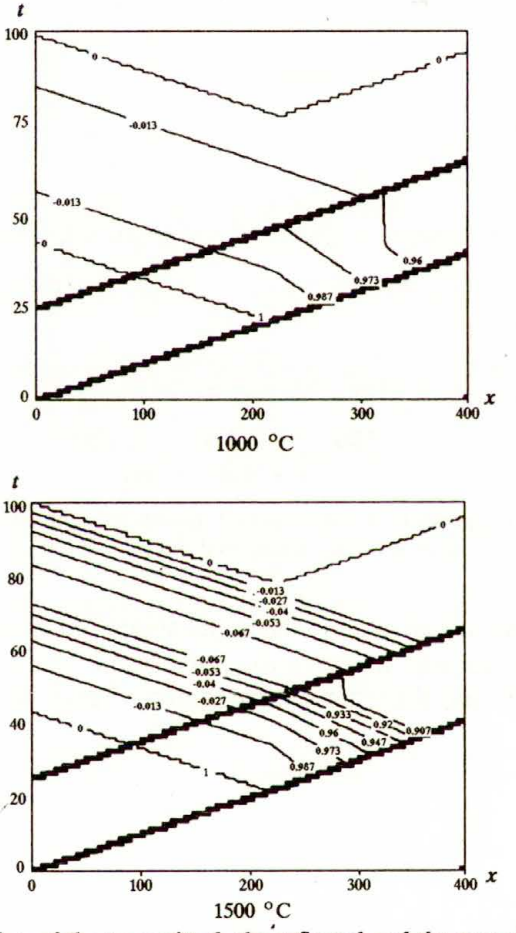

FIG. 11. Superposition of the transmitted, the reflected and the secondary reflected part of the pulse.

For the given temperature distribution in the bridging piece, one gets at the temperature of 1000°C in the furnace a transmission into the specimen of 96% of the initial pulse amplitude. The amplitude of the primary reflection is 2.5%,

http://rcin.org.pl

and the one of the secondary reflection is 0.1%. At 1500°C the initial pulse amplitude is transmitted in 89%. In this case the amplitude of the primary reflection increases to 7% and that of the secondary reflection to 0.3%. These results show that the secondary and higher order reflections are negligible.

The integration of the transmitted parts along their characteristic leads to formula (4.3), which shows that the transmitted pulse amplitude depends on the temperature in the furnace θ_f alone.

$$\sigma_t(\theta_f) = \sigma_i \sqrt{\frac{A_0 \varrho(\theta_f) c(\varrho_f)}{A(\theta_f) \varrho_0 c_0}}. \tag{4.3}$$

5. Experimental results

Commercial alumina bars of diameter 8 mm and length 200 mm have been tested in the whole range of temperature between the room temperature and 1500°C. The tests at the room temperature were conducted within the cold furnace, in order to check the compatibility of the results with those at the room temperature in the former experimental arrangement. Altogether 28 specimens were tested, at higher temperatures the number of experiments per temperature point was reduced from six to one due to increasing time cost.

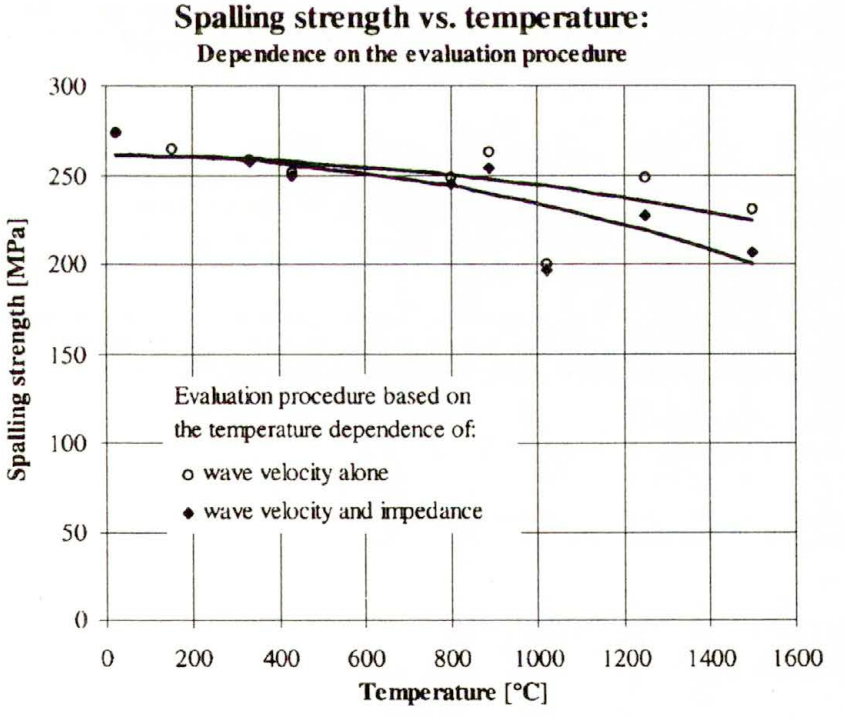

FIG. 12. Experimental results.

http://rcin.org.pl

The results of the tests can be therefore treated as preliminary ones only, not representing the full statistics of the strength at elevated temperatures. They prove, however, doubtlessly the applicability of the experimental method to testing at elevated temperatures.

The consideration of the incremental reflections of the pulse caused by the continuous drop of the impedance indicates that the decay of the strength with the increase of the temperature up to 1500°C is much stronger than that anticipated in preliminary tests, Fig. 12. The observations can be interpreted within a continuum damage model.

6. Conclusion

The new experimental set-up and evaluation procedure enable very efficient determination of the strength parameters in spalling of ceramics at a wide range of temperatures, combining low costs with relatively high accuracy of the results.

Acknowledgments

The work presented here has been performed in relation with the DFG project Na 218/1 on dynamic testing of high performance ceramics. Dr. S. BIERWIRTH and Dipl.-Ing. H.-J. KLUMPP participated in the construction of the set-up and conducted parts of the tests. Their input and the financial support of the German Research Foundation (DFG) is hereby gratefully acknowledged.

References

1. S. BIERWIRTH, *Verfahren zur Bestimmung dynamischer Zugbruchparameter von Hochleistungskeramik*, Fortschritt-Berichte VDI, Reihe 18, Mechanik/Bruchmechanik, Nr. 148, VDI-Verlag, Düsseldorf 1994.
2. M. MÜLLER-BECHTEL and J. NAJAR, *Spalling of alumina ceramics in uniaxial stress at elevated temperatures*, Material and structural modelling in collision research, Proc. 9th DYMAT Techn. Conf., TUM, 1995, Ch. 2, J. NAJAR [Ed.], Munich 1995.
3. J. NAJAR, *Dynamic tensile fracture phenomena at wave propagation in ceramic bars*, [in:] Mechanical and Physical Behaviour of Materials under Dynamic Loading, Proc. Int. Symp. EURODYMAT 94, Oxford, J. HARDING [Ed.], Les Editions de Physique, J. de Physique IV, **4**, 647–652, Sept. 1994.

DEPARTMENT A OF MECHANICS
UNIVERSITY OF TECHNOLOGY, MUNICH, GERMANY.

Received December 11, 1996.

http://rcin.org.pl

Arch. Mech., 49, 2, pp. 369–384, Warszawa 1997

Simple shear of metal sheets at high rates of strain

Dedicated to Professor Franz Ziegler
on the occasion of His 60th birthday

H. V. NGUYEN and W. K. NOWACKI (WARSZAWA)

THE TEST of dynamic (at high rates of strain) plane shear is discussed. Use is made of the new shear device in which the loading and displacements are controlled by the Split Hopkinson Pressure Bar acting in compression. This device allows to perform tests under the plane shear state in a specimen having the form of metal sheets. Simplified analytical solution of the boundary-value problem in the case of simple shear is prescribed. The analytical solution of the initial-boundary problem is compared with the experimental data.

1. Introduction

NUMERICAL SYSTEMS allow us to simulate the mechanical behaviour of thin-walled constructions, such as body of automobiles, buses, shells of wagons, air-planes, etc., subjected to the impact loading; required is the knowledge of the dynamical behaviour of thin sheets in which these constructions are made. Their mechanical characteristics are dependent on the metallurgical composition of the metal as well on the manner of its production. It is indispensable to have the experimental data concerning this specific form of material. Tests in the case of simple shear are very important for the experimental investigation of the constitutive equations of materials. These experiments are supplementary to other tests realized in the conditions of tension as well in the compression or in the pure shear.

Recently, a new shear device was used to perform tests on specimens having the form of slabs such as metal sheets [1]. The loading and the displacements of this device are controlled by a Split Hopkinson Pressure Bar (SHPB) acting in compression. The special device was used to transform the compression to simple plane shear. For thin sheets in dynamic simple plane shear tests, it is the only known method to obtain a very good homogeneity of the permanent strain field over the total length of the specimen, without the localization of deformations as in the case of torsion of thin-walled tubes [2, 3 and 13].

The analogous initial-boundary-value problem of simple shear was formulated in the case of finite strains. We consider the rate-independent constitutive relations for adiabatic process with combined isotropic-kinematic hardening at moderate pressures. The thermal expansion, the heat of elastic deformation and the heat of internal rearrangement are neglected. The analytical solution is compared with the experimental data. The performed numerical calculations enabled

http://rcin.org.pl

the evaluation of the optimal dimensions of the specimen used in the case of dynamic loading.

2. Experiment

Figure 1 presents the principle of the shear device. The shear device consists of two coaxial cylindrical parts (the external part is tubular and the internal part is massive). Both cylinders are divided into two symmetrical parts, and between them the sheet in testing is fixed using screws of high strength – Fig. 2. Two bands of the specimen between the internal and external parts of the device are in plane shear when these cylinders move axially one toward the other. The width of these bands is 3 mm. Each band before test is rectangular and becomes very near parallelogram having the constant length and the constant height. The specimens can have different thickness. There are two kinds of specimens: one is made of the steel XES (chemical composition: C–50, Ni–25, Cr–18, Mn–189, Cu–23, Al–57, Si–4, P–17 in 10^{-3} volume percent, thickness 0.74 mm) and the other is of steel 1H18N9T (chemical composition: C–10, Mn–200, Si–80, P–5, S–3 Cr–180, Ni–80, thickness 0.5 mm).

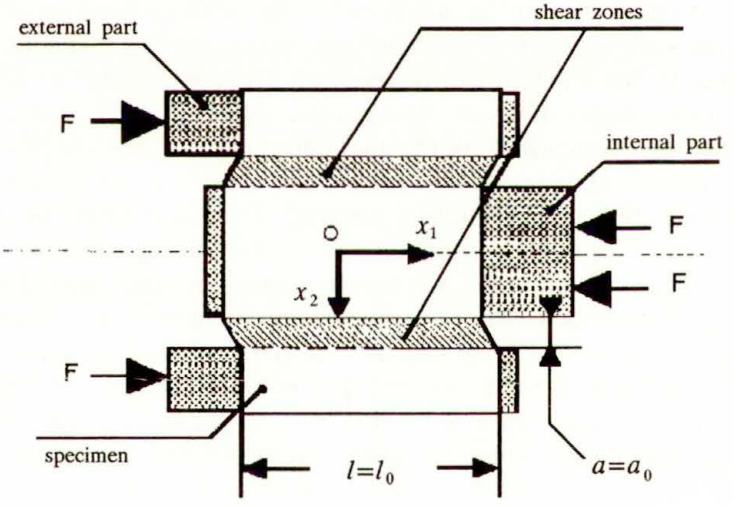

FIG. 1. Scheme of the shear device.

First, the system is tested under quasi-static loading for verifying the effectiveness. The presence of free bounds of specimen produces the heterogeneity of stress field because the stress vector normal to the free surfaces must be zero, therefore we have assumed that the dimensions of the perturbed zone are small compared to the dimensions of the specimen. This assumption is acceptable as shown in [1], where the mounting of the sheet is tested and the homogeneity of the field of deformation is observed. In general, we must take the ratio a_0/l_0

http://rcin.org.pl

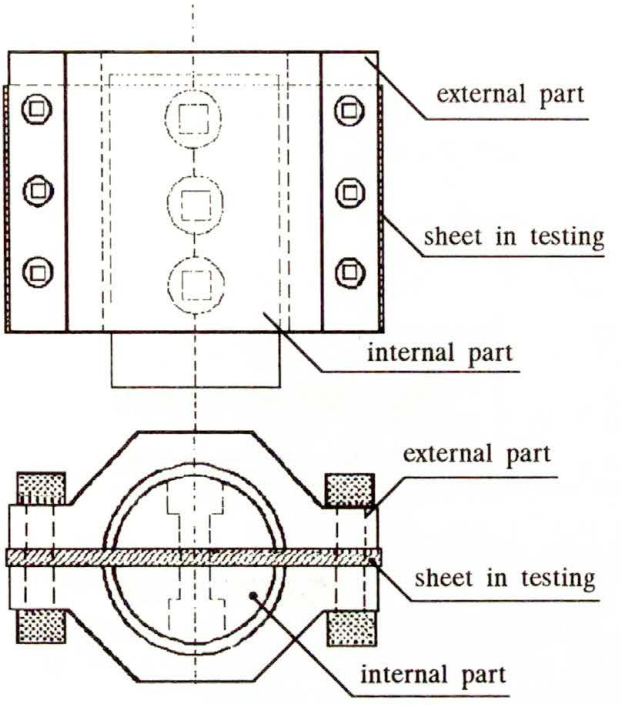

FIG. 2. Shear device in detail.

sufficiently small. It is shown in [8, 9] that when the ratio $a_0/l_0 \leq l/10$, the results of test are good for both static and dynamic cases. We take in our tests $a_0/l_0 = l/10$.

The dynamic test is similar but the loading is realized by the SHPB. The device with specimen is placed between two bars of the SHPB. In this case the mechanical impedance of the shear device and the SHPB must be the same to avoid the noise in the interface signal. The impulse is created by the third projectile bar: the usual compression technique. We have to register the input, the transmitted and the reflected impulse: ε_i, ε_t and ε_r. The highest strain rate in the specimen can be obtained using only one bar of the SHPB system. We use the transmitted bar only and the shearing device is placed in the front of this bar. The projectile bar strikes directly the device. We have to register only the transmitted impulse ε_t and the velocity of the projectile.

Measurement of quasi-static or dynamic deformation in the case of simple shear of the metal sheets is not very simple. The specimen is deformed not only between the grips, in the gauge section, the part under the grips is partially deformed too. The transversal strike lines, marked on the specimen before the test, for example the line AB shown in the Fig. 3 a becomes after deformation the curve AB' with the strike sections Aa, $b'c'$ and dB'. These curves observed under the optical microscope are shown by the photo – Fig. 3 b.

http://rcin.org.pl

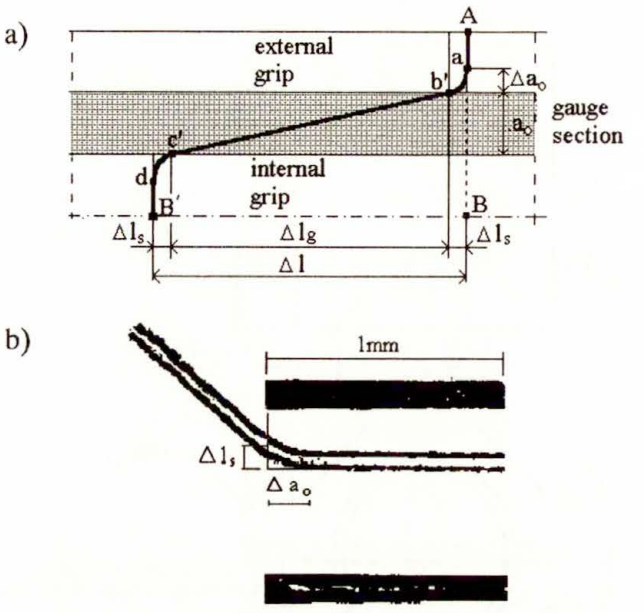

FIG. 3. Deformation in simple shear of the sheet, in the gauge section and under the grips: a) scheme, b) observed under the optical microscope.

Relative displacement of external and internal parts of shear device Δl is easy to measure in the case of quasi-static deformation (in the testing machine) as well in the case of dynamic deformation – in SHPB system. It is a sum of two terms: $\Delta l = \Delta l_g + 2\Delta l_s$, where Δl_g corresponds to the deformation in the simple shear defined as $\gamma = \Delta l_g / a_0$, and Δl_s correspond to the value of sliding under the grips. It was assumed that, in the case of simple plane shear, there is no change in the cross-section: $S_E = \text{const}$ ($S_E = l_0 d$; where d is the thickness of the specimen). Then the mean shear stress is defined by $\sigma_{12} = F/S_E$.

The estimations of the sliding value under the grips Δl_s can be obtained in the quasi-static test of loading-unloading. After this test, the permanent deformation of the specimen can be measured using the optical microscope. Comparisons of this measure with those obtained by an extensometer at the end of the unloading process yields the value of Δl_s, for the given range of deformation γ.

We can notice that the shear device can be also deformed during the test. It is desirable that the measurement of deformation should be performed as near as possible to the gauge section. In this case the best is the local optical measure of deformation made by the CCD camera, with simultaneous treatment of the picture. The principle of this method is described in [14]. Using this method, we can determine the shear deformation of the specimen with the accuracy of the order of $2 \cdot 10^{-5}$. In [14] it is proved that the measurement by the relative displacement of the grips is also good, on condition that the deformation of the specimen under the grips is taken into consideration.

http://rcin.org.pl

In the axis of Fig. 1 the stress tensor has the following components: σ_{11}, σ_{22} and σ_{12}. The presence of σ_{11} and σ_{22} is due to the fact that the distance between two parts of the shear device is constant during experiment i.e. $a = a_0 = \text{const}$. The strain tensor has only one non-zero component $\varepsilon_{12} = \gamma$. In this test, large deformations can be obtained without localisation of the deformation, contrary to the case of torsion of thin cylindrical specimens [2, 3 and 13], for example. The specimens deformed quasi-statically or dynamically to $70-90\%$ and observed under the optical microscope, have a similar structure. The transversal lines marked before the test on the specimens, on the gauge section, remain parallel after the test. This fact indicates that the deformation is homogeneous in the considerable part of the specimen. We have assumed that the dimensions of the perturbed zone are small compared to the dimensions of the specimen. The exceptional qualities of the homogeneity of the residual strain field show that the simplified analysis can be used in the zone of plastic deformations.

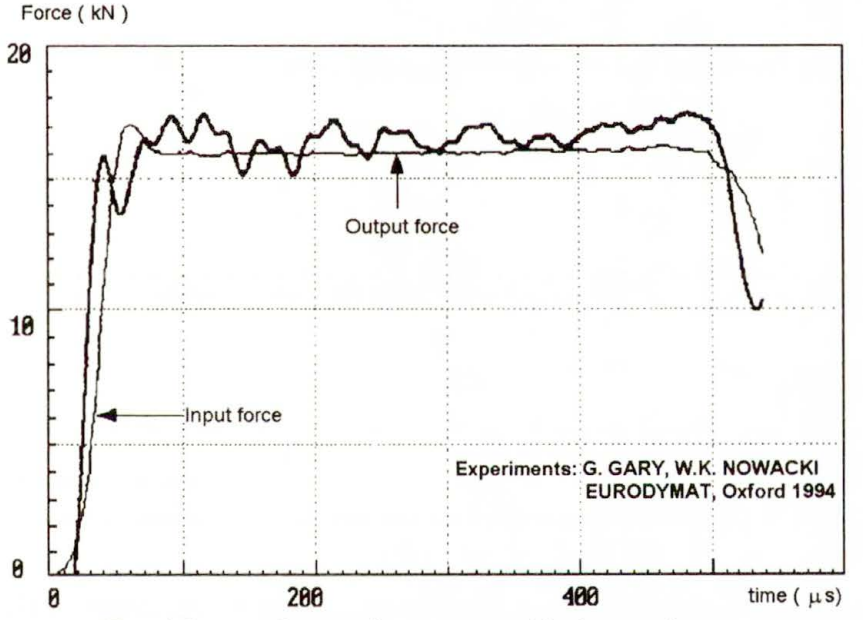

FIG. 4. Input and output forces measured in the experiment.

In the analysis, we must take into account that the loading of the specimen is not instantaneous. The loading compression wave must take some time to travel from one end to the other end of the device. However, we have in our tests very good equilibrium of forces on two sides of the shear device, see Fig. 4. We observe that the input force and the output are very similar in shape, neglecting the small oscillations of the input force. So, in the simplified analysis we suppose that the loading is homogeneous and we proceed as in the case of quasi-static loading. Knowing the velocities on bounds of the shear device, we can find the

http://rcin.org.pl

displacements. The force is taken to be equal to the mean value of the input and output forces.

The sensibility to the rate of deformation in compression and in the simple shear is presented in Fig. 5. The experiments made on the XES steel at low and moderate strain rate (quasi-static test in compression and dynamic compression test using SHPB system) are performed by G. GARY and described in [1]. These results are completed by investigations in dynamic simple shear. The diagrams in the Fig. 5 present the variation of the maximal stress versus logarithmic rate of deformation, for different kinds of experiments mentioned above.

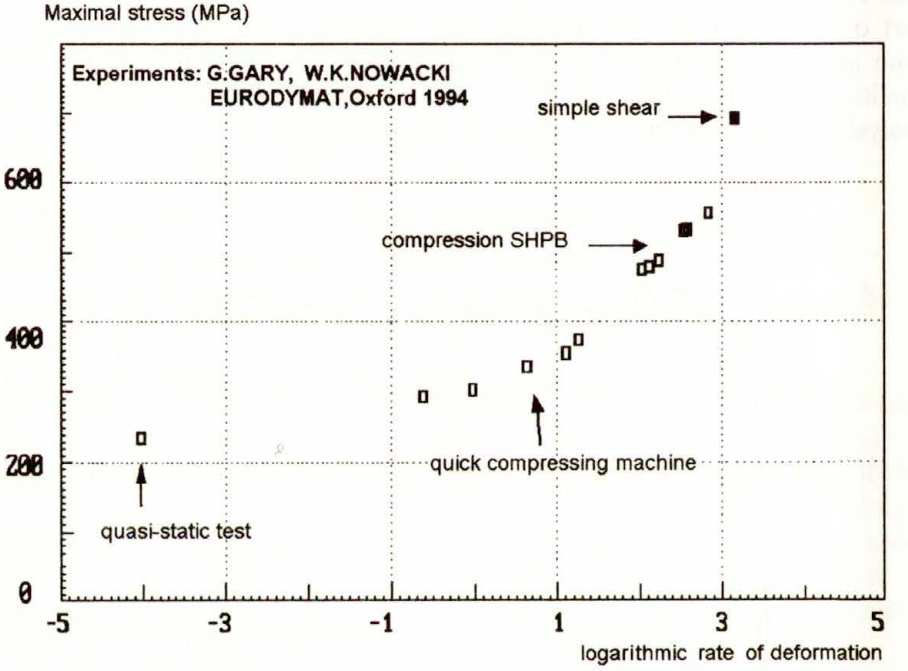

FIG. 5. Comparison of the simple shear test with the simple compression test [1].

In the paper [11] the quasi-static tests concerning the behaviour of 1H18N9T steel are discussed. The temperature field due to deformation is simultaneously registered. The goal of this paper was to obtain the mechanical curves as well as the temperature distributions in the shear regions. A change of temperature of the surface of these regions has been observed by the thermovision camera coupled with a system of data acquisition and conversion. The infrared radiation emitted by shear paths was measured. The results obtained enable us to present the temperature changes of the specimens subjected to the shear test with different rates of deformation, as well as to describe the macroscopic shear band developing at higher deformations. Finally, the experimental results were compared with the results of numerical simulations presented in Sec. 5 of the present paper.

http://rcin.org.pl

3. Theoretical simple shear analysis

The simple shear in the direction $\mathbf{e}_1$ of the coordinate system $(\mathbf{e}_1, \mathbf{e}_1)$ is defined by the relations

$$(3.1) \qquad \begin{aligned} u_1 &= \gamma(t)x_2, & u_2 &= u_3 = 0, \\ v_1 &= \dot{\gamma}x_2, & v_2 &= v_3 = 0, \end{aligned}$$

where $\gamma = \operatorname{tg}\phi$ (cf. Fig. 6) and $\dot{\gamma}$ are the plastic shear strain and shear strain

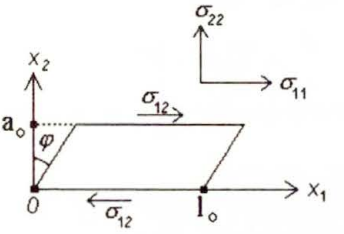

FIG. 6. Scheme of simple shear.

rate, respectively. From the velocity field $\mathbf{v}$, the velocity gradient $\mathbf{V}$, the rate of deformation $\mathbf{D}$ and the material spin $\boldsymbol{\omega}$ can be determined in the system $(\mathbf{e}_1, \mathbf{e}_1)$ as

$$(3.2) \qquad \mathbf{V} = \frac{\dot{\gamma}}{2}\begin{pmatrix} 0 & 1 \\ 0 & 0 \end{pmatrix}, \qquad \mathbf{D} = \frac{\dot{\gamma}}{2}\begin{pmatrix} 0 & 1 \\ 1 & 0 \end{pmatrix}, \qquad \boldsymbol{\omega} = \frac{\dot{\gamma}}{2}\begin{pmatrix} 0 & 1 \\ -1 & 0 \end{pmatrix}.$$

The Cauchy stress tensor $\boldsymbol{\sigma}$ and the back stress $\boldsymbol{\Pi}$ have the non-zero components

$$(3.3) \qquad \boldsymbol{\sigma} = \begin{pmatrix} \sigma_{11} & \sigma_{12} \\ \sigma_{21} & \sigma_{22} \end{pmatrix}, \qquad \boldsymbol{\Pi} = \begin{pmatrix} \pi_{11} & \pi_{12} \\ \pi_{21} & \pi_{22} \end{pmatrix}.$$

Using the constitutive relations for adiabatic process for rate-independent materials with combined isotropic-kinematic hardening at moderate pressures, when the thermal expansion, the heat of elastic deformation and the heat of internal rearrangement are neglected, we obtain the following constitutive equations [10]

$$(3.4) \qquad \overset{\circ}{\mathbf{T}} = \beta \mathbf{L}\,\mathbf{D} - \frac{3j\mu\beta \mathbf{D}\cdot(\overline{\mathbf{T}} - \boldsymbol{\Pi})}{\sigma_Y^2 \mathcal{H}}\,[(\overline{\mathbf{T}} - \boldsymbol{\Pi}) + \mathbf{P}],$$

$$j = \begin{cases} 1 & \text{if } f = 0 \text{ and } \mathbf{D}\cdot(\overline{\mathbf{T}} - \boldsymbol{\Pi}) \geq 0, \\ 0 & \text{if } f = 0 \text{ and } \mathbf{D}\cdot(\overline{\mathbf{T}} - \boldsymbol{\Pi}) < 0, \quad \text{or} \quad f < 0, \end{cases}$$

where $\beta = \varrho_0/\varrho$ is the ratio of densities in the reference and actual configurations, $\mathbf{T} = \beta\boldsymbol{\sigma}$, $\overset{\circ}{\mathbf{T}} = \dot{\mathbf{T}} - \boldsymbol{\omega}\mathbf{T} + \mathbf{T}\boldsymbol{\omega}$ is the Zaremba-Jaumann rate, $\overline{\mathbf{T}}$ is the deviatoric

http://rcin.org.pl

part of **T**, **L** is the fourth order tensor of elastic moduli, μ is the Lamé constant and f is the Huber-Mises yield criterion

$$f = \frac{3}{2}(\overline{\mathbf{T}} - \mathbf{\Pi})\cdot(\overline{\mathbf{T}} - \mathbf{\Pi}) - \sigma_Y^2(\vartheta, \alpha) = 0, \tag{3.5}$$

where σ_Y is the yield stress in simple tension, ϑ is the temperature and α corresponds to the size of the yield surface

$$\dot{\alpha} = (\overline{\mathbf{T}} - \mathbf{\Pi})\cdot\mathbf{D}^{\mathbf{P}}. \tag{3.6}$$

The shift of the yield surface is represented here by the back stress $\mathbf{\Pi}$ for which the evolution law has the form of linear kinematic hardening

$$\overset{\nabla}{\mathbf{\Pi}} = c\,\mathbf{D}^{\mathbf{P}}, \tag{3.7}$$

where c = const and $\mathbf{D}^{\mathbf{P}}$ is the plastic rate of deformation. The change in the temperature is described as

$$\varrho_0 c_v \dot{\vartheta} = (1-\pi)(\overline{\mathbf{T}} - \mathbf{\Pi})\cdot\mathbf{D}^{\mathbf{P}}, \tag{3.8}$$

c_v is specific heat at constant volume; the first term on the right-hand side of (3.8) represents the rate of energy dissipation and, therefore, $\pi < 1$. For numerous metals π takes the value from 0.02 to 0.1 [10]. In Eq. (3.4) $\mathcal{H}$ is the hardening function

$$\mathcal{H} = 1 + \frac{c}{2\mu\beta} + \frac{1}{6\mu\beta}\frac{\partial(\sigma_Y^2)}{\partial\alpha} + \frac{(1-\pi)}{6\mu\beta\varrho_0 c_v}\frac{\partial(\sigma_Y^2)}{\partial\vartheta}$$

and tensor $\mathbf{P}$ is obtained by expressing the term $(\boldsymbol{\omega}_p\mathbf{T} + \mathbf{T}\boldsymbol{\omega}^p)$ as a function of $\mathbf{D}^{\mathbf{P}}$ where $\boldsymbol{\omega}^p$ is the plastic spin.

The equation for plastic spin can be assumed, according to DAFALIAS [6], PAULUN and PĘCHERSKI [7] and others, in the following form

$$\boldsymbol{\omega}^p = \eta(\mathbf{\Pi}\,\mathbf{D}^{\mathbf{P}} - \mathbf{D}^{\mathbf{P}}\mathbf{\Pi}), \tag{3.9}$$

where η may depend on the invariants of $\mathbf{D}^{\mathbf{P}}$ and $\mathbf{\Pi}$.

In the case of plane simple shear we have $\beta = 1$ and the equations above lead to

$$\begin{aligned}
\dot{\sigma}_{11} - \dot{\gamma}\sigma_{12} &= -\frac{3j\mu}{\sigma_Y^2\mathcal{H}}\left[\dot{\gamma}(\sigma_{12} - \pi_{12})\right]\left[(\sigma_{11} - \pi_{11}) + \frac{\eta}{\mu}\mathcal{M}\sigma_{12}\right],\\
\dot{\sigma}_{12} - \dot{\gamma}\sigma_{11} &= \mu\dot{\gamma} - \frac{3j\mu}{\sigma_Y^2\mathcal{H}}\left[\dot{\gamma}(\sigma_{12} - \pi_{12})\right]\left[(\sigma_{12} - \pi_{12}) - \frac{\eta}{\mu}\mathcal{M}\sigma_{11}\right],\\
\dot{\pi}_{11} - \dot{\gamma}\pi_{12} &= \frac{3jc}{\sigma_Y^2\mathcal{H}}\left[\dot{\gamma}(\sigma_{12} - \pi_{12})\right](\sigma_{11} - \pi_{11}),\\
\dot{\pi}_{12} - \dot{\gamma}\pi_{11} &= \frac{3jc}{\sigma_Y^2\mathcal{H}}\left[\dot{\gamma}(\sigma_{12} - \pi_{12})\right](\sigma_{12} - \pi_{12});
\end{aligned} \tag{3.10}$$

http://rcin.org.pl

here $\sigma_{11} = -\sigma_{22}$, $\pi_{11} = -\pi_{22}$, and

$$\mathcal{M} = [\pi_{11}(\sigma_{12} - \pi_{12}) - \pi_{12}(\sigma_{11} - \pi_{11})]. \tag{3.11}$$

We use here the relation for the function η occurring in the expression of plastic spin (3.9), in the form proposed in the papers [6, 7, 15 and 16]:

$$\eta = \frac{3}{\left[\left(\frac{3c}{2}\right)^2 + \frac{3c}{2}\left(\frac{3}{2}\boldsymbol{\Pi}\cdot\boldsymbol{\Pi}\right)^{1/2}\right]^{1/2}}. \tag{3.12}$$

The Huber-Mises yield criterion (3.5) is

$$\begin{aligned} f &= \frac{3}{2}(\overline{\sigma} - \boldsymbol{\Pi})\cdot(\overline{\sigma} - \boldsymbol{\Pi}) - \sigma_Y^2 \\ &= 3\left[(\sigma_{11} - \pi_{11})^2 + (\sigma_{12} - \pi_{12})^2\right] - \sigma_Y^2(\alpha, \vartheta) = 0, \end{aligned} \tag{3.13}$$

and in the equations (3.10) we have

$$j = \begin{cases} 1 & \text{if } f = 0 \text{ and } \dot{\gamma}(\sigma_{12} - \pi_{12}) \geq 0, \\ 0 & \text{if } f = 0 \text{ and } \dot{\gamma}(\sigma_{12} - \pi_{12}) < 0, \quad \text{or} \quad f < 0. \end{cases} \tag{3.14}$$

The change in the temperature ϑ is described by

$$\varrho_0 c_v \dot{\vartheta} = j\frac{(1 - \pi)[\dot{\gamma}(\sigma_{12} - \pi_{12})]}{\mathcal{H}}. \tag{3.15}$$

The hardening function $\mathcal{H}$ now is

$$\mathcal{H} = 1 + \frac{c}{2\mu} + \frac{1}{6\mu}\frac{\partial(\sigma_Y^2)}{\partial\alpha} + \frac{(1 - \pi)}{6\mu\varrho_0 c_v}\frac{\partial(\sigma_Y^2)}{\partial\vartheta}. \tag{3.16}$$

In case of elasticity $j = 0$ and Eqs. (3.10) reduce to

$$\begin{aligned} \dot{\sigma}_{11} - \gamma\sigma_{12} &= 0, \\ \dot{\sigma}_{12} - \gamma\sigma_{11} &= \mu\dot{\gamma}, \\ \dot{\pi}_{11} - \gamma\pi_{12} &= 0, \\ \dot{\pi}_{12} + \gamma\pi_{11} &= 0. \end{aligned} \tag{3.17}$$

Under the initial conditions that for $\gamma = 0$, stresses $\sigma_{11} = \sigma_{12} = \pi_{11} = \pi_{12} = 0$, we have the analytical solution:

$$\begin{aligned} \sigma_{11} &= \mu(1 - \cos\gamma), \\ \sigma_{12} &= \mu\sin\gamma, \\ \pi_{11} &= 0, \\ \pi_{12} &= 0. \end{aligned} \tag{3.18}$$

http://rcin.org.pl

The stress-shear strain relations, in the range of elastic deformations, are shown in the Fig. 7, with $\mu = 8 \cdot 10^4$ MPa. The contribution of normal stress σ_{11} and σ_{22} is very small in comparison with that of the stress component σ_{12}.

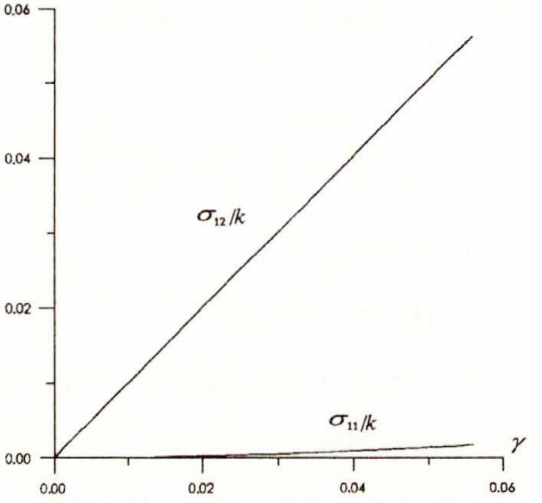

FIG. 7. Shear stress σ_{12} and normal stress σ_{11} vs. shear strain: elastic material.

We can show that in the case of plasticity with kinematic hardening, we also obtain analytical solutions. Then $\sigma_Y = \text{const}$ and now from (3.16) we have

$$\mathcal{H} = 1 + \frac{c}{2\mu}. \tag{3.19}$$

Introducing the new variable ϕ satisfying the yield condition

$$\begin{aligned} \sigma_{11} - \pi_{11} &= (1/\sqrt{3})\sigma_Y \cos\phi, \\ \sigma_{12} - \pi_{12} &= (1/\sqrt{3})\sigma_Y \sin\phi, \end{aligned} \tag{3.20}$$

the relation between ϕ and γ is now the following:

$$\frac{\sqrt{a^2-1}\tan\dfrac{\phi}{2} + (a-1)}{\sqrt{a^2-1}\tan\dfrac{\phi}{2} - (a-1)} \exp\left(-\sqrt{a^2-1}\gamma\right) = C, \tag{3.21}$$

where $a = \mu/k_0$, $k_0 = \sigma_Y/\sqrt{3}$ is the yield value in shear and

$$C = \frac{\sqrt{a^2-1}\tan\dfrac{\phi^*}{2} + (a-1)}{\sqrt{a^2-1}\tan\dfrac{\phi^*}{2} - (a-1)} \exp\left(-\sqrt{a^2-1}\gamma^*\right),$$

http://rcin.org.pl

and where γ^* and ϕ^* are described by the formula $\sin(\gamma^*/2) = k_0/2\mu$ and $\tan(\gamma^*/2) = \operatorname{ctg}\phi^*$.

The back stress π_{11} satisfies the equation

$$\frac{d\pi_{11}}{d\phi} - \pi_{11}\frac{\tan\phi}{a\cos\phi - 1} = \frac{c}{2\mathcal{H}}\frac{\sin\phi\cos\phi}{a\cos\phi - 1} \tag{3.22}$$

hence we can calculate π_{12} by the formula

$$\pi_{12} = \pi_{11}\tan\phi. \tag{3.23}$$

We find σ_{11}, σ_{12} from (3.20) and finally we determine

$$\begin{aligned}
\pi_{11} &= \frac{c}{2\mathcal{H}}(\cos\phi - \cos\phi^*)\frac{\cos\phi}{(1 - a\cos\phi)}, \\
\pi_{12} &= \frac{c}{2\mathcal{H}}(\cos\phi - \cos\phi^*)\frac{\sin\phi}{(1 - a\cos\phi)}, \\
\sigma_{11} &= \frac{c}{2\mathcal{H}}(\cos\phi - \cos\phi^*)\frac{\cos\phi}{(1 - a\cos\phi)} + k_0\cos\phi, \\
\sigma_{12} &= \frac{c}{2\mathcal{H}}(\cos\phi - \cos\phi^*)\frac{\sin\phi}{(1 - a\cos\phi)} + k_0\sin\phi.
\end{aligned} \tag{3.24}$$

The analytical solution for the normal and tangential components of the back stress tensor π_{11} and π_{12} could be used directly to evaluate the function η given in (3.12).

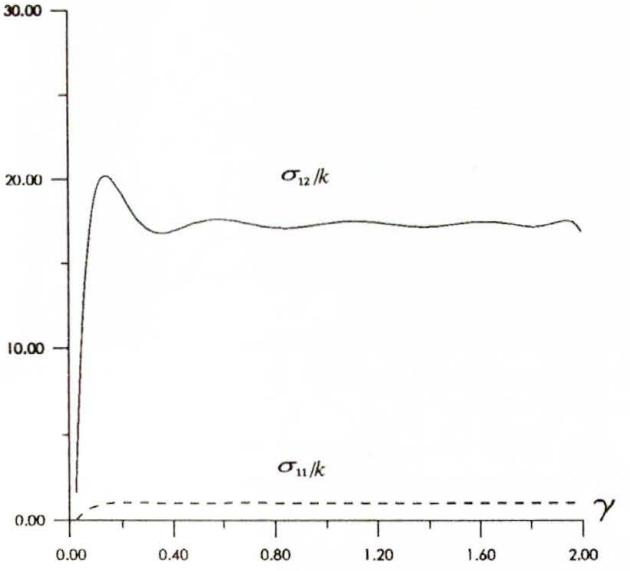

FIG. 8. Shear stress σ_{12} and normal stress σ_{11} vs. shear strain for kinematic hardening.

http://rcin.org.pl

Now, we can determine the stress – shear strain relations in the range of non-elastic deformations. Solutions for stresses σ_{11} and σ_{12} in dimensionless form vs. shear strain γ, illustrated in Fig. 8, are obtained for kinematic hardening, using the same material properties as in the paper [12], namely: $\mu = 8 \cdot 10^4$ MPa, $c = 5333,33$ MPa, $k_0/\mu = 0.0577$. Results of calculations for kinematic hardening are similar to those obtained in the paper [12]. In the case of large plastic deformations, the ratios σ_{11}/σ_{12} and σ_{22}/σ_{12} are much higher than in the case of small elastic deformations – cf. Fig. 7.

4. Metallurgical and thermomechanical observations

A portion of the gauge length of the specimen submitted to the simple shear test, with high strain rate, is shown in the Fig. 9. The shear deformation is of the order of 73%. An essential feature is the formation of the tangled structure and dislocations cells. Their elongation and arrangement tend to be aligned along the shear direction. In several grains the micro-bands of shear, parallel to the direction of x_1 axis are observed.

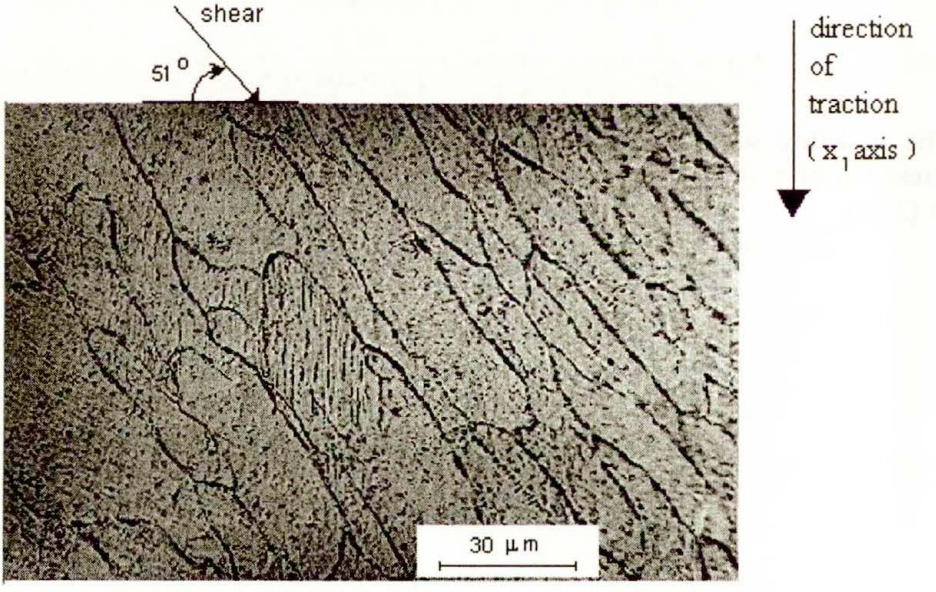

FIG. 9. Macro- and micro-bands of shear in the specimen subjected to simple shear.

At the very high strain rate, the shear macro-bands are observed. We can suppose that it is a critical strain at which the shear localization occurs. Before arriving at the critical strain, the deformation goes uniformly over the whole gauge length of the specimen. The work-hardening results from the creation, multiplication and interaction of the dislocations. In this case, a small part of the

http://rcin.org.pl

work of plastic deformation is stored in the material as elastic strain energy (about 6% cf. [13]) and the remaining part is converted into heat. In the paper [11] the temperature field due to plastic deformation is measured by the thermovision camera. With this technique, it is possible to evaluate the stored energy due to simple shear in the case of large deformations. The shear macro-bands are observed in the case of quasi-static deformations.

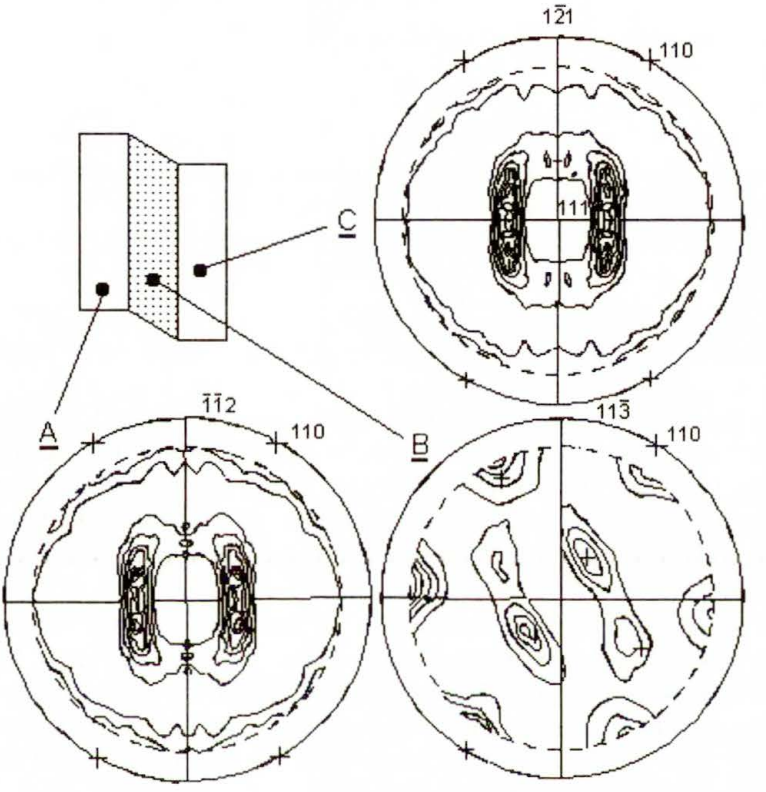

FIG. 10. a) and c) initial texture of the sheet (zones undeformed under grips), b) texture measured in the deformed zone after simple shear – permanent deformation 73%.

The initial texture is illustrated in Fig. 10a and Fig. 10c. The texture evolution after the large deformation of the order of 73% is shown in the Fig. 10b, which shows a clear loss of orthotropy with respect to the initial reference frame. The final textures found in different points of the shear zones after simple shear are very similar.

5. Numerical simulations of the experiment

The program of finite element method was used to the numerical simulations of the formulated problem of quasi-static and dynamic simple shear of thin

http://rcin.org.pl

sheets. We assume the initial and boundary conditions similar to those used in the experiment.

A. In the case of quasi-static loading, the boundary conditions have the following form:

In fixed ends of specimen (under grips) – cf. Fig. 6:

$$(5.1)\qquad \begin{aligned} &u_1(x_1, x_2, t)\Big|_{x_2=0} = u_2(x_1, x_2, t)\Big|_{x_2=0} = 0, \\ &v_1(x_1, x_2, t)\Big|_{x_2=a_0} = v_0 \qquad \text{and} \qquad u_2(x_1, x_2, t)\Big|_{x_2=a_0} = 0, \end{aligned}$$

where v_0 is the velocity of the testing machine in traction. In this case, the sliding of material under the grips is neglected.

At the free ends of the specimen (for $x_1 = 0$ and $x_1 = l_0$) we have:

$$(5.2)\qquad \sigma_{12}(x_1, x_2, t)\Big|_{\substack{x_1=0 \\ x_1=l_0}} = \sigma_{11}(x_1, x_2, t)\Big|_{\substack{x_1=0 \\ x_1=l_0}} = -\sigma_{22}(x_1, x_2, t)\Big|_{\substack{x_1=0 \\ x_1=l_0}} = 0.$$

B. In the case of dynamic deformations, conditions (5.1) must be replaced by conditions of balance of forces in the contact between the specimen and the measuring bars. We should remember that the shear device and bars of SHPB system have identical mechanical impedances. At the same time, a simplifying assumption is introduced, and the process of waves propagation in the specimen is neglected.

With a view to a perfect equilibrium of input and output forces and quasi-constant value of the time period $50\,\mu s < t < 500\,\mu s$ – cf. Fig. 5, we can treat our problem as quasi-static. The amplitude of loading is determined from the dynamic experiment. We assume that in the contact between the specimen and measuring bars, the force is constant in time, cf. Fig. 5, and equal to $F_{\max}$. The boundary conditions (4.1) take the form:

$$(5.3)\qquad \sigma_{12}(x_1, x_2, t)\Big|_{x_2=0} = -F_{\max}/S_E \qquad \text{and} \qquad u_2(x_1, x_2, t)\Big|_{\substack{x_2=0 \\ x_2=a_0}} = 0.$$

We assume the homogeneous zero initial conditions.

In the finite element method the rectangular mesh is introduced. Deformation of the mesh in time is determined. At the same time, the components of the stress tensor σ_{12} and $\sigma_{22} = -\sigma_{11}$, the stress intensity $\sigma_i = (3/2 s_{ij} s_{ij})^{1/2}$ and the equivalent strain $e_i = (2/3\, \varepsilon^p_{ij}\, \varepsilon^p_{ij})^{1/2}$ are determined. First, the numerical simulation was made for the quasi-static loading of the sheet made of the steel 1H18N9T, with $\mu = 8 \cdot 10^4$ MPa, $\varrho = 7.8\,\mathrm{g/cm^3}$ and $\sigma_y = 280$ MPa.

Results of numerical simulation in the specimen subjected to quasi-static simple shear are shown in the Fig. 11. The equivalent deformation field is shown

http://rcin.org.pl

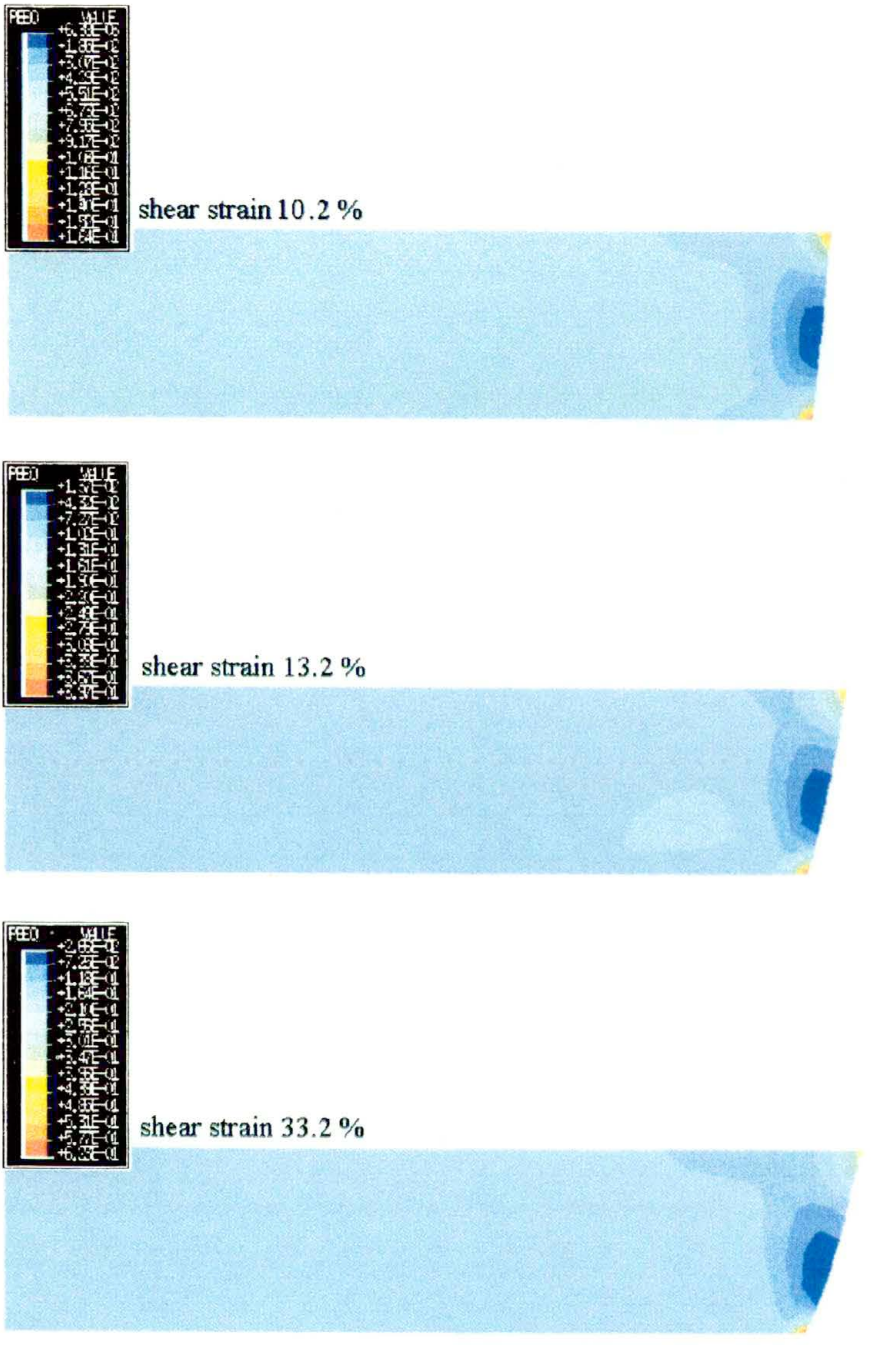

[FIG. 11]

http://rcin.org.pl

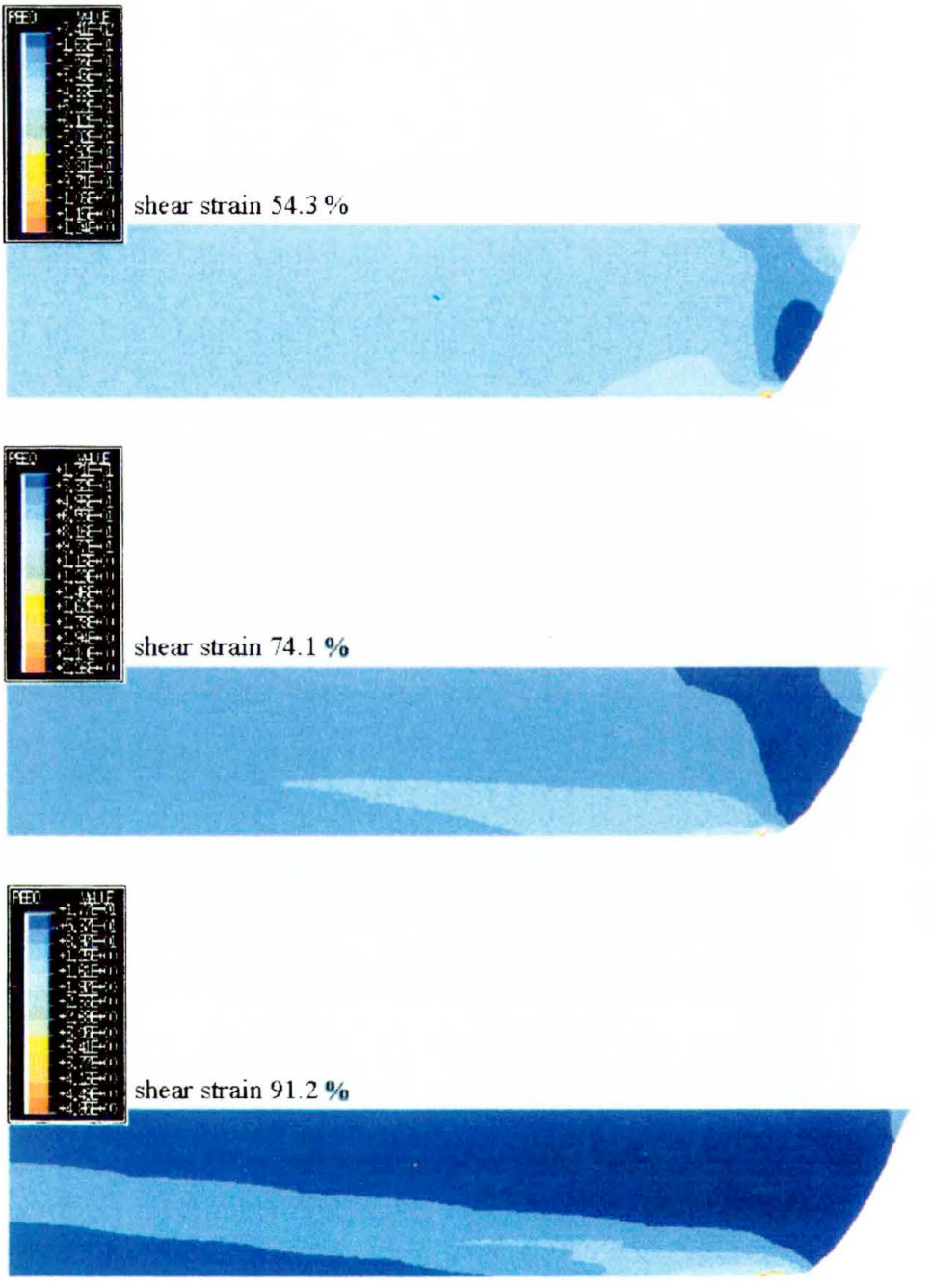

FIG. 11. Numerical simulation. Equivalent deformation.

http://rcin.org.pl

for one half of the shear zone of the specimen, in view of the symmetry of deformation process with respect to the axis x_2 – cf. Fig. 1. Successive sequences are presented for different values of shear strain defined as $\gamma = \Delta l(t)/a_0$, from $\gamma = 10.2\%$ to $\gamma = 91.2\%$. We observe for example the heterogeneity of the strain and stress fields at the free ends of the specimen, at the distance less than 1.7% (accurate to 0.01% of deformation) of the total length when the strain is 30%, and less than 6.6% of the total length when the strain is 70%, exactly as in the experiments.

The performed numerical calculations enabled the evaluation of the optimal dimensions of the specimen.

6. Conclusions

Considerable homogeneity of the permanent strain field at finite deformations over the total length of the specimens is observed in experiments and in the results of simulation. The proposed method is the only known test providing, in the case of a thin sheet, homogeneous stress and strain fields in both the dynamic and static tests. They can be used to verify the constitutive relations proposed in [10]. Simple shear test is particularly attractive, since the application of this type of loading path can result in large strains without the occurrence of plastic instability. The advantages of the method in the case of static deformation were discussed widely in [5]. The thermo-mechanical coupling was described in the paper [11].

Acknowledgments

The authors wish to express their thanks for the co-operation in the field of metallurgical examination of samples and valuable discussions to Dr. M. RICHERT, University of Mining & Metallurgy, Kraków.

This paper is supported by the Polish Committee for Scientific Research, KBN Project No. 7T07A02608 on "Dynamic fracture of materials".

Numerical computations were performed at the Computing Center of the Warsaw University of Technology, on Super Server CS 6400.

References

1. G. GARY and W.K. NOWACKI, *Essai de cisaillement plan appliqué à des tôles minces*, J.de Physics IV, Colloque C8, Supplément au J. de Physic III 4, pp. 65–70, 1994.
2. K.A. HARTLEY, J. DUFFY and R.H. HAWLEY, *Measurement of the temperature profile during shear band formation in steels deforming at high strain rates*, J. Mech. Phys. Solids, **35**, 3, pp. 283–301, 1986.
3. A. MARCHAND and J. DUFFY, *An experimental study of the formation process of adiabatic shear bands in structural steel*, J. Mech. Phys. Solids, **36**, 3, pp. 251–283, 1988.
4. B. BACROIX and ZAIQIAN HU, *Texture evolution induced by strain path changes in low carbon steel sheets*, Metallurgical and Materials Trans. A, **26A**, pp. 601–613, March 1995.

http://rcin.org.pl

5. B. BACROIX, P. GENEVOIS and C. TEODOSIU, *Plastic anisotropy in low carbon steels subjected to simple shear with strain path changes*, Eur. J. Mech., A/Solids, **13**, 5, pp. 661–675, 1994.
6. Y.F. DAFALIAS, *A missing link in the macroscopic constitutive formulation of large plastic deformations*, [in:] Plasticity Today, pp. 135–151, A. SAWCZUK, G. BIANCHI [Eds.], Elsevier, 1985.
7. J.E. PAULUN and R. PĘCHERSKI, *On the relation for plastic spin*, Arch. Appl. Mech., **62**, pp. 376–385, 1992.
8. E.F. RAUCH and C. G'SELL, *Flow localization induced by a change in strain path in mild steel*, Material Sci. and Engng., (A111), 71, 1989.
9. A. TOURABI, B. WACK, P. GUÉLIN, D. FAVIER, P. PEGON and W.K. NOWACKI, *Remarks on an experimental plane shear test and on an anisotropic elastic-plastic theory*, Technical Report, SMIRT, 1993, Stuttgart, August 15-20, Elsevier Sci. Publ., 1993.
10. NGUYEN HUU VIEM, *Isothermal and adiabatic flow laws of metallic elastic-plastic solids at finite strains and propagation of acceleration waves*, Arch. Appl. Mech., **44**, 5-6, pp. 595–602, 1992.
11. P.S. GADAJ, W.K. NOWACKI and E. PIECZYSKA, *Changes of temperature during the simple shear test of stainless steel*, Arch. Mech., **48**, 4, 1996.
12. L. SZABO and M. BALLA, *Comparison of some stress rates*, Int. J. Solids Structures, **25**, 3, pp. 279–297, 1989.
13. Y.B. XU, Y.L. BAI, Q. XUE and L.T. SHEN, *Formation, microstructure and development of the localized shear deformation in low-carbon steel*, Acta Mater., **44**, 5, pp. 1917–1926, 1966.
14. P.Y. MANACH, *Etude du comportement thermomécanique d'alliages à mémoire de forme NiTi*, Doctoral Thesis, Institut National Polytechnique de Grenoble, 1993.
15. J.E. PAULUN and R.B. PĘCHERSKI, *Study of corotational rates for kinematic hardening in finite deformation plasticity*, Arch. Mech., **37**, 6, pp. 661–677, 1985.
16. R.B. PĘCHERSKI, *Model of plastic flow accounting for the effects of shear banding and kinematic hardening*, ZAMM, Z. Angew. Math. Mech., **75**, pp. S 203–204, 1995.

INSTITUTE OF FUNDAMENTAL TECHNOLOGICAL RESEARCH
POLISH ACADEMY OF SCIENCES
e-mail: wnowacki@ippt.gov.pl

Received December 2, 1996.

http://rcin.org.pl

Arch. Mech., 49, 2, pp. 385–401, Warszawa 1997

Macroscopic measure of the rate of deformation produced by micro-shear banding

R. B. PĘCHERSKI (WARSZAWA)

PHYSICAL MODEL of shear strain rate produced by active micro-shear bands in metals is formulated and mathematical idealization of micro-shear bands system by means of the theory of singular surface of order one is proposed. Extension of the known averaging procedure over the representative volume element traversed by a strong discontinuity surface is presented. As a result, the macroscopic measure of velocity gradient produced in the course of elastic-plastic deformation with micro-shear banding is derived. The corresponding macroscopic measures of the rate of deformation and material spin, necessary to formulate constitutive description, are also determined.

1. Introduction

INTEGRATED STUDIES on physics and mechanics of large plastic deformations of metals accounting for micro-shear bands require careful analysis of the averaging procedure and proper setting of the resulting description of the effects of micro-shear bands within the continuum theory of materials. Formulation of a complete theory based on the precise micro-to-macro transition remains an open and challenging question. The aim of the paper is to approach this problem merely from the point of view of the contribution of micro-shear banding to kinematics of finite elastic-plastic deformations of metallic solids. The related macroscopic measures of velocity gradient, rate of deformation and material spin, which are necessary to formulate constitutive equations of elastoplasticity at finite strain, have been determined. The derivation is based on the following novel concepts:

(i) Mathematical idealization of a system (cluster) of active micro-shear bands as propagating singular surface of order one, having properties of a vortex sheet.

(ii) Formulation of the physical model, which enables to relate the macroscopic shear strain rate with microstructural features of active micro-shear bands and to identify the jump in velocity across the vortex sheet.

(iii) Extension of the known averaging procedure by introducing the representative volume element (RVE) traversed by the singular surface of vortex sheet type.

The possibility of modelling of the narrow zone of localization as a surface of strong discontinuity in the velocity field was suggested by THOMAS [1] and applied further by VALANIS [2] and SU [3]. The authors observed that the concentration of dislocation movement on a few slip planes can cause abrupt changes of the velocity field on the micro-scale and may lead to velocity jumps accompanying

http://rcin.org.pl

plastic deformation in macro-level. The theoretical characterization of a shear band, as a surface of discontinuity, across which the jumps in velocity, stress gradient and temperature are allowed, was considered recently by OLMSTED *et al.* [4] for the one-dimensional problem of unidirectional shearing of a slab, which is used typically in a variety of investigations of the so-called "adiabatic shear bands" formation. The results of this study can be applied to derive in a more rigorous manner the constitutive equations, accounting for micro-shear bands with their characteristic geometric pattern, which were obtained previously under certain simplifying assumptions, [5–7]. Standard symbolic notation is used throughout the paper with tensors denoted by boldface characters.

2. Physical motivation

The results of metallographic observations reveal that in heavily deformed metals or even at small strains, if they are preceded by the change of deformation path, a multiscale hierarchy of shear localization modes progressively replaces the crystallographic multiple slip or twinning. Different terminology is used depending on the level of observation. In our study, the term "micro-shear band" is understood as a long and very thin (of order 0.1 μm) sheet-like region of concentrated plastic shear, crossing grain boundaries without deviation and forming a definite pattern in relation to the principal directions of strain. It bears very large shear strains and can lie in a "non-crystallographic" position. The term "non-crystallographic" means that micro-shear bands are usually not parallel to a particular, densely packed crystallographic plane, of conventionally possible active slip system in the crystallites they intersect. This change of deformation mode contributes to the development of strain-induced anisotropy and modifies remarkably the material properties. The experimental information about mechanical behaviour and related structural features is reviewed, e.g. in [6, 8 and 9], where comprehensive lists of references are given. The experimental observations show that micro-shear bands, formed e.g. in rolling, are usually inclined by about $\pm 35°$ to the rolling plane and are orthogonal to the specimen lateral face, although there can be considerable deviations from this value within the 15° to 50° range, cf. [8] and [9].

3. Macroscopic averaging and continuum mechanics description in plasticity of metals

The physical constraint on any continuum mechanics approach to metal plasticity, i.e. the physical dimension of the smallest representative volume element (RVE) of crystalline material for which it is possible to define significant overall measures of stress and strain during plastic deformation, was thoroughly discussed by HILL [10–13] and HAVNER [14–16]. According to [10], p. 8: "... the

http://rcin.org.pl

dimensions must be large compared with the thickness of the glide packets separating the active glide lamellae (generally of order 10^{-4} cm in many metals at ordinary temperatures). Thus, the linear dimension of the smallest crystal whose behaviour can legitimately be considered from the standpoint of the theory of plasticity is probably of order 10^{-3} cm." On the other hand, HAVNER [14–16] argues that, to an observer who can resolve distances to 1 μm, the deformation of crystal grains (with the mean grain diameter of order 100 μm) within plastically deformed metal polycrystals is relatively smooth. At such a scale of observation, called microscopic level, one can just distinguish between slip lines on crystal surfaces. This slip lines appear on the submicroscopic level as slip line bundles and slip bands of the order of 0.1 μm width, containing numerous glide lamellae between which amounts of slip as great as 10^3 lattice spacings have occurred. Therefore, the minimum dimension of the RVE in the continuum microscopic description of elastic-plastic deformations of crystalline solids is taken in [14] to be of the order of 1 μm, i.e. $> 10^3$ lattice spacings. Consequently, the linear dimension of the RVE corresponding to the macroscopic level is often assumed to be of the order of several millimeters, for moderately fine-grained metals, e.g. in [15] the macro-element is assumed as a polycrystalline unit cube having the unit linear dimension $L_0 \approx 1$ mm. This discussion is valid under the general assumption that the dominant mechanism of inelastic behaviour is crystallographic slip. In such a case, the theory describing kinematics and constitutive structure of finite elastic-plastic deformations of crystalline solids is well established and the transition between the microscopic and macroscopic levels is well understood (cf. e.g. HILL [11–13], HAVNER [14–16] and MANDEL [17–18], as well as, HILL and RICE [19], PETRYK [20] and STOLZ [21]). In particular, relations between macro-measures of stress, strain and plastic work are related with the volume averages of their micro-measures. It has also been shown that certain structural features of the constitutive relations, as the normality rule or certain constitutive inequalities, are transmitted upwards through a hierarchy of observational levels unchanged, irrespective of the heterogeneity, no matter what is its origin (cf. HILL [22]).

In the averaging procedure, discussed in [11–20], quasi-static deformation processes with negligible body forces are typically assumed. This means that within the reference volume V_0 of the macroscopic RVE (macro-element), the nominal stress field $\mathbf{s}_m$, representing micro-stresses, and their rates $\dot{\mathbf{s}}_m$ are self-equilibrated

$$\text{Div}\mathbf{s}_m = 0, \qquad \text{Div}\dot{\mathbf{s}}_m = 0 \quad \text{in} \quad V_0 \tag{3.1}$$

and with boundary conditions

$$\boldsymbol{\nu}_0\mathbf{s}_m = \mathbf{t}_\nu, \qquad \boldsymbol{\nu}_0\dot{\mathbf{s}}_m = \dot{\mathbf{t}}_\nu \quad \text{on} \quad \partial V_0, \tag{3.2}$$

where $\boldsymbol{\nu}_0$ is the externally directed unit vector normal to the reference volume at a point on its boundary ∂V_0. The averaging procedure and micro-to-macro transition, studied within the framework of finite strain theory by HILL [11–13] and

http://rcin.org.pl

HAVNER [14–16] lead, in particular, to the following relations for the macroscopic measures of the deformation gradient $\mathbf{F}$ and its rate $\dot{\mathbf{F}}$, which are expressed, with use of Gauss' theorem (divergence theorem), by means of the surface data

$$\mathbf{F} \equiv \{\mathbf{f}\} = \frac{1}{V_0}\int_{V_0} \mathrm{Grad}\boldsymbol{\chi}_m \, dV_0 = \frac{1}{V_0}\int_{\partial V_0} \mathbf{x}_m \otimes \boldsymbol{\nu}_0 \, dA_0 , \tag{3.3}$$

$$\dot{\mathbf{F}} \equiv \{\dot{\mathbf{f}}\} = \frac{1}{V_0}\int_{V_0} \mathrm{Grad}\dot{\boldsymbol{\chi}}_m \, dV_0 = \frac{1}{V_0}\int_{\partial V_0} \dot{\boldsymbol{\chi}}_m \otimes \boldsymbol{\nu}_0 \, dA_0 . \tag{3.4}$$

Here the symbol $\boldsymbol{\chi}_m$ denotes a microscopic field of motion of the material point $\mathbf{X}_m$ in the reference configuration of the RVE into its current position $\mathbf{x}_m$

$$\mathbf{x}_m = \boldsymbol{\chi}_m(\mathbf{X}_m, t), \tag{3.5}$$

and the microscopic velocity $\mathbf{v}_m$ is determined in the current configuration

$$\mathbf{v}_m = \mathbf{v}_m(\mathbf{x}_m, t) = \mathbf{v}_m(\boldsymbol{\chi}_m(\mathbf{X}_m, t), t) \equiv \dot{\boldsymbol{\chi}}_m(\mathbf{X}_m, t). \tag{3.6}$$

The Gauss theorem applied above, was specified for any vector field $\mathbf{w} = \mathbf{w}(\mathbf{X}_m)$ defined on the closure $\overline{V}_0 = V_0 \cup \partial V_0$ and being of class $C^0(\overline{V}_0)$ and piecewise of class $C^1(V_0)$, so that $\mathbf{w}$ is continuous on the closure $\overline{V}_0$ and piecewise continuously differentiable on V_0 (cf. e.g. SMITH [23]). Similarly, the following relations for the macroscopic measures of the suitably smooth tensor field of nominal stress $\mathbf{S}$

$$\mathbf{S} \equiv \{\mathbf{s}_m\} = \frac{1}{V_0}\int_{V_0} \mathbf{s}_m \, dV_0 = \frac{1}{V_0}\int_{\partial V_0} \mathbf{X} \otimes \mathbf{t}_\nu \, dA_0 , \tag{3.7}$$

its rate $\dot{\mathbf{S}}$

$$\dot{\mathbf{S}} \equiv \{\dot{\mathbf{s}}_m\} = \frac{1}{V_0}\int_{V_0} \dot{\mathbf{s}}_m \, dV_0 = \frac{1}{V_0}\int_{\partial V_0} \mathbf{X} \otimes \dot{\mathbf{t}}_\nu \, dA_0 \tag{3.8}$$

and the Kirchhoff stress $\boldsymbol{\tau}$

$$\boldsymbol{\tau} \equiv \{\boldsymbol{\tau}_m\} = \{\mathbf{f}\mathbf{s}_m\} = \frac{1}{V_0}\int_{\partial V_0} \mathbf{x} \otimes \mathbf{t}_\nu \, dA_0 \tag{3.9}$$

can be obtained by application of Gauss' theorem and (3.1), cf. [11].

http://rcin.org.pl

4. Basic kinematical relations

In plasticity of single crystals, it is usually assumed that dislocations traversing a volume element produce a change of its shape, but they do not change its lattice orientation. This leads to the fundamental assumption in elastoplasticity models for metals, which says that distinction should be made between kinematics of the continuum and kinematics of the underlying crystallographic structure. The macroscopic counterpart of such a situation in finite deformation plasticity of polycrystals is Mandel's concept of the intermediate, relaxed, configuration, called isoclinic one, in which the chosen director triad preserves always the same orientation with respect to the fixed axes of the laboratory reference frame. In such a case, we can understand that the director vectors are introduced as a tool to monitor at any instant the state of the strain-induced anisotropy. Different visualizations of such a triad are discussed e.g. in [17], and [24–29], where more detailed discussion and further references can be found. The assumption that the continuum is endowed with the structure in the form of the director vectors leads to the concepts of the local, relaxed, intermediate isoclinic configurations, plastic spin and structure corotational rate. Due to this, the decomposition of the deformation gradient $\mathbf{F}$ becomes unique, [17]

$$\mathbf{F} = \mathbf{E}\,\mathbf{P}, \tag{4.1}$$

where $\mathbf{E}$ denotes the elastic transformation from the intermediate isoclinic configuration to the current one, and $\mathbf{P}$ is the plastic transformation from the reference configuration to the isoclinic one. The following basic kinematical relations hold:

$$\mathbf{L} = \dot{\mathbf{E}}\mathbf{E}^{-1} + \mathbf{E}\dot{\mathbf{P}}\mathbf{P}^{-1}\mathbf{E}^{-1}, \qquad \mathbf{L} = \mathbf{D} + \mathbf{W}, \tag{4.2}$$

$$\mathbf{D} = \mathbf{D}^e + \mathbf{D}^p, \qquad \mathbf{W} = \mathbf{W}^e + \mathbf{W}^p, \tag{4.3}$$

$$\mathbf{D}^e = \{\dot{\mathbf{E}}\mathbf{E}^{-1}\}_s, \qquad \mathbf{D}^p = \{\mathbf{E}\dot{\mathbf{P}}\mathbf{P}^{-1}\mathbf{E}^{-1}\}_s, \tag{4.4}$$

$$\mathbf{W}^e = \{\dot{\mathbf{E}}\mathbf{E}^{-1}\}_a, \qquad \mathbf{W}^p = \{\mathbf{E}\dot{\mathbf{P}}\mathbf{P}^{-1}\mathbf{E}^{-1}\}_a, \tag{4.5}$$

where $\mathbf{L} = \dot{\mathbf{F}}\mathbf{F}^{-1}$ is the velocity gradient, $\mathbf{D}$ and $\mathbf{W}$ correspond to the rate of deformation and material spin, respectively, and the superscripts e and p refer to elastic and plastic states, whereas the symbols $\{\mathbf{t}\}_s$ and $\{\mathbf{t}\}_a$ denote the symmetric and skew-symmetric parts of the second-order tensor $\mathbf{t}$. A similar decomposition, such as in (4.1), was proposed earlier by LEE [30] within the context of finite elastic-plastic deformation of continuous body, without explicit definition of a structure or director vectors and isoclinic configuration. Such an approach is completely different from that presented above and can be considered as an alternative to the plasticity theory of structured solids.

http://rcin.org.pl

5. Physical model of shear strain rate produced by active micro-shear bands

Consider certain RVE containing the region of progressive shear banding, depicted schematically in Fig. 1 a, where the traces of successive clusters of micro-shear bands are shown. The arrow points to the direction of expansion of the region. According to the results of experimental observations presented in [8–9] and [31], an active shear band consists of the clusters of micro-shear bands of

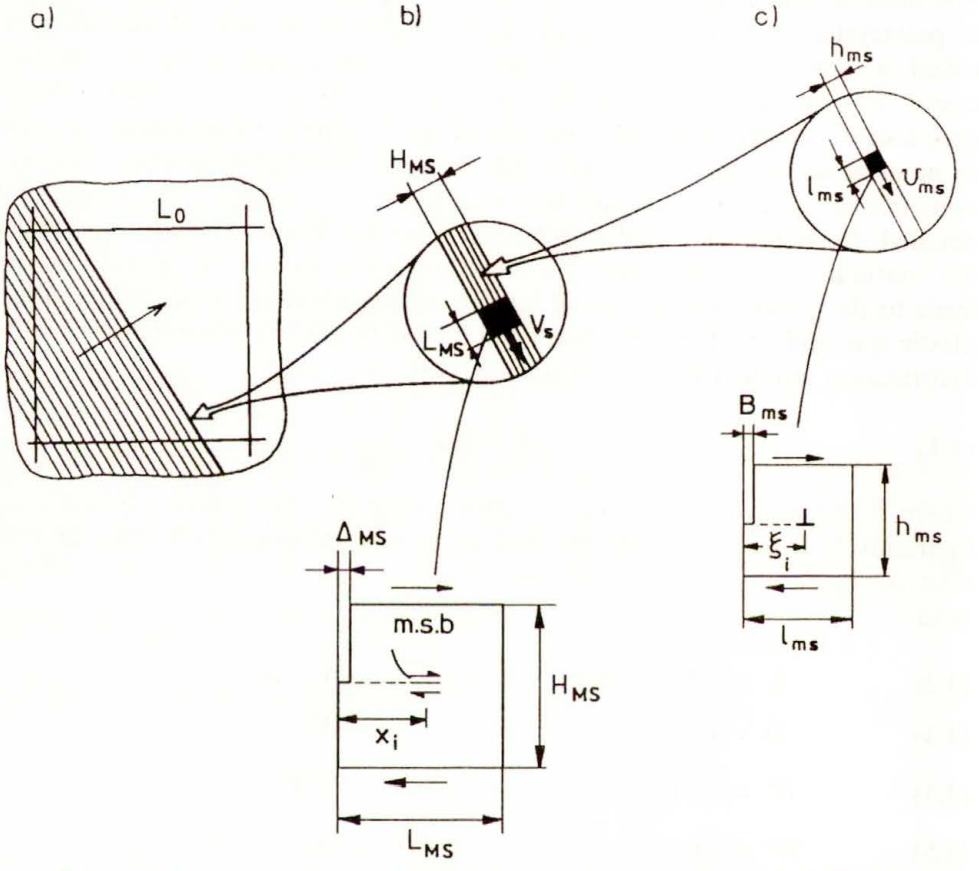

FIG. 1. Schematic illustration of the multiscale, hierarchically organized system of shear banding: a) The section of the unit cube of the RVE, having the dimension $L_0 \approx 1\,\text{mm}$, traversed by the region of shear banding progressing in the direction pointed by the arrow. b) The cluster of active micro-shear bands with the active zone of the thickness $H_{MS} \approx (10 \div 100)\mu\text{m}$ and the width L_{MS} being of the same order. Beneath, the fundamental mechanism of plastic shear strain generated by the active micro-shear bands (m.s.b.), which operate within the active zone, moving along the distances x_i, $i = 1, 2, 3, ..., N_{MS}$, during their "lifetime", and produce the total displacement Δ_{MS} of the top of the active zone relative to the bottom, is depicted. c) The active zone of a single micro-shear band of the thickness $h_{ms} \approx 0.1\mu\text{m}$ and the width l_{ms} of the same order. Below, the picture of an elementary dislocation model of plastic shear in the active zone is shown. The displacement B_{ms} of the top of the active zone with respect to the bottom is produced by n dislocations moving at the distances ξ_i, $i = 1, 2, 3, ..., n$.

http://rcin.org.pl

the thickness of order $(10 \div 100)\,\mu$m, which at this level of observation can be considered as elementary carriers of plastic strain. On the other hand, an active micro-shear band is produced as the effect of spatial and time organization of large number of dislocations, which generate and move collectively within a long and thin sheet-like regions, crossing grain boundaries without deviation and having the thickness of order $0.1\,\mu$m. Therefore, from the point of view of kinematics, the micro-shear band can be considered as a thin region of concentrated plastic shear. During the passage of the active zone, of thickness h_{ms} and width l_{ms}, the local perturbation, B_{ms}, of the microscopic displacement field is produced which travels at the head of the micro-shear band with the speed v_{ms} as a distortion wave, cf. Fig. 1 c. According to [31], l_{ms} can be interpreted as the mean diameter of the dislocation islands observed on TEM micrographs. Therefore, one can assume that approximately $l_{ms} \approx h_{ms}$. According to the discussion in [32], the width l_{ms} corresponds also to the dimension of the range of stress pulse produced by dynamic pile-up of a group of dislocations, which is necessary for the transmission process through the grain boundary and activation of a micro-shear band. In Fig. 1, two successive "magnifications" of the shear banding area are "zoomed in" and the related fundamental mechanisms of plastic shear are illustrated. The first one, depicted in Fig. 1 b, corresponds to the cluster of micro-shear bands, having the active zone of thickness H_{MS} and the width L_{MS}, in which the passage of large number of active micro-shear bands results in the local perturbation, Δ_{MS}, of the microscopic displacement field $\mathbf{u}_m = \mathbf{x}_m - \mathbf{X}_m$, which moves with the speed V_s. The second "magnification", shown in Fig. 1 c, represents the aforementioned active zone of a single micro-shear band.

Consider an elementary dislocation model of plastic shear produced in the active zone at the head of a single micro-shear band, as it is depicted in Fig. 1 c. According to the known approach, the shear strain results from the generation and movement of large number of dislocations through the active zone, (cf. GILMAN [33] and DIETER [34]), and the following relations hold

$$\delta_i = \frac{\xi_i b}{l_{ms}}, \qquad B_{ms} = \sum_i^n \delta_i = \frac{b}{l_{ms}} \sum_i^n \xi_i, \tag{5.1}$$

where δ_i is the displacement of the i-th dislocation at an intermediate position between $\xi_i = 0$ and $\xi_i = l_{ms}$, whereas B_{ms} corresponds, according to Fig. 1 c, to the displacement of the top of the active zone relative to the bottom for n dislocations. The corresponding shear strain γ reads

$$\gamma = \frac{B_{ms}}{h_{ms}} = \frac{b\,n}{l_{ms} h_{ms}} \overline{\xi}, \qquad \overline{\xi} = \frac{\sum_i^n \xi_i}{n}, \tag{5.2}$$

where $\overline{\xi}$ is the average distance that dislocations have moved. Assuming that the distance $\overline{\xi}$ and the number of dislocations n can change with the variable τ,

http://rcin.org.pl

corresponding to the duration of the microscopic process of plastic shear, the pertinent shear strain rate can be calculated

$$\frac{d\gamma}{d\tau} = \frac{b}{l_{ms}h_{ms}}\left(n\,v_d + \overline{\xi}\frac{dn}{d\tau}\right), \tag{5.3}$$

where

$$v_d = \frac{d\overline{\xi}}{d\tau} \tag{5.4}$$

is the average dislocation velocity. Finally, the shear strain rate, produced in a singular micro-shear band, can be expressed in terms of the speed v_{ms} of the head of micro-shear band

$$\frac{d\gamma}{d\tau} = \frac{v_{ms}}{h_{ms}}, \qquad v_{ms} = \frac{b}{l_{ms}}\left(n\,v_d + \overline{\xi}\frac{dn}{d\tau}\right). \tag{5.5}$$

According to (5.3), generation and movement of new dislocations contribute to the plastic strain rate. If we assume that the movement of a constant number of mobile dislocations plays the prevalent role, (5.3) transforms into the well known Orowan relation

$$\frac{d\gamma}{d\tau} = b\,\varrho\,v_d, \qquad \varrho = \frac{n}{l_{ms}h_{ms}}, \tag{5.6}$$

where ϱ denotes the dislocation density. In the case of micro-shear bands propagation, the systems which are not necessarily parallel to densely packed crystallographic planes are activated. The critical stress in such planes is very high and therefore, the generation of new dislocations may contribute remarkably to plastic shear strain rate. In such a case relation (5.5) seems to be justified. It is, however, difficult to follow experimentally the interplay of both the mechanisms of generation and movement of dislocations to provide a unique assessment of their contribution to the plastic strain rate (cf. e.g. KORBEL [35]).

Consider a certain number of active micro-shear bands N_{MS} of similar orientation and produced within certain time period, $\overline{\tau} = \tau_f - \tau_i$, which can be considered as an infinitesimal increment, Δt, of "time-like parameter" in the macroscopic description. As it is depicted schematically in Fig. 1 b, such a system (cluster) of micro-shear bands produces the microscopic shear strain γ_{ms}, which is given by the following relation

$$\gamma_{ms} = \frac{\Delta_{MS}}{H_{MS}}, \qquad \Delta_{MS} = \frac{\overline{B}_{ms}N_{MS}}{L_{MS}}\overline{x}_{MS}, \tag{5.7}$$

where $\overline{B}_{ms}$ is the total displacement produced by a single micro-shear band

$$\overline{B}_{ms} = h_{ms}\overline{\gamma} = \int_{\tau_i}^{\tau_f} v_{ms}\,d\tau, \tag{5.8}$$

http://rcin.org.pl

and

$$\overline{x}_{MS} = \frac{\sum_{i}^{n} x_i}{n}, \qquad n \equiv N_{MS}, \tag{5.9}$$

denotes the average distance that N_{MS} micro-shear bands have moved, during their "lifetime", in the active zone. Assuming that the distance $\overline{x}_{MS}$ and the number of active micro-shear bands N_{MS} can change during propagation of the active zone of the cluster, we have from (5.7)

$$\dot{\gamma}_{ms} = \frac{\overline{B}_{ms}}{L_{MS} H_{MS}} \left(N_{MS} \dot{\overline{x}}_{MS} + \overline{x}_{MS} \dot{N}_{MS} \right), \tag{5.10}$$

where the dot denotes differentiation with respect to the "time-like parameter" t. Let us observe that the rate $\dot{\overline{x}}_{MS}$ can be identified with the speed v_{ms} of the head of a single micro-shear band, $\dot{\overline{x}}_{MS} \equiv v_{ms}$, under the simplifying assumption that v_{ms} is approximately the same for each micro-shear band in the active zone of the cluster. Then, the speed of propagation of the disturbance of the microscopic displacement field, V_S, produced in the active zone of the cluster of N_{MS} active micro-shear bands, is given by

$$V_S = \frac{\overline{B}_{ms}}{L_{MS}} \left(N_{MS} v_{ms} + \overline{x}_{MS} \dot{N}_{MS} \right), \tag{5.11}$$

and the shear strain rate reads

$$\dot{\gamma}_{ms} = \frac{V_S}{H_{MS}}. \tag{5.12}$$

If the number of active micro-shear bands in the active zone can be assumed constant, the relation for the speed V_S is given by

$$V_S = \frac{\overline{B}_{ms}}{L_{MS}} N_{MS} v_{ms} \tag{5.13}$$

and (5.12) takes the form, which is formally similar to the Orowan relation (5.6)

$$\dot{\gamma}_{ms} = \overline{B}_{ms} \varrho_{MS} v_{ms}, \qquad \varrho_{MS} = \frac{N_{MS}}{L_{MS} H_{MS}}, \tag{5.14}$$

where ϱ_{MS} corresponds to the active micro-shear bands density. It is a matter of further investigations upon the evolution of clusters of micro-shear bands to confirm the usefulness of this hypothesis.

http://rcin.org.pl

The experimental observations and certain analogy with martensitic transformations, lead to the hypothesis that micro-shear bands propagate with the veloeity v_{ms} of constant value, which is close to the shear wave speed c_s (velocity of sound) in the considered metal or alloy. Thus, the following relation is physically justified

$$v_{ms} = \eta\, c_s = \eta \left(\frac{\mu}{\varrho}\right)^{1/2}, \qquad \eta \in (0,1), \tag{5.15}$$

where η corresponds to the factor accounting for the effect of dissipation related with nucleation and movement of dislocations in the activated systems. The value of η can be determined, at least theoretically, from $(5.5)_2$. However, it is difficult to evaluate experimentally, in a consistent way, all the structural parameters occurring in $(5.5)_2$. Therefore, the direct measurements of v_{ms} seem to be more appropriate. For instance, the results of shear band speed measurements in $C-300$ steel (a high strength maraging steel) have been reported recently by ZHOU *et al.* [36]. The highest speed observed is close to $1200\,\mathrm{ms}^{-1}$, i.e. approximately 40% of the shear wave speed c_s of the specimen material. This gives the estimate of $\eta \approx 0.40$. The investigated shear bands correspond to the clusters of micro-shear bands. According to (5.13), the speed of a single micro-shear band should be much higher, what will produce also higher value of η. The complementary evaluation of structural parameters, $\overline{B}_{ms}$, L_{MS} and N_{MS}, of the investigated shear bands is necessary to obtain more exact specification of η.

6. System of active micro-shear bands as a surface of strong discontinuity

The foregoing discussion of physical nature of micro-shear banding process, as well as the recent results of the microscopic observations *in situ*, presented by YANG and REY [37] and REY *et al.* [38], support the following hypothesis:

The passage of micro-shear bands within the active zone of the cluster, results in the perturbation of the microscopic displacement field travelling with the speed V_s, which produces a discontinuity of the microscopic velocity field in the RVE it traverses. The progression of clusters of micro-shear bands can be idealized mathematically by means of a singular surface of order one propagating through the macro-element (RVE) of the continuum.

The necessary mathematical formalism of the theory of propagating singular surfaces is given, e.g. by TRUESDELL and TOUPIN [39], ERINGEN and SUHUBI [40] and KOSIŃSKI [41]. The theory allows to identify the postulated discontinuity surface of the microscopic velocity field $\mathbf{v}_m$ in RVE as a singular surface $\Sigma(t)$ moving in the region V_0 of the reference configuration of the body, where for each instant of "time-like parameter" $t \in I \subset R$, the surface $\Sigma(t) \subset V_0$ has the dual counterpart $S(t) \subset V$, in the spatial configuration. There exists the jump

http://rcin.org.pl

discontinuity of derivatives of the function of motion χ_m, i.e. of the microscopic velocity field $[\![\dot{\chi}_m]\!] \neq \mathbf{0}$ and the deformation gradient $[\![\mathbf{f}]\!] \neq \mathbf{0}$, which are assumed to be smooth in each point of $V_0 \times I$ outside the discontinuity surface:

$$[\![\dot{\chi}_m]\!] = \dot{\chi}_m^+ - \dot{\chi}_m^- \neq 0, \qquad [\![\mathbf{f}]\!] = \mathbf{f}^+ - \mathbf{f}^- \neq 0. \tag{6.1}$$

According to [39] and [41], the considered surface of strong discontinuity of microscopic velocity field fulfills the properties of a vortex sheet with the jump discontinuity of the first derivatives of χ_m given by

$$[\![\mathbf{v}]\!] = V_S \boldsymbol{s}, \qquad [\![\mathbf{f}]\!] = -\frac{V_S}{U} \boldsymbol{s} \otimes \boldsymbol{n}\,\mathbf{f}, \qquad \text{for} \quad U \neq 0, \tag{6.2}$$

where $\boldsymbol{s}$ and $\boldsymbol{n}$ are, respectively, the unit tangent and the unit normal vectors to the discontinuity surface $S(t)$, while U corresponds to the local intrinsic speed of propoagation of $S(t)$, (cf. [39], p. 508). Similarly, for the material counterpart of a singular surface $\Sigma(t)$, the compatibility relations take the form

$$[\![\dot{\chi}_m]\!] = V_S \boldsymbol{s}, \qquad [\![\mathbf{f}]\!] = -\frac{V_S}{U_N} \boldsymbol{s} \otimes \boldsymbol{N} \qquad \text{for} \quad U_N \neq 0, \tag{6.3}$$

where $\boldsymbol{N}$ is the unit vector normal to the discontinuity surface $\Sigma(t)$ and U_N is the normal component of the surface velocity (cf. [40], p. 96).

7. Problem of macroscopic averaging and continuum mechanics description of micro-shear banding

Application of the generalized form of Gauss' theorem for the gradient of the microscopic velocity field $\dot{\chi}_m$, which is sufficiently smooth in each point of $V_0 \times I$ except the singular surface, where the discussed jump discontinuity $[\![\dot{\chi}_m]\!]$ appears, leads to (cf. e.g. [41], p. 68 or [42], p. 427)

$$\int_{V_0} \operatorname{Grad} \dot{\chi}_m \, dV_0 = \int_{\partial V_0 - \Sigma(t)} \dot{\chi}_m \otimes \boldsymbol{\nu}_0 \, dA_0 - \int_{\Sigma(t)} [\![\dot{\chi}_m]\!] \otimes \boldsymbol{N} \, dA_0 . \tag{7.1}$$

Due to (7.1), the averaging procedure (3.4) of the microscopic velocity field $\dot{\chi}_m$ over the macro-element V_0 can be generalized to the macroscopic RVE traversed by a singular surface of order one. The macroscopic measure of the deformation gradient $\mathbf{F}$ and its rate $\dot{\mathbf{F}}$ are expressed by means of surface data in the following way

$$\mathbf{F} \equiv \frac{1}{V_0} \int_{\partial V_0 - \Sigma(t)} \mathbf{x}_m \otimes \boldsymbol{\nu}_0 \, dA_0 , \tag{7.2}$$

http://rcin.org.pl

where according to (3.3) $\mathbf{F} = \mathbf{F}$, and

$$\dot{\mathbf{F}} \equiv \frac{1}{V_0} \int\limits_{\partial V_0 - \Sigma(t)} \boldsymbol{\chi}_m \otimes \boldsymbol{\nu}_0 \, dA_0 = \frac{1}{V_0} \int\limits_{V_0} \mathrm{Grad}\dot{\boldsymbol{\chi}}_m \, dV_0 + \frac{1}{V_0} \int\limits_{\Sigma(t)} [\![\dot{\boldsymbol{\chi}}_m]\!] \otimes \boldsymbol{N} \, dA_0 . \tag{7.3}$$

Similarly, application of the generalized form of Gauss' theorem for the stress field $\mathbf{s}_m$ over the macro-element V_0 with the singular surface, gives the formula for the average nominal stress

$$\mathbf{F} \equiv \frac{1}{V_0} \int\limits_{\partial V_0 - \Sigma(t)} \mathbf{X}_m \otimes \mathbf{t}_\nu \, dA_0 = \frac{1}{V_0} \int\limits_{V_0} \mathbf{s}_m \, dV_0 + \frac{1}{V_0} \int\limits_{\Sigma(t)} \boldsymbol{\xi} \otimes [\![\mathbf{t}_N]\!] \, dA_0 , \tag{7.4}$$

where

$$\mathbf{t}_N = \boldsymbol{N}\, \mathbf{s}_m(\boldsymbol{\xi}), \qquad \boldsymbol{\xi} \in \Sigma(t). \tag{7.5}$$

The dynamical compatibility condition for the jump of the tractions $[\![\mathbf{t}_N]\!]$ across the singular surface in the reference configuration $\Sigma(t)$ takes the form (cf. e.g. [40], p. 34)

$$\boldsymbol{N}[\![\mathbf{s}_m]\!] = -\varrho U_N [\![\dot{\boldsymbol{\chi}}_m]\!]. \tag{7.6}$$

Let us consider the processes in which the jump of inertia forces across the singular surface is negligible. This corresponds to the situation, in which the movement of the singular surface, being the mathematical idealization of the progressing shear banding zone, is approximated by a quasi-static process. In such a case $U_N = 0$ and the jump in the tractions, $[\![\mathbf{t}_N]\!]$, must vanish to ensure the equilibrium condition, what results in vanishing of the integral over $\Sigma(t)$ in (7.4) and restores the classical averaging formula (3.7) (cf. NEMAT-NASSER and HORI [43], p. 37).

Assuming that the singular surface of order one has the properties of the vortex sheet with the velocity jump of magnitude V_S, and accounting in (7.3) for $(6.3)_1$, we obtain

$$\dot{\mathbf{F}} = \frac{1}{V_0} \int\limits_{V_0} \mathrm{Grad}\dot{\boldsymbol{\chi}}_m \, dV_0 + \frac{1}{V_0} \int\limits_{\Sigma(t)} V_S \boldsymbol{s} \otimes \boldsymbol{N} \, dA_0 . \tag{7.8}$$

If we choose the current configuration of RVE, at time t, as the reference one, the rate of deformation gradient $\dot{\mathbf{F}}$ becomes then the rate of relative deformation

http://rcin.org.pl

gradient, $\dot{\mathbf{F}}_{(t)}(t)$, at time t (cf. [44], p.54) and the averaging formula (7.8) will take the following spatial form:

$$\mathbf{L} \equiv \frac{1}{V} \int_{\partial V - S(t)} \mathbf{v}_m \otimes \boldsymbol{\nu}\, dA = \frac{1}{V} \int_V \operatorname{grad} \mathbf{v}_m\, dV + \frac{1}{V} \int_{S(t)} V_S \boldsymbol{s} \otimes \boldsymbol{n}\, dA, \tag{7.9}$$

where $\mathbf{L}$ denotes the macroscopic measure of velocity gradient $\mathbf{L} \equiv \dot{\mathbf{F}}_{(t)}(t) = \dot{\mathbf{F}}(t)\mathbf{F}^{-1}(t)$, averaged over the macro-element V traversed by the vortex sheet $S(t)$.

The averaging formula (7.9) enables us to account for the contribution of micro-shear banding in the macroscopic measure of velocity gradient produced at finite elastic-plastic strain. According to (7.9), the velocity gradient $\mathbf{L}$ is decomposed as follows:

$$\mathbf{L} = \mathbf{L} + \mathbf{L}_{MS}, \qquad \mathbf{L}_{MS} = \frac{1}{V} \int_{S(t)} V_S \boldsymbol{s} \otimes \boldsymbol{n}\, dA. \tag{7.10}$$

Assuming that the singular surface $S(t)$ forms a plane traversing volume V, with the unit vectors $\boldsymbol{s}$ and $\boldsymbol{n}$ held constant, $(7.10)_2$ results in

$$\mathbf{L}_{MS} = \dot{\gamma}_{MS} \boldsymbol{s} \otimes \boldsymbol{n}, \tag{7.11}$$

where the macroscopic shear strain rate $\dot{\gamma}_{MS}$ is determined, according to (5.11) and (5.12), by the microscopic variables as an average over the RVE

$$\dot{\gamma}_{MS} = \frac{1}{V} \int_{S(t)} H_{MS} \dot{\gamma}_{ms}\, dA = \frac{1}{V} \int_{S(t)} \frac{B_{ms}}{L_{MS}} \left(N_{MS} v_{ms} + \bar{x}_{MS} \dot{N}_{MS} \right) dA. \tag{7.12}$$

Further experimental and theoretical studies are necessary to identify the structural variables appearing in (7.12) and to prepare more workable formula for the macroscopic shear strain rate produced by micro-shear banding. For instance, the following simplification could be verified. Consider the situation, when the number of the micro-shear bands N_{MS} operating in the active zone does not change much during the deformation process. Then, according to (5.14) and (5.15), the relation (7.12) takes the form

$$\dot{\gamma}_{MS} = \frac{1}{V} \int_{S(t)} H_{MS} \dot{\gamma}_{ms}\, dA = \frac{\eta c_s}{V} \int_{S(t)} H_{MS} B_{ms} \varrho_{MS}\, dA. \tag{7.13}$$

For the RVE being the unit cube of the dimension L_0, (7.13) reads

$$\dot{\gamma}_{MS} = \eta \frac{B_{ms} N_{MS}}{L_0 L_{MS}} c_s = \eta \frac{B_{ms}}{n_{SB} D_{SB} d_{MS}} c_s, \tag{7.14}$$

http://rcin.org.pl

where n_{SB} is the number of the clusters of micro-shear bands in the RVE, and D_{SB} is the mean distance between them, so that $L_0 = n_{SB}D_{SB}$, while d_{MS} is the mean distance between micro-shear bands in the cluster of the thickness $H_{MS} = N_{MS}d_{MS}$, under the assumption that $L_{MS} \approx H_{MS}$ (cf. Fig. 1).

The derived relations (7.12)–(7.14) are valid for a single system of micro-shear bands. This can be generalized for the case of a double shearing system

$$\mathbf{L} = \mathbf{L}_1 + \sum_{i=1}^{2} \dot{\gamma}_{MS}^{(i)} \boldsymbol{s}^{(i)} \otimes \boldsymbol{n}^{(i)}, \tag{7.15}$$

where $\dot{\gamma}_{MS}^{(i)}$ is the macroscopic shear strain rate and $\boldsymbol{s}^{(i)}$, $\boldsymbol{n}^{(i)}$ are the respective unit vectors of the i-th shearing system. It is worthy to note, that (7.15) is valid under the assumption that the active micro-shear bands in both systems operate in the time period, which can be considered as an infinitesimal increment of "time-like parameter" in the macroscopic description. Otherwise, the sequence of events should be taken into considerations. The above relations provide the following macroscopic measures of the rate of plastic deformations and plastic spin produced by active micro-shear bands

$$\mathbf{D}_{MS}^{p} = \frac{1}{2}(\mathbf{L}_{MS} + \mathbf{L}_{MS}^{T}), \qquad \mathbf{W}_{MS}^{p} = \frac{1}{2}(\mathbf{L}_{MS} - \mathbf{L}_{MS}^{T}). \tag{7.16}$$

The discussed averaging procedure over the RVE with the singular surface allows us to account for the characteristic geometric pattern of micro-shear bands which is transmitted upwards through a multiscale hierarchy of observational levels.

8. Concluding remarks

To capture the gross effects of active micro-shear bands, the simplified approach based on the mode of plane deformation of rigid-plastic solid was applied in [5–6]. The contribution of the mechanism of crystallographic multiple slip was approximated by the classical J_2 flow law and the contribution of active micro-shear bands was idealized by means of an additional double-shearing system. This resulted in the additive composition of the rates of plastic deformations as a combination of two modes of pure shear in the plane of plastic flow. The assessment of possible incorporation of the rate equations of plastic flow into an elastic-plastic material model was discussed in [6] and [7]. The approximate description of infinitesimally small elastic strains and large plastic deformations accounting for macroscopic effects of micro-shear banding was proposed in [45–47]. The derivation of the macroscopic measure of the velocity gradient $\mathbf{L}$ given in (7.9) and its additive decomposition $(7.10)_1$ makes it possible to formulate in a more rigorous manner the constitutive equations of elastoplasticity with

http://rcin.org.pl

an account of micro-shear banding. Due to (4.1)–(4.3), $(7.10)_1$ and (7.16), the following kinematical relations hold

$$\begin{aligned} \mathbf{D} &= \mathbf{D}^e + \mathbf{D}^p = \mathbf{D}^e + \mathbf{D}^p_S + \mathbf{D}^p_{MS}, \\ \mathbf{W} &= \mathbf{W}^e + \mathbf{W}^p = \mathbf{W}^e + \mathbf{W}^p_S + \mathbf{W}^p_{MS}, \end{aligned} \tag{8.1}$$

where $\mathbf{D}^p_S$ and $\mathbf{W}^p_S$ correspond, respectively, to the rate of plastic deformation and plastic spin produced by crystallographic multiple slip. The application of the aforementioned relations for constitutive modelling of elastic-plastic behaviour of metallic solids is presented in [47].

This work is focused mainly on the question how the effects of characteristic geometric pattern of micro-shear bands can be transmitted to the macroscopic level and included into the kinematics of finite elasto-plastic strains. Nevertheless, the kinetics of micro-shear banding phenomena with the related dynamic conditions on the strong discontinuity surface (7.6) and the pertinent micro-to-macro transition analysis is also very important. The results obtained by RANIECKI and TANAKA [48] within the context of continuum mechanics description of martensitic phase transformations, with use of the concepts of a surface of strong discontinuity and thermodynamical driving force, provide useful analogies. Further studies are necessary to shed more light on these problems. In particular, the possibility of application of the idea of thermodynamical driving force for the formulation of the criterion of micro-shear band formation deserves further examining.

A fundamental role in the rigorous analysis of the linkages between basic properties at two levels of description of elastic-plastic solids plays the theorem of product averages, which was studied in a general form by HILL [13]. The comprehensive bibliography of earlier papers, confined to small strains, is discussed in the work of NEMAT–NASSER and HORI [44]. The problem of extension of this theorem to the RVE, which is traversed by a propagating strong discontinuity surface, requires further studies.

Acknowledgment

This work was supported by the Committee for Research (KBN) Poland, under the project No. 7 T07A 017 08. The author is indebted to Prof. W. KOSIŃSKI for his critical comments after reading of the manuscript. Also discussions with Prof. H. PETRYK, in particular on the physical model and the averaging procedure, are greatly appreciated.

References

1. T.Y. THOMAS, *Plastic flow and fracture in solids*, Academic Press, New York and London 1961.
2. K.C. VALANIS, *Banding and stability in plastic materials*, Acta Mech., **79**, 113–141, 1989.
3. X.M. SU, *Localized banding with strong velocity jumps*, Arch. Appl. Mech., **62**, 172–180, 1992.

http://rcin.org.pl

4. W.E. OLMSTEAD, S. NEMAT-NASSER and L. NI, *Shear bands as surfaces of discontinuity*, J. Mech. Phys. Solids, **42**, 697–709, 1994.
5. R.B. PĘCHERSKI, *Physical and theoretical aspects of large plastic deformations involving shear banding*, [in]: Finite Inelastic Deformations. Theory and Applications, Proc. IUTAM Symposium Hannover, Germany 1991, D. BESDO and E. STEIN [Eds.], Springer Verlag, 167–178, 1992.
6. R.B. PĘCHERSKI, *Modelling of large plastic deformations based on the mechanism of micro-shear banding. Physical foundations and theoretical description in plane strain*, Arch. Mech., **44**, 563–584, 1992.
7. R.B. PĘCHERSKI, *Theoretical description of plastic flow accounting for micro-shear bands*, Arch. Metall., **38**, 205–219, 1993.
8. A. KORBEL, *Mechanical instability of metal substructure – catastrophic flow in single and polycrystals*, [in]: Z.S. Basinski International Symposium on Crystal Plasticity, D.S. WILKINSON and J.D. EMBURY [Eds.], Canadian Institute of Mining and Metallurgy, 42–86, 1992.
9. M. HATHERLY and A.S. MALIN, *Shear bands in deformed metals*, Scripta Metall., **18**, 449–454, 1984.
10. R. HILL, *The mechanics of quasi-static plastic deformation in metals*, [in]: Surveys in Mechanics, G.K. BATCHELOR, R.M. DAVIES [Eds.], Cambridge, 7–31, 1956.
11. R. HILL, *On constitutive macro-variables for heterogeneous solids at finite strain*, Proc. Roy. Soc. Lond., **A326**, 131–147, 1972.
12. R. HILL, *On the micro-to-macro transition in constitutive analyses of elastoplastic reponse at finite strain*, Math. Proc. Camb. Phil. Soc., **95**, 481–494, 1984.
13. R. HILL, *On macroscopic effects of heterogeneity in elastoplastic media at finite strain*, Math. Proc. Camb. Phil. Soc., **98**, 579–590, 1985.
14. K.S. HAVNER, *On the mechanics of crystalline solids*, J. Mech. Phys. Solids, **21**, 383–394, 1973.
15. K.S. HAVNER, *Aspects of theoretical plasticity at finite deformation and large pressure*, ZAMP, **25**, 765–781, 1974.
16. K.S. HAVNER, *Finite plastic deformation of crystalline solids*, Cambridge University Press, Cambridge, U.K. 1992.
17. J. MANDEL, *Plasticité classique et viscoplasticité*, C.I.S.M., Springer Verlag, Udine 1972.
18. J. MANDEL, *Mécanique des solides anélastiques. – Généralisation dans R9 de la règle du potentiel plastique pour un élément polycrystallin*, C. R. Acad. Sc. Paris, **290 B**, 481–484, 1980.
19. R. HILL and J.R. RICE, *Constitutive analysis of elastic-plastic crystals at arbitrary strain*, J. Mech. Phys. Solids, **20**, 401–413, 1972.
20. H. PETRYK, *On constitutive inequalities and bifurcation in elastic-plastic solids with a yield-surface vertex*, J. Mech. Phys. Solids, **37**, 265–291, 1989.
21. C. STOLZ, *On relationship between micro and macro scales for particular cases of nonlinear behaviour of heterogeneous media*, 617–628, [in]: Proc. of IUTAM/ICM Symposium on Yielding, Damage and Failure of Anisotropic Solids, J.-P. BOEHLER [Ed.], Mechanical Engineering Publications, London 1990.
22. R. HILL, *The essential structure of constitutive laws for metal composites and polycrystals*, J. Mech. Phys. Solids, **15**, 779–795, 1967.
23. D.R. SMITH, *An introduction to continuum mechanics*, Kluwer Academic Publishers, Dordrecht 1993.
24. J. MANDEL, *Thermodynamics and plasticity*, [in]: Foundations of Continuum Thermodynamics, 283–304, J.J. DELGADO DOMINGOS *et al.* [Eds], McMillan, London 1974.
25. M. KLEIBER and B. RANIECKI, *Elastic-plastic materials at finite strains*, [in]: Plasticity Today, Modelling, Methods and Applications, 3–46, A. SAWCZUK and G. BIANCHI [Eds.], Elsevier, London 1985.
26. R.B. PĘCHERSKI, *The plastic spin concept and the theory of finite plastic deformations with induced anisotropy*, Arch. Mech., **40**, 807–818, 1988.
27. B. RANIECKI and Z. MRÓZ, *On the strain-induced anisotropy and texture in rigid-plastic solids*, [in]: Inelastic Solids and Structures. A. Sawczuk Memorial Volume, 13–32, M. KLEIBER and A. KÖNIG [Eds.], Pineridge Press, Swansea 1990.
28. S.C. ŢIGOIU and E. SOÓS, *Elastoviscoplastic models with relaxed configurations and internal state variables*, Appl. Mech. Rev., **43**, 131–151, 1990.
29. J.F. BESSELING and E. VAN DER GIESSEN, *Mathematical modelling of inelastic deformation*, Chapman & Hall, London 1994.
30. E.H. LEE, *Elastic-plastic deformation at finite strains*, J. Appl. Mech., **36**, 1–6, 1969.

http://rcin.org.pl

31. A. KORBEL, *The real nature of shear bands – plastons?*, 325–335, [in:] Plastic Instability, Proc. Int. Symp. on Plastic Instability. Considère Memorial (1841–1914), Presses de l'Ecole Nationale des Ponts et Chaussées, Paris 1985.

32. A. PAWEŁEK and A. KORBEL, *Soliton-like behaviour of a moving dislocation group*, Phil. Mag., **61 B**, 829–842, 1990.

33. J.J. GILMAN, *Physical nature of plastic flow and fracture*, 43–99, [in]: Plasticity, Proc. of the Second Symp. on Naval Structural Mechanics, E.H. LEE and P.S. SYMONDS [Eds.], Pergamon Press, 1960.

34. G.E. DIETER, *Mechanical metallurgy*, SI Metric Edition — adapted by D. BACON, McGraw-Hill, London 1988.

35. A. KORBEL, *The analyses of the nonuniform deformation in the substitutional solid solutions* [in Polish], Metalurgia i Odlewnictwo, Z. 65, Zesz. Nauk. AGH, Kraków 1974.

36. M. ZHOU, A.J. ROSAKIS and G. RAVICHANDRAN, *Dynamically propagating shear bands in impact loaded prenotched plates. I. Experimental investigations of temperature signatures and propagation speed*, J. Mech. Phys. Solids, **44**, 981–1006, 1996.

37. S. YANG and C. REY, *Shear band postbifurcation in oriented copper single crystals*, Acta Metall., **42**, 2763–2774, 1994.

38. C. REY, P. VIARIS DE LESEGNO and R. CHIRON, *Etude de la localisation de la déformation plastique en bandes de cisaillement dans des monocristaux de fer déformés en traction simple*, Proc. 6ème Colloque Franco-Polonais, Hétérogénéités de déformation plastique: aspects microscopiques et macroscopiques, 13, 14 et 15 Novembre 1995, Ecole des Mines de Saint-Etienne [to appear].

39. C. TRUESDELL and R.A. TOUPIN, *The classical field theories*, Encyclopaedia of Physics, III/1, S. FLÜGGE [Ed.], Springer-Verlag, Berlin 1960.

40. A.C. ERINGEN and E.S. SUHUBI, *Elastodynamics*, Vol I. *Finite Motions*, Academic Press, New York 1974.

41. W. KOSIŃSKI, *Field singularities and wave analysis in continuum mechanics*, PWN, Warszawa and Ellis Horwood, Chichester 1986.

42. A.C. ERINGEN, *Mechanics of continua*, J. Wiley, New York 1967.

43. S. NEMAT-NASSER and M. HORI, *Micromechanics: Overall properties of heterogeneous materials*, North-Holland, Amsterdam 1993.

44. C. TRUESDELL and W. NOLL, *The non-linear field theories of mechanics*, Encyclopaedia of Physics, III/3, S. FLÜGGE [Ed.], Springer-Verlag, Berlin 1965.

45. R.B. PĘCHERSKI, *Model of shear banding based on the idea of potential surfaces forming a vertex on the extremal surface*, ZAMM, **74**, 190–192, 1994.

46. R.B. PĘCHERSKI, *Model of plastic flow accounting for the effects of shear banding and kinematic hardening*, ZAMM, **75**, 203–204, 1995.

47. R.B. PĘCHERSKI, *Macroscopic effects of micro-shear banding in plasticity of metals* [submitted for publication].

48. B. RANIECKI and H. TANAKA, *On the thermodynamic driving force for coherent phase transformations*, Int. J. Engng. Sci., **32**, 1845–1858, 1994.

INSTITUTE OF FUNDAMENTAL TECHNOLOGICAL RESEARCH
POLISH ACADEMY OF SCIENCES
e-mail: rpecher@ippt.gov.pl

Received October 1, 1996.

http://rcin.org.pl

Arch. Mech., 49, 2, pp. 403–412, Warszawa 1997

Bending of a symmetric piezothermoelastic laminated plate with a through crack

Y. SHINDO, W. DOMON and F. NARITA (SENDAI)

FOLLOWING the theory of linear piezoelectricity, we consider the response of a cracked composite plate with attached piezoelectric polyvinylidene fluoride layers subjected to mechanical, thermal and electric field loading. Piezoelectric layers are added to the upper and lower surfaces. Classical lamination theory is extended to include piezothermoelastic effects, and the bending problem of a symmetric piezoelectric laminated plate with a through crack is considered. Fourier transforms are used to reduce the problem to the solution of a pair of dual integral equations. The integral equations are solved exactly and the moment intensity factor is expressed in closed form.

Notations

c half of the crack length,
E_0 intensity of uniform electric field,
E_i x_i axis elastic modulus,
E_z z component of electric field vector,
d_{kl} piezoelectric compliance coefficients,
D_{ij} bending composite plate stiffnesses,
G_{ij} i-j plane shear modulus,
mm2 mm, piezoelectric material has planes of symmetry in the x_1- and x_2-axes; 2 denotes that the x_3-axis is a two-fold rotational axis,
M_0 intensity of uniform moment,
M_{xx}, M_{yy}, M_{xy} moment resultants,
$M^E_{xx}, M^E_{yy}, M^E_{xy}$ electric moment resultants,
$M^\theta_{xx}, M^\theta_{yy}, M^\theta_{xy}$ thermal moment resultants,
h half of the total thickness,
h_k thickness of the k-th layer,
$J_0(\ )$ zero-order Bessel function of the first kind,
K_I moment intensity factor,
Q_x, Q_y vertical shear forces,
T absolute temperature,
$T_0, -T_0$ temperature rises at bottom and top surfaces, respectively,
T_R stress-free reference temperature,
u_x, u_y, u_z rectangular displacement components,
V_y equivalent shear,
w middle surface displacement,
x, y, z coordinate axes of laminate,
x_1, x_2, x_3 coordinate axes of lamina [for PVDF, x_1: rolling direction, x_3: poling direction],
α_i x_i axis coefficient of thermal expansion,

http://rcin.org.pl

$\varepsilon_{xx}, \varepsilon_{yy}, \varepsilon_{xy}$ components of strain tensor,
θ $= T - T_R$, temperature rise,
θ_1 angle between the lamina x axis and lamina principal x_1 axis,
ν_{ij} i-j plane Poisson's ratio,
$\sigma_{xx}, \sigma_{yy}, \sigma_{xy}$ components of stress tensor.

Superscripts

E electrically induced component,
θ thermally induced component.

Subscript

k k-th layer.

1. Introduction

PIEZOELECTRIC materials and composites are an important branch of modern engineering materials, with wide applications in actuators and sensors in smart materials and structures [1]. Investigations on such smart materials and structures include the works of LEE and JIANG [2], who presented a state space approach for exact analysis of three-dimensional piezoelectric lamina, with the aim at developing an efficient analytical methodology for laminated piezoelectric structures, and BATRA *et al.* [3], who performed an analysis of a simply supported rectangular elastic plate forced into bending vibrations by the application of time harmonic voltages to piezoelectric actuators attached to its bottom and top surfaces. However, it is reported experimentally that flaws or defects produced during their manufacturing process in piezoelectric materials can adversely influence the performance of piezoelectric devices [4]. When piezoelectric materials are subjected to mechanical, thermal and electrical stresses in service, the propagation of defects such as cracks may result in premature failure of these materials. To prevent failure during service and to secure the structural integrity of piezoelectric devices, understanding of fracture behaviour of piezoelectric materials and composites is of great importance [5, 6].

In this investigation, the linear electro-thermoelastic analysis of a symmetric piezoelectric laminated plate with a through crack under a uniform electric field is discussed. The cracked composite plate with piezoelectric polyvinylidene fluoride layers attached to its bottom and top surfaces is loaded by mechanical and thermal bending moments. The electric field and the poling direction are perpendicular to the plate surfaces, and classical lamination theory including piezothermoelastic effects is applied. Fourier transforms are used to reduce the problem to the solution of a pair of dual integral equations. The integral equations are solved exactly and the moment intensity factor is expressed in closed form.

http://rcin.org.pl

2. Problem statement and basic equations

Consider a symmetric piezothermoelastic laminated plate containing a through crack of length $2c$ constructed of N layers of materials that exhibit the symmetry of an orthorhombic crystal of class mm2 with respect to axes x_1, x_2, x_3 as shown in Fig. 1. Let the coordinate axes x and y be such that they are in the middle plane of the hybrid laminate and the $z = x_3$ axis is perpendicular to this plane.

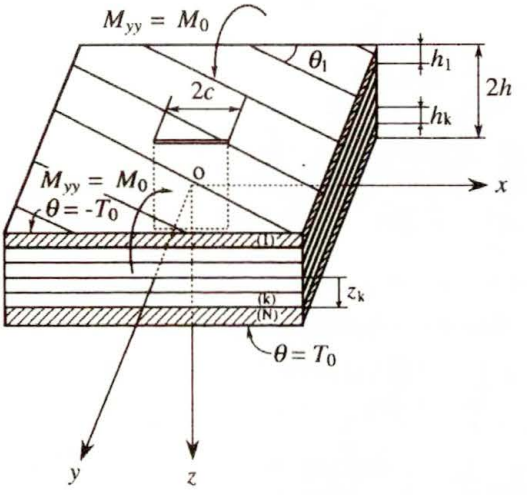

FIG. 1. A symmetric piezothermoelastic laminated plate with a through crack.

The crack is located on the line $y = 0$, $-c < x < c$. The total thickness is $2h$ and the k-th layer has thickness $h_k = z_k - z_{k-1}$ $(k = 1, ..., N)$, where $z_0 = -h$ and $z_N = h$. For the present investigation, in which a large uniform electric potential is applied to one or more layers of the cracked laminate, it is assumed that the electric field resulting from variations in stress and temperature (the so-called direct piezoelectric effect) is insignificant compared with the applied electric field [1]. The cracked composite plate is deformed by mechanical and thermal bending moments. If the midplane is a plane of material symmetry, it may be seen that the membrane and bending solutions of the problem would be fully uncoupled.

By employing the usual assumptions of classical lamination theory [7], the rectangular displacement components u_x, u_y, u_z may be expressed as follows:

$$u_x = -zw_{,x}, \qquad u_y = -zw_{,y}, \qquad u_z = w(x, y), \tag{2.1}$$

where a comma denotes partial differentiation with respect to the coordinate and $w(x, y)$ represents the deflection of the middle plane of the composite plate. The strain variations within the laminate are related to the middle surface displacement $w(x, y)$ by the expressions

$$\varepsilon_{xx} = -zw_{,xx}, \qquad \varepsilon_{yy} = -zw_{,yy}, \qquad \varepsilon_{xy} = -zw_{,xy}. \tag{2.2}$$

http://rcin.org.pl

The constitutive relations for a typical layer k ($k = 1, ..., N$), referred to arbitrary plate axes x, y and z, become

$$\begin{Bmatrix} \sigma_{xx} \\ \sigma_{yy} \\ \sigma_{xy} \end{Bmatrix}_k = -z \begin{bmatrix} \overline{Q}_{11} & \overline{Q}_{12} & \overline{Q}_{16} \\ \overline{Q}_{12} & \overline{Q}_{22} & \overline{Q}_{26} \\ \overline{Q}_{16} & \overline{Q}_{26} & \overline{Q}_{66} \end{bmatrix}_k \begin{Bmatrix} w_{,xx} \\ w_{,yy} \\ 2w_{,xy} \end{Bmatrix} - \begin{bmatrix} 0 & 0 & \overline{e}_{31} \\ 0 & 0 & \overline{e}_{32} \\ 0 & 0 & \overline{e}_{36} \end{bmatrix}_k \begin{Bmatrix} 0 \\ 0 \\ E_z \end{Bmatrix}_k - \begin{Bmatrix} \overline{\lambda}_1 \\ \overline{\lambda}_2 \\ \overline{\lambda}_6 \end{Bmatrix}_k \theta, \tag{2.3}$$

where $(\sigma_{xx}, \sigma_{yy}, \sigma_{xy})$ are the components of stress tensor, E_z is the z component of electric field vector, and $\theta = T - T_R$ is the temperature rise from the stress-free reference temperature T_R. For $\overline{Q}_{ij}$, $\overline{e}_{ij}$ and $\overline{\lambda}_i$ we have

$$\begin{aligned}
\overline{Q}_{11} &= Q_{11}\cos^4\theta_1 + 2(Q_{12}+2Q_{66})\sin^2\theta_1\cos^2\theta_1 + Q_{22}\sin^4\theta_1, \\
\overline{Q}_{12} &= (Q_{11}+Q_{22}-4Q_{66})\sin^2\theta_1\cos^2\theta_1 + Q_{12}(\sin^4\theta_1+\cos^4\theta_1), \\
\overline{Q}_{16} &= (Q_{11}-Q_{12}-2Q_{66})\sin\theta_1\cos^3\theta_1 + (Q_{12}-Q_{22}+2Q_{66})\sin^3\theta_1\cos\theta_1, \\
\overline{Q}_{22} &= Q_{11}\sin^4\theta_1 + 2(Q_{12}+2Q_{66})\sin^2\theta_1\cos^2\theta_1 + Q_{22}\cos^4\theta_1, \\
\overline{Q}_{26} &= (Q_{11}-Q_{12}-2Q_{66})\sin^3\theta_1\cos\theta_1 + (Q_{12}-Q_{22}+2Q_{66})\sin\theta_1\cos^3\theta_1, \\
\overline{Q}_{66} &= (Q_{11}+Q_{22}-2Q_{12}-2Q_{66})\sin^2\theta_1\cos^2\theta_1 + Q_{66}(\sin^4\theta_1+\cos^4\theta_1);
\end{aligned} \tag{2.4}$$

$$\begin{aligned}
Q_{11} &= \frac{E_1}{1-\nu_{12}\nu_{21}}, \\
Q_{12} &= \frac{\nu_{12}E_2}{1-\nu_{12}\nu_{21}}, \\
Q_{22} &= \frac{E_2}{1-\nu_{12}\nu_{21}}, \\
Q_{66} &= G_{12};
\end{aligned} \tag{2.5}$$

$$\begin{aligned}
\overline{e}_{31} &= (Q_{11}d_{31} + Q_{12}d_{32})\cos^2\theta_1 + (Q_{12}d_{31} + Q_{22}d_{32})\sin^2\theta_1, \\
\overline{e}_{32} &= (Q_{11}d_{31} + Q_{12}d_{32})\sin^2\theta_1 + (Q_{12}d_{31} + Q_{22}d_{32})\cos^2\theta_1, \\
\overline{e}_{36} &= [(Q_{11} - Q_{12})d_{31} + (Q_{12} - Q_{22})d_{32}]\sin\theta_1\cos\theta_1;
\end{aligned} \tag{2.6}$$

$$\begin{aligned}
\overline{\lambda}_1 &= (Q_{11}\alpha_1 + Q_{12}\alpha_2)\cos^2\theta_1 + (Q_{12}\alpha_1 + Q_{22}\alpha_2)\sin^2\theta_1, \\
\overline{\lambda}_2 &= (Q_{11}\alpha_1 + Q_{12}\alpha_2)\sin^2\theta_1 + (Q_{12}\alpha_1 + Q_{22}\alpha_2)\cos^2\theta_1, \\
\overline{\lambda}_6 &= [(Q_{11} - Q_{12})\alpha_1 + (Q_{12} - Q_{22})\alpha_2]\sin\theta_1\cos\theta_1;
\end{aligned} \tag{2.7}$$

in which E_i is x_i axis elastic modulus, ν_{ij} is the i-j plane Poisson's ratio, G_{ij} is the i-j plane shear modulus, d_{kl} are the piezoelectric compliance coefficients, α_i is

http://rcin.org.pl

the x_i axis coefficient of thermal expansion, and θ_1 is the angle between the lamina x axis and lamina principal x_1 axis. Additionally, the elastic moduli and Poisson's ratios are related by

$$\frac{\nu_{12}}{E_1} = \frac{\nu_{21}}{E_2}. \tag{2.8}$$

Integrating the constitutive relations of Eq. (2.3) through the composite plate thickness leads to the structure material stiffness relationships. The bending composite plate stiffnesses are given as

$$D_{ij} = \sum_{k=1}^{N} \int_{z_{k-1}}^{z_k} (\overline{Q}_{ij})_k z^2 \, dz \qquad (i,j = 1,2,6). \tag{2.9}$$

Electric and thermal moment resultants are given by

$$\begin{Bmatrix} M_{xx}^E \\ M_{yy}^E \\ M_{xy}^E \end{Bmatrix} = \sum_{k=1}^{N} \int_{z_{k-1}}^{z_k} \begin{Bmatrix} \overline{e}_{31} \\ \overline{e}_{32} \\ \overline{e}_{36} \end{Bmatrix}_k (E_z)_k z \, dz, \tag{2.10}$$

$$\begin{Bmatrix} M_{xx}^\theta \\ M_{yy}^\theta \\ M_{xy}^\theta \end{Bmatrix} = \sum_{k=1}^{N} \int_{z_{k-1}}^{z_k} \begin{Bmatrix} \overline{\lambda}_1 \\ \overline{\lambda}_2 \\ \overline{\lambda}_6 \end{Bmatrix}_k \theta z \, dz. \tag{2.11}$$

Combining the results of Eqs. (2.9)–(2.11), the moment resultants (M_{xx}, M_{yy}, M_{xy}) can be written as

$$\begin{Bmatrix} M_{xx} \\ M_{yy} \\ M_{xy} \end{Bmatrix} = - \begin{bmatrix} D_{11} & D_{12} & D_{16} \\ D_{12} & D_{22} & D_{26} \\ D_{16} & D_{26} & D_{66} \end{bmatrix} \begin{Bmatrix} w_{,xx} \\ w_{,yy} \\ 2w_{,xy} \end{Bmatrix} - \begin{Bmatrix} M_{xx}^E \\ M_{yy}^E \\ M_{xy}^E \end{Bmatrix} - \begin{Bmatrix} M_{xx}^\theta \\ M_{yy}^\theta \\ M_{xy}^\theta \end{Bmatrix}. \tag{2.12}$$

Note that M_{xy}^E, M_{xy}^θ and D_{16}, D_{26} are identically zero for the cross-ply construction, since the coefficients $\overline{e}_{36}$, $\overline{\lambda}_6$ in Eqs. (2.10), (2.11) and $\overline{Q}_{16}$, $\overline{Q}_{26}$ in Eq. (2.9) are zero for ply angles of 0° or 90°.

The usual plate equilibrium conditions in the case of zero mechanical loading are

$$\begin{aligned} M_{xx,x} + M_{xy,y} - Q_x &= 0, \\ M_{yx,x} + M_{yy,y} - Q_y &= 0, \end{aligned} \tag{2.13}$$

$$Q_{x,x} + Q_{y,y} = 0, \tag{2.14}$$

http://rcin.org.pl

where Q_x and Q_y are the vertical shear forces. Substituting Eq. (2.12) into Eqs. (2.13), (2.14) yields

$$Q_x = -\left[D_{11}w_{,xxx} + D_{26}w_{,yyy} + (D_{12} + 2D_{66})w_{,xyy} + 3D_{16}w_{,xxy}\right] - \left[M^E_{xx,x} + M^E_{xy,y} + M^\theta_{xx,x} + M^\theta_{xy,y}\right], \tag{2.15}$$

$$Q_y = -\left[D_{16}w_{,xxx} + D_{22}w_{,yyy} + 3D_{26}w_{,xyy} + (D_{12} + 2D_{66})w_{,xxy}\right] - \left[M^E_{xy,x} + M^E_{yy,y} + M^\theta_{xy,x} + M^\theta_{yy,y}\right], \tag{2.16}$$

$$D_{11}w_{,xxxx} + 2D_{12}w_{,xxyy} + 4D_{16}w_{,xxxy} + D_{22}w_{,yyyy} + 4D_{26}w_{,xyyy} + 4D_{66}w_{,xxyy} + (M^E_{xx,xx} + M^E_{yy,yy} + 2M^E_{xy,xy} + M^\theta_{xx,xx} + M^\theta_{yy,yy} + 2M^\theta_{xy,xy}) = 0. \tag{2.17}$$

Assuming a symmetric cross-ply panel having angles of 0° or 90°, the governing equation (2.17) simplifies to

$$D_{11}w_{,xxxx} + 2D_{12}w_{,xxyy} + D_{22}w_{,yyyy} + 4D_{66}w_{,xxyy} + M^E_{xx,xx} + M^E_{yy,yy} + M^\theta_{xx,xx} + M^\theta_{yy,yy} = 0. \tag{2.18}$$

The hybrid laminate with a through crack is bent by uniform moments of intensity M_0 at infinity and is subjected to an applied uniform electric field $E_z = E_0$ in addition to the upper and lower surface temperatures $\theta = -T_0, T_0$. The plate is subjected to the linear temperature variation

$$\theta(z) = \frac{T_0}{h}z\,. \tag{2.19}$$

Because of the assumed symmetry in geometry and loading, it is sufficient to consider the problem for $0 \le x < \infty$, $0 \le y < \infty$ only. The boundary conditions can be written as

$$V_y = M_{xy,x} + Q_y = 0 \qquad (y = 0, \quad 0 \le x < \infty), \tag{2.20}$$

$$\begin{aligned} M_{yy} &= 0 \qquad (y = 0, \quad 0 \le x < c), \\ u_y &= 0 \qquad (y = 0, \quad c \le x < \infty), \end{aligned} \tag{2.21}$$

where V_y is the equivalent shear.

3. Solution procedure

We assume that the solution w is of the form

$$w = \frac{D_{12} - D_{22}}{2(D_{11}D_{22} - D_{12}^2)}M_0x^2 + \frac{D_{12} - D_{11}}{2(D_{11}D_{22} - D_{12}^2)}M_0y^2 + \frac{2}{\pi}\int_0^\infty \left[A_1(s)e^{-s\gamma_1 y} + A_2(s)e^{-s\gamma_2 y}\right]\cos(sx)\,ds, \tag{3.1}$$

http://rcin.org.pl

where $A_1(s)$ and $A_2(s)$ are the unknown functions to be determined later, and γ_1 and γ_2 are

$$\gamma_1 = \left\{ \frac{(D_{12} + 2D_{66}) + (D_{12}^2 + 4D_{12}D_{66} + 4D_{66} - D_{11}D_{22})^{1/2}}{D_{22}} \right\}^{1/2}, \tag{3.2}$$

$$\gamma_1 = \left\{ \frac{(D_{12} + 2D_{66}) - (D_{12}^2 + 4D_{12}D_{66} + 4D_{66} - D_{11}D_{22})^{1/2}}{D_{22}} \right\}^{1/2}. \tag{3.3}$$

The boundary condition of Eq. (2.20) leads to the following relation between unknown functions:

$$\gamma_1 \left[D_{12} + 4D_{66} - D_{22}\gamma_1^2 \right] A_1(s) + \gamma_2 \left[D_{12} + 4D_{66} - D_{22}\gamma_2^2 \right] A_2(s) = 0. \tag{3.4}$$

Application of the boundary conditions (2.21) gives rise to a pair of dual integral equations:

$$\begin{aligned} C \int_0^\infty sA(s)\cos(sx)\,ds &= \frac{\pi}{2}(M_0 - M_{yy}^E - M_{yy}^\theta) \qquad (0 \le x < c), \\ \int_0^\infty A(s)\cos(sx)\,ds &= 0 \qquad\qquad\qquad\qquad (c \le x < \infty), \end{aligned} \tag{3.5}$$

in which C, M_{yy}^E and M_{yy}^θ are known as

$$\begin{aligned} C = (D_{22}\gamma_1^2 - D_{12})\frac{4D_{66} + D_{12} - D_{22}\gamma_2^2}{\gamma_1 D_{22}(\gamma_1^2 - \gamma_2^2)} \\ - (D_{22}\gamma_2^2 - D_{12})\frac{4D_{66} + D_{12} - D_{22}\gamma_1^2}{\gamma_2 D_{22}(\gamma_1^2 - \gamma_2^2)}, \end{aligned} \tag{3.6}$$

$$M_{yy}^E = \sum_{k=1}^{N} \frac{(\bar{e}_{32})_k}{2} E_0(z_k^2 - z_{k-1}^2), \tag{3.7}$$

$$M_{yy}^\theta = \sum_{k=1}^{N} \frac{(\bar{\lambda}_2)_k}{3h} T_0(z_k^3 - z_{k-1}^3). \tag{3.8}$$

The unknown $A(s)$ is related to $A_j(s)$ $(j = 1, 2)$ as follows:

$$A(s) = s\left[\gamma_1 A_1(s) + \gamma_2 A_2(s)\right]. \tag{3.9}$$

The set of dual integral equations (3.5) may be solved by using a new function $\Phi(\xi)$ defined by

$$A(s) = \frac{\pi}{2}\frac{c^2}{C}\int_0^1 \xi^{1/2}\Phi(\xi)J_0(cs\xi)\,d\xi, \tag{3.10}$$

http://rcin.org.pl

where $J_0(\ )$ is the zero-order Bessel function of the first kind. Having satisfied Eq. (3.5) for $c \leq x < \infty$, the remaining condition for $0 \leq x < c$ leads to an Abel integral equation for $\Phi(\xi)$. The solution for $\Phi(\xi)$ is expressed by

$$\Phi(\xi) = \left(M_0 - M_{yy}^E - M_{yy}^\theta\right) \xi^{1/2}. \tag{3.11}$$

The moment intensity factor is obtained as

$$K_I = \lim_{x \to c^+} \{2\pi(x-c)\}^{1/2} M_{yy}(x,0) = M_0(\pi c)^{1/2} \left(1 - \frac{M_{yy}^E + M_{yy}^\theta}{M_0}\right). \tag{3.12}$$

4. Numerical results and discussion

The thermoelastic response of a cracked piezoelectric laminated plate subjected to mechanical, thermal and electric field loading is considered. The hybrid laminate chosen is a graphite/epoxy composite with a symmetric construction of $[0°/90°/0°/90°]_s$ where $[\ ]_s$ denotes symmetry about the middle surface. Each graphite/epoxy lamina is of constant thickness. Two double thick layers of polyvinylidene fluoride (PVDF), piezoelectric polymers poled in $\mp z$-direction, are added to the upper and lower surfaces to make a ten-layer hybrid composite structure. Material and geometric properties for the graphite/epoxy lamina and the PVDF layer are given in Table 1.

Table 1. Properties of graphite/epoxy and PVDF.

Graphite/epoxy
$E_1 = 181\,\text{GPa},\ E_2 = 10.3\,\text{GPa}$
$G_{12} = 7.17\,\text{GPa}$
$\nu_{12} = 0.28$
$\alpha_1 = 0.02 \times 10^{-6}\,1/\text{K},\ \alpha_2 = 22.5 \times 10^{-6}\,1/\text{K}$
$h_{GE} = h_k = 1.25 \times 10^{-4}\,\text{m}\ \ (k = 2, \ldots, 9)$
$\varrho_{GE} = \varrho_k = 1580\,\text{kg/m}^3\ \ (k = 2, \ldots, 9)$
Polyvinylidene fluoride (PVDF)
$E_1 = E_2 = 2\,\text{GPa},\ G_{12} = 0.752\,\text{GPa},\ \nu_{12} = 0.33$
$\alpha_1 = \alpha_2 = 120 \times 10^{-6}\,1/\text{K}$
$d_{31} = d_{32} = 23 \times 10^{-12}\,\text{m/V}$
$h_P = h_1 = h_{10} = 2.5 \times 10^{-4}\,\text{m}$
$\varrho_P = \varrho_1 = \varrho_{10} = 1800\,\text{kg/m}^3$

Figure 2 exhibits the variation of the normalized moment intensity factor $|K_I/M_0(\pi c)^{1/2}|$ against the electric field E_0 for $M_0 = 5\,\text{Nm/m}$ and $T_0 = 40°\,\text{C}$.

http://rcin.org.pl

The existence of the electric field $E_z = E_0$ produces smaller values of the moment intensity factor.

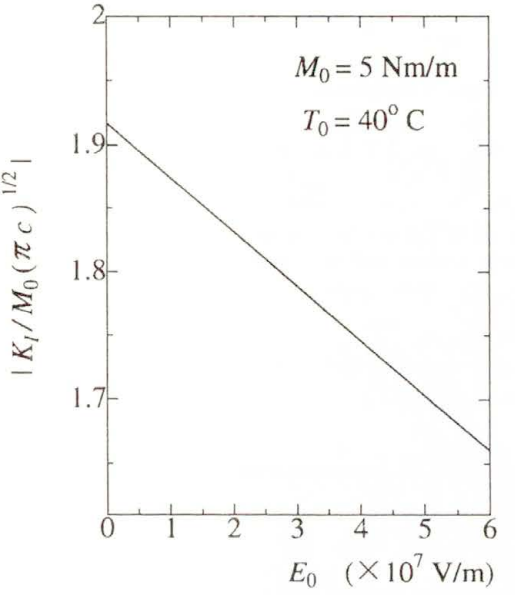

FIG. 2. Moment intensity factor $|K_I/M_0(\pi c)^{1/2}|$ versus E_0.

Only the converse piezoelectric effect has been considered here, whereby an electric field is applied to piezoelectric layers in order to suppress the structure's overall deformation and singular moment near the crack tip. However, advantage can also be taken of the direct piezoelectric effect by employing another piezoelectric layer as a sensor. By coupling the two effects with appropriate feedback control, a smart structure can be achieved [1]. Work in this area is currently being pursued.

5. Conclusions

The response of a cracked composite plate with attached piezoelectric polyvinylidene fluoride layers under mechanical, thermal, and electrical field loading has been analyzed theoretically. Classical lamination theory including piezothermoelastic effects is applied and the results are expressed in terms of the moment intensity factor. The moment intensity factor decreases with the increase of the electric field. The results presented demonstrate the feasibility of suppressing thermomechanically induced flexure and singular moment near the crack tip via the piezothermoelastic effects.

http://rcin.org.pl

References

1. T.R. TAUCHERT, *Piezothermoelastic behavior of a laminated plate*, J. Thermal Stresses, **15**, 1, pp. 25–37, 1992.
2. J.S. LEE and L.Z. JIANG, *Exact electroelastic analysis of piezoelectric laminae via state space approach*, Intern. J. Solids and Struct., **33**, 7, pp. 977–990, 1996.
3. R.C. BATRA, X.Q. LIANG and J.S. YANG, *The vibration of a simply supported rectangular elastic plate due to piezoelectric actuators*, Intern. J. Solids and Struct., **33**, 11, pp. 1597–1618, 1996.
4. Y.Y. TANG and K. XU, *Exact solutions of piezoelectric materials with moving screw and edge dislocations*, Intern. J. Engng. Sci., **32**, 10, pp. 1579–1591, 1994.
5. Y. SHINDO, K. TANAKA and F. NARITA, *Singular stress and electric fields of a piezoelectric ceramic strip with a finite crack under longitudinal shear*, Acta Mech., **120**, 1-4, pp. 31–45, 1997.
6. Y. SHINDO, F. NARITA and K. TANAKA, *Electroelastic intensification near anti-plane shear crack in orthotropic piezoelectric ceramic strip*, Theoret. and Appl. Fracture Mech., **25**, 1, pp. 65–71, 1996.
7. R.M. JONES, *Mechanics of composite materials*, Scripta Book Co., Washington, D.C. 1975.

DEPARTMENT OF MATERIALS PROCESSING
GRADUATE SCHOOL OF ENGINEERING, TOHOKU UNIVERSITY, SENDAI, JAPAN.
e-mail: shindo@msws.material.tohoku.ac.jp

Received October 21, 1996.

http://rcin.org.pl

Arch. Mech., 49, 2, pp. 413–419, Warszawa 1997

On the interface modelling of crystal growth processes Part II. Uncoupled thermoelastic theory

Dedicated to Professor Franz Ziegler on the occasion of His 60th birthday

S. TABACOVA (PLOVDIV) and W. KOSIŃSKI (WARSZAWA)

SOLIDIFICATION of an elastic sphere from melt in a quasi-static formulation has been investigated in "singular surface approach" and in "finite slab approach". Thermal stresses in the solid phase are derived for both approaches due to the uncoupled thermoelastic quasi-static theory. In the interfacial layer, which has been regarded as a boundary layer between the liquid and the solid phase, special constitutive relations for the purely mechanical problem are posed in order to have a continuous change from the liquid to solid phase. It has been found that the solutions corresponding to the "singular surface approach" are the zero order terms of the asymptotic expansions in the small parameter of the "finite slab approach" solutions.

1. Introduction

IN THE FIRST PART of the present paper [1] the different approaches treating the interface modelling during phase-change process (solidification or melting) are listed. A comparison between the two approaches: the "singular surface approach" and the "finite slab approach" is presented there. It is shown that under some physical hypotheses, the interfacial layer could be regarded as a "phase-change" boundary layer and its thickness depends only on the solidification mechanism specific for a given material. The surface fields (internal energy, density, evolution time) in the "singular surface approach" are obtained to be the zero order terms in the asymptotic expansion (in a small parameter related to the layer thickness) of the correspondent fields in the "finite slab approach". In the same paper, as a particular case, the quasi-static solidification of a sphere and its interface evolution in time is observed. In the "finite slab approach" an averaging procedure is applied, in which integration along the thickness is performed to get mean quantities defined as surface fields, and some preliminary phenomenological assumptions are necessary to obtain the field quantities. In some aspect this is shown in [1] for the internal energy and temperature distribution in the layer.

The aim of the present paper is to continue the comparison between the "singular surface approach" and the "finite slab approach" for the quasi-static axisymmetrical growth of an elastic sphere from a liquid phase. In the framework of the quasi-static uncoupled thermoelastic theory, the results obtained in [1]

http://rcin.org.pl

for the thermal problem will be used when solving the purely mechanical problem. For the case of solidification discussed here, it is appropriate to apply the uncoupled quasi-static thermoelastic theory [3]. The extension of the model to the thermal stresses necessitates the assumption of some constitutive law for the thermal stresses inside the layer. It will be shown that the solutions for the deformations, stresses and pressure corresponding to the "singular surface approach" are the zero order terms of the asymptotic expansion in a small parameter of the solutions obtained from the "finite slab approach".

2. Formulation of the problem

The crystal growth of an elastic sphere $\widehat{G}_t^-$ with radius R in a spherical container with radius R^* filled with its melt $\widehat{G}_t^+$ is considered as in [1]. The phase change process is due to a continuous negative heat flux $Q_0 < 0$ from a crystal seed of radius ε concentric with the spherical container. The solid and liquid phases are supposed to be at thermostatic equilibrium, isotropic, and the liquid phase is incompressible and ideal. A spherical coordinate system (r, φ, θ) is introduced connected with the container. The problem is 1D due to the symmetry with respect to φ and θ if the problem boundary conditions are independent of φ and θ. The interface evolution in time is $r = R(t)$ and the interface coordinates are $l^1 := \varphi$, $l^2 := \theta$. The second fundamental tensor of the surface is $b_{11} = -R\sin^2\theta$, $b_{22} = -R$, $b_{12} = b_{21} = 0$ and the mean and Gauss curvatures are $H = -1/R$ and $K = 1/R^2$ and $\mathrm{div}_s = 0$ (all the notations are the same as those in [1]).

The solidification process is treated in the solidification time scale, i.e., it is assumed to be quasi-static. The uncoupled quasi-static theory of thermoelasticity is applied for the solid phase. Then for both media the general balance laws for mass and momentum [1] give:

$$\varrho_l = \varrho^+ = \text{const}, \qquad \varrho_s = \varrho_s(r), \tag{2.1}$$

where ϱ_l and ϱ_s are the liquid and solid densities,(1) respectively;

$$\mathrm{div}\,\mathbf{T}_l = 0, \qquad \mathrm{div}\,\mathbf{T}_s = 0, \tag{2.2}$$

where $\mathbf{T}$ is the stress tensor. For the liquid phase, $\mathbf{T}_l = -p\mathbf{I}$, where $p = p(r)$ is the pressure and $\mathbf{I}$ is the identity tensor. From fluid incompressibility it follows that $\mathrm{div}\,\mathbf{u}_l = 0$, where $\mathbf{u}_l = (u_{l_r}, 0, 0)$ are the displacements in the fluid. For the solid phase as in [3], $\mathbf{T}_s = \lambda_s \mathrm{tr}\,\mathbf{E}_s\mathbf{I} + 2\mu_s\mathbf{E}_s - (3\lambda_s + 2\mu_s)\alpha_s(\theta_s - \theta_a)\mathbf{I}$, where λ_s, μ_s and α_s are the material constants, $\mathbf{E}_s$ is the deformation tensor with components

$$\varepsilon_{s_{rr}} = \frac{\partial u_{s_r}}{\partial r}, \qquad \varepsilon_{s_{\varphi\varphi}} = \varepsilon_{s_{\theta\theta}} = \frac{u_{s_r}}{r}, \qquad \varepsilon_{s_{r\varphi}} = \varepsilon_{s_{r\theta}} = \varepsilon_{s_{\varphi\theta}} = 0,$$

(1) Everywhere in the text index l refers to the liquid phase and index s – to the solid.

http://rcin.org.pl

$u_{s_r} = u_{s_r}(r)$ is the radial displacement and θ_a is some reference temperature, e.g. $\theta_a = \theta|_{r=\varepsilon}$.

The boundary conditions for the unknown functions have to be imposed on $\partial\widehat{G}_t^-$, $\partial\widehat{G}_t^+$ and on S_t – the interface boundary – for the "singular surface approach", or on S_t^- and S_t^+ – the two interface boundaries – for the "finite slab approach". Then on $\partial\widehat{G}_t^-$, which means $r = \varepsilon$ and ε – greater than the critical radius of a crystal nucleus [4]:

$$\begin{aligned} \varrho_s &= \varrho_{s_0} = \text{const}, \\ u_{s_r} &= 0. \end{aligned} \tag{2.3}$$

On $\partial\widehat{G}_t^+$, i.e., $r = R^*$:

$$p = p_\infty \,. \tag{2.4}$$

3. Singular surface approach

The interface $S_t : F = r - R(t) = 0$, is defined as the isotherm $\theta = \theta_m$ and the surface normal velocity is $c_n = \dot{R}$. On that surface the density and displacement are continuous, while the stress tensor suffers a jump [2]:

$$\begin{aligned} \varrho_s &= \varrho^+, \\ u_{l_r} &= u_{s_r}\,, \qquad \mathbf{T}_s \cdot \mathbf{n} - \mathbf{T}_l \cdot \mathbf{n} = \sigma H \mathbf{n}, \end{aligned} \tag{3.1}$$

where σ is the solid/liquid surface tension, and $\mathbf{n} = (1, 0, 0)$ is the unit normal.

The uncoupled thermoelastic problem (2.2) with $(2.3)_2$, (2.4), $(3.1)_2$, and with the expressions (4.4) and (4.3) for θ_l and θ_s found in [1], has the following solutions in $\widehat{G}_t^+$:

$$\begin{aligned} p &= p_\infty\,, \\ u_{l_r} &= \frac{C}{r^2}\,; \end{aligned} \tag{3.2}$$

and in $\widehat{G}_t^-$

$$\begin{aligned} u_{s_r} &= b_0 + b_1 r + \frac{b_2}{r^2}\,, \\ \tau_{s_{rr}} &= 2(\lambda_s + \mu_s)\left(\frac{b_0}{r} + b_1\right) - 4\mu_s \frac{b_2}{r^3} + \lambda_s b_1 + A, \\ \tau_{s_{\varphi\varphi}} &= \tau_{s_{\theta\theta}} = 2(\lambda_s + \mu_s)\left(\frac{b_0}{r} + b_1\right) + 2\mu_s \frac{b_2}{r^3} + \lambda_s b_1 + A, \end{aligned} \tag{3.3}$$

http://rcin.org.pl

where

$$A = -(3\lambda_s + 2\mu_s)\alpha_s \left[\theta_m - \theta_a - \frac{Q_0}{4\pi\kappa_s}\left(\frac{1}{R} - \frac{1}{r}\right)\right], \quad b_0 = \frac{(3\lambda_s + 2\mu_s)\alpha_s Q_0}{8\pi\kappa_s(\lambda_s + 2\mu_s)},$$

$$C = C' = b_0\left(R^2 - \varepsilon^2\right) + b_1\left(R^3 - \varepsilon\right), \qquad b_2 = -b_0\varepsilon^2 - b_1\varepsilon,$$

$$b_1 = b_1' = \frac{-\frac{\sigma}{R} - p_\infty - \left[\frac{2\lambda_s}{R} + \frac{4\mu_s}{R^3}\varepsilon^2\right] b_0 + (3\lambda_s + 2\mu_s)\alpha_s(\theta_m - \theta_a)}{3\lambda_s + 2\mu_s + \frac{4\mu_s}{R^3}\varepsilon}.$$

Here b_1' and C' correspond to the "singular surface approach". In the next section dealing with the "finite slab approach" we shall give another value of b_1.

4. Finite slab approach

In this approach the two subregions $\hat{G}_t^{\pm}$ are divided by a narrow layer Z_t with regular surface boundaries $S_t^{\pm}$, and a reference surface S_t is located between them, to which the mean interfacial fields will be referred. The surface boundaries $S_t^{\pm}$ are defined as $S_t^- : r = R + z^-$ and $S_t^+ : r = R + z^+$ and a coordinate $l \in [z^-, z^+]$ is ascribed to the layer, such that $r = R + l$.

Suppose that the physical assumptions i) – vi) from [1] hold. Therefore, the interfacial layer is a phase change boundary layer between the liquid and the solid phase with thickness $\delta R_0 \ll 1$ and $z^+ - z^- = \delta R_0$, where δ is a small parameter. Moreover, from (4.14) of [1] the quantities z^+ and z^- depend only on the thermal properties of the media in contact. All the interfacial fields are represented as polynomial functions of l, while their corresponding mean values F – in an asymptotic expansion of the small parameter δ:

$$F = F_0 + \delta F_1 + \delta^2 F_2 + \dots, \tag{4.1}$$

where F_0 relates to the "singular surface approach" solution.

As a result, for the density in the solid bulk we get:

$$\varrho_s(R + z^-) = \varrho^+ \quad \text{or} \quad \varrho_s(R) = \varrho^+ + O(\delta) \tag{4.2}$$

which confirms the result of the "singular surface approach" $(3.1)_1$ and the surface density ϱ^S in the interfacial layer is given by (4.17) of [1]. Similarly, the temperature solutions θ_l and θ_s in the bulks are (4.19), (4.20) of [1], which have as zero order terms the "singular surface approach" solutions (4.4) and (4.3) from [1]. The surface energy density $\varrho^s e^s$ is represented by (4.18) of [1]. It is evident that the zero order terms of (4.17) and (4.18) of [1] vanish, as it was assumed in the "singular surface approach".

http://rcin.org.pl

Some additional assumption for the interfacial layer material rheology must be introduced before formulating the mean surface stress $\mathbf{W}^s$, i.e., the assumption:

vii) The stress tensor $\mathbf{T}(l)$ has only non-zero diagonal elements $\tau_{ij} = 0$, $(i \neq j)$. Then for the stress tensor in the layer we assume the form

$$\mathbf{T}(l) = -p(l)\mathbf{I} + \lambda(l)\operatorname{tr}\mathbf{E}(l)\mathbf{I} + 2\mu(l)\mathbf{E}(l) - [3\lambda(l) + 2\mu(l)]\,\alpha(l)\,[\theta(l) - \theta_{\min}]\,\mathbf{I},$$

where the material coefficients λ, μ and α, $p(l)$, the volume deformation $\operatorname{tr}\mathbf{E}$ and the radial displacement u_r are regular functions of l. The coefficients of these unknown functions are found by a matching procedure with the corresponding values from both media, and their final form is:

$$\begin{aligned}
&\lambda(l) = \frac{\lambda_s}{\delta R_0}(z^+ - l), \quad \mu(l) = \frac{\mu_s}{\delta R_0}(z^+ - l), \quad \alpha(l) = \frac{\alpha_s}{\delta R_0}(z^+ - l),\\
&p(l) = \left[\frac{p_\infty}{\delta R_0} - \frac{p_2 \delta R_0 (c_\nu^- - c_\nu^+)}{(c_\nu^- + c_\nu^+)}\right](l - z^-) + p_2(l^2 - z^{-2}),\\
&\operatorname{tr}\mathbf{E}(l) = \frac{\varepsilon_s}{\delta R_0}(z^+ - l),\\
&u_r(l) = \frac{D_0}{(R+l)^2} + \frac{\varepsilon_s(R + z^+)}{3\delta R_0}(R + l) - \frac{\varepsilon_s}{4\delta R_0}(R + l)^2,
\end{aligned} \tag{4.3}$$

where

$$D_0 = (R + z^-)^2\left\{b_0\left[1 - \frac{\varepsilon^2}{(R+z^-)^2}\right] + b_1''\left[(R + z^-) - \frac{\varepsilon}{(R+z^-)^2}\right] - \frac{\varepsilon_s(R + z^-)}{12\delta R_0}(R + 3\delta R_0 + z^+)\right\},$$

$$\varepsilon_s = \frac{2b_0}{R + z^-} + 3b_1'', \qquad C'' = D_0 + \frac{\varepsilon_s(R + z^+)^4}{12\delta R_0}.$$

With

$$j(l) = 1 + (l/R)^2, \qquad \mathbf{A}_s(l) = (1 + l/R)\mathbf{I}_s, \qquad \operatorname{div}_s\mathbf{I}_s = -\frac{2}{R}\mathbf{n},$$

the case of the linear momentum balance in the layer (from (3.2) of [1])

$$\psi = \varrho v = 0, \qquad \psi^s = \varrho^s\mathbf{V} = \mathbf{0}, \qquad \mathbf{w} = -\mathbf{T}, \qquad \mathbf{v} = \mathbf{0}, \qquad \mathbf{W}^s = <-\mathbf{T}(l)\mathbf{A}_s(l)>$$

is:

$$\operatorname{div}_s\mathbf{W}^s = \left[1 + \left(\frac{z^+}{R}\right)^2\right]\mathbf{T}_l(R + z^+)\mathbf{n} - \left[1 + \left(\frac{z^-}{R}\right)^2\right]\mathbf{T}_s(R + z^-)\mathbf{n}. \tag{4.4}$$

http://rcin.org.pl

The unknown coefficients p_2 and b_1'' will be found after taking into account that

$$\mathrm{div}_s \mathbf{W}^s = -2 < \left(1 + \frac{l}{R}\right) \tau_{\varphi\varphi}(l) > H\mathbf{n},$$

and that $< p(l) > = 0.5\sigma + O(\delta)$ is the classical surface tension:

$$p_2 = \frac{-3\sigma}{(\delta R_0)^3}, \tag{4.5}$$

$$b_1'' = b_1' + \delta B + O(\delta^2); \tag{4.6}$$

here B can be calculated from (4.3).

Evidently, if we replace b_1 with b_1'' and C with C'' in $(3.2)_2$, $(3.3)_1$ and $(3.3)_2$, the resultant displacements and the stresses will possess zero order terms with respect to δ which will coincide with the respective ones from the "singular surface approach". Here, it is interesting to note that in the layer all the considered functions are regular, i.e., they obey Eq. (4.1), but only the pressure function $p(l)$ contains a term of order $O(\delta^{-1})$ like a "smoothed" Dirac function contributing to the surface tension as a mean interfacial quantity. In the singular surface case the interface is of zero thickness and we can regard the surface tension as a result of some Dirac function similar to the pressure function.

5. Conclusions

An extension of authors' previous paper [1] dealing with the elastic sphere solidification from melt in a quasi-static formulation has been obtained in two approaches: "singular surface approach" and "finite slab approach". Using the results for the temperature and density distribution everywhere in the solid/liquid system from [1], the purely mechanical uncoupled thermoelastic quasi-static problem is treated in both approaches. In the interfacial layer special constitutive relations are posed for the stress tensor, displacements, material coefficients λ, μ and α, the volume deformation and pressure, in order to ensure their continuous change from liquid to solid.

The comparison between the two approaches leads to the conclusion that the solutions for the density, temperature, thermal stresses, displacements and pressure obtained by the "singular surface approach" are the zero order terms in the asymptotic expansion of the corresponding solutions due to the "finite slab approach".

The classical surface tension is due to the pressure function in the interfacial layer. It occurs that the pressure function is singular with respect to the layer thickness and depends only on the thermal parameters of the material.

http://rcin.org.pl

References

1. W. KOSIŃSKI and S. TABACOVA, *On the interface modelling of crystal growth processes.* Part I. *Thermostatic considerations*, Arch. Mech., **46**, 6, 839–854, 1994.
2. W. KOSIŃSKI, *A phenomenological approach to fluid-phase interfaces*, [in:] Modelling Macroscopic Phenomena at Liquid Boundaries, pp. 65–107, CISM, W. KOSIŃSKI & A.I. MURDOCH [Eds.], Springer Verlag, 1991.
3. B.A. BOLEY and J.H. WEINER, *Theory of thermal stresses*, John Wiley and Sons, Inc., New York – London 1960.
4. B. CHALMERS, *Principle of solidification*, Robert E. Kriger Publishing Company, Malabar, Florida 1982.

DEPARTMENT OF MECHANICS,
TECHNICAL UNIVERSITY - PLOVDIV,
61, Sankt Peterburg blvd., 4000 Plovdiv, BULGARIA
and
INSTITUTE OF FUNDAMENTAL TECHNOLOGICAL RESEARCH
POLISH ACADEMY OF SCIENCES
e-mail: wkos@ippt.gov.pl

Received November 4, 1996.

http://rcin.org.pl

Arch. Mech., 49, 2, pp. 421–441, Warszawa 1997

Internal variables in dynamics of composite solids with periodic microstructure

Dedicated to Professor Franz Ziegler on the occasion of His 60th birthday

Cz. WOŹNIAK (CZĘSTOCHOWA)

A NEW UNIFIED micromechanical approach to dynamics of micro-periodic composite solids is formulated. The proposed approach introduces the concept of internal variables in order to describe the effect of the microstructure size on the global body behaviour. It is shown that the evolution equation for internal variables can be obtained without any specification of the material properties of the composite.

1. Introduction

IT IS KNOWN that the behaviour of the composite solids with periodic microstructure can be examined on two levels. On the micro-level the interactions between constituents of a composite are detailed while the global body response is investigated in the framework of macromechanics. The passage from micro- to macromechanics is realized by so-called micromechanical approaches, [1], leading to various mathematical models of the composite solid on the macro-level. The best known ones are those based on the concept of homogeneous equivalent body where the micro-heterogeneous composite is modelled as made of a certain "homogenized" material. The above models can be obtained by some special procedures, [1, 12], derived by means of the asymptotic methods, [3, 5, 11], by the Fourier expansions, [23], or using so-called micro-local parameters, [15, 32]. However, following the concept of a homogeneous equivalent body we neglect the effect of the microstructure size on the global body behaviour. This effect plays an important role mainly in the vibration and wave propagation analysis. In order to describe dynamic problems in the framework of macromechanics, a number of mathematical models, mainly based on the concept of the continuum with extra local degrees of freedom, or obtained by finding the higher-order terms of the asymptotic expansions, was proposed, [2, 9, 14, 15, 22, 24]. Models of this kind have a rather complicated analytical form and, applied to the investigation of boundary-value problems, often lead to a large number of boundary conditions which may be not well motivated from the physical viewpoint. Between the models using the concept of a homogeneous equivalent body and those applying the continua with extra local degrees of freedom, are situated the models of

http://rcin.org.pl

refined macrodynamics, [32]. The effect of periodic microstructure size on the dynamic body behaviour in the framework of refined macrodynamics is described by certain unknown fields, called macro-internal variables (MIV). These variables, being governed by ordinary differential equations involving time derivatives, do not enter the boundary conditions. So far, the internal variables were mainly used in formulations of the constitutive relations, [7]. Applications of this concept to the micromechanical approach in dynamics of periodic composite solids were recently investigated in a series of papers [4, 6, 8, 10, 13, 16, 18–21, 26–30, 33–44].

In the aforementioned papers the micromechanical approach to macromechanics, using the macro-internal variables, was based on certain heuristic assumptions related to the specification of materials and the expected motions of the body. The aim of this contribution is to derive the governing equations for models with MIV without those assumptions. The main result is that the evolution equations for MIV can be obtained without any specification of the material properties of a composite solid. The considerations in Secs. 1–5 are restricted to the periodic composites. Certain generalization of the MIV-model, describing microstructures which may be non-periodic in some directions, are proposed in Sec. 6, where two kinds of what are called the quasi-internal variable models (QIV-models) are introduced. The investigations are related to composites with perfectly bonded constituents and are carried out in the framework of the small displacement gradient theory.

Throughout the paper all capital Roman superscripts run over $1, \ldots, N$ (summation convention holds unless otherwise stated). Points of the physical space E are denoted by $\mathbf{x}$, $\mathbf{y}$ or $\mathbf{z}$ and their distance by $\|\mathbf{x} - \mathbf{y}\|$. The letter t stands for the time coordinate and $t \in [t_0, t_f]$. By $|\ |$ we define both the absolute value of a real number and the length of a vector. It is assumed that all introduced functions satisfy the regularity conditions required in the subsequent analysis.

2. Analytical preliminaries

Let Ω be a region in the Euclidean 3-space E occupied by the composite solid in the reference configuration. Setting $Y := (-l_1/2, l_1/2) \times (-l_2/2, l_2/2) \times (-l_3/2, l_3/2)$ we assume that the solid in this configuration has the Y-periodic heterogeneous structure (is Y-periodic) and that the microstructure length parameter defined by $l := \sqrt{l_1^2 + l_2^2 + l_3^2}$ is negligibly small as compared to the smallest characteristic length dimension L_Ω of Ω. We shall use the notation $Y(\mathbf{x}) = \mathbf{x} + Y$; if $Y(\mathbf{x}) \subset \Omega$ then $Y(\mathbf{x})$ will be called the cell or the volume element of Ω. The set $\Omega_0 := \{\mathbf{x} \in \Omega;\ Y(\mathbf{x}) \subset \Omega\}$ is said to be the macro-interior of Ω. For an arbitrary integrable function $f(\cdot)$, defined almost everywhere on

http://rcin.org.pl

Ω, we define the averaged value of $f(\cdot)$ on $V(\mathbf{x})$ by means of

$$(2.1) \qquad <f(\mathbf{z})>(\mathbf{x}) = \frac{1}{l_1 l_2 l_3} \int_{V(\mathbf{x})} f(\mathbf{z})\, dv(\mathbf{z}), \qquad \mathbf{x} \in \Omega_0 .$$

If $f(\cdot)$ is a V-periodic function then $< f(\mathbf{z}) > (\mathbf{x})$ is a constant which will be denoted by $< f >$. Now we shall recall two auxiliary concepts which will be used in the subsequent analysis, [32].

Let $\Phi(\cdot)$ be a real-valued function defined on Ω, which represents a certain scalar field. Let us assume that the values of this field in the problem under consideration have to be calculated and/or measured up to a certain tolerance determined by the tolerance parameter ε_Φ, $\varepsilon_\Phi > 0$. It means that an arbitrary real number Φ_0 satisfying condition

$$|\Phi(\mathbf{x}) - \Phi_0| < \varepsilon_\Phi$$

can be also treated as describing with sufficient accuracy the value of this field at the point $\mathbf{x}$. The triple $(\Phi(\cdot), \varepsilon_\Phi, l)$ will be called the *ε-macrofunction* (related to the region Ω) if the following condition holds

$$(\forall (\mathbf{x}, \mathbf{y}) \in \Omega^2)\ [\|\mathbf{x} - \mathbf{y}\| < l \ \Rightarrow\ |\Phi(\mathbf{x}) - \Phi(\mathbf{y})| < \varepsilon_\Phi].$$

Roughly speaking, from both the calculation and measurement viewpoints, every ε-macrofunction restricted to an arbitrary cell $V(\mathbf{x})$, $\mathbf{x} \in \Omega_0$, can be treated as constant. Now assume that $\Phi(\cdot, t)$, $t \in [t_0, t_f]$, for every t is a differentiable function defined on Ω, having piecewise continuous time derivatives. Moreover, let Ψ stand for Φ as well as for an arbitrary derivative of Φ and assume that the value of Ψ has to be calculated and/or measured up to a certain tolerance given by the tolerance parameter ε_Ψ. If every triple $(\Psi(\cdot), \varepsilon_\Psi, l)$ is the ε-macrofunction, then the n-tuple $(\Phi(\cdot), \varepsilon_\Phi, \varepsilon_{\nabla\Phi}, \varepsilon_{\dot{\Phi}}, ..., l)$ is said to be the regular ε-macrofunction (related to the region Ω). In the sequel we shall tacitly assume that all tolerance parameters ε_Φ, $\varepsilon_{\nabla\Phi}$, $\varepsilon_{\dot{\Phi}}$, ..., as well as the microstructure length parameter l are known and hence $\Phi(\cdot)$ will be referred to as the regular ε-macrofunction. This concept will be also extended to vector and tensor functions by assuming that all their components in an arbitrary coordinate system are regular ε-macrofunctions.

To the concept of ε-macrofunction certain approximations are strictly related which will be used in this contribution. Let $f(\cdot)$ be an integrable function defined almost everywhere on Ω and $\Phi(\cdot)$ stand for an arbitrary ε-macrofunction (the tolerance parameter ε_Φ as well as the microstructure length parameter l are assumed to be known). Denote by $\mathcal{O}(\varepsilon_\Phi)$ a set of possible local increments $\Delta\Phi$ of Φ such that $|\Delta\Phi| < \varepsilon_\Phi$. Due to the meaning of the ε-macrofunction in calculations of integrals of the form

$$\int_{V(\mathbf{x})} f(\mathbf{z})[\Phi(\mathbf{z}) + \mathcal{O}(\varepsilon_\Phi)]dv, \qquad \mathbf{x} \in \Omega_0 ,$$

http://rcin.org.pl

terms $\mathcal{O}(\varepsilon_\Phi)$ can be neglected. This statement will be called the *Macro-Averaging Approximation* (MAA). Using the MAA we assign to every $f(\cdot)$ the tolerance relation $\approx$ (i.e., the binary relation which is reflexive and symmetric) defined on a set of integrals over $V(\mathbf{x})$ and given by

$$\int_{V(\mathbf{x})} f(\mathbf{z})[\Phi(\mathbf{z}) + \mathcal{O}(\varepsilon_\Phi)]dv \approx \int_{V(\mathbf{x})} f(\mathbf{z})\Phi(\mathbf{z})\,dv, \qquad \mathbf{x} \in \Omega_0. \tag{2.2}$$

Since

$$\int_{V(\mathbf{x})} f(\mathbf{z})dv\Phi(\mathbf{x}) = \int_{V(\mathbf{x})} f(\mathbf{z})[\Phi(\mathbf{z}) + \mathcal{O}(\varepsilon_\Phi)]dv,$$

where now $\mathcal{O}(\varepsilon_\Phi) = \Phi(\mathbf{x}) - \Phi(\mathbf{z})$ for every $\mathbf{z} \in V(\mathbf{x})$, then (2.1) yields

$$\int_{V(\mathbf{x})} f(\mathbf{z})\Phi(\mathbf{z})dv \approx \int_{V(\mathbf{x})} f(\mathbf{z})dv\Phi(\mathbf{z}), \qquad \mathbf{x} \in \Omega_0. \tag{2.3}$$

It has to be emphasized that terms $\mathcal{O}(\varepsilon_\Phi)$ will be neglected only in the course of averaging procedure, i.e., only in the tolerance relations of the form (2.2). Using the notation $\approx$ in (2.2) and (2.3), we have tacitly assumed that every tolerance relation $\approx$ is assigned to a certain integrable function $f(\cdot)$ and is not transitive. It means that in the formula

$$\int_{V(\mathbf{x})} f(\mathbf{z})\Phi_1(\mathbf{z})\Phi_2(\mathbf{z})dv \approx \int_{V(\mathbf{x})} f(\mathbf{z})\Phi_1(\mathbf{z})dv\Phi_2(\mathbf{x}) \approx \int_{V(\mathbf{x})} f(\mathbf{z})dv\Phi_1(\mathbf{x})\Phi_2(\mathbf{x}), \tag{2.4}$$

where $\Phi_1(\cdot)$, $\Phi_2(\cdot)$ are ε-macrofunctions, symbol $\approx$ stands for two different tolerance relations.

In order to introduce the second auxiliary concept used in the subsequent analysis, define by $h^A(\cdot)$, $A = 1, 2, \ldots$, the system of linear independent continuous V-periodic functions (and hence defined on E) having continuous first-order derivatives. Let the above functions satisfy conditions

$$< h^A >= 0, \qquad < h^A h^B >= \delta^{AB} l^2, \qquad (\forall \mathbf{x}) \left[|h^A(\mathbf{x})| \leq l \right]$$

and constitute a basis in the space of sufficiently regular functions defined on an arbitrary cell $V(\mathbf{x})$ and having on $V(\mathbf{x})$ the averaged values equal to zero. We also assume that for every $h^A(\cdot)$ there exists a V-periodic lattice Λ_A of points in E such that $h^A/_{\partial V(\mathbf{x})} = 0$ for every $\mathbf{x} \in \Lambda_A$. It means that $(\forall h^A)((\exists \mathbf{x})[h^A/_{\partial V(\mathbf{x})} = 0]$. Under the aforementioned conditions the system $h^A(\cdot)$, $A = 1, 2, \ldots$, will be called *the local oscillation basis*.

The concepts of the regular ε-macrofunction and the local oscillation basis as well as the macro-averaging approximation (MAA) formulated above constitute

http://rcin.org.pl

the fundamental tools of the micromechanical approach to the macrodynamics of composites which will be proposed in Secs. 3–5 of this contribution.

In Sec. 6 the aforementioned concepts and definitions will be adapted to the cases in which the composite solids have the periodic heterogeneous structures only in one or two directions. Setting $\Omega = \Pi \times (0, H)$, where Π stands for the plane region, we shall deal in Sec. 6 with ε-macrofunctions related to Π or $(0, H)$. Similarly, the functions $h^A(\cdot)$ will be defined either on $\mathbf{R}^2$ or on $\mathbf{R}$, and the averaging operation (2.1) will be restricted either to the area element or to the straight-line element.

3. Foundations of kinematics

Let $\mathbf{u}(\cdot, t)$ stand for a displacement field defined on Ω for every instant t. Define on Ω_0 the averaged displacement field by means of

$$\mathbf{U}(\mathbf{x}, t) := <\mathbf{u}(\mathbf{z}, t)>(\mathbf{x}), \qquad \mathbf{x} \in \Omega_0 . \tag{3.1}$$

By the local displacement oscillations we shall mean the vector functions $\mathbf{w}_\mathbf{x}(\cdot, t)$ defined independently on every $V(\mathbf{x})$, $\mathbf{x} \in \Omega_0$, such that

$$\mathbf{w}_\mathbf{x}(\mathbf{y}, t) = \mathbf{u}(\mathbf{y}, t) - \mathbf{U}(\mathbf{y}, t) + \mathbf{r}_\mathbf{x}(\mathbf{y}, t), \qquad \mathbf{y} \in V(\mathbf{x}), \tag{3.2}$$

where $\mathbf{r}_\mathbf{x}(\cdot)$ satisfy condition

$$<\mathbf{r}_\mathbf{x}(\mathbf{z}, t)> (\mathbf{y}) = <\mathbf{U}(\mathbf{z}, t)>(\mathbf{x}) - \mathbf{U}(\mathbf{x}, t),$$

and will be specified at the end of this section. It can be seen that

$$<\mathbf{w}_\mathbf{x}(\mathbf{z}, t)>(\mathbf{x}) = 0, \qquad \mathbf{x} \in \Omega_0 ,$$

and hence, under the known regularity conditions, every function $\mathbf{w}_\mathbf{x}(\cdot, t)$ can be represented by the Fourier series in the local oscillation basis $h^A(\cdot)$, $A = 1, 2, \ldots$. Denoting the Fourier coefficients by

$$\mathbf{W}^A(\mathbf{x}, t) := <\mathbf{w}_\mathbf{x}(\mathbf{z}, t) h^A(\mathbf{z})>(\mathbf{x}) l^{-2}, \qquad \mathbf{x} \in \Omega_0 , \tag{3.3}$$

we obtain

$$\mathbf{w}_\mathbf{x}(\mathbf{y}, t) = \sum_{A=1}^{\infty} \mathbf{W}^A(\mathbf{x}, t) h^A(\mathbf{y}), \qquad \mathbf{y} \in V(\mathbf{x}), \quad \mathbf{x} \in \Omega_0 . \tag{3.4}$$

The kinematics of the composites under consideration will be based on two assumptions.

Truncation Assumption (TA) states that the Fourier series (3.4) can be approximated by the sum of the first N terms for some $N \geq 1$, where N has to be specified in every problem under consideration.

http://rcin.org.pl

From TA it follows that instead of (3.4) we assume

$$\mathbf{w}_{\mathbf{x}}(\mathbf{y}, t) = \mathbf{W}^A(\mathbf{x}, t)h^A(\mathbf{y}), \qquad \mathbf{y} \in V(\mathbf{x}), \quad \mathbf{x} \in \Omega_0, \tag{3.5}$$

where here and in the sequel the Roman superscripts run over $1, ..., N$ (summation convention holds). The functions $h^A(\cdot)$, $A = 1, 2, ..., N$ are called *the micro-shape functions*.

Kinematic Macro-Regularity Assumption (KRA) restricts the class of motions in every problem under consideration by assuming that fields $\mathbf{U}(\cdot, t)$, $\mathbf{W}^A(\cdot, t)$, $A = 1, 2, ..., N$, are regular ε-macrofunctions.

It can be seen that the formulation of KRA takes into account TA by means of which the number N of the micro-shape function is postulated in every problem under consideration. Under the KRA, fields $\mathbf{U}(\cdot, t)$, $\mathbf{W}^A(\cdot, t)$, $A = 1, 2, ..., N$, are said to be *the macrodisplacements and the macro-internal variables* (MIV), respectively. The meaning of the term MIV will be explained in Sec. 5. The ε-macrofunctions $\mathbf{U}(\cdot, t)$, $\mathbf{W}^A(\cdot, t)$ describe the kinematics of composites on the macro-level (macro-kinematics) and will constitute the basic kinematic unknowns in the framework of the proposed model. The results of this section are summarized by the following lemma.

LEMMA. Under TA the displacements on the micro-level are related to the macrodisplacements and the macro-internal variables by the formulae

$$\mathbf{u}(\mathbf{y}, t) = \mathbf{U}(\mathbf{y}, t) + h^A(\mathbf{y})\mathbf{W}^A(\mathbf{y}, t). \tag{3.6}$$

The proof of the above lemma is based on the specification of fields $\mathbf{r}_{\mathbf{x}}(\cdot, t)$ in (3.2) to the form

$$\mathbf{r}_{\mathbf{x}}(\mathbf{y}, t) = h^A(\mathbf{y})\left[\mathbf{W}^A(\mathbf{x}, t) - \mathbf{W}^A(\mathbf{y}, t)\right], \qquad \mathbf{y} \in V(\mathbf{x}), \quad A = 1, ..., N. \tag{3.7}$$

Substituting the right-hand sides of (3.7) into (3.2) and using (3.5) we arrive at (3.6), which ends the proof.

COROLLARY. From the above lemma it follows that the MIV are related to the displacements $\mathbf{u}(\cdot, t)$ by means of the system of equations

$$< h^A(\mathbf{z})h^B(\mathbf{z})\mathbf{W}^B(\mathbf{z}, t) >(\mathbf{x}) = < [\mathbf{u}(\mathbf{z}, t) - \mathbf{U}(\mathbf{z}, t)]h^A(\mathbf{z}) >(\mathbf{x}), \qquad \mathbf{x} \in \Omega_0,$$

which under KRA and MAA can be replaced by

$$\mathbf{W}^A(\mathbf{x}, t) > = < \mathbf{u}(\mathbf{z}, t)h^A(\mathbf{z}) >(\mathbf{x}), \qquad \mathbf{x} \in \Omega_0. \tag{3.8}$$

Formula (3.8) yields the simple interpretation of the macro-internal variables as certain weighted averages of displacements.

http://rcin.org.pl

4. From micro- to macrodynamics

Let $\mathbf{s}(\cdot, t)$ denote the Cauchy stress tensor field defined for every t on $\Omega \backslash \Gamma$ where Γ is a set of all interfaces between the components of the composite. Let us define on Ω_0 the following averaged stress fields

$$
\begin{aligned}
&\mathbf{S}(\mathbf{x}, t) := <\mathbf{s}(\mathbf{z}, t)>(\mathbf{x}), \\
&\mathbf{H}^A(\mathbf{x}, t) := <\mathbf{s}(\mathbf{z}, t) \cdot \nabla h^A(\mathbf{z})>(\mathbf{x}), \qquad \mathbf{x} \in \Omega_0 .
\end{aligned} \tag{4.1}
$$

In order to pass from micro- to macrodynamics, two extra assumptions will be required.

Stress Macro-Regularity Assumption (SRA) restricts the class of stress fields in the problem under consideration to that in which the fields $\mathbf{S}(\cdot, t)$, $\mathbf{H}^A(\cdot, t)$ are regular ε-macrofunctions.

Under SRA the fields defined by (4.1) will be called *the macrostresses* and *the micro-dynamic forces*, respectively. The meaning of the latter term will be explained at the end of this section.

Let $\varrho(\cdot)$ stand for the mass density field (which is the V-periodic function defined almost everywhere on Ω), and assume that the body force $\mathbf{b}$ is constant. Let us denote by $\mathbf{n}(\mathbf{y})$ the unit normal outward to $\partial V(\mathbf{x})$ at $\mathbf{y}$. The starting point of the proposed micromechanical procedure will be the weak form of equations of motion in micromechanics. Taking into account the symmetry of the stress tensor, these equations can be assumed in the form of conditions

$$
\begin{aligned}
\int_{V(\mathbf{x})} \mathbf{s}(\mathbf{y}, t) : \nabla \overline{\mathbf{u}}(\mathbf{y})\, dv = \oint_{\partial V(\mathbf{x})} [\mathbf{s}(\mathbf{y}, t) \cdot \mathbf{n}(\mathbf{y})] \cdot \overline{\mathbf{u}}(\mathbf{y})\, da \\
+ \int_{V(\mathbf{x})} \varrho(\mathbf{y}) \left[\mathbf{b} - \ddot{\mathbf{u}}\,(\mathbf{y}, t)\right] \cdot \overline{\mathbf{u}}(\mathbf{y})\, dv
\end{aligned} \tag{4.2}
$$

which have to hold for every $\mathbf{x} \in \Omega_0$ and for an arbitrary test function $\overline{\mathbf{u}}(\cdot)$. In order to pass from micro- to macrodynamics we have to specify the set of test functions in (4.2). Taking into account (3.6) we assume that

$$
\overline{\mathbf{u}}(\mathbf{y}) = \overline{\mathbf{U}}(\mathbf{y}) + h^A(\mathbf{y}) \overline{\mathbf{W}}^A(\mathbf{y}), \tag{4.3}
$$

where $\overline{\mathbf{U}}(\cdot)$, $\overline{\mathbf{W}}^A(\cdot)$ are arbitrary linearly independent regular ε-macrofunctions defined on Ω.

Now we shall explain the meaning of the micro-shape functions in the modelling procedure. To this end denote $\Gamma(\mathbf{x}) := V(\mathbf{x}) \cap \Gamma$, $\mathbf{x} \in \Omega_0$. Hence $\Gamma(\mathbf{x})$ is a set of all interfaces in the volume element $V(\mathbf{x})$ across which the tensor $\mathbf{s}(\cdot, t)$ can suffer jump discontinuities. Let us also introduce the residual fields in every

http://rcin.org.pl

cell $V(\mathbf{x})$ given by

$$\mathbf{r}(\mathbf{y},t) := \varrho(\mathbf{y})\,\ddot{\mathbf{u}}\,(\mathbf{y},t) - \varrho(\mathbf{y})\mathbf{b} - \operatorname{Div}\mathbf{s}(\mathbf{y},t) \quad \text{if} \quad \mathbf{y} \in V(\mathbf{x})\backslash\Gamma(\mathbf{x}),$$
$$\mathbf{j}(\mathbf{y},t) := [\mathbf{s}](\mathbf{y},t)\cdot\mathbf{n}(\mathbf{y}) \quad \text{if} \quad \mathbf{y} \in \Gamma(\mathbf{x}), \quad \mathbf{x} \in \Omega_0,$$

where $[\mathbf{s}]$ is a jump of the stress tensor across $\Gamma(\mathbf{x})$ in the direction of the unit normal $\mathbf{n}(\mathbf{y})$ to $\Gamma(\mathbf{x})$. Obviously, in the framework of micromechanics the residual fields are identically equal to zero. It can be verified that, under the above notations, Eqs. (4.2) can be written in the equivalent form of conditions

$$\int_{V(\mathbf{x})} \mathbf{r}\cdot\bar{\mathbf{u}}\,dv + \int_{\Gamma(\mathbf{x})} \mathbf{j}\cdot\bar{\mathbf{u}}\,da = 0, \qquad \mathbf{x} \in \Omega_0,$$

which have to hold for an arbitrary test function $\bar{\mathbf{u}}(\cdot)$ defined on Ω. In the framework of the proposed approach, we shall assume that the piecewise constant (discontinuous across Γ) distribution of heterogeneity is approximated in the vicinity of interfaces by the continuous one. Hence $\Gamma = \emptyset$ and the integrals over $\Gamma(\mathbf{x})$ drop out. Taking into account (4.3) and using MAA, the above conditions reduce to the following ones

$$\int_{V(\mathbf{x})} \mathbf{r}\,dv = 0, \qquad \int_{V(\mathbf{x})} \mathbf{r}h^A\,dv = 0, \qquad A = 1,\ldots,N, \quad \mathbf{x} \in \Omega_0.$$

The second of the above formulae represents the interrelation between the residual field $\mathbf{r}$ and the form and number of the micro-shape functions. More general models will be presented in the separate paper.

Taking into account the above approximation we shall formulate the fundamental assertion of the micromechanical approach to macrodynamics proposed in this contribution. For the sake of simplicity we shall also assume that the micro-shape functions $h^A(\cdot)$ satisfy the extra conditions $<\varrho h^A>= 0$, $A = 1,\ldots,N$.

Fundamental Assertion. Under TA, KRA, SRA and in the framework of MAA, the equations of motion (4.2) imply the following interrelation between the macrodisplacements $\mathbf{U}(\cdot,t)$ and the macrostresses $\mathbf{S}(\cdot,t)$:

$$\operatorname{Div}\mathbf{S}(\mathbf{x},t) - <\varrho>\ddot{\mathbf{U}}\,(\mathbf{x},t) + <\varrho>\mathbf{b} = 0, \tag{4.4}$$

as well as between the macro-internal parameters $\mathbf{W}^A(\cdot,t)$ and the micro-dynamic forces $\mathbf{H}^A(\cdot,t)$:

$$<\varrho h^A h^B>\ddot{\mathbf{W}}^B(\mathbf{x},t) + \mathbf{H}^A(\mathbf{x},t) = 0, \qquad A = 1,\ldots,N; \tag{4.5}$$

the above relations hold for every $\mathbf{x} \in \Omega_0$ and $t \in (t_0, t_f)$.

http://rcin.org.pl

The relations given by (4.4), (4.5) will be called *the equations of motion* and *the dynamic evolution equations*, respectively. Since the moduli $< \varrho h^A h^B >$ are of the order $\mathcal{O}(l^2)$, then the above equations describe the effect of the microstructure size l on the body dynamic response. For this reason Eqs. (4.4), (4.5) are said to represent *the refined macrodynamics* of the composites under consideration, [30]. Let us observe that both in the quasi-stationary processes and for the problems in which the above effect can be neglected we obtain $\mathbf{H}^A(\mathbf{x}, t) = 0$. That is why the fields defined by the second of Eqs. (4.1) were called the micro-dynamic forces. It has to be emphasized that under the aforementioned assumptions, Eqs. (4.4), (4.5) are related to a composite solid with periodic microstructure made of arbitrary materials. Hence, the aforementioned equations represent the averaged laws of motion in the framework of the proposed refined macrodynamics.

At the end of this section we shall prove the fundamental assertion. To this end let us substitute the right-hand side of (4.3) into (4.2). Using (2.1) we obtain

$$
\begin{aligned}
&\int\limits_{V(\mathbf{x})} \mathbf{s}(\mathbf{y}, t) \,:\, \nabla \overline{\mathbf{u}}(\mathbf{y})\, dv = \int\limits_{V(\mathbf{x})} \mathbf{s}(\mathbf{y}, t) \,:\, \nabla \overline{\mathbf{U}}(\mathbf{y})\, dv \\
&\qquad + \int\limits_{V(\mathbf{x})} \left[\nabla h^A(\mathbf{y}) \cdot \mathbf{s}(\mathbf{y}, t)\right] \cdot \overline{\mathbf{W}}^A(\mathbf{y})\, dv, \\
&\oint\limits_{\partial V(\mathbf{x})} \left[\mathbf{s}(\mathbf{y}, t) \cdot \mathbf{n}(\mathbf{y})\right] \cdot \overline{\mathbf{u}}(\mathbf{y})\, da \approx \oint\limits_{\partial V(\mathbf{x})} \left[\mathbf{s}(\mathbf{y}, t) \cdot \mathbf{n}(\mathbf{y})\right] \cdot \overline{\mathbf{U}}(\mathbf{y})\, da \\
&\qquad + \oint\limits_{\partial V(\mathbf{x})} h^A(\mathbf{y}) \left[\mathbf{s}(\mathbf{y}, t) \cdot \mathbf{n}(\mathbf{y})\right] \cdot \overline{\mathbf{W}}^A(\mathbf{y})\, da, \\
&\int\limits_{V(\mathbf{x})} \varrho(\mathbf{y}) \left[\mathbf{b} - \ddot{\mathbf{u}}\,(\mathbf{y}, t)\right] \cdot \overline{\mathbf{u}}(\mathbf{y})\, dv \approx \int\limits_{V(\mathbf{x})} \varrho(\mathbf{y}) \left[\mathbf{b} - \ddot{\mathbf{u}}\,(\mathbf{y}, t)\right] \cdot \overline{\mathbf{U}}(\mathbf{y})\, dv \\
&\qquad + \int\limits_{V(\mathbf{x})} \varrho(\mathbf{y}) h^A(\mathbf{y}) \left[\mathbf{b} - \ddot{\mathbf{u}}\,(\mathbf{y}, t)\right] \cdot \overline{\mathbf{W}}^A(\mathbf{y})\, dv.
\end{aligned}
\tag{4.6}
$$

Combining (4.6) and (4.2) and bearing in mind that $\overline{\mathbf{U}}(\cdot)$, $\overline{\mathbf{W}}^A(\cdot)$ are linearly independent ε-macrofunctions, we conclude that the equations of motion (4.2) imply the following conditions

$$
\begin{aligned}
\int\limits_{V(\mathbf{x})} \mathbf{s}(\mathbf{y}, t) \,:\, \nabla \overline{\mathbf{U}}(\mathbf{y})\, dv &= \oint\limits_{\partial V(\mathbf{x})} \left[\mathbf{s}(\mathbf{y}, t) \cdot \mathbf{n}(\mathbf{y})\right] \cdot \overline{\mathbf{U}}(\mathbf{y})\, da \\
&\quad + \int\limits_{V(\mathbf{x})} \varrho(\mathbf{y}) \left[\mathbf{b} - \ddot{\mathbf{u}}\,(\mathbf{y}, t)\right] \cdot \overline{\mathbf{U}}(\mathbf{y})\, dv,
\end{aligned}
\tag{4.7}
$$

http://rcin.org.pl

(4.7) [cont.]
$$\int_{V(\mathbf{x})} \left[\mathbf{s}(\mathbf{y},t)\cdot\nabla h^A(\mathbf{y})\right]\cdot\overline{\mathbf{W}}^A(\mathbf{y})\,dv = \oint_{\partial V(\mathbf{x})} [\mathbf{s}(\mathbf{y},t)\cdot\mathbf{n}(\mathbf{y})]\cdot\overline{\mathbf{W}}^A(\mathbf{y})h^A(\mathbf{y})\,da + \int_{V(\mathbf{x})} \varrho(\mathbf{y})\left[\mathbf{b}-\ddot{\mathbf{u}}\,(\mathbf{y},t)\right]\cdot\overline{\mathbf{W}}^A(\mathbf{y})h^A(\mathbf{y})\,dv, \qquad \mathbf{x}\in\Omega_0,$$

which have to hold for arbitrary regular ε-macrofunctions $\overline{\mathbf{U}}(\cdot)$, $\overline{\mathbf{W}}^A(\cdot)$ defined on Ω. By means of (2.2), (2.1) and bearing in mind the remark following (2.3), the integrals on the left-hand sides of (4.7) can be transformed as follows

(4.8)
$$\begin{aligned}\int_{V(\mathbf{x})} \mathbf{s} : \nabla\overline{\mathbf{U}}(\mathbf{y})\,dv &\approx \int_{V(\mathbf{x})} \mathbf{s}\,dv : \nabla\overline{\mathbf{U}}(\mathbf{x}) = l_1l_2l_3\mathbf{S}(\mathbf{x},t) : \nabla\overline{\mathbf{U}}(\mathbf{x})\\ &\approx \int_{V(\mathbf{x})} \mathbf{S}\,dv : \nabla\overline{\mathbf{U}}(\mathbf{x}) \approx \int_{V(\mathbf{x})} \mathbf{S} : \nabla\overline{\mathbf{U}}\,dv\\ &= \oint_{\partial V(\mathbf{x})} (\mathbf{S}\cdot\mathbf{n})\cdot\overline{\mathbf{U}}\,dv - \int_{V(\mathbf{x})} \operatorname{Div}\mathbf{S}\cdot\overline{\mathbf{U}}\,dv,\end{aligned}$$
$$\int_{V(\mathbf{x})} (\mathbf{s}\cdot\nabla h^A)\overline{\mathbf{W}}^A\,dv \approx \int_{V(\mathbf{x})} (\mathbf{s}\cdot\nabla h^A)\,dv\cdot\overline{\mathbf{W}}^A(\mathbf{x}) \approx \int_{V(\mathbf{x})} \mathbf{H}^A\cdot\overline{\mathbf{W}}^A\,dv.$$

For the sake of simplicity, in (4.8) and in the subsequent formulas the argument $\mathbf{y}\in V(\mathbf{x})$ is not specified in all integrands. Using (2.2) and the first of formulas (3.7) as well as the conditions $<\varrho h^A>=0$, $<h^A>=0$, the integrals over $V(\mathbf{x})$ on the right-hand sides of (4.7) can be given

$$\begin{aligned}\int_{V(\mathbf{x})} \varrho(\mathbf{b}-\ddot{\mathbf{u}})\cdot\overline{\mathbf{U}}\,dv &\approx \int_{V(\mathbf{x})} \varrho\,dv\,\mathbf{b}\cdot\overline{\mathbf{U}}(\mathbf{x}) - \int_{V(\mathbf{x})} \varrho(\ddot{\mathbf{U}} + h^A\,\ddot{\mathbf{W}}^A)\,dv\cdot\overline{\mathbf{U}}(\mathbf{x})\\ &\approx l_1l_2l_3\left[<\varrho>\mathbf{b}\cdot\overline{\mathbf{U}}(\mathbf{x}) - <\varrho>\ddot{\mathbf{U}}\,(\mathbf{x},t)\cdot\overline{\mathbf{U}}(\mathbf{x})\right]\\ &\approx \int_{V(\mathbf{x})} <\varrho>(\mathbf{b}-\ddot{\mathbf{U}})\cdot\overline{\mathbf{U}}\,dv,\end{aligned}$$

(4.9)
$$\begin{aligned}\int_{V(\mathbf{x})} \varrho(\mathbf{b}-\ddot{\mathbf{u}})\cdot\overline{\mathbf{W}}^{\mathbf{A}}h^A\,dv &\approx \int_{V(\mathbf{x})} \varrho h^A\,dv\,\mathbf{b}\cdot\overline{\mathbf{W}}^{\mathbf{A}}(\mathbf{x})\\ &- \int_{V(\mathbf{x})} \varrho(\ddot{\mathbf{U}} + h^B\,\ddot{\mathbf{W}}^B)h^A\,dv\cdot\overline{\mathbf{W}}^{\mathbf{A}}(\mathbf{x}) \approx \int_{V(\mathbf{x})} \varrho h^A\,dv\;\ddot{\mathbf{U}}\,(\mathbf{x},t)\cdot\overline{\mathbf{W}}^{\mathbf{A}}(\mathbf{x})\\ &- \int_{V(\mathbf{x})} \varrho h^Ah^B\,dv\;\ddot{\mathbf{W}}^B(\mathbf{x},t)\cdot\overline{\mathbf{W}}^{\mathbf{A}}(\mathbf{x}) \approx \int_{V(\mathbf{x})} <\varrho h^Ah^B>\ddot{\mathbf{W}}^B\cdot\overline{\mathbf{W}}^{\mathbf{A}}\,dv.\end{aligned}$$

http://rcin.org.pl

Taking into account (4.8) and (4.9) we shall represent (4.7) in the form

$$
\begin{aligned}
&\int_{V(\mathbf{x})} \left(\operatorname{Div}\mathbf{S} - <\varrho>\ddot{\mathbf{U}} + <\varrho>\mathbf{b}\right)\cdot\overline{\mathbf{U}}\,dv - \oint_{\partial V(\mathbf{x})} (\mathbf{S}\cdot\mathbf{n} - \mathbf{s}\cdot\mathbf{n})\cdot\overline{\mathbf{U}}\,da = 0,\\
&\int_{V(\mathbf{x})} \left(<\varrho h^A h^B>\ddot{\mathbf{W}}^B + \mathbf{H}^A\right)\overline{\mathbf{W}}^A\,dv - \oint_{\partial V(\mathbf{x})} (\mathbf{s}\cdot\mathbf{n})h^A\cdot\overline{\mathbf{W}}^{\mathbf{A}}\,da = 0.
\end{aligned}
\tag{4.10}
$$

The first of equations (4.10) has to hold for every $\overline{\mathbf{U}}(\cdot)$ and the second one for every $\overline{\mathbf{W}}^A(\cdot)$. Moreover, $\overline{\mathbf{U}}(\cdot)$, $\overline{\mathbf{W}}^A(\cdot)$, $\operatorname{Div}\mathbf{S}(\cdot,t)$, $\mathbf{H}^A(\cdot,t)$ and $\ddot{\mathbf{U}}(\cdot,t)$, $\ddot{\mathbf{W}}^B(\cdot,t)$ are ε-macrofunctions. It follows that using MAA, from Eqs. (4.10) we obtain

$$
\begin{aligned}
&l_1 l_2 l_3\left[\operatorname{Div}\mathbf{S}(\mathbf{x},t) - <\varrho>\ddot{\mathbf{U}}(\mathbf{x},t) + <\varrho>\mathbf{b}\right]\cdot\overline{\mathbf{U}}(\mathbf{x})\\
&\qquad - \oint_{\partial V(\mathbf{x})} (\mathbf{S}\cdot\mathbf{n} - \mathbf{s}\cdot\mathbf{n})\cdot\overline{\mathbf{U}}\,da = 0,\\
&l_1 l_2 l_3\left[<\varrho h^A h^B>\ddot{\mathbf{W}}^B(\mathbf{x},t) + \mathbf{H}^A(\mathbf{x},t)\right]\cdot\overline{\mathbf{W}}^A(\mathbf{x})\\
&\qquad - \oint_{\partial V(\mathbf{x})} (\mathbf{s}\cdot\mathbf{n})\cdot\overline{\mathbf{W}}^A h^A\,da = 0.
\end{aligned}
\tag{4.11}
$$

Introducing the local coordinate $\mathbf{p}\in V$ we also obtain

$$
\begin{aligned}
\oint_{\partial V(\mathbf{x})} (\mathbf{S}\cdot\mathbf{n})\cdot\overline{\mathbf{U}}\,da &= \int_{V(\mathbf{x})} \operatorname{Div}(\mathbf{S}\cdot\overline{\mathbf{U}})\,dv \approx l_1 l_2 l_3 \operatorname{Div}\left[\mathbf{S}(\mathbf{x},t)\cdot\overline{\mathbf{U}}(\mathbf{x})\right]\\
&\approx \operatorname{Div}\int_{V(\mathbf{x})} \mathbf{s}\cdot\overline{\mathbf{U}}\,dv = \operatorname{Div}_{\mathbf{x}}\int_V \mathbf{s}(\mathbf{x}+\mathbf{p},t)\cdot\overline{\mathbf{U}}(\mathbf{x}+\mathbf{p},t)\,dv(\mathbf{p})\\
&= \int_V \operatorname{Div}_{\mathbf{x}}\left[\mathbf{s}(\mathbf{x}+\mathbf{p},t)\cdot\overline{\mathbf{U}}(\mathbf{x}+\mathbf{p},t)\right]dv(\mathbf{p})\\
&= \int_{V(\mathbf{x})} \operatorname{Div}(\mathbf{s}\cdot\overline{\mathbf{U}})dv = \oint_{\partial V(\mathbf{x})} (\mathbf{s}\cdot\mathbf{n})\cdot\overline{\mathbf{U}}\,da.
\end{aligned}
\tag{4.12}
$$

Hence, the surface integral in the first of equations (4.11) can be neglected and we arrive at (4.4). Bearing in mind that $\ddot{\mathbf{W}}^B(\cdot,t)$, $\overline{\mathbf{W}}^A(\cdot)$ and $\mathbf{H}^A(\cdot,t)$ are ε-macrofunctions, we conclude that the surface integrals in the second of equation (4.11) are values of a certain ε-macrofunction; at the same time $h^A = 0$ on $\partial V(\mathbf{x})$ for every $\mathbf{x}\in\Lambda_A$, cf. Sec. 2. It follows that for an arbitrary $\mathbf{x}\in\Omega_0$ the above surface integrals attain the values which in the framework of MAA can be neglected. Hence the second equation (4.11) reduces to (4.5), which ends the proof. An alternative proof of the above fundamental assertion can be found in [35].

http://rcin.org.pl

5. MIV-model

In order to describe the dynamic response of the composite body in the framework of the MIV-model, we have to complete equations (4.4), (4.5) by introducing the constitutive equations for macrostresses $\mathbf{S}$ and micro-dynamic forces $\mathbf{H}^A$. Taking into account the definitions (4.1), the second of the formulae (3.7) and applying MAA to the integrals in (4.1), this can be done for arbitrary periodic composites the components of which are simple materials. To simplify the subsequent considerations we shall restrict ourselves to the linear visco-elastic materials governed by the constitutive equations of the form

$$\mathbf{s} = \mathbf{C}(\mathbf{z}) : \mathbf{e} + \mathbf{D}(\mathbf{z}) : \dot{\mathbf{e}}, \qquad \mathbf{e} := 0.5\left[\nabla\mathbf{u} + (\nabla\mathbf{u})^T\right], \tag{5.1}$$

where $\mathbf{C}(\cdot)$, $\mathbf{D}(\cdot)$ are Y-periodic piecewise constant functions the values of which are the fourth order tensors of elastic and viscous moduli, respectively, for the component materials. Define the linearized macro-strain tensor by means of

$$\mathbf{E}(\mathbf{x}, t) := 0.5\left[\nabla\mathbf{U}(\mathbf{x}, t) + (\nabla\mathbf{U}(\mathbf{x}, t))^T\right]. \tag{5.2}$$

Now, we shall prove that the following formula holds for an arbitrary sufficiently regular Y-periodic tensor field $\mathbf{F}(\cdot)$:

$$< \mathbf{F}\cdot\nabla(h^A\mathbf{W}^A) > (\mathbf{x}) \approx < \mathbf{F}\cdot\nabla h^A > \otimes\mathbf{W}^A(\mathbf{x}). \tag{5.3}$$

To this end let us observe that

$$< \mathbf{F}\cdot\nabla h^A > (\mathbf{x}) = -\frac{1}{|\mathbf{Y}|}\int\limits_{\Gamma(\mathbf{x})} h^A[\mathbf{F}]\cdot\mathbf{n}\, da - < h^A \operatorname{Div}\mathbf{F} > (\mathbf{x}), \tag{5.4}$$

where $[\mathbf{F}]$ is a jump of $\mathbf{F}$ across all interfaces $\Gamma(\mathbf{x})$, oriented by a unit normal $\mathbf{n}$ in $Y(\mathbf{x})$. At the same time, for every A we obtain (no summation over A!)

$$\begin{aligned} < \mathbf{F}\cdot\nabla(h^A\mathbf{W}^A) > (\mathbf{x}) &= < \operatorname{Div}(\mathbf{F}\otimes\mathbf{W}^A h^A) > (\mathbf{x}) - < \operatorname{Div}\mathbf{F}\otimes\mathbf{W}^A h^A > \\ &\approx \frac{1}{|\mathbf{Y}|}\oint\limits_{\partial Y(\mathbf{x})} h^A(\mathbf{F}\cdot\mathbf{n})\otimes\mathbf{W}^A\, da \\ &+ \left(\frac{1}{|\mathbf{Y}|}\int\limits_{\Gamma(\mathbf{x})} h^A[\mathbf{F}]\cdot\mathbf{n}\, da - < h^A\operatorname{Div}\mathbf{F} > (\mathbf{x})\right)\otimes\mathbf{W}^A(\mathbf{x}, t). \end{aligned} \tag{5.5}$$

For every $\mathbf{x}\in\Lambda_A$ the value of the first integral on the right-hand side of (5.5) is equal to zero. At the same time, this integral represents a certain ε-macrofunction defined on Ω_0 (since $\mathbf{W}^A(\cdot, t)$ is the ε-macrofunction) and hence bearing in mind

http://rcin.org.pl

(5.4), we conclude that (5.3) holds true, which ends the proof. Using this result we also have

$$(5.6) \qquad <\mathbf{F}\cdot\nabla h^A>\cdot\mathbf{W}^A(\mathbf{x},t)+<\mathbf{F}h^A>:\nabla\mathbf{W}^A(\mathbf{x},t)\approx<\mathbf{F}\cdot\nabla h^A>\cdot\mathbf{W}^A(\mathbf{x},t).$$

Substituting (5.1) into definitions (4.1), taking into account the second of equations (3.7) and using MAA, by means of (5.6) we obtain

$$(5.7) \quad \begin{aligned} \mathbf{S}(\mathbf{x},t) &= <\mathbf{C}>:\mathbf{E}(\mathbf{x},t)+<\mathbf{C}\cdot\nabla h^A>\cdot\mathbf{W}^A(\mathbf{x},t) \\ &\quad + <\mathbf{D}>:\dot{\mathbf{E}}(\mathbf{x},t)+<\mathbf{D}\cdot\nabla h^A>\cdot\dot{\mathbf{W}}^A(\mathbf{x},t), \\ \mathbf{H}^A(\mathbf{x},t) &= <\nabla h^A\cdot\mathbf{C}>:\mathbf{E}(\mathbf{x},t)+<\nabla h^A\cdot\mathbf{C}\cdot\nabla h^B>\cdot\mathbf{W}^B(\mathbf{x},t) \\ &\quad + <\nabla h^A\cdot\mathbf{D}>:\dot{\mathbf{E}}(\mathbf{x},t)+<\nabla h^A\cdot\mathbf{D}\cdot\nabla h^B>\cdot\dot{\mathbf{W}}^B(\mathbf{x},t), \end{aligned}$$

for every $\mathbf{x}\in\Omega_0$ and $t\in(t_0,t_f)$. The above equations will be referred to as the macro-constitutive equations for the linear visco-elastic composites.

Equations (4.4), (4.5) and (5.2), (5.7) represent the macro-internal variable model (MIV-model) of micro-periodic composites made of perfectly bonded visco-elastic constituents. For the linear elastic materials the above equations reduce to those of the refined macromechanics, which were obtained independently in [30] by means of certain heuristic hypotheses. For every micro-periodic composite solid (with constituents modelled as simple materials) the proposed model is uniquely determined by the choice of the micro-shape functions $h^A(\cdot)$, $A=1,\ldots,N$.

It has to be emphasized that for every class of motions specified by conditions (3.6), we obtain the pertinent MIV-model. In the analysis of special problems we have to take into account only these classes of motions which seem to be relevant from the viewpoint of the engineering applications of the theory.

Substituting the right-hand sides of Eqs. (5.7) into (4.4), (4.5), we obtain the system of three partial differential equations for the macrodisplacements $\mathbf{U}$ coupled with the system of $3N$ ordinary differential equations for the macro-internal variables $\mathbf{W}^A$. Hence, in formulations of the initial-boundary value problems, unknowns $\mathbf{W}^A(\cdot,t)$ do not enter the boundary conditions. That is why they were called the macro-internal variables (MIV). It can be shown that for homogeneous bodies and homogeneous initial conditions for MIV, we obtain the trivial solution $\mathbf{W}^A=\mathbf{0}$, $A=1,\ldots,N$, to every boundary value problem. Hence, the macro-internal variables play a crucial role in a description of the dynamic behaviour of solids with periodic microstructure, and that is why the models proposed were referred to as the macro-internal variable models. It has to be emphasized that solutions to special problems in the framework of MIV-models have the physical sense only if the fields $\mathbf{U}(\cdot,t)$, $\mathbf{W}^A(\cdot,t)$ as well as $\mathbf{S}(\cdot,t)$, $\mathbf{H}^A(\cdot,t)$, for every instant t, are the regular ε-macrofunctions. This requirement can be verified only *a posteriori*.

http://rcin.org.pl

6. QIV-models

The MIV-model can be applied to composites which are periodic along every coordinate axis appearing in the problem under consideration. It means that the above models are applicable also to plane problems or to one-dimensional problems, provided that the corresponding basic cell of the composite is plane or one-dimensional, respectively. However, MIV-models cannot be applied if the dimension of the cell is smaller than the number of spatial coordinates in the problem under consideration. In this case the micro-shape functions are independent of some of the spatial coordinates, and hence the surface integral in the second Eqs. (4.11) cannot be neglected and the formula (5.3) does not hold. In this section we shall modify the previously obtained results for two important special types of composite materials.

6.1. Composites reinforced by a system of parallel fibres

Let $\Omega = \Pi \times (0, H)$, where Π is a regular region on the plane $0x_1x_2$. Assume that the composite has a material structure periodic only in the directions of the x_1-axis and x_2-axis. Let l_1, l_2 stand for the corresponding periods and define $A \equiv (-l_1/2, l_1/2) \times (-l_2/2, l_2/2)$. Such situation takes place, e.g., for composites reinforced by a system of periodically distributed fibres parallel to the x_3-axis. In these cases we shall deal with the A-periodic composites. Setting $\mathbf{X} := (x_1, x_2)$ and $A(\mathbf{X}) := \mathbf{X} + A$, we define the averaging operator on $A(\mathbf{X})$ given by

$$(6.1) \qquad < f(\mathbf{z}, t) > (\mathbf{x}) := \frac{1}{l_1 l_2} \int\limits_{A(\mathbf{X})} f(z_1, z_2, x_3, t)\, dz_1\, dz_2\,,$$

which will be used throughout this subsection. Denoting $l = \sqrt{(l_1)^2 + (l_2)^2}$ we introduce the concept of ε-macrofunction (related to the region Π) as a function $\Phi(\cdot)$ defined on Π and such that

$$(\forall\, (\mathbf{X}, \mathbf{Y}) \in (\Pi)^2)[\|\mathbf{X} - \mathbf{Y}\| < l \;\Rightarrow\; |\Phi(\mathbf{X}) - \Phi(\mathbf{Y})| < \varepsilon_\Phi].$$

A function Φ can also depend on x_3 and/or t as parameters. Moreover, the micro-shape functions $h^A(\cdot)$ are now independent of the x_3-coordinate since the disturbances in displacements caused by the micro-periodic heterogeneity of the medium take place only in the x_α-axes directions, $\alpha = 1, 2$. The equations of motion for the class of composites under consideration can be obtained from Eqs. (4.11) by setting $V = A \times (-\delta, \delta)$, $\delta > 0$ and passing with δ to zero, $\delta \to 0$. Let $\mathbf{a}_3$ be the versor (unit vector) of the x_3-axis. Introducing kinematic fields averaged over $A(\mathbf{X})$

$$(6.1') \qquad \mathbf{U}(\mathbf{x}, t) := <\mathbf{u}(\mathbf{z}, t)>(\mathbf{x}), \qquad \mathbf{W}^A(\mathbf{x}, t) := <\mathbf{w}_\mathbf{x}(\mathbf{z}, t) h^A(\mathbf{Z})>(\mathbf{x}) l^{-2},$$

http://rcin.org.pl

and the stress fields averaged over $A(\mathbf{X})$

$$
\begin{aligned}
\mathbf{S}(\mathbf{x},t) &:= <\mathbf{s}(\mathbf{z},t)>(\mathbf{x}),\\
\mathbf{H}^A(\mathbf{x},t) &:= <\mathbf{s}(\mathbf{z},t)\cdot\nabla h^A(\mathbf{Z})>(\mathbf{x}),\\
\mathbf{R}^A{}_3(\mathbf{x},t) &:= <\mathbf{a}_3\cdot\mathbf{s}(\mathbf{z},t)h^A(\mathbf{Z})>(\mathbf{x}),
\end{aligned}
\tag{6.2}
$$

we shall assume that $\mathbf{U}(\cdot,x_3,t),\ldots,\mathbf{R}^A{}_3(\cdot,x_3,t)$ are regular ε-macrofunctions (related to Π) for every $x_3\in(0,H)$, $t\in(t_0,t_f)$. From (4.11), after some manipulations we obtain

$$
\begin{aligned}
&\operatorname{Div}\mathbf{S}(\mathbf{x},t)-<\varrho>(x_3)\,\ddot{\mathbf{U}}(\mathbf{x},t)+<\varrho>(x_3)\mathbf{b}=\mathbf{0},\\
&-\mathbf{R}^A{}_{3,3}(\mathbf{x},t)+<\varrho h^A h^B>(x_3)\,\ddot{\mathbf{W}}^{\mathbf{B}}(\mathbf{x},t)+\mathbf{H}^A(\mathbf{x},t)=\mathbf{0}.
\end{aligned}
\tag{6.3}
$$

For the sake of simplicity let us confine ourselves to the elastic materials, setting $\mathbf{s}=\mathbf{C}(\mathbf{X},x_3)$: $\mathbf{e}$, $\mathbf{e}=\operatorname{sym}\nabla\mathbf{u}$, where $\mathbf{C}(\cdot,x_3)$ is A-periodic for every $x_3\in(0,H)$. Substituting the right-hand side of the above constitutive relations into (6.2), by means of $\nabla\mathbf{u}=\mathbf{U}+h^A\nabla\mathbf{W}+\nabla h^A\otimes\mathbf{W}$, and using the procedure given in Sec. 5, we obtain

$$
\begin{bmatrix}\mathbf{S}\\ \mathbf{H}^{\mathbf{A}}\\ \mathbf{R}^A{}_3\end{bmatrix}=\begin{bmatrix}<\mathbf{C}>, & <\mathbf{C}\cdot\nabla h^B>, & <\mathbf{C}\cdot\mathbf{a}_3h^B>\\ <\nabla h^A\cdot\mathbf{C}>, & <\nabla h^A\cdot\mathbf{C}\cdot\nabla h^B>, & <\nabla h^A\cdot\mathbf{C}\cdot\mathbf{a}_3h^B>\\ <h^A\,\mathbf{a}_3\cdot\mathbf{C}>, & <h^A\,\mathbf{a}_3\cdot\mathbf{C}\cdot\nabla h^B>, & <h^A\,\mathbf{a}_3\cdot\mathbf{C}\cdot\mathbf{a}_3h^B>\end{bmatrix}\times\begin{bmatrix}\mathbf{E}\\ \mathbf{W}^{\mathbf{B}}\\ \mathbf{W}^{\mathbf{B}}{}_{,3}\end{bmatrix},
\tag{6.4}
$$

where the elements of the above matrix can be functions of an argument x_3. Equations (6.3), (6.4) together with (5.2) represent a model of the class of composites under consideration. In general we now deal with composites which can be non-periodic in the x_3-axis direction; if $\varrho(\cdot)$ and $\mathbf{C}(\cdot)$ are independent of x_3 then (6.3), (6.4) are equations with constant coefficients.

Substituting the right-hand sides of Eqs. (6.4) into Eqs. (6.3) we obtain the system of three partial differential equations of the second order for macrodisplacements $\mathbf{U}$ coupled with the system of $3N$ equations for $\mathbf{W}^A$. The latter are the second order partial differential equations with respect to arguments t and x_3. Hence, in formulations of boundary-value problems, we have to prescribe on $\partial[\Pi\times(0,H)]$ three conditions for three components of $\mathbf{U}$. At the same time on $\Pi\times\{0\}$ and $\Pi\times\{H\}$ we have also to introduce $3N$ extra boundary conditions for $3N$ components of $\mathbf{W}^A$, $A=1,\ldots,N$. It follows that $\mathbf{W}^A$ can be treated as internal variables only as functions of the argument $\mathbf{X}=(x_1,x_2)$. That is why they will be called the quasi-internal variables. Hence, Eqs. (6.3), (6.4), (5.2) represent what will be called the quasi-internal variables model (QIV-model) of the fibre-reinforced composites.

http://rcin.org.pl

6.2. Laminates

Following the line of approach performed in Subsec. 6.1 we also define $\Omega = \Pi \times (0, H)$ and assume that a laminate under consideration has the periodic material structure (with a period $l = l_3$) along the x_3-axis. The averaging operator used throughout this subsection will be given by

$$<f(\mathbf{z})>(\mathbf{x}) := \frac{1}{l} \int_{x_3 - l/2}^{x_3 + l/2} f(x_1, x_2, z_3)\, dz_3 .$$

Moreover, we introduce the concept of ε-macrofunction $\Phi(\cdot)$ (related to the line interval $(0, H)$) by means of

$$(\forall\ (x_3, y_3) \in (0, H)^2)[|x_3 - y_3| < l \ \Rightarrow\ |\Phi(x_3) - \Phi(y_3)| < \varepsilon_\Phi].$$

A function $\Phi(\cdot)$ can also depend on x_1, x_2 and/or t as parameters. The micro-shape functions $h^A(\cdot)$ depend now only on the argument x_3 since the oscillations of displacements caused by the periodic micro-heterogeneity of the medium take place only in the direction of the x_3-axis. Setting $V = (-\delta_1, \delta_1) \times (-\delta_2, \delta_2) \times (-l/2, l/2)$ and passing to the limit $\delta_1 \to 0$, $\delta_2 \to 0$, we obtain from Eqs. (4.11) the equations of motion for the composite under consideration. To this end we define by $\mathbf{a}_\alpha$ the versors of x_α-axes, $\alpha = 1, 2$, and introduce the fields

$$\begin{aligned} \mathbf{U}(\mathbf{x}, t) &:= <\mathbf{u}(\mathbf{z}, t)>(\mathbf{x}), \\ \mathbf{W}^A(\mathbf{x}, t) &:= <\mathbf{w}_\mathbf{x}(\mathbf{z}, t) h^A(z_3)>(\mathbf{x}) l^{-2}, \end{aligned} \tag{6.5}$$

and

$$\begin{aligned} \mathbf{S}(\mathbf{x}, t) &:= <\mathbf{s}(\mathbf{z}, t)>(\mathbf{x}), \\ \mathbf{H}^A(\mathbf{x}, t) &:= <\mathbf{s}(\mathbf{z}, t) \cdot \nabla h^A(z_3)>(\mathbf{x}), \\ \mathbf{R}^A{}_\alpha(\mathbf{x}, t) &:= <\mathbf{a}_\alpha \cdot \mathbf{s}(\mathbf{z}, t) h^A(z_3)>(\mathbf{x}). \end{aligned} \tag{6.6}$$

Moreover, let $\mathbf{U}(x_1, x_2, \cdot, t), \ldots, \mathbf{R}^A{}_\alpha(x_1, x_2, \cdot, t)$ be regular ε-macrofunctions (related to $(0, H)$) for every $\mathbf{X} = (x_1, x_2) \in \Pi$ and $t \in (t_0, t_f)$. In this case from (4.11) we obtain (summation over $\alpha = 1, 2$ holds!)

$$\begin{aligned} &\operatorname{Div} \mathbf{S}(\mathbf{x}, t) - <\varrho>(\mathbf{X})\, \ddot{\mathbf{U}}(\mathbf{x}, t) + <\varrho>(\mathbf{X})\mathbf{b} = \mathbf{0}, \\ &-\mathbf{R}^A{}_{\alpha,\alpha}(\mathbf{x}, t) + <\varrho h^A h^B>(\mathbf{X})\, \ddot{\mathbf{W}}^B(\mathbf{x}, t) + \mathbf{H}^A(\mathbf{x}, t) = \mathbf{0}. \end{aligned} \tag{6.7}$$

Using the procedure explained in Sec. 5, from (6.6), after some manipulations, we arrive at (α, β run over 1, 2; summation convention over β holds!)

http://rcin.org.pl

$$(6.8)\qquad \begin{bmatrix} \mathbf{S} \\ \mathbf{H}^A \\ \mathbf{R}^A{}_\alpha \end{bmatrix} = \begin{bmatrix} <\mathbf{C}>, & <\mathbf{C}\cdot\nabla h^A>, & <\mathbf{C}\cdot\mathbf{a}_\beta h^A> \\ <\nabla h^A\cdot\mathbf{C}>, & <\nabla h^A\cdot\mathbf{C}\cdot\nabla h^B>, & <\nabla h^A\cdot\mathbf{C}\cdot\mathbf{a}_\beta h^B> \\ <h^A\,\mathbf{a}_\alpha\cdot\mathbf{C}>, & <h^A\,\mathbf{a}_\alpha\cdot\mathbf{C}\cdot\nabla h^B>, & <h^A\,\mathbf{a}_\alpha\cdot\mathbf{C}\cdot\mathbf{a}_\beta h^B> \end{bmatrix} \times \begin{bmatrix} \mathbf{E} \\ \mathbf{W}^B \\ \mathbf{W}^B{}_{,\beta} \end{bmatrix},$$

where the elements of the above matrix can depend on $\mathbf{X} \in \Pi$. Equations (6.7), (6.8) together with (5.2) constitute a model of the laminates which are periodic in x_3-axis direction. In the directions of the x_1 and x_2-axes, the material structure of those composites can be non-periodic. If $\varrho(\cdot)$ and $\mathbf{C}(\cdot)$ re independent of $\mathbf{X} = (x_1, x_2)$ then (6.7), (6.8) are equations with constant coefficients.

Substituting the right-hand sides of Eqs. (6.8) into Eqs. (6.7) we obtain the system of three second-order partial differential equations for $\mathbf{U}$ coupled with the system of $3N$ differential equations for $\mathbf{W}^A$. The latter are the second-order differential equations with respect to x_1, x_2 and t. It follows that in formulations of boundary-value problems we have to prescribe on $\partial\Omega$ three conditions for three components of $\mathbf{U}$. Moreover, on $\partial\Pi \times (0, H)$ we have also introduced $3N$ extra boundary conditions for $3N$ components of $\mathbf{W}^A$, $A = 1, ..., N$. Similarly to Subsec. 6.1, the unknowns $\mathbf{W}^A$ will be called the quasi-internal variables and hence the model given by Eqs. (6.7), (6.8) will be referred to as the quasi-internal variable model (QIV-model) of the laminated composites.

6.3. Final remarks

It can be seen that if the problem under consideration is independent of x_3-coordinate then the QIV-model for the fibre-reinforced composites reduces to the MIV-model. Similarly, if the problem is independent of x_1, x_2-coordinates then the QIV-model for laminates reduces to the MIV-model. The main feature of the QIV-models is that they can describe with a sufficient accuracy the conditions on these parts of boundary which are intersecting the periodic structure of a composite material. Using QIV-models we can also describe certain class of composites which are non-periodic in directions normal to the basic cell.

7. Conclusions

Let us summarize the advantages and drawbacks of both the MIV- and QIV-models of composites in the light of their possible applications to dynamics of composite solids. The main advantages can be listed as follows.

1. The MIV- and QIV-models describe the effect of the microstructure size on the dynamic behaviour of a composite body, contrary to models based on the concepts of the homogeneous equivalent body. Hence, using these models we

http://rcin.org.pl

can investigate dispersion phenomena and determine higher wave propagation speeds and free vibration frequencies in composite materials. It can be observed that the MIV-models describe the length-scale effect on the composite body behaviour only in dynamic problems while QIV-models – also in the quasi-stationary problems.

2. The form of the governing equations of the MIV-models is relatively simple since all macro-internal variables as the extra unknowns are governed by the ordinary differential equations, involving only time derivatives of $\mathbf{W}^A$. Hence, the boundary conditions for the MIV-models have the form similar to that met in solid mechanics. Moreover, QIV-models make it possible to describe conditions on the boundary cross-sections of fibre composites and on lateral boundaries of laminates with the required accuracy. It has to be noticed that in the micromorphic models of composites, based on the concept of the extra local degrees of freedom (like the Cosserat-type continua), we deal with the large number of boundary conditions which may be not well motivated from the physical or engineering viewpoint. The same situation also holds for the asymptotic models involving higher-order approximations; this problem will be analyzed in a separate paper.

3. The governing equations of an arbitrary MIV-model have constant coefficients which can be easily determined by calculating the integrals over V and do not require any previous solution to the boundary value problem on the unit cell, contrary to models obtained via the asymptotic methods. Coefficients in the equations of QIV-models can also be easily obtained by the calculation of integrals over the basic area or line element.

4. The MIV- and QIV-models have a wide scope of applications since they can be postulated in the unified way for composites made of arbitrary simple materials. Moreover, the formal procedure presented in this contribution can be easily generalized to include the problem of finite deformations.

5. In some special problems, the MIV- and QIV-models have an adaptive character similar to that of the FEM. It means that they can be formulated on different levels of accuracy either by applying different truncations of the Fourier series or by changing the form of micro-shape functions. Moreover, the error of the obtained solutions to boundary value problems can be evaluated *a posteriori* by the evaluation of the residual fields $\mathbf{r}(\cdot, t)$ introduced in Sec. 4, provided that the stresses and displacements have been previously calculated in terms of macrodisplacements $\mathbf{U}$ and macro-internal variables $\mathbf{W}^A$ with a sufficient accuracy.

Among the drawbacks of the MIV- and QIV-models, the following ones seem to be the most relevant:

1. The analysis of the microdynamic effects is confined almost exclusively to the behaviour of a composite on a macro-level. The passage to microdynamics by using formulae (3.6) may require a very large number N of the micro-shape functions, which make the problem very difficult to solve.

http://rcin.org.pl

2. The choice of the Fourier expansion of local oscillations and its truncation leading to the proper MIV- or QIV-models for the problem under consideration is not specified by the proposed approach. For some special problems (e.g. for laminated structures), the choice of the micro-shape functions can be based on the intuition of the researcher as a certain *a priori* postulated kinematic hypothesis not related to the aforementioned Fourier expansion.

3. Every MIV- and QIV-model is restricted only to the analysis of a special class of motions which from a qualitative viewpoint has to be postulated *a priori* by the choice of the micro-shape functions. Hence the above models can be applied mostly to problems in which we are interested in a dynamic body behaviour, under motions which can be assumed *a priori* as relevant for the problem under consideration.

Summarizing the above conclusions and taking into account the recently obtained results in this field (cf. the references mentioned in Introduction), one can suppose that the MIV- and QIV-models of composite material structures deserve a certain attention both from the theoretical and engineering point of view.

Acknowledgments

This research work was supported by KBN under grant No. 7 T07A 017 11.

References

1. J. ABOUDI, *Mechanics of composite materials: a unified micromechanical approach*, Elsevier, Amsterdam 1991.
2. J.D. ACHENBACH and G. HERMANN, *Wave motions in solids with laminar structuring*, [in:] Dynamics of Structured Solids, G. HERMANN [Ed.], Am. Soc. Mech. Engng., New York 1968.
3. N.S. BAKHVALOV and G.P. PANASENKO, *Averaged processes in periodic media* [in Russian], Nauka, Moskva 1984.
4. E. BARON and C. WOŹNIAK, *On the microdynamics of composite plates*, Arch. Appl. Mech., **66**, 126–133, 1995.
5. A. BENSOUSSAN, J.L. LIONS and G. PAPANICOLAOU, *Asymptotic analysis for periodic structures*, North-Holland, Amsterdam 1978.
6. I. CIELECKA, *On the continuum the dynamic behaviour of certain composite lattice-type structures*, J. Theor. Appl. Mech., **33**, 351–360, 1995.
7. B.D. COLEMAN and M.E. GURTIN, *Thermodynamics with internal state variables*, J. Chem. Phys., **47**, 597–613, 1967.
8. F. DELL'ISOLA, L. ROSA and C. WOŹNIAK, *Dynamics of solids with micro-periodic non-connected fluid inclusions*, Arch. Appl. Mech., [in the course of publication].
9. G.A. HEGEMIER, *On a theory of interacting continua for wave propagation in composites*, [in:] Dynamics of Composite Materials, E.H. LEE [Ed.], Am. Soc. Mech. Engng., New York 1972.
10. J. JĘDRYSIAK and C. WOŹNIAK, *On the elastodynamics of thin microperiodic plates*, J. Theor. Appl. Mech., **33**, 337–350, 1995.
11. V.V. JIKOV, O.A. KOZLOV and O.A. OLEINIK, *Homogenization of differential operators and integral functionals*, Springer-Verlag, Berlin 1994.
12. R. JONES, *Mechanics of composite materials*, Mc Graw-Hill, New York 1972.

http://rcin.org.pl

13. S. KONIECZNY and M. WOŹNIAK, *On the wave propagation in fibre-reinforced composites*, J. Theor. Appl. Mech., **33**, 375–384, 1995.
14. T. LEWIŃSKI and ST. KUCHARSKI, *A model with length scales for composites with periodic structure*, Part I, Comp. Mechanics, **9**, 249–265, 1992.
15. A. MAEWAL, *Construction of models of dispersive elastodynamic behaviour of periodic composites: a computational approach*, Comp. Meth. Appl. Mech. Engng., **57**, 191–205, 1986.
16. S.J. MATYSIAK and W. NAGÓRKO, *On the wave propagation in periodically laminated composites*, Bull. Polon Acad. Sci., Tech. Sci., **43**, 1–12, 1995.
17. S.J. MATYSIAK and C. WOŹNIAK, *Micromorphic effects in a modelling of periodic multilayered elastic composites*, Int. J. Engng. Sci., **25**, 549–551, 1987.
18. K. MAZUR-ŚNIADY, *Macro-dynamics of micro-periodic elastic beams*, J. Theor. Appl. Mech., **31**, 781–793, 1993.
19. B. MICHALAK, C. WOŹNIAK and M. WOŹNIAK, *The dynamic modelling of elastic wavy plates*, Arch. Appl. Mech., **66**, 177–186, 1996.
20. G. MIELCZAREK and C. WOŹNIAK, *On the dynamic modelling of fibrous composites*, J. Tech. Phys., **36**, 103–111, 1995.
21. G. MIELCZAREK and C. WOŹNIAK, *On the micro-dynamics of composite materials*, J. Theor. Appl. Mech., **33**, 731–745, 1995.
22. R.D. MINDLIN, *Microstructure in linear elasticity*, Arch. Rat. Mech. Anal., **16**, 51–78, 1964.
23. S. NEMAT-NASSER and M. HORI, *Micromechanics: overall properties of heterogeneous materials*, North-Holland, Amsterdam 1993.
24. C.T. SUN, J.D. ACHENBACH and G. HERMANN, *Time-harmonic waves in a stratified medium propagating in the direction of the layering*, J. Appl. Mech., **35**, 408–411, 1968.
25. H.F. TIERSTEN and M. JAHANMIR, *The theory of composites modelled as interpenetrating solid continua*, Arch. Rat. Mech. Anal., **65**, 153–192, 1977.
26. M. WĄGROWSKA and C. WOŹNIAK, *Macro-modelling of dynamic problems for visco-elastic composite materials*, Int. J. Engng. Sci., **34**, 923–932, 1996.
27. E. WIERZBICKI, *On the wave propagation in micro-periodic elastic media*, Bull. Acad. Polon Sci., Tech. Sci., **41**, 323–327, 1993.
28. E. WIERZBICKI, *Nonlinear macro-micro dynamics of laminated structures*, J. Theor. Appl. Mech., **33**, 291–307, 1995.
29. E. WIERZBICKI, C. WOŹNIAK and M. WOŹNIAK, *Finite rotations in the refined macrodynamics of elastic composites*, J. Theor. Appl. Mech., **33**, 15–25, 1995.
30. E. WIERZBICKI, C. WOŹNIAK and M. WOŹNIAK, *Thermal stresses in nonstationary problems for composite materials*, Int. J. Engng. Sci., [in the course of publication].
31. C. WOŹNIAK, *A nonstandard method of modelling of thermo-elastic periodic composites*, Int. J. Engng. Sci., **25**, 133–141, 1987.
32. C. WOŹNIAK, *Refined macrodynamics of periodic structures*, Arch. Mech., **45**, 295–304, 1993.
33. C. WOŹNIAK, *Micro-macro dynamics of periodic material structures*, [in:] Structural Dynamics, pp. 573–575, Eurodyn'93, Balkema, Rotterdam 1993.
34. C. WOŹNIAK, *Nonlinear macro-elastodynamics of microperiodic composites*, Bull. Acad. Polom Sci., Tech. Sci., **41**, 315–321, 1993.
35. C. WOŹNIAK, *Microdynamics: continuum modelling the simple composite materials*, J. Theor. Appl. Mech., **33**, 267–289, 1995.
36. C. WOŹNIAK, Z.F. BACZYŃSKI and M. WOŹNIAK, *Modelling of nonstationary heat conduction problems in micro-periodic composites*, ZAMM, **76**, 223–229, 1996.
37. C. WOŹNIAK and M. WOŹNIAK, *On the micro-modelling of dynamic response for thermoelastic periodic composites*, [in:] Proc. IUTAM Symp. "Microstructure Property Interactions in Composite Materials", pp. 387–395, Aalborg, 1994.
38. C. WOŹNIAK and M. WOŹNIAK, *A generalization of the internal-variable model for dynamics of solids with periodic microstructure*, J. Theor. Appl. Mech., [submitted for publ.].
39. C. WOŹNIAK, M. WOŹNIAK and S. KONIECZNY, *A note on dynamic modelling of periodic composites*, Arch. Mech., **45**, 779–783, 1993.

http://rcin.org.pl

40. M. WOŹNIAK, *On 2D-models of stratified subgrades*, J. Theor. Appl. Mech., **32**, 689–700, 1994.
41. M. WOŹNIAK, *Averaged formulation of nonstationary problems for stratified porous media*, J. Theor. Appl. Mech., **33**, 401–413, 1995.
42. M. WOŹNIAK, *On the dynamic behaviour of micro-damaged stratified media*, Int. J. Fract., **73**, 223–232, 1995.
43. M. WOŹNIAK, *On the description of consolidation processes in saturated reinforced subsoils*, Arch. Mech., **47**, 635–643, 1995.
44. M. WOŹNIAK, *2D dynamics of a stratified elastic subsoil layer*, Arch. Appl. Mech., **66**, 284–290, 1996.

INSTITUTE OF MATHEMATICS AND COMPUTER SCIENCE
TECHNOLOGICAL UNIVERSITY OF CZĘSTOCHOWA
ul. Dąbrowskiego 69, 42-200 CZĘSTOCHOWA.

Received October 14, 1996.

http://rcin.org.pl

Arch. Mech., 49, 2, pp. 443–445, Warszawa 1997

LETTERS TO THE EDITOR

Some thoughts on thermodynamics of internal variables

K. C. VALANIS (VANCOUVER)

THE THOUGHTS and ideas expressed here are meant to address the remarks and comments that were made by various speakers during the 31st Polish Solid Mechanics Conference. It was felt at the time that a complete picture of the theory on thermodynamics of internal variables appeared to be lacking in some issues that are of critical interest technically as well as historically. These comments are meant to address these issues.

The first point concerns the question of entropy. As is known, entropy is not a primitive quantity like energy. Its existence as a thermodynamic state function can be established only by integration of the First Law, if the First Law is integrable – as in the case of a perfect gas. The conditions of integrability of the 1st Law, which is basically a Pfaffian form, were established by Caratheodory, on the basis of inaccessibility of thermodynamic states. This, however, was done only for non-dissipative, i.e., reversible processes. The application of the Caratheodory principle to irreversible processes, associated with the deformation of materials with memory, leading to a proof of existence of entropy in the presence of such processes, was done by VALANIS [1, 2], using the concept of internal variables. These were used not so much as agents of dissipation, as is commonly done, but as additional variables necessary to render such quantities as energy and entropy as STATE FUNCTIONS, which they are not if the internal variables are missing.

One important aspect of the proof is that dissipative processes, associated with the deformation of materials with memory, do possess entropy at levels *far* removed from equilibrium – i.e., not just for processes near equlibrium as was the case with the traditional "thermodynamics of irreversible processes". Thus in the case of thermodynamics of internal variables, *equilibrium* does *not* enjoy a *special place* in the theory, so that the Kestin "paradox" in plasticity, that a succession of "equilibrium states" constitutes none-the-less a dissipative process, is resolved by means of the endochronic theory, where time is the length of the strain path.

The alternative is to begin with a functional form of a constitutive theory of materials with memory and to assume that such materials possess entropy as a primitive state function and further, to assume the existence of entropy inequalities. This is nothing short of a leap of faith since there is no fundamental mathematical or physical basis neither for the existence of entropy in this mathematical framework, nor for the associated inequalities.

http://rcin.org.pl

The second point regards the contention that the thermodynamical theory of internal variables is not fully general since it cannot describe Markov processes. To the extent that such processes are a mathematical model for viscocity (and diffusion), it is much more satisfactory if one deals with viscosity *per se*. It was said, on one occasion of an invited address, that internal variables cannot describe viscous materials such as viscous liquids of the Navier–Stokes type. But on the contrary, internal variables do describe the constitutive behaviour of viscous liquids, albeit in an *asymptotic* sense!! In other words, viscous liquids are asymptotic ideals of "linear" viscoelastic solids!

To show that this is in fact the case, first for small deformation and then for large, we first consider the deviatoric response of a linear viscoelastic solid where the deviatoric stress is a linear memory integral of the history of the deviatoric strain as in Eq. (1). Its large deformation counterpart is given in Eq. (2).

$$s_{ij} = \int_0^t 2\mu(t-t')\, de_{ij}/dt'\, dt', \tag{1}$$

$$\tau_{\alpha\beta} = \int_0^t \mu(t-t')\, dC_{\alpha\beta}/dt'\, dt' + pC_{\alpha\beta}\,. \tag{2}$$

In Eq. (1) $\mathbf{s}$ is the deviatoric stress tensor, $\mathbf{e}$ the deviatoric strain tensor and μ the memory kernel. In Eq. (2) $\boldsymbol{\tau}$ is the (covariant) Piola stress and $\mathbf{C}$ the Right Cauchy–Green tensor, and again μ is the memory kernel. Also p is the (indeterminate) hydrostatic stress for incompressible materials.

In the linear theory of internal variables the memory kernel is a sum of positive decaying exponential terms. It is shown in the Appendix that when the relaxation times tend to zero, the memory kernel becomes a Dirac delta function so that the material becomes a viscous liquid. The theory is remarkable in this sense. No material can have, physically speaking, a zero relaxation time, simply because relaxation processes take a finite time to be completed. Thus a zero relaxation time is an idealization and the viscous liquid is a mathematical construction, true only in an asymptotic sense.

The same is true in plasticity where the constitutive behaviour is represented by an endochronic integral. In this case, a perfectly plastic solid is an "ideal" which results when the endochronic relaxation times tend to zero.

Appendix

We begin with Eq. (1). The interest is to show that the material, whose constructive behaviour is given by Eq. (1), degenerates into a viscous liquid, when its relaxation times tend to zero. Since, according to the theory of internal variables,

http://rcin.org.pl

the memory function $\mu(t)$ in Eq. (1) is the sum of decaying exponential terms, one such term suffices in the proof. Thus, let:

$$\mu(t) = \mu_0 e^{-\alpha t}, \tag{3}$$

where α is the inverse relaxation time λ and is equal to μ_0/η. We note that μ_0 is the (instantaneous) modulus of the material while η is the viscosity. Evidently λ is equal to η/μ_0 and tends to zero as μ_0 tends to infinity. In the light of Eq. (3), Eq. (1) becomes:

$$\alpha \mathbf{s} + d\mathbf{s}/dt = 2\mu_0 \, d\mathbf{e}/dt \tag{4}$$

or

$$\mathbf{s} + (\eta/\mu_0) \, d\mathbf{s}/dt = 2\eta \, d\mathbf{e}/dt. \tag{5}$$

Thus, as μ_0 tends to infinity:

$$\operatorname{Lim} \mathbf{s} = \eta \, d\mathbf{e}/dt. \tag{6}$$

Hence viscous behaviour is the mathematical ideal of zero relaxation time s.

In a similar manner Eq. (2) becomes:

$$\tau_{\alpha\beta} = pC_{\alpha\beta} + \eta \, dC_{\alpha\beta}/dt. \tag{7}$$

The Cauchy stress T_{ij} is related to $\tau_{\alpha\beta}$ by the transformation:

$$T_{ij} = x^{\alpha}{}_{,i} \, x^{\beta}{}_{,j} \, \tau_{\alpha\beta}, \tag{8}$$

where x^{α} and y_i are the material and spatial coordinates, respectively, and a comma denotes a derivative with respect to y_i. In view of Eqs. (7) and (8)

$$T_{ij} = p \, \delta_{ij} + 2\eta \, d_{ij} \tag{9}$$

since

$$x^{\alpha}{}_{,i} \, x^{\beta}{}_{,j} \, dC_{\alpha\beta}/dt = 2d_{ij}, \tag{10}$$

where d_{ij} is the deformation rate tensor. We remark that Eq. (9) is the Navier–Stokes equation for a linear incompressible viscous liquid.

References

1. K.C. VALANIS, *Irreversibility and existence of entropy*, Int. J. Non-Lin. Mech., **6**, 337–360, 1971.
2. K.C. VALANIS, *Partial integrability as the basis of existence of entropy in irreversible systems*, ZAMM, **63**, 73–80, 1983.

ENDOCHRONICS, VANCOUVER, USA.

Received November 20, 1996.

http://rcin.org.pl

DIRECTIONS FOR THE AUTHORS

The journal *ARCHIVES OF MECHANICS (ARCHIWUM MECHANIKI STOSOWANEJ)* deals with the printing of original papers which should not appear in other periodicals.

As a rule, the volume of a paper should not exceed 40 000 typographic signs, that is about 20 type-written pages, format: 210 × 297 mm, leaded. The papers should be submitted in two copies. They must be set in accordance with the norms established by the Editorial Office. Special importance is attached to the following directions:

1. The title of the paper should be as short as possible.

2. The text should be preceded by a brief introduction; it is also desirable that a list of notations used in the paper should be given.

3. The formula number consists of two figures: the first represents the section number and the other the formula number in that section. Thus the division into subsections does not influence the numbering of formulae. Only such formulae should be numbered to which the author refers throughout the paper, and also the resulting formulae. The formula number should be written on the left-hand side of the formula; round brackets are necessary to avoid any misunderstanding. For instance, if the author refers to the third formula of the set (2.1), a subscript should be added to denote the formula, viz. $(2.1)_3$.

4. All the notations should be written very distincly. Special care must be taken to write small and capital letters as precisely as possible. Semi-bold type should be underlined in black pencil. Explanations should be given on the margin of the manuscript in case of special type face.

5. It has been established to denote vectors by semi-bold type. Trigonometric functions are denoted by sin, cos, tg and ctg, inverse functions – by arc sin, arc cos, arc tg and arc ctg; hyperbolic functions are denoted by sh, ch, th and cth, inverse functions – by Arsh, Arch, Arth and Arcth.

6. Figures in square brackets denote reference titles. Items appearing in the reference list should include the initials of the first name of the author and his surname, also the full title of the paper (in the language of the original paper); moreover;

a) In the case of books, the publisher's name, the place and year of publication should be given, e.g.,
5. S. Ziemba, *Vibration analysis*, PWN, Warszawa 1970;

b) In the case of a periodical, the full title of the periodical, consecutive volume number, current issue number, pp. from ... to ..., year of publication should be mentioned; the annual volume number must be marked in black pencil so as to distinguish it from the current issue number, e.g.,
6. M. Sokołowski, *A thermoelastic problem for a strip with discontinuous boundary conditions*, Arch. Mech., **13**, 3, 337–354, 1961.

7. The authors should enclose a summary of the paper. The volume of the summary is to be about 100 words.

8. The authors are kindly requested to enclose the figures prepared on diskettes (format PCX, BitMap or PostScript).

Upon receipt of the paper, the Editorial Office forwards it to the reviewer. His opinion is the basis for the Editorial Committee to determine whether the paper can be accepted for publication or not.

The printing of the paper completed, the author receives 10 copies of reprints free of charge. The authors wishing to get more copies should advise the Editorial Office accordingly, not later than the date of obtaining the galley proofs.

The papers submitted for publication in the journal should be written in English. No royalty is paid to the authors.

Please send us, in addition to the typescript, the same text prepared on a diskette (floppy disk) 3 1/2″ or 5 1/4″ as an ASCII file, in Dos or Unix format.

EDITORIAL COMMITTEE
ARCHIVES OF MECHANICS
(ARCHIWUM MECHANIKI STOSOWANEJ)

http://rcin.org.pl